INFINITE DILUTION ACTIVITY COEFFICIENT MEASUREMENTS OF ORGANIC SOLUTES IN FLUORINATED IONIC LIQUIDS BY GAS-LIQUID CHROMATOGRAPHY AND THE INERT GAS STRIPPING METHOD

Submitted in fulfillment of the academic requirements for the degree of Master of Science,
Faculty of Engineering, School of Chemical Engineering,
University of KwaZulu-Natal

by

Kaniki Armel Tumba

[BSc. Eng (Chem)]

Supervisor: Prof. Deresh Ramjugernath

Co-Supervisor: Dr. Paramespri Naidoo

March 2010

DECLARATION

I, Kaniki Armel Tumba, declare that:

(i) The research reported in this thesis, except where otherwise indicated, is my original work.

(ii) This thesis has not been submitted for any degree or examination at any other university.

(iii) This thesis does not contain other persons' data, pictures, graphs or other information, unless specifically acknowledged as being sourced from other persons.

(iv) This thesis does not contain other persons' writing, unless specifically acknowledged as being sourced from other researchers. Where other written sources have been quoted, then:

a) their words have been re-written but the general information attributed to them has been referenced;

b) where their exact words have been used, their writing has been placed inside quotation marks, and referenced.

(v) Where I have reproduced a publication of which I am an author, co-author or editor, I have indicated in detail which part of the publication was actually written by myself alone and have fully referenced such publications.

(vi) This thesis does not contain text, graphics or tables copied and pasted from the internet, unless specifically acknowledged, and the source being detailed in the thesis and in the References sections.

_____ _____

Kaniki A. Tumba (Candidate) Date

As the candidate's Supervisor I agree/do not agree to the submission of this thesis.

_____ _____

Prof. Deresh Ramjugernath Date

ABSTRACT

Environmental and safety concerns have prompted an active quest for “green” alternatives to molecular solvents currently used in industrial chemical processes. In recent years, ionic liquids have been reported as potentially good replacements for conventional solvents. Activity coefficients at infinite dilution, γ_i^∞ of various organic solutes have been measured in the temperature range from 313.15 to 373.15 K by gas-liquid chromatography and the inert gas stripping techniques in seven fluorinated ionic liquids (FILs). Partial molar excess enthalpies at infinite dilution of the solutes in the ionic liquids have been derived from the temperature-dependence of experimental γ_i^∞ values. Selectivities and capacities have been calculated for various separation problems and compared to literature values for other ionic liquids, as well as conventional solvents. The effect of structure on the selectivity has been investigated.

The present work, initiated in the context of South Africa’s Fluorochemical Expansion Initiative is a contribution to the understanding of how structure influences FILs selectivity and capacity in different separation problems. FILs are interesting for South Africa as its geology contains large amounts of fluorine ores.

For the n-hexane/benzene, and n-hexane/hex-1-ene systems which represent the aliphatics/aromatics and paraffins/olefins separation problems, higher selectivities at infinite dilution were obtained with FILs consisting of short-chained cations and small anions. The opposite trend was observed for the methanol/acetone and the ethanol/butan-2-one systems as representatives of the alcohols/ketones separation problem as well as the methanol/benzene system which refers to the alcohols/aliphatics mixtures. FILs with long cation alkyl chains and large anions tend to be the most selective for the benzene/ butan-2-one system, indicative of the aliphatics/ketones separation problem.

The natural logarithm of γ_i^∞ has been found to vary linearly with the carbon number of the alkyl chain attached to the methylpyrrolidinium or methylimidazolium group. On this ground, a simple equation correlating γ_i^∞ as well as selectivity with the cation alkyl chain length has been proposed. It has been successfully tested using experimental data related to pyrrolidinium and imidazolium-based ionic liquids.

Additionally, an inert gas stripping apparatus suitable for γ_i^∞ measurements in ionic liquids has been constructed. Results obtained with the two different methods showed a good agreement.

ACKNOWLEDGEMENTS

Glory and Praise to Jehovah, the all mighty God who allowed me to achieve this research work.

I express my utmost gratitude to Prof. Deresh Ramjugernath for his dedicated supervision and his priceless assistance throughout this study. Dr Paramespri Naidoo, the co-supervisor is sincerely acknowledged for her pertinent suggestions and skillful guidance.

This work is based upon research supported by the South African Research Chairs Initiative of the Department of Science and Technology and National Research Foundation (NRF) which is acknowledged for its financial support.

I would be remiss if I do not extend my appreciations to the following individuals as well:

- My wife Fanny Tshabu Kaniki who deserves a medal for her patience and support;
- My parents, brothers and sisters for their encouragements;
- Messers Lindinkosi Mkinze and Ayanda Khanyile, The Thermodynamics Research Unit laboratory technicians;
- Messers Ken Jack and Kelly Robertson, Mechanical workshop staff in the School of Chemical Engineering;
- Glass blower Peter Siegling and UKZN Chemical Engineering ICT manager P. Nayager;
- Prof. Urszula Domańska and Dr. Andrzej Marciniak (Warsaw University of Technology, Poland) for insightful discussions on the behavior of ionic liquids;
- Dr. Fabrice Mutelet (Laboratoire de Thermodynamique des Milieux Polyphasés, Nancy, France) for his availability to answer some tricky questions on the GLC experimental procedure;
- Dr. Christophe Coquelet (Laboratoire des Equilibres Thermodynamiques, ENSM, Fontainebleau, France) who helped in advising on the construction of the inert gas stripping apparatus;
- All Thermodynamics Research Unit postgraduate students and friends: J. Chiyen, M. Tshibangu, J. Kapuku, T. P. Benecke, M. Tadie, S. Iwarere, B. Moller, F. Kabulu, P.N. Thokozani, ...
- E. Olivier and N. Gwala who authorized the use of their experimental data in this study;
- All UKZN Chemical Engineering lecturers who expressed interest in this project: Prof. J.D. Raal, Prof. D. Arnold, Mr Baah,…

TABLE OF CONTENTS

LIST OF FIGURES

LIST OF PHOTOGRAPHS

LIST OF TABLES

NOMENCLATURE

Symbols

A -- Solute peak area detected by gas chromatography (mV.min)

a -- Slope (min^{-1})

B -- Second virial coefficient ($cm^3\ mol^{-1}$)

C -- Concentration ($mol\ cm^{-3}$)

D -- Pure carrier gas flow rate ($cm^3 min^{-1}$)

D_2 -- Total gas flow at still exit ($cm^3 min^{-1}$)

D_1 -- Solvent gas flow in the stream entering the still ($cm^3 min^{-1}$)

D_{ij} -- Diffusion constant of solute i in solvent j ($cm^2\ s^{-1}$)

D_b -- Diameter of bubbles (cm)

f -- Fugacity for pure species

$\hat{f}$ -- Fugacity for species in solution

G -- Gibbs energy

g -- Gravitational acceleration ($cm^2 s^{-1}$)

H -- Henry's law constant

H --Enthalpy (J)

h -- Path length of bubbles in solution (cm)

I -- Poynting correction

K -- Partitioning coefficient

k -- Capacity

k_i -- Correction factors

k_L -- Mass transfer coefficient in the liquid ($mol.s^{-1}.cm^2$)

M -- Molar mass ($g.mol^{-1}$)

m -- Mass (g)

N -- Amount of solvent in the still

n -- Amount of solute in the still

P -- Pressure (kPa)

P^o or P^* - vapour pressure (kPa)

P_i -- Partial pressure (kPa)

R -- Gas constant ($J.mol^{-1}\ K^{-1}$)

R_b -- Radius of bubbles (cm)

S -- Selectivity

T -- Absolute temperature (K)

T_b -- Boiling point temperature (K)

V -- Volume (cm^3)

V_G -- Volume of the vapour space in the still (cm^3)

x -- Mole fraction in the liquid phase

y -- Mole fraction in the vapour phase

Z -- Compressibility factor

Greek letters

γ -- Activity coefficient, species in solution

φ -- Fugacity coefficient

ρ -- Density ($g.cm^{-3}$)

α -- Separation factor

κ -- Calibration detector constant

τ_L -- Ratio of mass transfer in the cell to mass transfer to reach equilibrium taking into account liquid phase resistance only

τ_G -- Same as τ_L taking into account gas phase diffusion only

u^{∞} -- Limiting speed of bubbles in solution ($cm.s^{-1}$)

$\gamma^{\infty,II}$ -- Corrected activity coefficient at infinite dilution

ν -- Kinematic viscosity (cSt)

η -- Dynamic viscosity (cP)

ω -- Acentric factor

Subscripts

1-- Solute

2-- Carrier gas

3-- Solvent.

CG-- Carrier gas

i -- Properties related to pure component i

ij -- Interaction properties

c -- Critical Properties

r -- Reduced Properties

L -- Liquid phase

o -- Initial value

f -- Final value

FM --Flowmeter

G --Gas phase

V --Vapour phase

Superscripts

id --Ideal solution

l --Liquid phase

v --Vapor phase

∞ -- Infinite dilution

o -- Initial value

sat --At saturation

E -- Excess properties

v -- Property in vapour phase

L -- Property in liquid phase

exp -- Experimentally determined

lit -- Literature value

ABBREVIATIONS

CG -- Carrier gas

IDAC -- Infinite dilution activity coefficient

IGST -- Inert Gas Stripping Technique

GLC -- Gas-Liquid Chromatography

COSMO-RS -- Conductor-like Screening Model for Real Solvents

DCT -- Double Cell Technique

SCT -- Single Cell Technique

GC -- Gas Chromatography

VLE -- Vapour Liquid Equilibrium

LLE --Liquid Liquid Equilibrium

RD-- Relative Deviation

GCMs -- Group Contribution Methods

FILs – Fluorinated Ionic Liquids

Cations

$[EMIM]^+$-- 1-ethyl-3-methylimidazolium

$[HMIM]^+$-- 1-hexyl-3-methylimidazolium

$[MOIM]^+$-- 1-methyl-3-octylimidazolium

$[BMIM]^+$-- 1-butyl-3-methylimidazolium

$[3C_4C_1P]^+$-- Tributylmethylphosphonium

$[3C_6C_{14}P]^+$-- Trihexyltetradecylphosphonium

[Py]-- Pyridinium

[Epy]-- Ethylpyridinium

$[BMPy]^+$-- n-butyl-4-methylpyridinium

$[MOPyrr]^+$-- 1-octyl-1-methyl-pyrrolidinium

$[BMPyrr]^+$-- 1-butyl-1-methyl-pyrrolidinium

$[HMPyrr]^+$-- 1-hexyl-1-methyl-pyrrolidinium

$[Et_3S]^+$-- Triethylsulfonium

$[C_13C_8N]^+$-- Methyltrioctylammonium

$[3C_1C_4N]^+$-- Trimethylbutylammonium

$[C_{16}MIM]^+$-- 1-hexadecyl-3-methylimidazolium

$[CpMIM]^+$-- 1-butyronitrile-3-methylimidazolium

$[EDMIM]^+$-- 1-ethyl-3-dimethylimidazolium

$[CpMMIM]^+$-- 1-butyronitrile-2, 3-dimethylimidazolium

$[PDMIM]^+$-- 1-propyl-3-dimethylimidazolium.

$[MMIM]^+$--1-methyl-3-methylimidazolium.

$[PBA\text{-}MIM]^+$-- 1-propyl boronic acid-3-methylimidazolium

$[PBA\text{-}OMIM]^+$-- 1-propyl boronic acid-3-octylimidazolium

$[PBA\text{-}C_{10}MIM]^+$-- 1-propyl boronic acid-3-decylimidazolium

$[PBA\text{-}C_{12}MIM]^+$-- 1-propyl boronic acid-3-dodecylimidazolium

$[PropOMIM]^+$-- 1-propenyl-3-methyloctylimidazolium

$[PropC_{10}MIM]^+$--1-propenyl-3-decylimidazolium

$[PropC_{12}MIM]^+$-- 1-propenyl-3-dodecylimidazolium

$[H\text{-}O\text{-}MIM]^+$--1-hexyloxymethyl-3-methylimidazolium

$[DH\text{-}O\text{-}MIM]^+$--1, 3-dihexyloxymethylimidazolium

Anions

$[SCN]^-$-- Thiocyanide

$[Tf_2N]^-$-- Bis (trifluoromethylsulfonyl) Imide

$[BF_4]^-$-- Tetrafluoroborate

$[TOS]^-$-- Tosylate

$[MeSO_4]^-$-- Methyl sulfate

$[(C_2F_5)_3PF_3]^-$-- Tris (pentafluoroethyl) trifluorophosphate

$[TFA]^-$-- Trifluoroacetate

$[TfO]^-$-- Trifluoromethylsulfonate

$[SbF_6]^-$-- Hexafluoroantimonate

$[PF_6]^-$-- Hexafluorophosphate

$[MDEGSO_4]^-$-- Diethyleneglycolmonoethylethersulfate

$[Me_2PO_4]^-$-- Dimethylphosphate

$[C_1OC_2SO_4]^-$-- Methoxyethylsulfate

$[FeCl_4]^-$-- Tetrachloridoferrate (III)

$[Et\text{-}SO_4]^-$-- Ethylsulfate

$[Oc\text{-}SO_4]^-$-- Octylsulfate

$[N(CN)_2]^-$ -- Dicyanamide

$[(C_8H_{17})_2PO_2]^-$-- Dimethylpentylphosphinate

$[n\text{-}C_{18}H_{35}OO]^-$-- Stearate

$[n\text{-}C_{16}H_{33}OO]^-$-- Palmitate

CHAPTER ONE: INTRODUCTION

Organic molecular solvents are used in different industrial chemical processes with satisfying technical results. However, most of these chemicals represent a risk to human health and are ecologically unfriendly due to their volatility. A good illustration of how destructive modern chemical products can be is given by this non-exhaustive list of disasters (Moutiers et al., 2003):

- Toxic cloud over Seveso in Italy, 1976;
- 3500 lives claimed when in 1984, the Bhopal based pesticide factory released toxic emissions in India;
- The devastating explosion of the AZF chemical plant in the French city of Toulouse in 2001.

Such accidents contribute to the increased awareness of environmental and health threats resulting from the large number of industrial processes. The development of less-polluting solvents and safe processes is nowadays a high priority on the agenda for "green chemistry". There is a pressing need to rethink the design of unsafe chemical processes so that younger generations inherit a healthy and safer environment.

In recent years, ionic liquids, salts that are liquids at low temperatures (Plechkova and Seddon, 2008) received the most attention as alternatives to volatile organic solvents in reactive chemistry, as well as, separation processes due to their negligible vapour pressure and wide liquid range.

Researchers at the Thermodynamics Research Unit, in the School of Chemical Engineering, University of KwaZulu-Natal in South Africa along with other academic institutions carried out systematic measurements of infinite dilution activity coefficients (γ_i^{∞}) for a wide range of organic solutes in various ionic liquids in order to assess their effectiveness as extracting solvents.

Though encouraging results were achieved, there is still an obvious appeal for more investigations in order to:

- Assess the solvent potential of the large number of ionic liquids that have not yet been investigated;
- Correlate the ionic liquid's structure and its ability to separate particular mixtures.

The present work has been conducted to increase the understanding of these two phenomena. Moreover, South Africa has nearly a third of the world's fluorspar (CaF_2) reserves (Meshri, 2000) and in the context of the Fluorochemical Expansion Initiative recently launched by its government, there are no better candidates for investigation than fluorinated ionic liquids. Thus this work is a focus on the measurement of infinite dilution activity coefficients in Fluorinated Ionic Liquids (FILs), bearing in mind their performance in separation processes.

An inert gas stripping apparatus for measurement of infinite dilution activity coefficients, (IDACs), for systems involving ionic liquids was constructed. The objective of this work was to answer the following questions:

- What performance can be expected from FILs as extracting solvents in extractive distillation and liquid-liquid extraction?
- How is the selectivity towards various systems affected by the anion-cation combination found in the structure of FILs?
- Can a reliable dilutor technique apparatus be locally designed, constructed and commissioned for use with small amounts of ionic liquids as solvent?

To address the above questions the methodological approach in this work consisted of:

- Generating new experimental activity coefficient data for organic solutes in selected fluorinated ionic liquids;
- Using experimental IDACs to determine limiting selectivity and capacity values for all FILs newly investigated, as well as, data reported in the literature;
- Analyzing the trends of variation of IDACs to gain insight into the influence of structure on limiting selectivity and capacity;
- Reviewing advances recorded in the use of the inert gas stripping technique;
- Constructing an apparatus similar to one developed previously in the Thermodynamics Research Unit (George, 2008) and reported in the open literature;
- Assessing its reliability in measuring infinite dilution activity coefficients by comparison of IDAC results obtained for the same systems using both Gas-Liquid Chromatography (GLC) and the Inert Gas Stripping Technique (IGST).

All experimental procedures have been conducted in the Thermodynamics Research Unit laboratories, in the School of Chemical Engineering, University of KwaZulu-Natal. All appropriate experimental equipment and necessary facilities were available to undertake the research work. Experimentally investigated ionic liquids are:

- Trihexyltetradecylphosphonium tetrafluoroborate, [$3C_6C_{14}P$] [BF_4]
- Trihexyltetradecylphosphonium bis(trifluoromethylsulfonyl) imide, [$3C_6C_{14}P$] [Tf_2N]
- Trihexyltetradecylphosphonium hexafluorophosphate, [$3C_6C_{14}P$] [PF_6]
- Methyltrioctylammonium bis (trifluoromethylsulfonyl) imide, [C_13C_8N] [Tf_2N]
- 1-ethyl-3-methylimidazolium trifluoromethanesulfonate, [EMIM] [TfO]
- 1-butyl-3-methylimidazolium hexafluoroantimonate, [BMIM] [SbF_6]
- 1-methyl-3-octylimidazolium hexafluorophosphate. [MOIM][PF_6]

Data have been generated at temperatures ranging from (313.15 to 373.15) K whereas solutes were selected among n-alkanes, alk-1-enes, alk-1-ynes, cycloalkanes, alkan-1-ols, alkylbenzenes and ket-2-ones. Separation problems are discussed through the n-hexane /benzene, methanol/benzene, methanol/acetone, n-hexane/hex-1-ene, ethanol/butan-2-one and benzene/butan-2-one systems.

During this study, contributions were made to publications by Olivier et al. (2010a, b and c), as well as, Gwala et al. (2010). This consisted of producing part of the published data i.e. infinite dilution activity coefficients in [EMIM] [TfO], [MOIM][PF_6], [BMIM] [SbF_6] and [C_13C_8N] [Tf_2N]. Full results obtained by these authors are used in this dissertation with their authorization.

This thesis is organized as follows. After this brief introduction (as chapter one), previous scientific work related to ionic liquids, generalities on activity coefficient at infinite dilution and recent advances in the design of inert gas stripping equipment are reviewed in chapter two. The third chapter provides details about the theory behind GLC and the IGST, as well as, equations used to compute infinite dilution activity coefficients. Chapter four is a description of the materials, the experimental set up and the experimental procedure used in this work. Infinite dilution activity coefficient experimental data are presented in chapter five. Results are discussed in the sixth chapter. Lastly, chapter seven is devoted to the conclusion and the recommendations for future investigations.

CHAPTER TWO: LITERATURE REVIEW

Chapter overview

In order to assist in determining the significance of previous similar works and understand the impact of the present study, this chapter reviews the following:

- Ionic liquids in the chemical industry;
- Generalities on activity coefficient at infinite dilution;
- Recent advances in the design of inert gas stripping equipments.

Experimental and predictive methods for infinite dilution activity coefficient determination are outlined. Only the two experimental techniques used in this work, gas-liquid chromatography and the inert gas stripping method are discussed. A closer look is taken at attempts made in the open literature to predict γ_i^{∞} in ionic liquids. The most promising predictive methods for systems involving ionic liquids are discussed in terms of accuracy and reliability. Since the objective of this study involves understanding the effect of fluorinated ionic liquids' structure on their ability to separate various mixtures and the construction of a dilutor cell, the results obtained from previous scientific investigation in these regards are reviewed. A treatment of ionic liquids in general and the fluorinated ones, in particular, is provided.

2.1. Ionic liquids

2.1.1. Definition and structure

Ionic liquids are materials that are solely composed of cations and anions, and melt at or below 100 ^{o}C (Endres and El Abedin 2006). The most commonly found structures of ionic liquids are given in figure 2-1.

2.1.2. History

In 1914, Paul Walden (1914) reported the physical properties of the first useful ionic liquid, ethylammonium nitrate, which had a melting point of 12 ^{o}C. It was synthesized by the reaction of concentrated nitric acid with ethylamine. Thereafter, Hurley and Weir (1951) stated the possibility of preparing room temperature ionic liquids by simply mixing and warming 1-ethylpyridinium in the presence of aluminum chloride; Chum et al. (1975), Robinson et al. (1979), Wilkes et al. (1982), Seddon et al. (1983) and Appleby et al. (1986) directed extensive research works towards new aluminum chloride-based ionic liquids in 1970s and 1980s. These ionic liquids did not find many practical applications due to their hydroscopic nature which required both preparation and handling to take place in an inert gas atmosphere. In 1992, water

and air stable 1-ethyl-3-imidazolium-based ionic liquids were reported by Cooper and O'Sullivan (1992), as well as Zaworotko and Wilkes (1992) in separate works. They developed imidazolium-based ionic liquids which consisted of alternative anions: acetate ($[CH_3CO_2]^-$), nitrite ($[NO_2]^-$), tetrafluoroborate ($[BF_4]^-$), trifluoromethane sulfonate ($[CF_3SO_3]^-$) and methylsulfate, ($[CH_3SO_4]^-$). Since then, new anions were incorporated in the structure of ionic liquids: hexafluorophosphate ($[PF_6]^-$), biscyanamide ($[N(CN)_2]_2^-$), trifluoroacetate ($[C_2F_3O_2]^-$), sulfate ($[SO_4]^{2-}$), hydrogensulfate ($[HSO_4]^-$), alkylsulfate ($[R\text{-}SO_4]^-$) , nitrate,($[NO_3]^-$). Contrary to chloroaluminates salts, these ionic liquids can be prepared on the bench. However, they can absorb water from the atmosphere, and they do not react with water. The development of more hydrophobic ionic liquids started in the second half of the 1990s through the work of Bonhôte et al. (1996). They reported the synthesis and characterization of ionic liquids containing hydrophobic anions such as trifluoromethane sulfonate ($[CF_3SO_3]^-$), triflate ($[OTf]^-$), tris (trifluoromethylsulfonyl) methanide {$[C(CF_3SO_2)_3]^-$} and bis (trifluoromethylsulfonyl) imide. As scientific research chemicals, ionic liquids were commercially available in 1999 (Letcher 2007). Nowadays, around 10^{18} ionic liquids have been predicted (Endres and El Abedin 2006) and could be synthesized by combining different ions like the ones shown in figure 2-1.

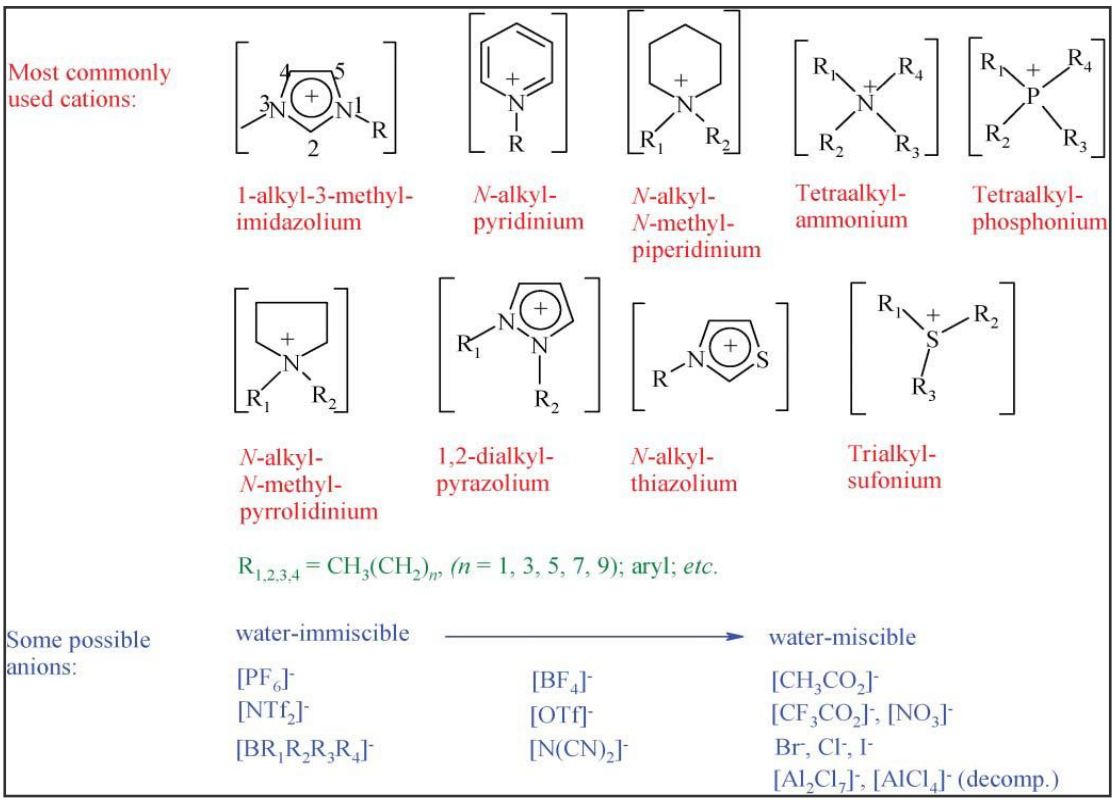

Figure 2-1: Structure of ionic liquids (Plechkova and Seddon 2008)

2.1.3. Properties of ionic liquids

It is because of their advantageous properties that ionic liquids attracted much attention from the scientific and industrial spheres. The most interesting properties of these compounds are listed below:

a) Extremely low vapour pressure: they are eco-friendly. (Welton 1999, and Wasserscheid and Keim 2000);
b) Low or reduced flammability hazards (Fox et al. 2008);
c) Tunable properties (Rogers and Seddon 2003);
d) Excellent solvation properties for a variety of organic and inorganic compounds (Rogers and Seddon 2003);
e) High electric conductivities (Trulove and Mantz 2003);
f) High thermal stability (Dupont 2004);
g) Wide liquid range (Huddleston et al. 2001);
h) Wide electrochemical window (Shröder et al. 2000).

Though ionic liquids are generally known as safe and benign compounds, some of them are volatile (Earl et al. 2006) and others are flammable (Smiglak et al. 2006).

2.1.4. Potential applications of ionic liquids in the chemical industry

The properties of a given ionic liquid are determined by the nature of its ions (Rogers and Seddon 2003). Any desired set of properties can be imparted to an ionic liquid by a proper selection of the anion-cation pair. This tunability of ionic liquids' properties allows a very wide range of applications as shown in the table below.

Table 2-1: Potential applications of ionic liquids in the chemical industry. (Plechkova and Seddon 2008)

Chemical engineering	**Electrochemistry**	**Biochemistry**
Mass separating agents	Electrolyte batteries	Biomass processing
Catalyst	Metal plating	Drug delivery
Coatings	Solar panels	Personal care
Lubricants	Fuel cells	Biocides
Plasticizers	Electro-optics.	Embalming
Dispersing agents		

2.1.5. Commercial applications of ionic liquids

Many companies have recently invested considerably in the development of ionic liquids-based commercial processes. Examples of publicly reported achievements regarding industrial uses of ionic liquids, as reviewed by Plechkova and Seddon (2008) are briefly discussed in this section.

2.1.5.1. BASIL Process

The Biphasic Acid Scavenging utilizing Ionic Liquids (BASIL) process is the most popular industrial application of ILs. It has been used by the German company BASF in the production of alkophenyl phosphines. 1-methylimidazolium chloride is used to scavenge the acid formed during the reaction. Results are better than in the original process where triethylamine was used.

2.1.5.2. Isobutene alkylation

Petro China performs isobutene alkylation with an ionic liquid. This is the largest commercial use of ionic liquids.

2.1.5.3. DIMERSOL Process

In this process, IFP (Institut Français du Pétrole) utilizes chloroaluminate (III) ionic liquids for alkenes dimerisation.

2.1.5.4. Other commercial uses

The following success stories have also been reported:

a) Pharmaceutical intermediate production by Central glass Co, Ltd in Japan;

b) 2, 5-dihydrofuran production by Eastman Chemical Company from 1996 to 2004;

c) Production of lithium ion rechargeable battery by Pionics in Japan.

2.1.5.5. Advanced projects

Besides the very small number of established industrial processes, one can list many promising projects, some at pilot plant stage. The most known ones include:

a) Metathesis and olefin trimerisation by SASOL in South Africa;

b) Azeotrope-breaking for water –ethanol and water –tetrahydrofuran with reduced; costs of solvent recovery by BASF;

c) Cellulose dissolution by BASF;

d) Aluminum plating by BASF;

e) Phosgene replacement by an ionic liquid in 1, 4-dichlorobutane production, achieved by BASF.

2.1.6. Use of ionic liquids as solvents in separation processes

2.1.6.1. Ionic liquids versus molecular solvents

Due to properties stated in section 2.1.3, ionic liquids attracted much attention in recent years as potential replacements to conventional molecular organic solvents.

With hundreds of thousands of ion combinations, it is possible to design an ionic liquid with the desired properties to suit a particular application by a proper anion and cation selection. One can adjust and tune ionic liquids to provide a specific property, including density, melting point, viscosity, hydrophobicity, miscibility and selectivity in separation processes. The tunability of ionic liquids provides flexibility for both reaction and combined reaction/separation schemes. And, since thermodynamics and kinetics of reactions taking place in ionic liquids differ from those in conventional solvents, it is clear that ionic liquids open new opportunities for both separation and combined reaction/separation processes. In ionic liquids, ions are held together by wide range interactions such as high coulombic forces and in some cases, hydrogen bondings resulting in near-zero vapour pressure and therefore no emission to the atmosphere. This non-volatile nature of ionic liquids allows the design and development of new environmentally-friendly separation processes. Another benefit is of course the reduced losses of solvents used in such processes. In addition, ionic liquids being generally non flammable, they should lead to safety benefits compared to molecular solvents commonly used in chemical engineering nowadays. Table 2-2 highlights more advantages of ionic liquids over molecular solvents that have enhanced their popularity.

Table 2-2: Ionic liquids versus molecular solvents (Plechkova and Seddon 2008).

Property	**Organic solvents**	**Ionic liquids**
Number of solvents	1000	1 000 000
Applicability	Single function	Multifunction
Catalytic ability	Rare	Common and tuneable
Chirality	Rare	Common and tuneable
Vapour pressure	Obeys the Clausius–Clapeyron equation	Negligible vapour pressure under normal conditions
Flammability	Usually flammable	Usually nonflammable
Solvation	Weakly solvating	Strongly solvating
Polarity	Conventional polarity concepts	Polarity concept questionable
Tuneability	Limited range of solvents available	Virtually unlimited range means ‘‘designer solvents’’
Cost	Normally cheap	Typically between 2 and 100 times the cost of organic solvents
Recyclability	Green imperative	Economic imperative
Viscosity/ Cp	0.2 – 100	22- 40 000
Density/g cm^3	0.6- 1.7	0.8- 3.3
Refractive index	1.3- 1.6	1.5- 2.2

2.1.6.2. Recent scientific investigations

Investigations on the suitability of ionic liquids as separation solvents are reviewed by Heintz (2005). In the last four years, the list of ionic liquids investigated is in steady progression. A large number of data have been experimentally generated to deal with various separation problems (David 2004). Some recent examples are studies on the basis of experimental VLE (Zhao et al. 2006, and Zhang et al. 2009) and LLE (Deenadayalu et al. 2006b and Meindersma et al. 2006) data which are available in the literature. All available experimental infinite dilution activity coefficient data for organic solutes in fluorinated and non-fluorinated ionic liquids can be found in publications listed in appendix A. The chemical quantum approach has also been used in the open literature to deal with problems such as:

a) Olefins-paraffins separation (Lei et al. 2007);

b) Diesel desulphurization (Kumar and Banerjee 2009);

c) Alkanols/ olefins separation (Banerjee 2008).

Patents have been granted for these processes involving ionic liquids as mass separation agents for organic liquid mixtures:

a) Separation of ionic compounds (Roetteger et al. 2003);

b) Separation of close-boiling or azeotropic mixtures (Arlt et al. 2002);

c) Separation of dienes from olefins (Boudreau et al. 2002);

d) Removal of polarizable impurities from hydrocarbons and hydrocarbon mixtures (Wasserscheid et al. 2002);

e) Mercaptans removal from hydrocarbon streams (O' Rear et al. 2001);

f) Extraction of aromatic hydrocarbons from aromatic petroleum streams (Gmehling and Krummen 2001).

All these research works established that ionic liquids are potentially good alternatives to currently used organic molecular solvents. As illustrated by table 2-3, for the separation of aromatic from aliphatic compounds, represented by the n-hexane/benzene and cyclohexane/ benzene systems, many ionic liquids can lead to higher limiting selectivities, and sometimes higher capacities than commonly used molecular solvents such as sulfolane and NMP. Regarding the influence of structure on extraction capacity, it is worthy to mention that only imidazolium and ammonium-based ionic liquids have been widely investigated with respect to aromatic/aliphatic compounds separation problems. It has been found that selectivity for aromatic hydrocarbons/aliphatic hydrocarbons increases with decreasing length of the alkyl chain on the cation (Letcher et al. 2009). Favorable anions are those with small volume and sterical shielding around the charge centre. An investigation on olefins/ paraffins separation problem revealed the same trends (Lei et al. 2006, 2007b). More thermodynamic data is needed

for a better understanding of the effect of structure on the extracting capacities for other types of ionic liquids and separation problems.

Table 2-3: Literature selectivity S_{12}^{∞} and capacity k_2^{∞} data at infinite dilution of selected ionic liquids, NMP and sulfolane for different separation problems at T = 313.15 K.

Solvent	S_{12}^{∞} **for Hexane/Benzene**	S_{12}^{∞} **for Cyclohex. /Benz.**	k_2^{∞}	**Reference**
[BMIM][SCN]	84.55	23.90	0.46	Domańska and Laskowska (2009)
[EMIM][SCN]	78.41	28.37	0.29	Domańska and Marciniak (2008b)
[EMIM][BF_4]	45.87	20.06	0.41	Foco et al. (2006)
[BMPy][BF_4]	36.88	-	0.61	Heintz et al. (2001)
[MMIM][$CH_3OC_2H_4SO_4$]	-	25.45	0.23	Kato and Gmehling (2004)
[BMIM][$MDEGSO_4$]	33.66	15.35	0.50	Letcher et al. (2005a)
[MMIM][BTI]	27.26	-	0.74	Krummen et al. (2002)
[MMIM][$(CH_3)_2PO_4$]	-	13.13	0.28	Kato and Gmehling (2004)
[BMIM][TFA]	27.00	12.96	0.36	Domańska and Marciniak (2007)
[EMIM][Et-SO_4]	25.77	11.11	0.34	Sumartschenkowa et al. (2006)
[Et_3S][BTI]	25.10	12.76	0.90	Domańska and Marciniak (2009)
Sulfolane	18.20	9.84	0.43	Möllmann et al. (1997)
NMP+6 %(w/w)H_2O	16.08	9.07	0.52	Krummen et al. (2004)
[BMPyrr][BTI]	15.47	-	1.16	Kato and Gmehling (2005b)
[MMIM][Me-SO_4]	14.33	17.55	0.15	Kato and Gmehling (2004)
NMP + 3 %(w/w)H_2O	13.79	10.00	0.71	Krummen et al. (2004)
NMP	11.49	7.72	0.99	Krummen et al. (2004)
[Py][[$C_2H_5OC_2H_4SO_4$]	11.18	8.47	0.26	Kato and Gmehling (2004)
[$3C_4C_1P$][Me-SO_4]	9.90	5.50	1.00	Letcher and Reddy (2007)
[BMPyr][TOS]	9.65	5.54	0.25	Letcher et al. (2009)
[MOIM][Cl]	8.71	5.40	0.56	David et al. (2003)
[MOIM][$MDEGSO_4$]	8.69	4.99	0.73	Deenadayalu et al. (2006)
[BMIM][Oc-SO_4]	5.27	3.49	0.69	Letcher et al. (2005b)
[$3C_6C_{14}P$][$(C_8H_{17})_2PO_2$]	1.52	1.125	2.08	Letcher et al. (2008)

2.1.7. Barriers to the commercial use of ionic liquids

In December 2002, Chemical vision 2020 Technology partnership (Ford et al. 2004), an american industry-led organization appointed a task force to reflect on the barriers to the widespread use of ionic liquids and how to overcome them. Two years later, the vision 2020 ionic liquid task force (Ford et al. 2004) identified six barriers to the widespread use of ionic liquids in the chemical industry, including separation processes:

a) Lack of performance data under industrial conditions;

b) Lack of environmental and safety data for many ionic liquids;

c) Lack of economic benefit analyses;

d) Lack of fundamental understanding of compositional structure versus performance;

e) Ionic liquid manufacturing cost and scale-up;

f) Institutional issues such intellectual property and communication between researchers.

Seven years later, these obstacles still stand on the promising way leading to a wide scale incorporation of ionic liquids in chemical engineering processes. The present study falls under the fourth barrier.

2.1.8. Fluorinated ionic liquids (FILs)

For apparently unknown reasons, Fluoroanions and fluorocations ionic liquids are often respectively referred to as fluorous and fluorinated ionic liquids (Heitzman et al. 2006). Interesting reviews on fluorinated ionic liquids discuss specific features of this subset of ionic liquids (Xue et al. 2006 and Hagiwara and Ito 2000). Ionic liquids with fluorine-containing anions are the most commercially available and the most investigated as potential separation agents. Commonly found anions include $[BF_4]^-$, $[PF_6]^-$, $[CF_3SO_3]^-$, $[(CF_3SO_2)_2N]^-$, $[CF_3CO_2]^-$ and $[SbF_6]^-$. Fluorine-containing ionic liquids are of great interest for South Africa. Its government launched recently the Fluorochemical Expansion Initiative aimed at researching and developing South Africa's fluorinated products. The move is expected to put an end to the paradox pointed out by Prof. Deresh Ramjugernath[1], the South Africa's Research Chair in Fluorine process engineering and separation technology in these terms: "South Africa possesses the second to largest supply of Fluorspar; it currently imports all its fluorinated products." Synthesizing FILs at reasonable costs is therefore a possibility in this country. First direct measurements of IDACs in a fluorinated ionic liquid were reported by Heintz et al. (2001).

[1]http://www.caes.ukzn.ac.za/Collegeboastsnewresearchchairs, accessed 15 February 2009.

2.2. Infinite dilution activity coefficients

2.2.1. Definition

The activity coefficient γ_i of species i in a solution is defined by the following ratio:

$$\gamma_i = \frac{\hat{f}_i}{x_i f_i} \tag{2-1}$$

where, $\hat{f}_i$ is the fugacity of component i in solution, f_i its pure component fugacity and x_i, its molar fraction. Activity coefficient is also defined as the proportionality constant between the activity of a substance and its mole fraction in a given solution.

$$a_i = \gamma_i x_i \tag{2-2}$$

In the study of phase equilibria and therefore the design and optimization of separation processes, the concept of activity coefficient is used rather than activity.

2.2.2. Importance and use of infinite dilution activity coefficient data

The infinite dilution activity coefficient γ_i^{∞}, also referred to as limiting activity coefficient is the limiting value of the activity coefficient of a solute when its concentration tends towards zero. Alessi et al. (1991) defined the infinite dilution region as one where each molecule of the solute is surrounded by molecules of the solvent only. Only solute-solvent interactions take place. This can be assumed for mole fractions ranging between 10^{-7} and 10^{-4}, depending on components under investigation. The infinite dilution region of solutions attracted much interest for couple of reasons underlining its great importance (Raal and Mühlbauer 1998):

a) The system behavior in the very dilute regions is instrumental in obtaining high purity products;
b) The most difficult and costly stage of a separation process is the removal of the last traces of impurity;
c) The greatest departure from ideality occurs in the very dilute regions;
d) Environmental concerns are based on the very dilute regions in the gas phase which is air.

Sandler (1996) discusses theoretical and practical applications of infinite dilution activity coefficient (IDAC) values in chemical and environmental engineering. The most important ones that are related to chemical engineering are listed below:

a) Synthesis, design and optimization of separation processes;

b) Calculation of Henry's law constants;

c) Predicting the existence of an azeotrope;

d) Development of predictive methods for G^E

e) Characterization of behavior for liquid mixtures.

2.2.2.1. Synthesis, design and optimization of separation processes

Separation is a critical stage in most of chemical processes by virtue of its sensitive impact on the global cost, as well as the quality of the product. One of the most important applications of IDACs is found in separation processes. IDAC values are used in the preliminary selection of solvent in view of extractive distillation, as well as, liquid-liquid extraction (Tiegs et al. 1986). The potentially best separating agent, called entrainer, is the one allowing the highest selectivity and capacity values. In other words, when solvents are investigated to find out the most suitable separating agent for a mixture containing two components i and j , their respective IDAC values in each solvent are determined. Equation (2-3) is then used to calculate the selectivity at infinite dilution β_{ij}^{∞} of each solvent with respect to the i/j system.

$$\beta_{ij}^{\infty} = \frac{\gamma_{is}^{\infty}}{\gamma_{js}^{\infty}} \tag{2-3}$$

γ_{is}^{∞} and γ_{js}^{∞} represent the limiting activity coefficients of i and j respectively in the solvent, s . β_{ij}^{∞} is the limiting selectivity of solvent s for the system consisting of components i and j . Thus, selectivity values at infinite dilution are important for a preliminary selection of an entrainer. A second quantity to look at is the solvent capacity at infinite dilution, k_j^{∞} which is numerically the maximum amount of species j that can be dissolved in the solvent.

$$k_j^{\infty} = \frac{1}{\gamma_j^{\infty}} \tag{2-4}$$

Additionally, capacity reveals how much solvent is used during the separation process. The greater the solvent capacity, the smaller the amount of solvent used. In principle, the solvent to use as separating agent is supposed to have the greatest value of both selectivity and capacity. But in practice, a compromise is to be found, since these two quantities are in inverse variation with respect to one another. A criterion that incorporates both selectivity and capacity together

is called performance index, $\boldsymbol{PI}$ given by the product of these properties (Kumar and Banerjee 2009). Thus, at infinite dilution,

$$PI^{\infty} = \beta_{ij}^{\infty} . k_j^{\infty} \tag{2-5}$$

The determination of γ^{∞} permits one to evaluate the potential use of solvents. Therefore, it serves as a preselection criterion. Other criteria (Lydersen 1983) leading to the definitive choice of a solvent include: recoverability, distribution coefficient, solvent solubility, density, interfacial tension, viscosity, cost, corrosiveness, non-flammability, low toxicity, etc.

2.2.2.2. Calculation of Henry's law constants

There is a relationship between the Henry's law constant of a solute i in a solvent and its limiting activity coefficient:

$$\gamma_i^{\infty} = \frac{H_i}{P_i^*} \tag{2-6}$$

H_i represents the Henry's law constant for solute *i* in the solvent and P_i^* is the vapour pressure of solute *i* at the temperature for which the IDAC is determined. Equation (2-6) shows that Henry's law constants can be found through IDAC values. In cases where the temperature of the system is above the critical temperature of the solute, the Henry's law constant, rather than the IDAC is useful (Eike et al. 2004). Design calculations for gas separation applications commonly involve the use of Henry's law constants.

2.2.2.3. Predicting the existence of an azeotrope

Conditions for the occurrence of an azeotrope in binary systems can be established using infinite dilution activity coefficient data (Gmehling and Möllmann 1998). For a system showing positive deviation from Raoult's law, an azeotrope with a temperature-minimum (pressure-maximum) takes place when

$$\ln \gamma_j^{\infty} > \frac{\ln P_i^{sat}}{\ln P_j^{sat}} > \ln \gamma_i^{\infty} \tag{2-7}$$

For a system exhibiting negative deviation from Raoult's law, an azeotrope with a temperature-maximum (pressure-minimum) takes place when:

$$\ln \gamma_j^{\infty} < \frac{\ln P_i^{sat}}{\ln P_j^{sat}} < \ln \gamma_i^{\infty} \quad (2\text{-}8)$$

From equations 2-7 and 2-8, it obviously appears that the knowledge of the IDAC values can help in predicting conditions leading to an azeotropic mixture.

2.2.2.4. Development of predictive methods for G^E

Values of infinite dilution activity coefficient are important for the development of new thermodynamic models, the adjustment of parameters, as well as the expansion of the applicability for the existing group contribution models (Gmehling 2003 and Nebig et al. 2009). With the aid of an appropriate correlation, one can use infinite dilution activity coefficient values to come up with VLE data in the intermediate concentration range. Additionally, it is recommended to fit group interaction parameters simultaneously to all available VLE, LLE and infinite dilution activity coefficient experimental data (Weidlich and Gmehling 1987).

2.2.2.5. Characterization of behavior for liquid mixtures

The infinite dilution activity coefficient value is an indication of the nature of interactions between solute and solvent molecules (McMillan and Mayer 1945). A high IDAC value is synonymous of weak solute-solvent interactions i.e. low solubility (Cheong 2003). The IDAC value is also a limiting measurement of the nonideality (Bao and Han 1995) of a solution. For an ideal system, $\gamma_i^{\infty} = 1$ whereas a departure from ideality corresponds to IDAC values greater or smaller than unity.

2.2.3. Temperature dependence of activity coefficient

The Gibbs-Helmholtz equation (2-9) depicts the effect of temperature change on activity coefficient.

$$\left[\frac{\partial\left(G^E / RT\right)}{\partial T}\right]_{P,x} = -\frac{H^E}{RT^2} \quad (2\text{-}9)$$

This leads to the following significant relations:

$$\left(\frac{\partial \ln \gamma_i}{\partial T}\right)_{P,x} = -\frac{H_i^E}{RT^2} \quad (2\text{-}10)$$

$$\left(\frac{\partial \ln \gamma_i^{\infty}}{\partial(1/T)}\right)_{P,x} = \frac{H_i^{E,\infty}}{R} \tag{2-11}$$

Using experimental γ^{∞} data, the partial excess enthalpy at infinite dilution for a given solute *i*, $H_i^{E,\infty}$ can be directly obtained from the slope of a straight line derived from equation (2-11), where R is the gas constant. It only takes an approximation of experimental γ_i^{∞} values by the linear regression,

$$\ln \gamma_i^{\infty} = A + \frac{B}{T} \tag{2-12}$$

This procedure is widely used in the experimental section of this thesis.

2.2.4. Predictive activity coefficient models

Predictive thermodynamic models are very important in separation processes (Lei et al. 2008) as they allow:

a) A rapid solvent selection at reduced costs (Novak et al. 1987);
b) Accessing data that are difficult or impossible to obtain experimentally;
c) The development of process simulators (Gmehling 2003).

It is beyond the scope of this study to review all the thermodynamic models used to predict infinite dilution activity coefficients. Only the most promising models used for systems involving ionic liquids are dealt with in this section. The most successful models used by various researchers to predict activity coefficients of various solutes in ionic liquids can be classified into two categories:

a) Group contribution methods;
b) COSMO-based methods.

2.2.4.1 Group Contribution methods. (GCMs)

These methods are based on the group contribution concept which assumes that the interaction energy of a system is the sum of functional groups interaction energies, provided that groups are properly defined (Gmehling 2009). Molecules are therefore split into smaller structures called groups to which parameters are assigned. These activity coefficient models are mostly based on the relationship between the latter and the excess free energy.

The ASOG (Analytical Solution of Group) Model

The ASOG (Analytical Solution of Group) model was developed by Derr and Deal (1969) who exploited previous works by Wilson and Deal (1962). It was redefined by Kojima and Tochigi (1979) who modified several parameters in order to account for the effect of temperature changes. In this method, the expression of the activity coefficient is composed of two parts: the size contribution term and the group interaction one. Go et al. (2007) used the ASOG model to correlate experimental infinite dilution activity coefficient data of n-octane, n-nonane and n-decane in the ionic liquid 4-methyl-*n*-butylpyridinium tetrafluoroborate in the temperature range from 297 to 344 K. Their results were in good agreement with the experimental measurements. Twelve interaction parameters related to three structural groups, $CH_{2,}$ pyridinium and BF_4 were determined.

The UNIFAC model and its modifications

After its publication by Fredenslund et al. (1975), the UNIFAC (Uniquac Quasi-Chemical Functional Activity Coefficient) underwent a plethora of revisions and extensions which are outlined in reviews by Lei et al. (2008) and Castells et al. (1999).

The original UNIFAC, as stated by Lohmann and Gmehling (2001), presented the following advantages:

a) Availability through commercial processes simulators;
b) Reliability in predicting VLE results;
c) Applicability over a wide range of mixtures.

The same authors highlight its weaknesses as follows:

a) Incorrect description of the temperature-dependence of the activity coefficient and other related properties;
b) Unsatisfactory results when predicting properties in the dilute region, as well as for asymmetric systems.

In an attempt to remedy these limitations, more advanced versions of the UNIFAC model were developed, the most important ones being UNIFAC (Dortmund) by Weidlich and Gmehling (1987) and UNIFAC (Lynby) by Larsen et al. (1987). The modified UNIFAC (Dortmund) differs from the original UNIFAC model in that it uses a different combinatorial part and it reliably takes into account the temperature dependence of group interaction parameters. Its developers introduced new van der Waals quantities as well. No thermodynamic model can claim as much popularity as UNIFAC (Do). This is attributed to the amount of research work and publications related to it in the last twenty years. Moreover, around fifty companies and

institutions work actively in the UNIFAC Consortium to support directly or indirectly its perfections. The Thermodynamics Research Unit, at the University of KwaZulu-Natal is part of this organization. Successes recorded in improving the predictability of properties using UNIFAC (Dortmund) are presented in publications by Gmehling and Schiller (1993), Hansen et al. (1991), Gmehling (1995), Gmehling et al.(1998), Gmehling et al.(2002), Gmehling et al.(2009), Lohmann and Gmehling (2001), Wittig et al.(2001) and Jakob et al. (2006). Recently, Prof. Gmehling's group started to assess the predictive ability of UNIFAC (Do) for systems involving ionic liquids. The parameter matrix of this model has been expanded, allowing for the prediction of infinite dilution activity coefficients of:

a) n-alkanes and alk-1-enes in [BMPyr] [BTI], [HMPyr] [BTI] and [OMPyr] [BTI] (Nebig et al. 2009);
b) Methylcyclohexane and toluene in [HMIM] [BTI] (Liebert et al. 2008);
c) n-alkanes, benzene and toluene in [MMIM] [BTI] [BMIM] [BTI] [HMIM] [BTI], as well as benzene and toluene in [BMIM] [BTI] (Nebig et al. 2007);
d) n-alkanes, alk-1-enes, cycloalkanes, cycloalkenes, aromatics, alcohols, ketones, esters, ethers and water in [HMIM][BTI], [OMIM][BTI], [BMPyr][BTI];
e) The binary mixture of [BMIM] [BTI] and [EMIM] [BTI] (50:50 weight percent) (Kato and Gmehling 2005b).

It is clear that the parameter matrix remains very limited when one looks at the number of ions involved in the structure of ionic liquids. The major weakness of GCMs is their inability to deal with isomers, proximity effects and systems involving groups for which experimental data have never been compiled (Putnam et al. 2004).

2.2.4.2. COSMO-based methods

The conductor–like screening model (COSMO) is a predictive method for thermophysical properties using a quantum chemical approach. Its two most widely used variants for infinite dilution activity coefficients in ionic liquids are COSMO-RS (The conductor–like screening model for real solvents), developed by Klamt (1995) and COSMO-SAC (The conductor–like screening model, solvation activity coefficients) (Lin and Sandler 2002). These two models involve statistical thermodynamics, along with quantum chemical calculation (Eckert and Klamt 2003). They require σ -profiles of molecules in the same manner as group contribution methods rely on group interaction parameters. A σ -profile is defined by Klamt and Eckert (2000) as "a distribution function of the amount of surface having a screening charge density between σ and $\sigma + d\sigma$". COSMO-based models are parameterized for 9 elements so far: hydrogen, carbon, nitrogen, oxygen, fluorine, chlorine, bromine, iodine and sulfur. They rely on a very small

number of parameters (Eckert and Klamt 2003) which are not specific regarding molecules types or functional groups. This represents a great advantage as compared to GCMs which involve a large number of functional groups. Even components that have never been synthesized before can be studied since no experimental data are needed to carry out predictions as shown by Klamt et al. (1998). Long computation time and high computation costs are the major disadvantages of these COSMO-based models. In a paper discussing comparisons between COSMO-RS and GCMs, Grensemann and Gmehling (2005), taking into account another article to which Klamt himself contributed (Putnam et al. 2004) reveal the following:

a) COSMO-RS achieves poor results in the applicability limits of GCM's, more especially, UNIFAC (Do);

b) COSMO-RS is advisable in cases of unknown GCMs parameters, isomer and proximity effects.

This paper prompted a strong reaction from the developer of COSMO-RS (Klamt 2005) who found its conclusions biased in order to clearly favour the Modified UNIFAC (Do). From a neutral point of view, more time is required to confirm whether COSMO-RS is inferior or superior to GCMs (Klamt and Eckert 2008). More importantly, extensions are under way to improve both models. Infinite dilution activity coefficients of a large spectrum of solutes in some ionic liquids have been predicted using COSMO-RS. In a study on the removal of thiophene from diesel oil (Kumar and Banerjee 2009), COSMO-RS predictions of infinite dilution activity coefficient of alkanes, alk-1-enes and cycloalkanes in [HMIM] [PF_6], [HMIM] [BF_4], [MOIM] [Cl] and [EMIM] [Tf_2N] are reported. The average absolute deviation of their predictions was found to be 12% with respect to experimental data. Larger errors are observed in a quantum chemical approach work by Sumon (2005) when predicting γ_i^{∞} of toluene and heptane in a large number of ionic liquids. Other similar predictive works (Banerjee and Khanna 2006, and Lei et al. 2007b) were in fair agreement with experimental measurements, exhibiting the same range of errors.

2.2.5. Experimental techniques for IDACs measurements

Various experimental methods exist for determining infinite dilution activity coefficients:

a) Gas-Liquid Chromatography (Letcher 1980);

b) Inert Gas Stripping Method (Leroi et al. 1977 and Richon et al. 1980);

c) Headspace Analysis Method (Hussam and Carr 1985);

d) Indirect Headspace Chromatography. (Li and Carr 1993);

e) Dew Point Method (Eckert and Sherman 1996);

f) Differential Static Cell Method (Alessi et al. 1986);

g) Differential Ebulliometry Method (Gautreaux and Coates 1955);
h) Rayleigh Distillation Method (Dohnal and Horakova 1991).

The two methods used in this work, are the most popular ones for ionic liquids. They are discussed here, with an emphasis on their suitability for this class of solvents. A useful review paper by Kojima et al. (1997) gives more details on other experimental techniques used for direct IDAC measurements.

2.2.5.1. Gas liquid chromatography (GLC)

In this technique, the solvent, used as stationary phase, is loaded onto the column. The solute, which is the mobile phase, is injected in a carrier gas through the column. The eluted solute is detected and its retention time, along with other experimental parameters, is used in an equation to compute the IDAC. Gas-liquid chromatography can be used for IDACs of volatile solutes in non-volatile or low volatility solvents. It is not applicable to systems involving a mixture of solvents. Table 2-4 summarizes the advantages and disadvantages of Gas-Liquid Chromatography.

Table 2-4: Advantages and disadvantages of the Gas Liquid Chromatographic method

Advantages	Disadvantages
Sample purity is not required	The method is suited to low volatility or non-volatile solvents only
The method is rapid as many solutes can be injected at once	The IDAC of the solvent in the solute cannot be determined
Reactive systems can be investigated	

2.2.5.2. The inert gas stripping technique. (IGS)

In this method, a highly dilute solute is stripped from a solution by a constant inert gas flow under isothermal conditions. The vapour leaving the cell is periodically analyzed by gas chromatography. It is observed that the peak area depicting the solute concentration in the vapour phase decreases exponentially with time. Under this particular condition of exponential dilution, the infinite dilution activity coefficient of the solute in the solvent is related to the decreasing rate of its corresponding peak area with time. The IGS method is used to measure γ^{∞} of volatile solutes in non-volatile or volatile solvents. Systems with solvent mixtures can be investigated. The method is alternatively called the dilutor technique, as well as continuous gas

extraction technique (Vitenberg 2003; Dobryakov and Vitenberg 2006). Table 2-5 presents the advantages and disadvantages of this technique.

Table 2-5: Advantages and disadvantages of the inert gas stripping method

Advantages	Disadvantages
GC calibration is not required since only peak area ratios are involved in calculations	Solutes must be purified.
A mixture of solvents can be investigated.	Low volatility solutes are difficult to measure.
Systems with high volatility solvents can be measured	A good gas-liquid contact is critical to obtain reliable results.
Many solutes can be investigated at once	

2.3. Advances in the design of IGS equipment

2.3.1. Major developments in the use of the IGSM

Since its establishment by Leroi et al. (1977), the IGSM underwent some improvements in terms of modernization of the analytical tool (GC), temperature and pressure sensors, achievement of isothermal conditions during experiments, etc. But the most important advance in this technique lies in a better understanding of factors affecting the accuracy of measurements provided by many research works. This resulted in various cell designs in order to suit different types of systems. Bao and Han (1995) sum up the major advances in the inert gas stripping technique as follows:

a) Establishment of the IGS technique by Leroi et al. (1977);
b) Correction by Duhem and Vidal (1978) for the liquid concentration of the solute by taking into account its partition between the two phases in the dilutor cell;
c) Modification of the dilutor cell structure by Richon and coworkers (Richon et al. 1980 and Richon and Renon 1980);
d) Use of the two-cell technique in order to investigate low boiling solvents. (Doležal et al. 1981, and Doležal and Holub 1985);
e) Extension of the technique to viscous or foaming systems by Richon et al. (1985);
f) Further extension to mixtures containing food or oil (Lebert and Richon 1984a, b).

More recent developments involve the liquid analysis gas stripping method (Hradetzky et al. 1990), the use of the inert gas stripping technique for systems with ionic liquids (Krummen et al. 2002) and its extension to more delicate solvents of environmental interest involving semi-volatile and surface tension solutes (Kutsuna and Hori 2008).

2.3.2. The number of cells required for IDAC measurements

Either one or two cells can be used to measure infinite dilution activity coefficients by the inert gas stripping method. The single cell technique is suitable for systems with low volatility solvents and relatively high volatility solutes. The double cell technique is required when the solvent is a high volatile compound or mixture. In this variant, a presaturation cell is used to saturate the stripping gas with the solvent before the solute stripping process. This prevents any transfer of the solvent from the liquid to the vapour phase which would lead to changes of the amount of solvent in the dilutor cell. The single cell technique is appropriate to systems involving ionic liquids since they are generally very high boiling compounds and non volatile. Krummen et al. (2002) reported infinite dilution activity coefficient data for n-alkanes and alk-1-enes, cyclic hydrocarbons, aromatic hydrocarbons, ketones, alcohols, and water in the ionic liquids 1-methyl-3-methylimidazolium bis (trifluoromethylsulfonyl) imide, 1-ethyl-3-methylimidazolium bis (trifluoromethyl sulfonyl) imide, 1-butyl-3-methylimidazolium bis (trifluoromethylsulfonyl) imide, and 1-ethyl-3-methylimidazolium ethylsulfate in the temperature range between 293.15 K and 333.15 K. Activity coefficients at infinite dilution of alkanols in the ionic liquids 1-butyl-3-methylimidazolium hexafluorophosphate, 1-butyl-3-methylimidazolium methylsulfate, [BMIM][$MeSO_4$], and 1-hexyl-3-methylimidazolium bis(trifluoromethylsulfonyl) imide, [HMIM][Tf_2N], were measured by Dobryakov et al (2008). Using the same method, Nebig et al. (2009) determined γ_i^∞ for n-alkanes and alk-1-enes in the ionic liquids 1-butyl-1-methylpyrrolidinium bis (trifluoromethylsulfonyl) imide, 1-hexyl-1-methyl pyrrolidinium bis (trifluoromethylsulfonyl) imide and 1-methyl-1-octylpyrrolidinium bis (trifluoromethylsulfonyl) imide. Kato and Gmehling (2005a, b) presented infinite dilution activity coefficient data for seven solutes in the ionic liquids 1-butyl-3-methylimidazolium bis (trifluoromethylsulfonyl) imide and 1-ethyl-3-methylimidazolium bis (trifluoromethylsulfonyl) imide using the methods of gas liquid chromatography and the inert gas stripping technique. Their results show a good agreement between the two methods.

2.3.3. Cell design parameters

Thermodynamic equilibrium between the gas leaving the dilutor cell and the remaining liquid is instrumental in obtaining accurate infinite dilution activity coefficient data.To achieve this, three conditions must be met (Leroi et al. 1977):

a) Large total mass transfer area;
b) Sufficiently long contact time;
c) Good dispersion of bubbles in the liquid.

Studies mentioned in the two previous sections threw light on these factors which affect the performance of the IGSM:

a) Dispersion device;
b) Bubble rise height;
c) Stripping gas flow rate;
d) Bubble size;
e) Liquid viscosity;
f) Range of IDACs to be measured.

For accurate measurements of IDAC, it is essential to take into account these factors when designing dilutor cells. The impact of each of these parameters is briefly explained in the light of expressions derived by Richon et al. (1980) which are reviewed in Chapter 3 of this thesis.

2.3.3.1. Dispersion device

In the original version of the method by Leroi et al (1977) (See Figure 2-2), a fine porosity fritted glass was used as dispersion device. Recently constructed dilutor cells are generally provided with stainless steel capillaries with very small inner diameters. Stainless steel is known as a non corrosive material. To ensure that the total mass transfer area is large, the inert gas, generally helium or nitrogen, is dispersed into very small bubbles. Capillaries must be in reasonable number and well spaced to avoid any bubble coalescence. Dobryakov et al. (2008) designed a very small cell, of volume 5 cm^3, with just a single capillary tube used as the dispersion device.

2.3.3.2. Bubble rise height

The liquid level in the cell must be high enough for sufficient contact time between the bubbles and the investigated solution. This is a very important condition in view of attaining the required thermodynamic equilibrium.

2.3.3.3. Stripping gas flow rate

Efficient solute mass transfer from the liquid phase to the gaseous phase requires low inert gas flow rates as this results in longer contact times. The optimum flow rate depends on the system under investigation. It has been shown that when thermodynamic equilibrium has been attained between the two phases inside the dilutor cell, measured infinite dilution activity coefficients do not depend on the flow rate value. Additionally, the size of bubbles is affected by the flow rate, increasing up when the flow rate is increased. In previous works, experiments were performed with inert gas flow rates ranging between some tenths to tens of cm^3 (Kutsuna and Hori 2008, and Krummen et al. 2002)

2.3.3.4. Bubble size

The smaller the bubble size, the more efficient is the mass transfer. In effect, when the inert gas is dispersed into the solution as small bubbles, the total mass transfer area is increased. If bigger bubbles are used, the height of the cell must be high enough to ensure a long residence time of the gaseous phase in the solution.

2.3.3.5. Liquid viscosity

A high viscosity hinders mass transfer. Its other effect consists of reducing the bubble rise and consequently allowing larger contact times. The two effects with regards to mass transfer and equilibrium conditions in the cell compensate each other. However, more sophisticated features need to be incorporated in the design of the dilutor cell, more especially its stirrer, for very viscous mixtures (Richon et al. 1985).

2.3.3.6. Range of IDACs to be measured

When very high infinite dilution activity coefficient values have to be measured, large amounts of solute are stripped out of the solution in a very short period of time, since there are very weak interactions between the components involved in the mixture. If care is not taken, this will compromise the attainment of equilibrium and reduce the mass transfer extent as the contact time may be insufficient. It is not therefore surprising that the worst agreement between infinite dilution activity coefficient data obtained with the GLC method and the dilutor technique were observed for very high activity coefficients (Leroi et al. 1977). The designer should take into account the range of IDACs values the cell is supposed to deal with in order to tune other parameters such as the height and the dispersion device.

2.3.4. Review of previous equilibrium cells

Various cell designs have been reported over the last forty years as part of the inert gas stripping set up for the determination of infinite dilution activity coefficient, Henry's law constant and partition coefficient. The most efficient ones, taken from the open literature are reviewed. The various researchers who designed the cells discussed in this section reported a good agreement with infinite dilution activity coefficient data obtained by the GC method. And, reproducibilities better than 2% were obtained. However, the reliability seemed to be compromised when very high γ_i^{∞} values had to be measured. The other issue of concern is the determination of γ_i^{∞} in viscous mixtures.

2.3.4.1. Leroi et al. (1977)

Leroi et al. (1977) used the pyrex glass cell represented in figure 2-2 to measure infinite dilution activity coefficient for n-hexane and benzene in ten different nonvolatile solvents, including N-methyl-2-pyrrolidone (NMP), dimethylsulfoxide (DMSO), dimethylformamide (DMF), nitrobenzene, ethylene glycol and hexadecane. A solution of volume 25 cm^3 could be accommodated by the still and an experiment lasted one to two hours. Solutes were introduced into the cell by means of a 10 μl syringe via the septum. Inert gas flow rates ranged from 50 to 150 $cm^3 .min^{-1}$. To ensure accurate measurements, liquid drop entrainment was limited by a dead space above the solution. This gas phase volume was kept small enough to ensure accurate measurements. The dispersion device consisted of a fine porosity fritted glass disk as mentioned previously.

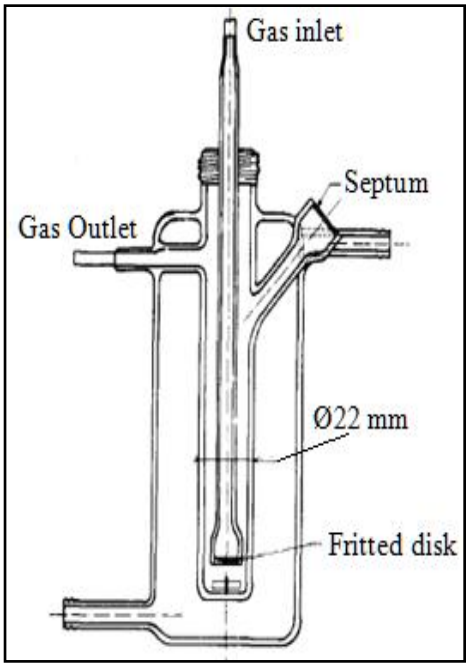

Figure 2-2: Dilutor cell constructed by Leroi et al. (1977)

2.3.4.2 Richon et al. (1980)

Richon et al. (1980) designed the dilutor cell shown in figure 2-3, similarly to the one constructed by Leroi et al. (1977). Their major improvements to the first cell include the following features:

a) Equal sized bubbles are introduced from the bottom by means of fine capillaries;
b) A conical outlet gas collector is adopted to minimize liquid entrainment.

They investigated infinite dilution activity coefficients of alkanes from C_1 to C_9 in hexadecane. Experiments undertaken concluded that the inert gas stripping method could be easily extended to Henry's law constant measurements. For Henry's law constants greater than 30 atm., their work showed the necessity to keep a very small and homogeneous vapour phase in the cell.

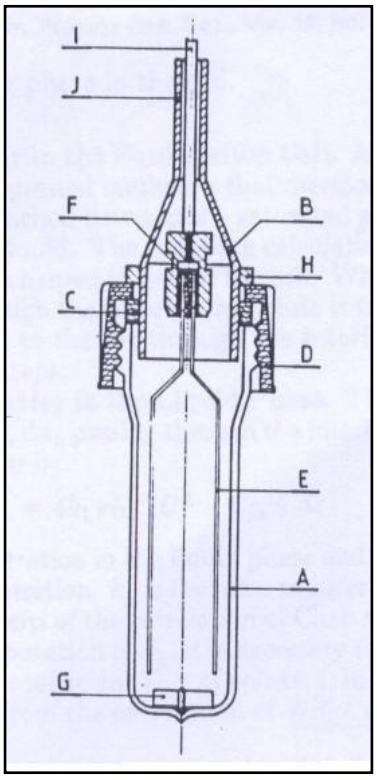

Figure 2-3: Equilibrium cell constructed by Richon et al. (1980)

A – glass still body, B – conical collector of gas outlet, C – gasket, D – plug, E – capillaries, F – Teflon seal, G – magnetic stirrer, H – metallic ring used to adjust the depth of the conical collector B in the still, I – tube for carrier gas inlet, J – gas outlet.

2.3.4.3. Richon and Renon (1980)

In this design, Richon and Renon (1980) abandoned the previous conical shape in favour of a simpler shape as shown in figure 2-4. A considerably reduced 1 cm high gas phase is kept above the solution inside the dilutor cell. Their cell was used to determine infinite dilution activity coefficients of light hydrocarbons in n-hexadecane, n-octadecane and 2, 2, 4, 4, 6, 8, 8-heptamethylnonane.

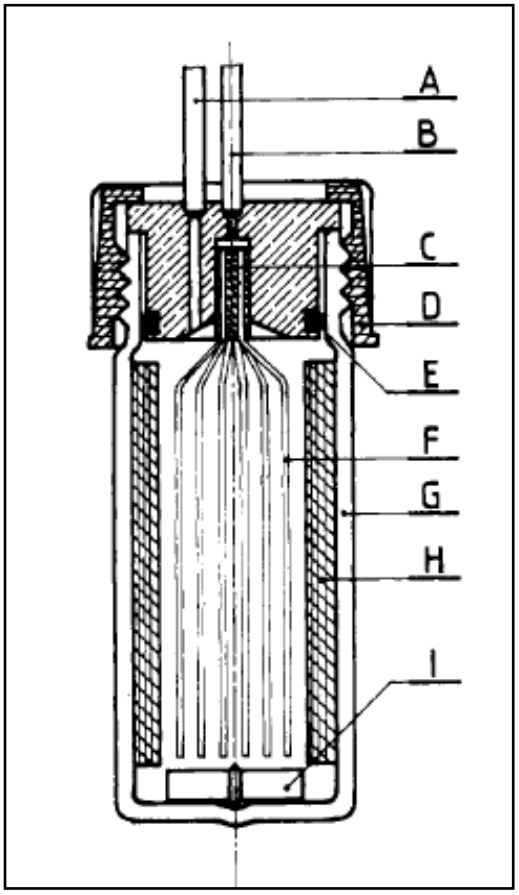

Figure 2-4: Dilutor cell used by Richon and Renon (1980).
A – vapour phase outlet, B – inert gas inlet, C – Teflon seal, D – plug, E - O-ring, F – capillaries, G – glass still body, H – baffles, I –magnetic stirrer.

2.3.4.4. Legret et al. (1983)

Legret et al. (1983) used the cell below (figure 2-5) to determine partition coefficients which are related to activity coefficients at infinite dilution. Their study involved some alkanes as solutes in the methane/n-decane system. The pre-saturator and the dilutor cell were fitted with 20 and 50 capillaries respectively. The capillary inner diameter was 0.3 mm for the pre-saturation cell and 0.1 mm for the dilutor cell. Both cells contained 40 cm^3 of solvent.

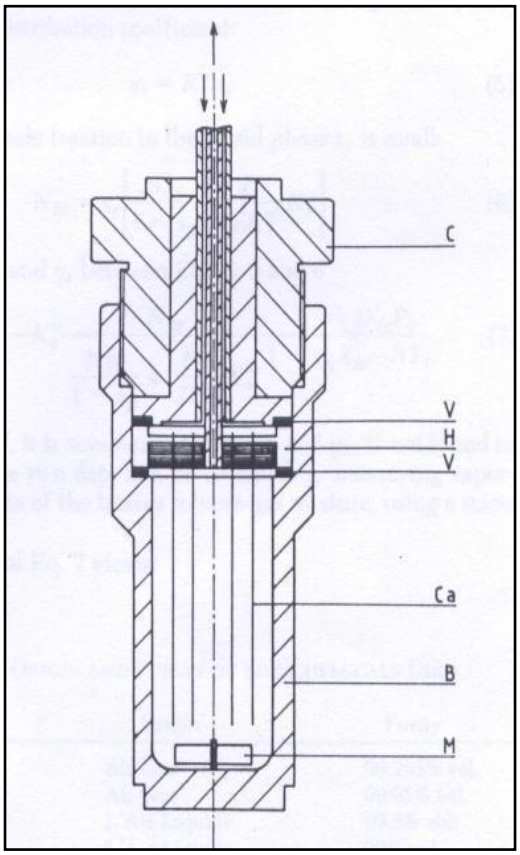

Figure 2-5: Dilutor cell design by Legret et al. (1983)

B – body, C – cap, Ca – capillaries, H – capillary holder, M – magnet, V – "O"-ring

2.3.4.5. Richon et al. (1985)

Richon et al. (1985) designed the cell presented in figure 2-6 in order to extend the use of the inert gas stripping technique to foaming and viscous mixtures. Examples of these are aqueous mixtures of glucides, polyols and proteins whose viscosities can be as high as 1000 cP. Since a magnetic stirrer would be inefficient due to high viscosity, the mixture is circulated inside the internal cylinder from top to bottom, by means of an Archimedes screw that is maintained by two pivots and activated by a permanent magnet. A special device is used to break foams without disturbing phase equilibrium inside the cell. The cell is provided with a bladed screw which prevents liquid rotation in the cell and promotes the coalescence of gas bubbles.

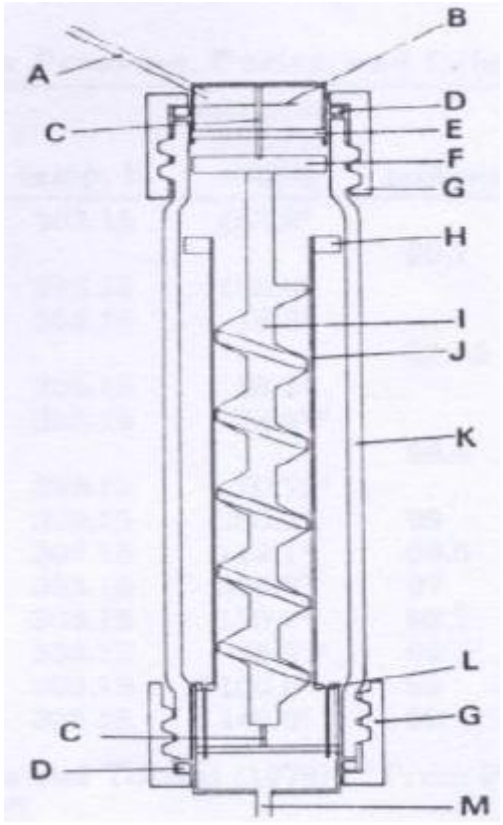

Figure 2-6: Dilutor cell designed by Richon et al. (1985) for viscous and foaming mixtures. A – vapour phase outlet, B – deflector, C – pivot, D – gasket, E – foam-breaking device, F – permanent magnet, G – plug, H – bladed screw, I – Archimedes screw, J – internal cylinder, K – dilutor cell, L – carrier gas capillary injectors and M – carrier gas inlet.

2.3.4.6. Bao et al. (1994)

In the design given in figure 2-7 proposed by Bao et al. (1994), a liquid-conducting tube is placed between the capillaries and the cell body to create a countercurrent flow of circulating solution to the stripping bubbles. This is aimed at enhancing mass transfer as well as making the stripping process more efficient. Bao et al. (1994) used stainless steel capillary tubes of 0.1 mm inner diameter as dispersion device.

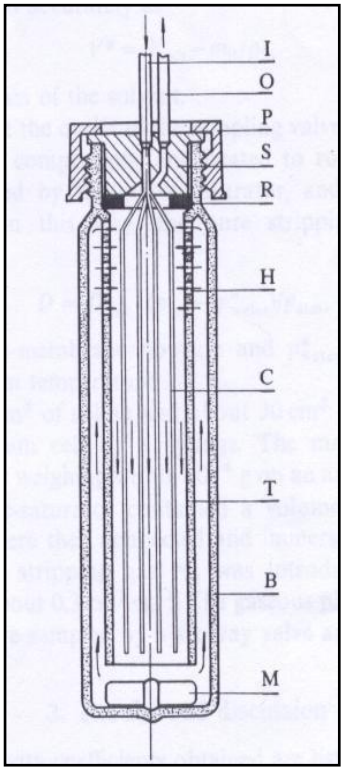

Figure 2-7: Equilibrium cell designed by Bao et al. (1994).
B – Body, C – capillaries, H – small holes, I – inert gas inlet, M – magnet, O – vapour phase outlet, P – plug, R – O-ring, S-seal, T – liquid-conducting tube.

2.3.4.7. Hovorka and Dohnal (1997)

As shown in figure 2-8, Hovorka and Dohnal (1997) designed an all-glass jacketed device accommodating both the pre-saturator and the dilutor cell. The pre-saturation compartment is divided by fritted glass disks into plates in order to allow efficient saturation of the inert gas with the solvent vapour, yet maintaining a small pressure drop across it. The saturated inert gas is dispersed in small bubbles into the diluted solution through a fine porosity fritted glass tip. Liquid droplet entrainment is prevented by the vapour space of the cell and a special design of the gas outlet. Their set up allowed measuring infinite dilution activity coefficients in the range from 230 to 70000.

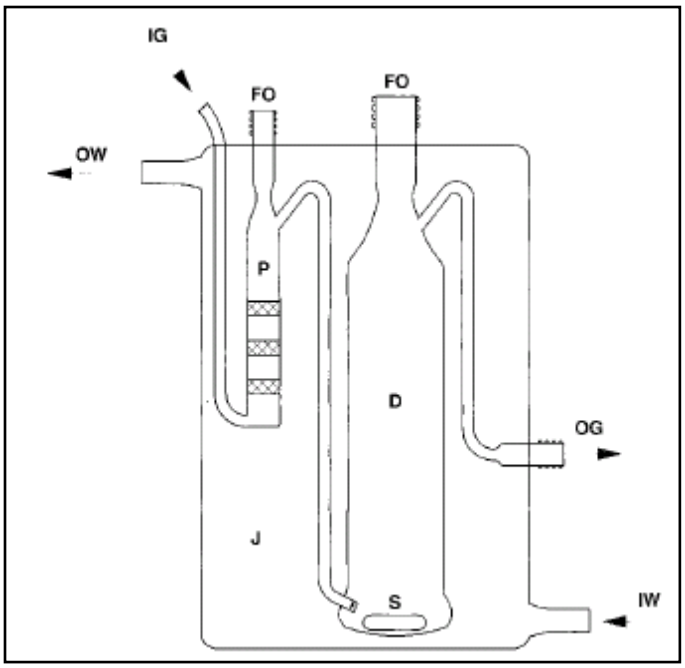

Figure 2-8: Equilibrium cell designed by Hovorka et al. (1997).

P – Pre-saturator with fritted glass disks, D – dilutor cell, S – stirrer, J – thermo-statted jacket, IW – input of thermo-statted water, OW – output of thermo-statted water, IG – input of stripping gas, OG – outlet of saturated stripping gas, FO – filling openings.

2.3.4.8. Miyano et al (2003)

The cell shown in figure 2-9 was used by Miyano et al (2003) to determine Henry's law constants and the infinite dilution activity coefficients of butane, isobutane, 1-butene and isobutene in methanol from (255 to 320) K. A counter flow of liquid against the rising bubbles is achieved in the inner tube of the cell to increase the contact time. They used a maximum inert gas flow rate of 2 cm^3. min^{-1}.

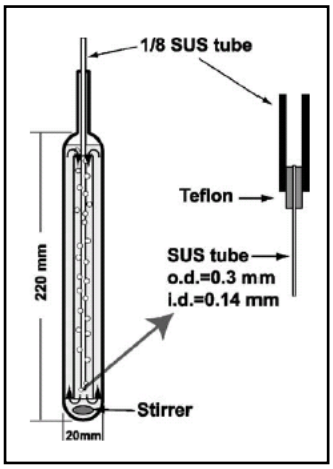

Figure 2-9: Equilibrium cell designed by Miyano et al. (2003) for the determination of Henry's law constants using the dilutor technique.

2.3.4.9. Dobryakov et al. (2008)

In order to investigate infinite dilution activity coefficient of alcohols in three different ionic liquids, Dobryakov et al. (2008) constructed a 5 cm^3 dilutor cell which was filled with 3 cm^3 of solvent during experiments. Their still which is shown in figure 2-10 used a single capillary tube plumbed in at the bottom as a dispersion device. Measurements were done with inert flow rates between 8 and 20 cm^3. min^{-1}.

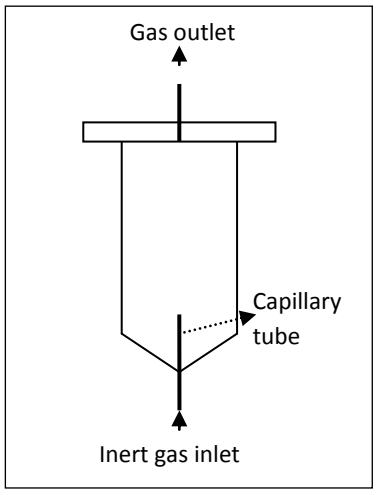

Figure 2-10: Dilutor cell designed by Dobryakov et al. (2008).

2.3.4.10. Kutsuna and Hori (2008)

Drawing inspiration from previous work by Lei et al (2007a) and Shunthirasingham et al. (2007), which established that the IGSM led to inaccurate Henry's law constants in case of semi-volatile and surface active solutes, particularly when small gas bubbles such as those with < 1 mm in radius were used, Kutsuna and Hori (2008) proposed the design shown in figure 2-11 and photograph 2-1. They determined Henry's law constants of perfluorooctanic acid (PFOA) in aqueous sodium chloride and sulfuric acid mixtures. To deal with semi-volatile and surface active solutes, their design incorporated a helical plate that increased the residence time. In addition, the dispersion device allows the formation of larger bubbles. Kutsuna and Hori performed experiments with 300 cm^3 of solvent in the dilutor cell, achieving a residence time of 15 seconds and using bubbles larger than 3 mm in radius and an inert gas flow rated as high as 80 $cm^3. min^{-1}$. Photograph 2-1 shows bubbles rising up along the underside of the glass helix from the bottom to the top of the solution placed in the cell.

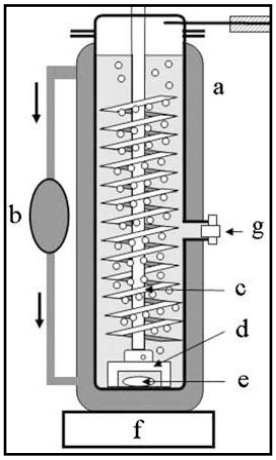

Figure 2-11: The dilutor cell designed by Kutsuna and Hori (2008).

a- Jacketed Duran glass column; b- Temperature-controlled water circulator; c- Gas-introduction tube with a glass helix; d- Polytetrafluoroethylene support; e- Magnetic bar; F-magnetic stirrer; g- Sampling port for injection.

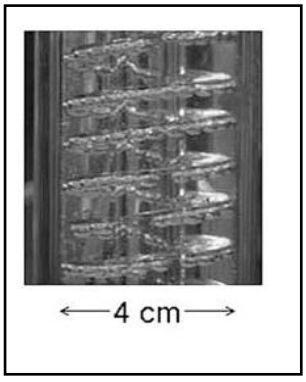

Photograph 2-1: The helical plate used in the dilutor cell designed by Kutsuna and Hori (2008).

CHAPTER THREE: THEORETICAL CONSIDERATIONS

Chapter overview

The theory and equations used to compute infinite dilution activity coefficients by two selected methods are presented. Where necessary, enough details on derivation procedures are provided. Assumptions leading to the derivation of these mathematical relationships are highlighted. They determine the reliability of the experimentally generated data. The modeling of mass transfer in the dilutor cell, as presented in the literature, is reviewed. It represents an important basis on which the dilutor cell constructed for this work was designed.

3.1. Gas liquid chromatography

Gas liquid chromatography is a well established method for determining infinite dilution activity coefficient of volatile solutes in nonvolatile solvents (Letcher 1980). It is logically used in this study of ionic liquids which are generally known as high boiling solvents. Equations involved in IDAC's computations, discussed by Letcher (1980) as well as Condor and Young (1979) and used in this work are given below. As the solute (1) moves through the column, it is assumed that:

- The mobile or gas phase is an ideal mixture composed of the carrier gas (2) and the solute (1);
- The stationary gas is a real liquid mixture, containing the solute and the solvent (3);
- The gas phase (mobile phase denoted as M) and the liquid phase (stationary phase, denoted as L, i.e. ionic liquid) are in thermodynamic equilibrium, well described by the modified Raoult's law.

The distribution coefficient, K_L of the solute between the two phases, according to Condor and Young (1979), is:

$$K_L = \frac{C^L}{C^M} \tag{3-1}$$

Concentration of the solute in the liquid and gas phases are given by

$$C^L = \frac{x\ n_3}{V_L} \tag{3-2}$$

and,

$$C^M = \frac{y n_2}{V_G} \tag{3-3}$$

where x and y are the mole fractions of the solute in the liquid and gas phases respectively, n_2 is the number of moles of the carrier gas in the mobile phase, n_3 is the number of moles of the solvent in the stationary phase, V_G is the volume of the gas phase and V_L is the volume of the stationary phase. From equations (3-1) through (3-3), it can be found that:

$$K_L = \frac{xn_3V_G}{yn_2V_L} \tag{3-4}$$

Taking into account the ideality of the gas phase,

$$V_G = \frac{n_2RT}{P} \tag{3-5}$$

and using modified Raoult's law, i.e.

$$yP = x\gamma_{13}^{\infty}P_1^* \tag{3-6}$$

Equation (3-4) can be written in a simplified form as:

$$K_L = \frac{n_3RT}{\gamma_{13}P_1^*V_L} \tag{3-7}$$

At mean column pressure (Laub and Peacsok 1978), the net retention volume, V_N , is related to the distribution coefficient and the volume of the stationary phase by:

$$V_N = K_L.V_L \tag{3-8}$$

When this expression is used in equation (3-7), the following equation determined by Porter et al. (1956) is obtained:

$$\gamma_{13}^{\infty} = \frac{n_3RT}{V_NP_1^*} \tag{3-9}$$

When the solute-solute and solute-carrier gas imperfections, as well as the pressure drop along the column are considered, a more accurate equation (Everett 1965, Cruickshank et al. 1966a and 1969) is derived:

$$\ln \gamma_{13}^{\infty} = \ln \frac{n_3 RT}{V_N P_1^*} - \frac{(B_{11} - v_1^*)P_1^*}{RT} + \frac{(2B_{12} - v_1^{\infty})J_2^3 P_o}{RT} \quad (3\text{-}10)$$

where $\ln \gamma_{13}^{\infty}$ is the infinite dilution activity coefficient of a solute (1) in a solvent (3), T is the column temperature, P_O is the column outlet pressure, the same as the atmospheric pressure, P_i is the column inlet pressure, $P_O J_2^3$ is the mean column pressure, P_1^*, the saturated pressure vapour of the solute at temperature *T*, v_1^* is the molar volume of the solute, v_1^{∞} is the partial molar volume at infinite dilution, equal to v_1^*, in this particular case. J_2^3 is the pressure correction term given by

$$J_2^3 = \frac{2}{3}\left[\frac{\left(\frac{P_i}{P_o}\right)^3 - 1}{\left(\frac{P_i}{P_o}\right)^2 - 1}\right] \quad (3\text{-}11)$$

V_N is the net retention volume given by

$$V_N = J_2^3 D_O (t_R - t_D) \quad (3\text{-}12)$$

D_O, the column outlet flow-rate, t_R the retention time for the solute and t_D is the inert gas retention time.

The second virial coefficients of pure solutes B_{11} were calculated using the McGlashan and Potter equation (1962).

$$B/V_C = 0.43 - 0.886(T_C/T) - 0.694(T_C/T)^2 - 0.0375(n-1)(T_C/T)^{4.5} \quad (3\text{-}13)$$

The same equation allowed the calculation of mixed virial coefficients B_{12}. Other mixed properties are determined by means of Hudson and McCourbey's (1960) mixing rules as follows:

$$T_{C12} = 128\left(T_{C11}.T_{C22}\right)^{\frac{1}{2}}\left(I_{C11}.I_{C22}\right)^{\frac{1}{2}}\left(V_{C11}.V_{C22}\right)/I_{C12} \quad (3\text{-}14)$$

$$I_{C12}.V_{C12}^2 = \left(I_{C11} + I_{C22}\right)\left(V_{C11}^{\frac{1}{3}} + V_{C22}^{\frac{1}{3}}\right)^6 \quad (3\text{-}15)$$

$$V_{C12} = \frac{1}{8}\left(V_{C11}^{\frac{1}{3}} + V_{C22}^{\frac{1}{3}}\right)^3 \quad (3\text{-}16)$$

$$n_{12} = \frac{n_1 + n_2}{2} \quad (3\text{-}17)$$

In the last four expressions, subscripts '1', '2' and '12' refer to the solute, the carrier gas and the mixture of these two components, *n* is the number of carbon atoms and is equated to one for compounds with no carbon atom. Critical properties T_C and V_C as well as the ionization energies, I_C are found in the literature (CRC Handbook 2005). Modified Rackett equation (Poling et al. 2001) gives the values of molar volumes as follows:

$$v = V_C\left(0.29056 - 0.08775\omega\right)^{\left(1-\frac{T}{T_C}\right)^{\frac{2}{7}}} \quad (3\text{-}18)$$

Saturated vapour pressures involved in equation (3-10) were calculated using the Antoine, modified Antoine or Wagner equations in compliance with the applicability range of each correlation. Constants for vapour pressure correlations which are required in equation (3-10) as well as acentric factors ω were taken from the literature (Poling et al. 2001).

3.2. Inert gas stripping method

3.2.1. Equations for IDACs computation

3.2.1.1. Equations proposed by Leroi et al. (1977)

3.2.1.1(a) General equations proposed by Leroi et al. (1977)

Leroi et al. (1977) derived basic equations to compute infinite dilution activity coefficients from the dilutor technique. The starting point of their formulation is the assumption that the two phases in the cell are in thermodynamic equilibrium. The equilibrium equations for each of the components are:

$$x_1\gamma_1 f_1^{oL^*} I_1 = y_1\varphi_1 P \quad (3\text{-}19)$$

$$x_3\gamma_3 f_3^{oL^*} I_3 = y_3\varphi_3 P \quad (3\text{-}20)$$

$$x_2 H = y_2 \varphi_2 P \tag{3-21}$$

where the subscripts refer to the solute (1), the carrier gas (2) and the solvent (3), x is the mole fraction in the liquid phase, y is the mole fraction in the vapour phase, P is the pressure, f is the fugacity, φ is the fugacity coefficient, f^{oL*} is the reference fugacity for a liquid at pure state and zero pressure, γ is the activity coefficient, H is the Henry's law constant and I is the Poynting correction given by:

$$I_i = \exp\left(\int_0^P \frac{v_i}{RT} dP\right) \tag{3-22}$$

In the above equation, v_i is the molar volume of the component i at temperature T. The reference state is the pure component at zero pressure for both solvent and solute. At low pressure, (conditions at which all the experiments in this study were carried out), the vapour phase corrections can be derived from second virial coefficients. Fugacity coefficients, which can be determined at low pressures from second virial coefficients, are used to account for the vapour phase imperfections as follows:

$$\ln \varphi_i = 2\sum_{j=1}^{n}\left(y_j B_{ij} - B_M\right)\frac{P}{RT} \tag{3-23}$$

$$B_M = \sum_i \sum_j y_i y_j B_{ij} \tag{3-24}$$

T is the system temperature, B_{ij} is the virial coefficient related to bimolecular interactions between i and j molecules, B_M is the mixed second virial coefficient at temperature T. R is the gas constant. The equation below can be used to determine reference fugacity values, f_i^{oL*} that are required in equations (3-19) and (3-20).

$$f_i^{oL*} = P_i^v \varphi_i^o\left(T, P_i^v\right)\exp\left(-\frac{v_i^{oL*} P_i^v}{RT}\right) \tag{3-25}$$

where v_i^{oL*} is the reference molar volume of liquid component i, P_i^v is the vapour pressure of component i and φ_i^o is the fugacity coefficient in the vapour phase at saturation. If the solute is considered infinitely dilute in the solvent and the carrier gas is insoluble or of negligible

solubility in the liquid phase, then the activity coefficient of the solute, γ_1 can be equated to its infinite dilution activity coefficient in the solvent (3), and both the activity coefficient of the solvent, γ_3 and its mole fraction, x_3 in the liquid phase to 1. Neglecting vapour phase imperfections, equilibrium equations (3-19) and (3-20) can be written as follows:

$$x_1 \gamma_1^{\infty} P_1^{v} = y_1 P \tag{3-26}$$

$$P_3^{v} = y_3 P \tag{3-27}$$

Amounts of solute and solvent removed from the equilibrium cell by the carrier gas flow can be calculated with the aid of these equations:

$$dn = y_1 P \frac{D_2 dt}{RT} \tag{3-28}$$

$$dN = y_3 P \frac{D_2 dt}{RT} \tag{3-29}$$

where n and N are respectively the number of moles for the solute and the solvent in the equilibrium cell at time t, dn and dN give the change in the amount of the two components with time. D_2 is the total volumetric rate of the gas phase leaving the still, converted to pressure P and temperature T. A combination of equations (3-26) through (3-29) leads to:

$$\frac{dn}{dt} = x_1 \gamma^{\infty} P_1^{v} \frac{D_2}{RT} \tag{3-30}$$

$$\frac{dN}{dt} = -P_3^{v} \frac{D_2}{RT} \tag{3-31}$$

From overall mass balance calculations around the equilibrium cell, D_2 the total volumetric rate of the gas phase leaving the still can be related to D, the pure carrier gas flow rate measured at system pressure P and system temperature T.

$$D_2 = D - \frac{RT}{P}\left(\frac{dn}{dt} + \frac{dN}{dt}\right) \tag{3-32}$$

Combining equations (3-30) through (3-32) gives:

$$D_2 = \frac{D}{1 - x_1 \gamma_1^{\infty} \frac{P_1^v}{P} - \frac{P_3^v}{P}} \tag{3-33}$$

At infinite dilution, it can be deduced that

$$x_1 = \frac{n}{n+N} \tag{3-34}$$

and

$$x_1 \cong \frac{n}{N} \tag{3-35}$$

The differential equations (3-30) and (3-31) describe the variations of the number of moles in the cell with time for both the solute and the solvent. Substituting D_2 in these two equations by equation (3-33) and replacing x_1 by (3-35) result in:

$$\frac{dn}{dt} = -\frac{n}{N} \gamma^{\infty} \frac{P_1^{sat}}{RT} \frac{D}{1 - \frac{n}{N} \gamma^{\infty} \frac{P_1^{sat}}{P} - \frac{P_3^{sat}}{P}} \tag{3-36}$$

$$\frac{dN}{dt} = \frac{P_3^{sat}}{RT} \frac{D}{1 - \frac{n}{N} \gamma^{\infty} \frac{P_1^{sat}}{P} - \frac{P_3^{sat}}{P}} \tag{3-37}$$

where P_i^{sat} is the saturated vapour pressure of component i. The last two equations have been derived using the following three assumptions:

- the vapour phase is ideal;
- The carrier gas solubility in the liquid phase is negligible;
- The solute is infinitely diluted in the solvent.

In quest of simplification, Leroi et al. (1977) added more assumptions depending on the volatility of the solvent.

3.2.1.1(b) Equation proposed by Leroi et al. (1977) for non-volatile solvents.

A non-volatile solvent is one with negligible vapour pressure equal or less than 1 mmHg (George 2008). Leroi et al. (1977) added the following assumptions with reference to equations (3-36) and (3-37):

- N is constant due to the non-volatile nature of the solvent;

- The ratio $\frac{P_3^{sat}}{P}$ is negligible with respect to 1 since the vapour pressure of the solvent is close to zero;
- The term $\frac{n}{N}\gamma^{\infty}\frac{P_1^{sat}}{P}$ is ignored due to the infinite dilution assumption.

Thus, equation (3-37) does not exist any longer whereas equation (3-36) can be written as

$$\frac{dn}{dt} = -\frac{n}{N}\gamma^{\infty}\frac{P_1^{sat}}{RT}D \tag{3-38}$$

Its solution is:

$$\ln\frac{n}{n_o} = -\frac{D}{RT}\frac{P_1^{sat}}{N}\gamma^{\infty}t \tag{3-39}$$

where n_o is the initial number of moles for the solute in the cell. During infinite dilution activity coefficient measurements, it is advisable to maintain the gas sampling valve at constant temperature and to ensure that the GC detector linearity is satisfied. If these requirements are met, the amount of the solute injected into the column given by the corresponding peak area A from the GC, will be proportional to its partial pressure over the solution y_3.

$$A = \kappa y_1 P \tag{3-40}$$

κ is the proportionality constant depending on the GC used. From equations (3-26), (3-35), (3-39) and (3-40), an equation showing an exponential decrease of the solute peak area with time can be obtained.

$$\ln\frac{A}{A_o} = \frac{D}{RT}\frac{P_1^{sat}}{N}\gamma^{\infty}t \tag{3-41}$$

A_o is the initial solute peak area. Finally, the infinite dilution activity coefficient γ_{13}^{∞} of the solute (1) in the solvent (3) is determined by means of this equation derived from expression (3-41):

$$\gamma_{13}^{\infty} = \frac{NRT}{DP_1^{sat}}\frac{1}{t}\ln\frac{A_1}{(A_1)_{t=0}} \tag{3-42}$$

where N is the number of solvent moles in the dilutor cell and $(A_1)_{t=0}$ expresses the initial solute peak area.

3.2.1.1(c) Equation proposed by Leroi et al. (1977) for volatile solvents

When a volatile solvent is used, its amount in the cell varies with time. Therefore, the two equations (3-36) and (3-37) are worked out simultaneously to give the following solution.

$$\ln\frac{A}{A_o}=\left(\frac{\gamma_{13}^{\infty}P_1^{sat}}{P_3^{sat}}-1\right)\ln\left(1-\frac{P}{P-P_3^{sat}}\frac{DP_3^{sat}}{N_oRT}t\right) \tag{3-43}$$

3.2.1.2. Equation proposed by Duhem and Vidal (1978) for non volatile solvents

Leroi et al. (1977) derived equation (3-43) on the basis of some assumptions such as neglecting the term $\frac{n}{N}\gamma^{\infty}\frac{P_1^{sat}}{P}$ appearing in equations (3-36) and (3-37). Duhem and Vidal established that for large infinite dilution activity coefficients, this particular assumption is no longer valid. Apart from dropping this assumption, they expressed the mole fraction of the solute in the liquid phase by

$$x_1=\frac{n}{N\left(1+\frac{V_G}{RT}\frac{P_1^{sat}\gamma_1^{\infty}}{N}\right)} \tag{3-44}$$

This allowed them to come up with the following equation:

$$\frac{dn}{dt}=-\frac{n}{N\left(1+\frac{V_G}{RT}\frac{P_1^{sat}\gamma_1^{\infty}}{N}\right)}\gamma_1^{\infty}P_1^{sat}\frac{D}{RT\left(1-\frac{n}{N\left(1+\frac{V_G}{RT}\frac{P_1^{sat}\gamma_1^{\infty}}{N}\right)}\gamma_1^{\infty}\frac{P_1^{sat}}{P}\right)} \tag{3-45}$$

Assuming a constant inert gas flow rate D, after incorporating a vapour space correction into equation (3-45), Duhem and Vidal derived the following equation which is more accurate for systems with large activity coefficients at infinite dilution:

$$\ln\frac{A}{A_o}=-\frac{D}{NRT\left(1+\frac{V_G}{RT}\frac{P_1^{sat}\gamma_1^{\infty}}{N}\right)}\frac{P_1^{sat}}{1-\frac{\tilde{n}}{N\left(1+\frac{V_G}{RT}\frac{P_1^{sat}}{N}\right)}\frac{\gamma_1^{\infty}P_1^{sat}}{P}}\gamma_1^{\infty}t \tag{3-46}$$

where $\tilde{n}$ is given by:

$$\tilde{n} = \frac{n - n_o}{\ln \frac{n}{n_o}} \tag{3-47}$$

In the above equation n and n_o are the number of moles of the solute in the still at a certain time t and the initial number of moles for the solute respectively. V_G is the volume of the vapour phase evaluated from equation (3-48) (Bao et al. 1993a, b).

$$V_G = V_c - \frac{m_s}{\rho_s} \tag{3-48}$$

3.2.1.3. Equation proposed by Bao and Han (1995) for a volatile solvent

Following the example of Duhem and Vidal (1978), Bao and Han (1995) used equation (3-44) to express the solute mole fraction in the liquid phase. Neglecting the correction term suggested by Bao and Han, they solved the differential equations (3-36) and (3-37) to obtain the following final result, applicable to a volatile solvent:

$$\ln \frac{A}{A_o} = \left(\frac{1}{1 + \frac{\gamma_1^\infty P_1^{sat} V_G}{N_o RT}} \frac{\gamma_1^\infty P_1^{sat}}{P_3^{sat}} - 1 \right) \ln \left(1 - \frac{P_3^{sat}}{P - P_3^{sat}} \frac{PD}{N_o RT} t \right) \tag{3-49}$$

3.2.1.4. Equation proposed by Hovorka and Dohnal (1997)

According to Leroi et al. (1977), under the assumption that the solvent is non-volatile, the partial pressure of the solute is negligible as compared to the total pressure in the cell, the vapour phase is ideal and neglecting the effect of the vapour space, the limiting activity coefficient can be determined as follows:

$$\gamma_1^\infty = \frac{NRT}{P_1^{sat} D} \left(- \frac{d \ln A_1}{dt} \right) \tag{3-50}$$

For a volatile solvent, a presaturation cell is used as explained in section 2.3.2. It is Hovorka and Dohnal's statement that after presaturation the flow rate of the stripping gas is increased by a factor $1/(1 - P_3^{sat}/P)$ where P_3^{sat} is the saturation vapour pressure of the solvent. Thus, for the double cell technique, the activity coefficient at infinite dilution is computed as

$$\gamma_1^{\infty} = \frac{NRT}{P_1^{sat} D}\left(-\frac{d\ln A_1}{dt}\right)\left(1-\frac{P_3^{sat}}{P}\right) \tag{3-51}$$

These last two equations provide the first order approximation of the infinite dilution activity coefficient, denoted as $\gamma_1^{\infty,I}$, with a sufficient degree of accuracy in most cases. However, for improved accuracy, the second order approximation $\gamma_1^{\infty,II}$ can be used.

$$\gamma_1^{\infty,II} = \gamma_1^{\infty,I} \prod k_i \tag{3-52}$$

where $\gamma_1^{\infty,I}$ is given by equation (3-50) or (3-51). Correction factors k_i are defined as follows:

- k_1, correction factor associated with the change of the inert stripping gas flow rate due to the saturation in the cell is given for the single cell technique (Equation 3-53) and the double cell technique (Equation 3-53) respectively by:

$$k_1 = 1-\left(\bar{n}_1 / n_2\right)\gamma_1^{\infty,I}\left(P_1^{sat}/P\right)-\left(P_3^{sat}/P\right) \tag{3-53}$$

and

$$k_1 = \left[1-\left(\bar{n}_1 / n_2\right)\gamma_1^{\infty,I}\left(P_1^{sat}/P\right)-\left(P_3^{sat}/P\right)\right]/(1-P_3^{sat}/P) \tag{3-54}$$

where $\bar{n}_1$ is the mean amount of the solute in the cell during the measurement and is given by:

$$\bar{n}_1 = \frac{n_1^o\left(A_1^f / A_1^o - 1\right)}{\ln\left(A_1^f / A_1^o\right)} \tag{3-55}$$

$\bar{n}_1^o$ is the initial amount of the solute in the cell, A_1^f and A_1^o are solute peak areas at the end and the beginning of the experiment, respectively. k_1 is always less than unity and rises with increasing volatility of the solvent and the solute.

- k_2 is the correction factor associated with solvent removal due to its volatility. When a presaturation cell is not used, this correction term is written as:

$$k_2 = \frac{1-\left(P_3^{sat} Dt\right)}{2N_o RT} \tag{3-56}$$

where t is the total stripping time, N_o denotes the initial amount of the solvent in the cell and D is the stripping gas flow rate. If the stripping gas is saturated, k_2 will become equal to unity; it is always less than unity and rises with decreasing cell volume and increasing solvent volatility.

- k_3 is related to the amount of the solute in the vapour space above the solution in the cell. It is calculated by

$$k_3 = \left[1 - \left(-d \ln A_1 / dt\right)(V / D)\right]^{-1} \cong \left[1 - \left(\gamma_1^{\infty,I} P_1^{sat} V_G\right) / NRT\right]^{-1} \tag{3-57}$$

where V_G is the vapour space volume. k_3 is greater than unity and rises with the solute volatility and with the increasing ratio of the vapour space volume to the amount of the solvent in the equilibrium cell.

- k_4 is the vapour phase nonideality correction factor given by:

$$k_4 = \left[1 + B_{22} / (RT)\right] \exp\left\{\left[P(2B_{12} - B_{22} - v_1^L) - P_1^{sat}(B_{11} - v_1^L)\right] / RT\right\} \tag{3-58}$$

where subscripts '1' and '2' refer to the solute and the stripping gas, respectively. v_1^L is the pure solute molar volume, B_{ij} is the second virial coefficient. Depending on the system and experimental conditions, k_4 can be either greater or smaller than unity.

3.2.1.5. Equation proposed by Krummen et al. (2000)

Krummen et al. (2000) proposed a formulation which takes into account the saturation fugacity of the components under investigation and the increase of the stripping gas flow rate caused by its saturation with the solvent. Assuming that the liquid phase is in equilibrium with the gas phase in the cell, these equations can be written:

$$x_1 \gamma_1 \varphi_1^{sat} P_1^{sat} I_1 = y_1 \varphi_1^{v} P \tag{3-59}$$

$$x_3 \gamma_3 \varphi_3^{sat} P_3^{sat} I_3 = y_3 \varphi_3^{v} P \tag{3-60}$$

Further assumptions are:

- The solute is highly dilute in the solvent. This implies that:

$$\gamma_1 = \gamma_1^{\infty} \tag{3-61}$$

$$\gamma_3 = 1 \tag{3-62}$$

$$x_3 = 1 \tag{3-63}$$

- Measurements are carried out at low pressures or pressure differences $(P - P_1^{sat})$. Thus,

$$I_1 \cong 1 \tag{3-64}$$

- The stripping gas is of negligible solubility in the liquid phase. Therefore,

$$\varphi_1^v = 1 \tag{3-65}$$

And for the solvent, it is assumed that:

$$\frac{\varphi_3^{sat} I_3}{\varphi_3^v} \cong 1 \tag{3-66}$$

The above simplifications allow writing equations (3-59) and (3-60) as follows:

$$x_1 \gamma_1 \varphi_1^{sat} P_1^{sat} = y_1 P \tag{3-67}$$

$$P_3^{sat} = y_3 P \tag{3-68}$$

The flow rate D_{in} of the stripping gas stream entering the dilutor cell is made up of the flow rate of the stripping gas stream entering the saturation cell, D and the flow rate of the solvent stream, D_3.

$$D_{in} = D + D_3 \tag{3-69}$$

The amount of solvent leaving the presaturator is provided by its saturation vapour pressure and mixes with the pure stripping gas entering the dilutor cell.

$$D_3 = D y_3 \tag{3-70}$$

Combining equations (3-68) through (3-70) leads to:

$$D_{in} = D \left(1 + \frac{P_3^{sat}}{P} \right) \tag{3-71}$$

According to Krummen et al. (2000), the solvent content in the stripping gas stream cannot be neglected when P_3^{sat} is greater than 5 mbar. D_{out}, the flow rate of the stripping gas stream leaving the dilutor cell, is given by:

$$D_{out} = D_{in} + D_1 \tag{3-72}$$

where D_1 is the flow rate of the solute removed from the measurement cell, which under the assumption of an ideal gas, can be calculated as follows:

$$D_1 = \frac{RT}{P} \frac{dn_1}{dt} \tag{3-73}$$

D_1 decreases with time. When the last two equations are combined, it follows that:

$$D_{out} = D_{in} - \frac{RT}{P} \frac{dn_1}{dt} \tag{3-74}$$

In order to determine activity coefficients at infinite dilution by the inert gas stripping technique, the variation of the amount of solute in the dilutor cell is measured as a function of time. This variation can be expressed by the following equation:

$$\frac{dn_1}{dt} = - y_1 \frac{PD_{out}}{RT} \tag{3-75}$$

Since the stripping gas is saturated with the solvent,

$$\frac{dN}{dt} = 0 \tag{3-76}$$

Taking into account equation (3-75), equation (3-74) can be written as:

$$D_{in} = D_{out}\left(1 - y_1\right) \tag{3-77}$$

Combining equations (3-77) and (3-67) results in:

$$D_{out} = \frac{D_{in}}{1 - \frac{x_1 \gamma_1^{\infty} \varphi_1^{sat} P_1^{sat}}{P}} \tag{3-78}$$

When equation (3-77) is used in equation (3-75) and combined with equation (3-67), the result is:

$$\frac{dn_1}{dt} = x_1 \gamma_1^{\infty} \varphi_1^{sat} P_1^{sat} \frac{1}{1 - \frac{x_1 \gamma_1^{\infty} \varphi_1^{sat} P_1^{sat}}{P}} \frac{D_{in}}{RT} \tag{3-79}$$

For relatively volatile solutes, high saturation vapour pressures of the solvent or large infinite dilution activity coefficient values, Krummen et al. (2000) suggest that only the solute content in the liquid phase should be taken into account when determining the solute molar fraction.

$$n_1 = n_1^L + n_1^v = x_1 n_3 + n_1^v \tag{3-80}$$

Assuming ideal gas behaviour, the content of the solute in the gas phase can be calculated as follows:

$$n_1^v = y_1 \frac{PV_G}{RT} \tag{3-81}$$

When equations (3-81) and (3-67) are combined and the resulting expression is inserted into equation (3-80), the result is:

$$x_1 = \frac{n_1}{N\left(1 + \frac{\gamma_1^{\infty} \varphi_1^{sat} P_1^{sat} V_G}{NRT}\right)} \tag{3-82}$$

If equation (3-82) is used in equation (3-79), the variation of the amount of solute with time can be expressed by:

$$\frac{dn_1}{dt} = -\frac{n_1}{N\left(1 + \frac{\gamma_1^{\infty} \varphi_1^{sat} P_1^{sat} V_G}{NRT}\right)} \gamma_1^{\infty} \varphi_1^{sat} P_1^{sat} \frac{1}{1 - \frac{\gamma_1^{\infty} \varphi_1^{sat} P_1^{sat} n_1}{PN(1 + \gamma_1^{\infty} \varphi_1^{sat} P_1^{sat} V_G / (NRT))}} \frac{D_{in}}{RT} \tag{3-83}$$

In the above equation, $1 - \frac{\gamma_1^{sat} \varphi_1^{sat} P_1^{sat} n_1}{PN(1 + \gamma_1^{\infty} \varphi_1^{sat} P_1^{sat} V_G / (NRT))}$ is the corrective term used to take into account the variation of the solute gas stream during measurements. If the change in the solute flow rate is neglected with respect to the inert gas stream, the corrective term is equated to unity. In this particular case, the integration of equation (3-83) yields:

$$\ln \frac{n_1}{n_o} = -\frac{\gamma_1^{\infty} \varphi_1^{sat} P_1^{sat}}{N\left(1+\frac{\gamma_1^{\infty} \varphi_1^{sat} P_1^{sat} V_G}{NRT}\right)} n_1 \tag{3-84}$$

If the linearity of the detector is assured and condensation effects in the sample loop and other tubes are avoided, the solute peak area A_1 is given by:

$$A_1 = k y_1 P \tag{3-85}$$

k is the proportionality constant. When equations (3-82), (3-67) and (3-85) are combined, the result is:

$$A_1 = k \frac{\gamma_1^{\infty} \varphi_1^{sat} P_1^{sat}}{N\left(1+\frac{\gamma_1^{sat} \varphi_1^{sat} P_1^{sat} V_G}{NRT}\right)} n_1 \tag{3-86}$$

All the quantities on the right–hand side of this equation do not vary during the measurements except the number of moles for the solute, n_1 Using n_1 from equation (3-86) in equation (3-84) leads to:

$$\frac{\ln(A_1 / A_o)}{t} = -\frac{\gamma_1^{\infty} \varphi_1^{sat} P_1^{sat}}{N\left(1+\frac{\gamma_1^{\infty} \varphi_1^{sat} P_1^{sat} V_G}{NRT}\right)} \frac{D_{in}}{RT} \tag{3-87}$$

Solving the equation for γ_1^{∞} gives:

$$\gamma_1^{\infty} = -\frac{NRT}{\varphi_1^{sat} P_1^{sat}\left(\frac{D_{in}}{a}+V_G\right)} \tag{3-88}$$

where a is the slope of the graph of the natural logarithm of the solute peak area versus time.

$$a = \frac{\ln(A_1 / A_o)}{t} \tag{3-89}$$

Using equation (3-71), expression (3-88) can be written as:

$$\gamma_1^{\infty} = -\frac{NRT}{\varphi_1^{sat} P_1^{sat} \left(\frac{D\left(1 + P_3^{sat}/P\right)}{a} + V_G \right)} \tag{3-90}$$

where V_G is the vapour phase volume and D is the stripping gas flow rate as it enters the presaturator at the system temperature T.

Equation (3-90) is also applicable to solvent mixtures with the aid of these formulae:

$$P_3^{sat} = \sum_1^i P_{3(i)}^{sat} \tag{3-91}$$

$$N = \sum_1^i N_{(i)} \tag{3-92}$$

where $P_{3(i)}^{sat}$ and $N_{(i)}$ are respectively saturation vapour pressures and amounts of individual solvents involved in the solution. Equation (3-90) shows that activity coefficients at infinite dilution can be determined from the experimentally measured slope a, the saturation vapour pressures of the solute and the solvent, the saturation fugacity coefficient of the solute, the system pressure and temperature, the inert gas flow rate and the vapour phase volume. The inert gas flow rate D needs to be converted to the cell conditions using the following equations, depending on the type of flowmeter used:

$$D = D^{\exp} \frac{T}{T_{FM}} \frac{P_{FM}}{P} \qquad \text{(Electronic flowmeter)} \tag{3-93}$$

$$D = D^{\exp} \frac{T}{T_{FM}} \frac{P_{FM} - P_W^{sat}}{P} \qquad \text{(Soap bubble flowmeter)} \tag{3-94}$$

where $D^{\exp}$ is the inert gas flow rate at the flowmeter, P_{FM} is the pressure at the flowmeter, P_W^{sat} is the saturation vapour pressure for water, P is the pressure in the measurement cell. Equation (3-94) was also useful for determining the corrected flow of the carrier gas when using GLC.

3.2.2. Mass Transfer considerations in the equilibrium cell.

Richon et al. (1980) developed a useful model to calculate mass transfer of the solute from the solution to the vapour phase in the still. A condition of validity of their method is that thermodynamic equilibrium should be achieved between the saturated gas leaving the still and

the liquid. Assuming that there is a very quick diffusion of solute into the bubble, the modified Raoult's law describes the existing vapour-liquid equilibrium in the still, bubbles are perfectly spherical and the carrier gas is not soluble in the solvent, they derived equations (3-95) and (3-96) for the attainment of equilibrium in the liquid phase and in the vapour phase respectively.

$$\tau_L = 1 - \exp\left(-\frac{3\rho_L k_L R \ T \ h}{R_b M_L \gamma_i^{\infty} P_i^s u^{\infty}} \right) \tag{3-95}$$

$$\tau_G = 1 - \frac{6}{\pi^2} \sum_{l=1} \frac{1}{l^2} \exp\left[-\frac{D_{ij}^G l^2 \pi^2 h}{R_b^2 u^{\infty}} \right] \tag{3-96}$$

where τ_L is the ratio of mass transfer in the cell to mass transfer to reach equilibrium, taking into consideration only the liquid phase resistance τ_G is the same as τ_L, taking into consideration gas phase diffusion only. As the system approaches equilibrium, τ_L as well as τ_G approach unity. h is the path length of the bubbles in the equilibrium still. ρ is the density in g .cm^{-3}, T is the temperature in Kelvin, D_{ij}^G is the diffusion coefficient of solute, i, in solvent, j, in the gas phase, R_b is the bubble radius, M_L is the solvent molar mass in g/mol., P_1^S is the solute vapour pressure at temperature T in atm and u^{∞} is the limiting bubble speed given by

$$(u^{\infty})^{1.4} = 7.2 \times 10^{-2} \nu_L^{-0.6} D_b^{1.6} g \tag{3-97}$$

υ_L, kinematic viscosity in cP and D_b is the diameter of bubbles. Many authors have designed dilutor cells on the basis of mass transfer calculation proposed by Richon et al. (1980).

Of particular importance is equation (3-95) which allows the determination of the optimal cell height (Li et al. 1993). It has been used for this end in this work. Infinite dilution activity coefficients values were computed using equation (3-90). Saturation fugacity coefficients were determined from second virial coefficients (See appendix D)

CHAPTER FOUR: EXPERIMENTAL APPARATUS AND PROCEDURE

Chapter overview

For each of the two techniques used in this work, the materials used, the experimental set up and the experimental procedure are described. Solvents and solutes preparation and purification before measurements by Gas Liquid Chromatography and the Inert Gas Stripping Technique are explained. This chapter also presents the main features of the dilutor cell designed for this study with emphasis on the procedure used to determine its optimal height. Uncertainties on the experimental parameters and variables are provided as they allowed determining the errors attached to the experimental data reported in this work.

4.1. Limiting activity coefficient measurements by gas liquid chromatography

4.1.1. Chemicals

The reliability and accuracy of an experimental procedure has to be checked by comparison with data available in the literature. In this study, systems involving n-hexadecane as the solvent has been used to test the exactness of the procedure. The following ionic liquids have been used as solvents:

- Trihexyltetradecylphosphonium tetrafluoroborate, [$3C_6C_{14}P$] [BF_4]
- Trihexyltetradecylphosphonium bis(trifluoromethylsulfonyl) imide, [$3C_6C_{14}P$] [BTI]
- Trihexyltetradecylphosphonium hexafluorophosphate, [$3C_6C_{14}P$] [PF_6]
- Trioctylmethylammonium bis(trifluoromethylsulfonyl) imide, [$3C_8C_1N$] [BTI]
- 1-ethyl-3-methylimidazolium trifluoromethanesulfonate, [EMIM] [TfO]
- 1-n-Butyl-3-methylimidazolium hexafluoroantimonate, [BMIM] [SbF_6]
- 1-Octyl-3-methylimidazolium hexafluorophosphate. [OMIM][PF_6]

The above fluorinated ionic liquids, whose structures are given in appendix B, have been selected because IDAC data for phosphonium-based FILs were found to be rare. In addition, these ionic liquids were selected because of their availability. Before use, they were heated at T = 353.15 K for seven hours under vacuum, using a vacuum pump, to remove all possible traces of impurities, including moisture. For all solvents, stated purities, densities and refractive indices are provided in tables C-1 through C-3 in appendix C. Densities of purified samples were measured by the vibrating tube method using a DMA 5000 Anton Paar densitometer. Refractive index measurements were carried out using an RX-7000α automatic digital refractometer. Both properties were measured in the Thermodynamics Research Unit laboratory. Solutes, including n-alkanes, alk-1-enes, alk-1-ynes, alkanols, cycloalkanes, alkylbenzenes and

ketones were used without any purification since impurities were separated by the GC during the measurement process. Diatomaceous earth, celite (Chromosorb W HP 80/100 mesh) was used as inert solid support onto which the solvent was coated. It was purified by vacuum heating under the same conditions as the ionic liquid. Dichloromethane was used as solvent to aid uniform coating of the ionic liquid onto the inert solid support and removed afterwards by evaporation. Dry helium was used as carrier gas.

4.1.2. Experimental set up

Experiments were performed using a Shimadzu GC-2014 gas chromatograph apparatus, equipped with a thermal conductivity detector, an auto-sampler and auto-injector. Retention times and chromatograms related to each run were made available on a PC monitor by means of a GC solution workstation software. The set up, shown in Photograph 4-1, is programmable so that it can carry out injections of samples from 125 different vials and acquire data with minimum human supervision.

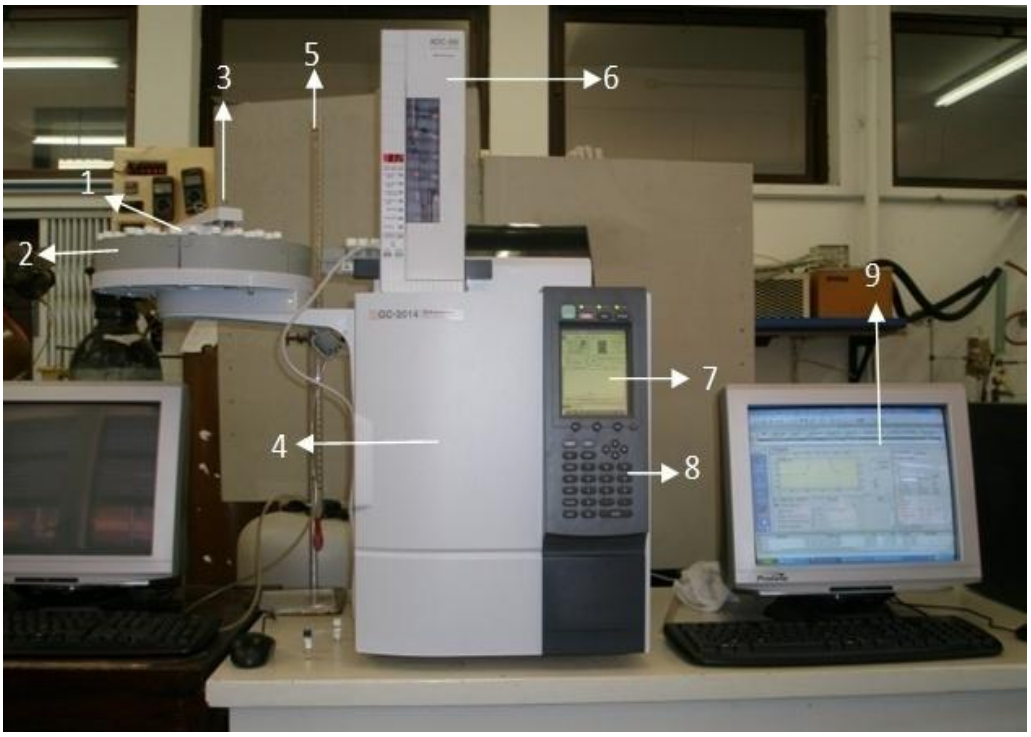

Photograph 4-1: Gas-Liquid Chromatography equipment.

1. Vials; 2. Tray; 3. Auto-sampler (arm); 4. Column oven; 5. Soap bubble flow-meter; 6. Auto-injector; 7. GC screen; 8. Operation panel; 9. PC monitor

4.1.3. Experimental procedure

The experimental procedure used in this work has been well documented by numerous authors (David et al. 2003, Letcher et al. 2003a,b and Deenadayalu et al. 2005). To check for adsorption problems, two different stainless steel columns of length 1 m and 4.1 mm inner diameter were used with two different mass percent packings. To avoid adsorption effects, mass percent packings of the ionic liquid that are large enough were used. Before packing, the columns were washed with hot soapy water, rinsed with cold water and flushed with acetone to minimize the drying time. The original and final masses of the ionic liquid and chromosorb mixture were in agreement to within 0.0005 g. Measurements were done at different temperatures between (303.15 and 373.15) K, i.e. (303, 313.15, 323.15, 333.15, 353.15, 363.15 and 373.15) K. Reproducibility was checked by undertaking three experimental runs. It was observed that retention times were reproducible within 0.05 minutes. The flow rate of dry helium, the carrier gas, was determined with the aid of a soap bubble flow meter placed at the outlet of the detector. The flow rates were corrected for water vapour pressure and varied from 0.3 to 0.7 $\mu m^3.s^{-1}$ .The carrier gas flow rate was allowed to stabilize for at least 15 min prior to any series of runs. The pressure drop through the column varied from (25 to 50) kPa, providing conducive retention times and sharp peaks. The injected volumes ranged between 0.1 and 0.5 µl and were considered small enough to comply with the condition of infinite dilution of the solutes on the column. Both the injector and the detector were at T = 523.15 K. More details on the experimental parameters and variables needed to compute infinite dilution activity coefficients by means of equation (3-10), are discussed below.

4.1.3.1 Temperature control

The equipment, not only controls the temperature using a thermostat, but also displays its value on the monitor. The column oven temperature was known with an accuracy of ± 0.01 K and a stability of 0.05 K. The design of the GC was such that an electronically controlled thermostat was used to reliably control the column temperature.

4.1.3.2 Pressure measurement

The outlet pressure which is the same as the atmospheric pressure was measured with the aid of a digital barometer with an uncertainty of ±0.30 %. The pressure drop through the packed column was fixed by the equipment, depending on the inert gas flow-rate set by the operator. The uncertainty in the inlet pressure measurement was ±0.50 %.

4.1.3.3 Flow-rate measurement

A bubble soap flow-meter consisting of a 100 ml calibrated cylinder was used for the determination of helium flow rate. The uncertainty in the flow rate measurement was estimated as ±0.20 %.

4.1.3.4 Infinite dilution range

Injections between 0.1 and 0.5µl were considered small enough to comply with the infinite dilution requirement. It is however advisable to check whether the retention time for a solute at the selected injection volume and flow rate remains the same as when it is part of a mixture.

4.1.3.5 Column packing

This is the most critical step when undertaking measurements via the Gas-Liquid Chromatography technique. Large error margins are caused by a careless column packing. The uncertainty in determining the mass of the solvent loaded into the column was ±0.03 %.

Column cleaning

The column was washed with soapy water and flashed with acetone to facilitate drying with air.

Determination of solvent number of moles

The following procedure was employed:

1. The mass of an empty flask was measured using a digital balance;
2. Chromosorb, the solid support for the solvent was added to the flask and weighed;
3. The amount of solvent to be added was roughly calculated on the basis of the desired percent loading of the solvent;
4. The solvent was added and its weight found accurately.

Coating the support with the IL

Dichloromethane was added to the flask content to distribute the solvent evenly on chromosorb. Thereafter, a rotary evaporator was used to remove the Dichloromethane. This step ended when the mass of the mixture in the content was equal to the one measured before adding dichloromethane.

Filling the column

The support loaded with IL was filled in the column with the aid of a vacuum pump. One had to make sure that the load was equally distributed inside the column. The mass of the packed

column had to be known before and after each series of runs to check for a probable elution of the solvent.

4.2. The inert gas stripping technique

4.2.1. Chemicals

To validate the method, experiments were performed with NMP as solvent whereas n-hexane, hex-1-ene, hex-1-yne, methanol, cyclohexane, benzene and acetone were used as solutes in the ionic liquid trihexyltetradecylphosphonium bis (trifluoromethylsulfonyl) imide, $[3C_6C_{14}P]$ [BTI]. Appendix C provides additional information about the solvents, including their source, purity, density and refractive index. No further purification was undertaken for the solutes as they were of high purity. Solvents were purified by heat treatment under vacuum.

4.2.2. Experimental Set-up

As part of this study, it was intended to construct an entire inert gas stripping set up with an equilibrium cell able to accommodate small volumes of samples, less than 50 g. This was a necessity since ionic liquids are very expensive chemicals. The second reason why a dilutor cell was needed is for systems that are not suitable when using the GLC technique. Examples of these are systems involving solutes that are solid at room temperature, solvent mixtures and those leading to a very long retention time. Design parameters for the dilutor cell were discussed in the previous chapter. The greatest part of the design work was centered on the dilutor cell as it is the most determinant piece of the set up performance. Figure 4-1 presents the simplified flow diagram of the set up used in this study, which is similar to the one described by Krummen et al. (2000) and Coquelet and Richon (2005). Photograph 4-2 gives the experimental set up of the inert gas stripping apparatus.

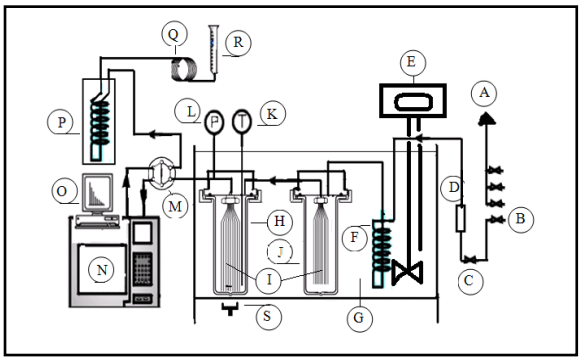

Figure 4-1: Flow diagram of the experimental set up for the inert gas stripping method. A-Helium, Nitrogen and air supply for the GC; B- Nitrogen line; C-Valve; D- flow regulator; E-Immersion temperature controller; F-Coil tube (Heat exchanger); G-Transparent acrylic bath; H- Dilutor cell; I-Capillaries; J-Presaturation cell; K-Platinum resistance thermometer; L-Pressure transducer; M-Sampling valve; N-GC apparatus; O-PC monitor; P-Cold trap; Q- Coil tube (Heat exchanger); R-Soap bubble flow-meter; S-Magnetic stirrer.

4.2.2.1. Gas cylinders

Four gases are used in this work:

- Nitrogen as stripping gas;
- Helium as carrier gas for the GC apparatus;
- Air and Hydrogen to produce the ignition flame for the GC (FID only).

The four cylinders containing the above gases are fitted with regulators. Nitrogen flow rate is controlled by a smaller regulator. Its value is determined by means of a soap bubble flow meter.

4.2.2.2. Water bath

An 18-litre transparent acrylic water bath, with maximum allowed temperature of 70 ^{o}C, was used to accommodate the cells during experiments. During experiments, leaks could be easily detected by the observation of gas bubbles, due to the transparency of the bath. A Haake Difisons temperature controller kept the water in the bath at a constant temperature set before each run. The nitrogen line (1/4 inch inner diameter and 12 m long) was coiled and immersed in the water bath to allow the gas to equilibrate to the set-point temperature before entering the cells. In order to reduce heat loss to the atmosphere, the water surface in the bath was completely covered with polystyrene chips. The temperature stability of the bath was ±0.1 K.

4.2.2.3. Cells

The two glass cells are identical and have a total volume of 50 cm^3 each. They were made for the purpose of this work by a Durban glass blower, Mr. Peter Siegling. Metallic parts were manufactured and fitted by the School of Chemical Engineering workshop staff members, Mr. Ken Jack and Mr. Kelly Robertson. The shape is similar to the cells previously used by other researchers (Coquelet and Richon 2005). Mass transfer considerations discussed by Richon et al. (1980) were taken into account to determine the cell height using equation (3-95), assuming the degree of the equilibrium attainment τ_L = 0.99 From the literature, ranges of different properties related to FILs (See table 2-2) were used in equation (3-95) to find out the most suitable height for the cell. The same procedure was used by Li et al. (1993) to find out the optimum height of the dilutor cell used in the study of IDAC's for nonelectrolytes solutes in water. For systems involving ionic liquids, the presaturator cell was removed. As shown in Photograph 4-3, the dilutor cell is fitted with ten stainless steel capillaries (0.1 mm inner diameter) purchased from Anatech, through which the stripping gas is introduced. During experiments, they should be placed in such a way that bubbles are not directed to the vortex. This will prevent bubbles coalescence (George 2008). A class A Pt-100 temperature sensor (length 250 mm, outer diameter 3 mm and limiting error of 0.25 ^{o}C) fitted with stainless steel pot seal and a Sensotec pressure transducer are inserted in order to measure the temperature of

the mixture and the pressure in the dilutor cell. To obtain accurate readings, both sensors had to be calibrated. A CTH 6500 digital thermometer (accuracy: ±0.03 %) and a CPH 6000 pressure calibration standard (accuracy: ±0.1 %) for temperature and pressor sensor calibrations, respectively. The bolt (G) along with the Teflon piece (H) seal the cell to ensure that no portion of nitrogen flows through other channels than the provided capillaries. Agitation of the solution contained in the cell is achieved by means of a magnetic stirrer. Other features of the designed cell are given by Photograph 4-3.

4.2.2.4. Cold trap

The stream leaving the dilutor cell contains not only nitrogen, but also solute and probably solvent vapours. A cold trap serves as a separation unit to ensure that the flow rate determined by the soap bubble flow-meter is actually the one of nitrogen which is required in the infinite dilution activity coefficient computation equation. Failure to condense solute and solvent vapours will lead to inaccurate data. The cold trap as shown in figure 4-2 consists of two chambers. The upper chamber (A) contains an ice-acetone solution in which a ¼ inch ID copper coil is completely immersed. The outlet gas stream from the dilutor cell flows through the coils and ends its path in the lower chamber (B) where the condensate is trapped. Nitrogen, the only gaseous component after this process, rises up to exit through the pipe (C) and makes its way to the soap bubble flow-meter (J). Valve (E) can be opened to drain out the liquid captured in chamber (B).

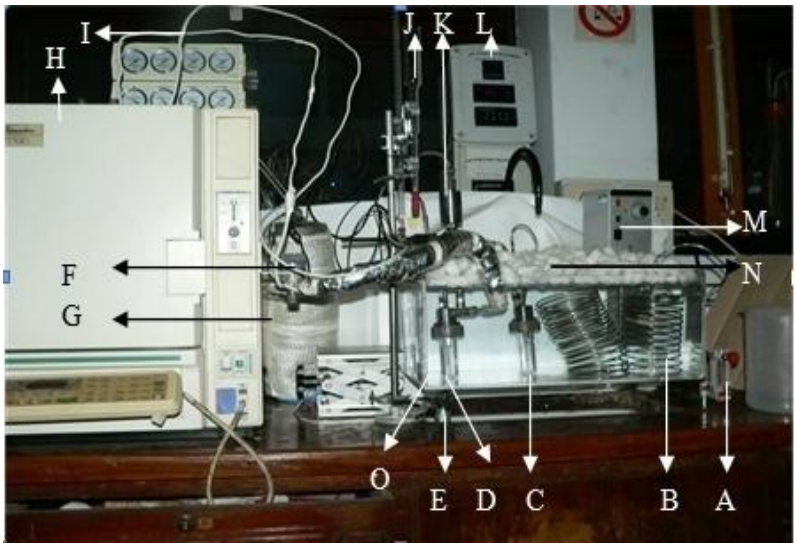

Photograph 4-2: Set-up of the inert gas stripping apparatus. A-flow regulator; B-Coil tube (Heat exchanger); C-Presaturation cell; D- Dilutor cell; E-Magnetic stirrer; F-Sampling valve; G-Cold trap; H-GC apparatus; I-GC lines; J-Soap bubble flow-meter; K-Pressure transducer; L-Pressure and temperatures displays; M-Immersion temperature controller; N-Polystyrene chips; O-Transparent acrylic bath.

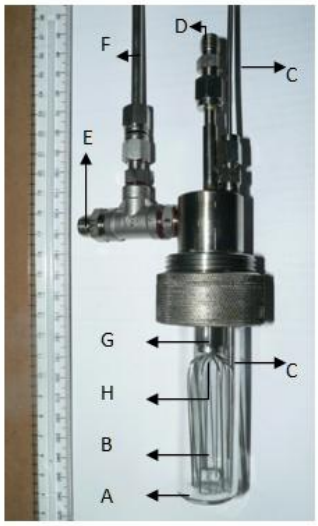

Photograph 4.3: The dilutor cell. A-Glass still; B-Capillaries; C-Temperature probe (Pt 100); D-Gas inlet; E-Gas outlet; F-Pressure transducer tube; G-Bolt (seal); H-Teflon plug (seal).

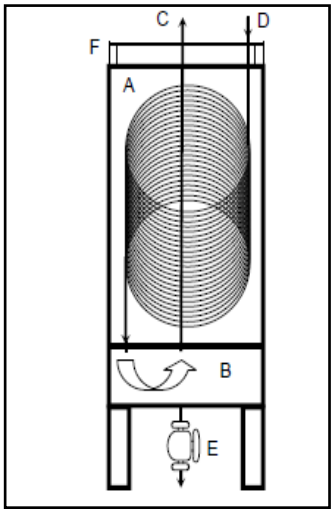

Figure 4-2: Cross Section of the cold trap to illustrate its inner workings (George 2008) A – Upper chamber, B – lower chamber, C – gas inlet, D – non-condensable gas outlet, E – release valve, F – lid.

4.2.2.5. Gas Chromatography apparatus

In this work, a SHIMADZU GC 14A gas chromatograph equipped with a FID detector was used. The FID has the advantage over the TCD to be very sensitive to small amounts of solutes injected. GC settings and column conditions during experiments are displayed in table 4-1. To avoid condensation of the solute as the stream flows from the dilutor cell outlet to the GC injection port via the six-port sampling valve, these lines had to be heated and thermostated at a temperature approximately 40 ^{o}C higher than the system temperature (Krummen et al. 2000).

Table 4-1: GC specification and set-up.

Column	CRS; 2m x 1/8'; Packed column
GC Program	Clarity work station
Detector type	FID
Carrier gas	Helium
Injection Port Temperature	493.15 K
Column Oven Temperature	393.15 K-453.15 K
Detector Temperature	493.15 K

4.2.3. Experimental procedure

First, the cells were cleaned and thereafter filled with the required components. The solvent was poured into each cell. The mass of the solvent in the dilutor cell had to be known accurately. The solute was injected into the dilutor cell in very small concentration to comply with the infinite dilution requirement, less than 0.001 mole fraction. The injected volume ranged between (10 and 25) μl . Density data of the solvent (given in appendix C) were used to determine by difference the vapour phase volume. The cells were then sealed and fitted onto the set up. The equipment was checked for leaks, the cold trap upper chamber was filled with acetone-ice mixture, the GC apparatus and all electrical equipments with desired settings were switched on. Thereafter the procedure below was followed:

1. The water bath, the sampling valve, the mixture in the dilutor cell and all other tubing were allowed to equilibrate to their respective set-point temperatures, the magnetic stirrer being switched on;
2. The inert gas was allowed to flow through the cell. A bubble soap flow-meter was used to measure the flow rate. Li et al. (1993) suggested that the infinite dilution activity coefficient obtained should be independent of the flow rate;
3. The gas sampling valve was set to the "fill" position, allowing the inert gas to flow for some minutes;
4. The gas sampling valve was set to the "inject" position for one to two minutes;
5. The sampling valve was set back to the "fill" position;
6. Steps 4 and 5 were repeated periodically. The time interval between two successive injections depended on the system under investigation. The natural logarithm of the solute peak area was expected to decrease linearly with time as illustrated by figure 4-3 which was taken from a publication by Krummen et al. (2000);
7. After a number of runs with sufficient data to compute infinite dilution activity coefficient values, the experiment was ended. Equation (3-90) was used to determine experimental IDAC values.

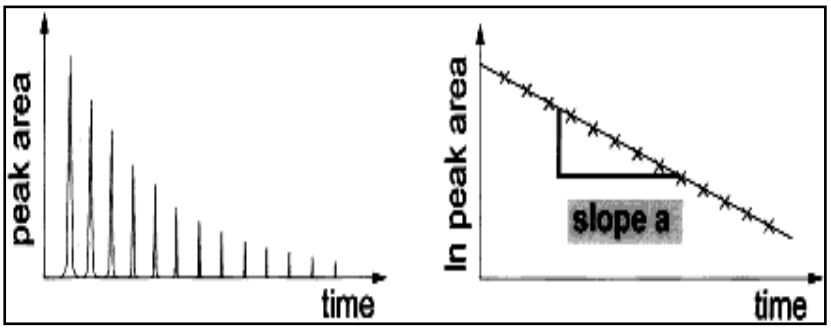

Figure 4-3: Typical plots of solute GC peak area and ln (solute peak area) versus time.

CHAPTER FIVE: RESULTS

Chapter overview

Results presented in this work consist of the following:

- Infinite dilution activity coefficients data for various organic solutes in n-hexadecane and seven different FILs, obtained from Gas-Liquid Chromatography;
- Excess molar enthalpies at infinite dilution of the same solutes in the fluorinated ionic liquids, calculated from experimental infinite dilution activity coefficients data;
- Correlation of experimental infinite dilution activity coefficient data with temperature and the carbon chain length of solutes;
- Infinite dilution activity coefficients data for six organic solutes in NMP and one fluorinated ionic liquid;
- Limiting selectivities and capacities of the seven investigated fluorinated ionic liquids for selected separation problems;
- Estimation of experimental errors in determining activity coefficients, Excess molar enthalpies, selectivities and capacities at infinite dilution.

Equations (3-10) and (3-90) were used to calculate IDACs from experimental parameters obtained by the GC method and the IGST respectively. Excess molar enthalpies at infinite dilution were determined using equation (2-11). Some experimental data obtained in this study have been published as part of collaborative work with Prof. Nirmala Deenadayalu ($[C_13C_8]$ $[Tf_2N]$) and Mr. Eugene Olivier ([EMIM] [TfO], [BMIM] $[SbF_6]$ and [MOIM] $[PF_6]$). These results are also included in this chapter.

5.1. Results from Gas-Liquid Chromatography

5.1.1. Hexadecane

Table 5-1: Infinite dilution activity coefficients of selected organic solutes in n-hexadecane.

Solutes	T /K	$\gamma_{13}^{\infty,\exp}$	$\gamma_{13}^{\infty,lit}$	$R.D^{\#}./\ \%$
n-pentane	323.15	0.839	0.814[a]	3.1
n-pentane	333.15	0.870	0.833 [a]	4.4
n-hexane	303.15	0.882	0.880-0.904[bc]	1.8
n-hexane	313.15	0.892	0.870-0.910 [b]	1.4
n-hexane	323.15	0.896	0.860-0.905 [a bd]	0.6
n-heptane	303.15	0.882	0.916-0.927 [b]	4.3
n-heptane	323.15	0.890	0.867-0.921 [ad]	0.4
Hex-1-ene	323.15	0.862	0.855 [a]	0.8
Hept-1-ene	323.15	0.866	0.902 [a]	4.0
Cyclopentane	323.15	0.695	0.686 [a]	1.3
Cyclohexane	303.15	0.775	0.795 [b]	2.5
Cyclohexane	313.15	0.776	0.778 [b]	0.3
Cyclohexane	323.15	0.736	0.739-0.787 [ad]	3.5
Benzene	303.15	1.071	1.105-1.110 [be]	3.3
Benzene	313.15	1.010	1.006-1.051 [b]	0.4
Benzene	323.15	0.953	0.932-0.995 [ad]	2.1
Toluene	323.15	0.953	0.941 [a]	1.3
Dichloromethane	303.15	1.428	1.440[b]	0.8

[a] Schult et al. (2001); [b]Chien et al (1981) [c] Cruickshank et al. (1966b); [d] Castells et al. (1990); [e] Gainey and Young (1968)

[#] Relative deviation, R.D., given by $\frac{\left(\gamma_{13}^{\infty,\exp} - \gamma_{13}^{\infty,lit}\right)}{\gamma_{13}^{\infty,lit}} \times 100$

5.1.2. Trihexyltetradecylphosphonium bis (trifluoromethylsulfonyl) imide, $[3C_6C_{14}P]$ $[Tf_2N]$

Table 5-2: Activity coefficients at infinite dilution γ_{13}^{∞} of organic solutes in trihexyltetradecylphosphonium bis (trifluoromethylsulfonyl) imide with solvent column loading n_3 = 1.577 mmol (29.5 %) at T = (313.15, 333.15, 353.15 and 373.15) K.

Experimental γ_{13}^{∞} at T /K					
Solute	n_3/ mmol	T=313.15	T=333.15	T=353.15	T=373.15
n-pentane	1.577	0.970	0.976	0.988	0.990
n-hexane	1.577	1.101	1.119	1.126	1.130
n-heptane	1.577	1.163	1.249	1.315	1.434
n-octane	1.577	1.405	1.443	1.459	1.495
n-nonane	1.577	1.607	1.681	1.769	1.871
Pent-1-ene	1.577	0.810	0.833	0.841	0.862
Hex-1-ene	1.577	0.909	0.932	0.941	0.943
Hept-1-ene	1.577	1.030	1.064	1.102	1.123
Oct-1-ene	1.577	1.163	1.384	1.610	1.905
Pent-1-yne	1.577	0.611	0.640	0.662	0.701
Hex-1-yne	1.577	0.691	0.707	0.718	0.730
Hept-1-yne	1.577	0.730	0.747	0.764	0.780
Oct-1-yne	1.577	0.841	0.872	0.890	0.899
Nony-1-ne	1.577	0.850	0.912	0.954	0.977
Cyclopentane	1.577	0.686	0.696	0.714	0.723
Cyclohexane	1.577	0.797	0.800	0.802	0.805
Cycloheptane	1.577	0.865	0.882	0.895	0.910
Cyclooctane	1.577	0.965	1.000	1.065	1.119
Methanol	1.577	1.077	1.025	0.921	0.865
Ethanol	1.577	1.270	1.096	0.953	0.880
Propan-1-ol	1.577	1.279	1.155	1.070	0.954
Butan-1-ol	1.577	1.425	1.194	1.090	0.949
Benzene	1.577	0.390	0.403	0.414	0.432
Toluene	1.577	0.450	0.471	0.485	0.512
Acetone	1.577	0.299	0.318	0.328	0.332
Butan-2-one	1.577	0.317	0.329	0.331	0.333

Table 5-3: Activity coefficients at infinite dilution γ_{13}^{∞} of organic solutes in trihexyltetradecylphosphonium bis (trifluoromethylsulfonyl) imide with solvent column loading n_3 =2.236 mmol (31.7 %) at T = (313.15, 333.15, 353.15 and 373.15) K.

Experimental γ_{13}^{∞} at T /K					
Solute	n_3/ mmol	T=313.15	T=333.15	T=353.15	T=373.15
n-pentane	2.236	0.950	0.980	0.992	1.014
n-hexane	2.236	1.091	1.103	1.122	1.130
n-heptane	2.236	1.139	1.257	1.309	1.412
n-octane	2.236	1.403	1.439	1.463	1.491
n-nonane	2.236	1.593	1.659	1.777	1.867
Pent-1-ene	2.236	0.802	0.815	0.843	0.838
Hex-1-ene	2.236	0.905	0.910	0.919	0.941
Hept-1-ene	2.236	1.034	1.066	1.100	1.121
Oct-1-ene	2.236	1.159	1.382	1.606	1.901
Pent-1-yne	2.236	0.615	0.632	0.664	0.697
Hex-1-yne	2.236	0.695	0.711	0.722	0.734
Hept-1-yne	2.236	0.722	0.751	0.760	0.784
Oct-1-yne	2.236	0.831	0.858	0.882	0.899
Nony-1-ne	2.236	0.856	0.918	0.958	0.981
Cyclopentane	2.236	0.688	0.700	0.712	0.719
Cyclohexane	2.236	0.793	0.794	0.794	0.795
Cycloheptane	2.236	0.875	0.880	0.887	0.900
Cyclooctane	2.236	0.961	0.996	1.073	1.121
Methanol	2.236	1.089	1.027	0.923	0.861
Ethanol	2.236	1.268	1.094	0.949	0.884
Propan-1-ol	2.236	1.281	1.149	1.074	0.952
Butan-1-ol	2.236	1.421	1.188	1.080	0.959
Benzene	2.236	0.392	0.407	0.420	0.442
Toluene	2.236	0.454	0.473	0.487	0.508
Acetone	2.236	0.295	0.300	0.320	0.330
Butan-2-one	2.236	0.325	0.326	0.333	0.335

Table 5-4: Average activity coefficients at infinite dilution γ_{13}^{∞} of organic solutes in trihexyltetradecylphosphonium bis (trifluoromethylsulfonyl) imide at T = (313.15, 333.15, 353.15 and 373.15) K.

Experimental γ_{13}^{∞} at T /K				
Solute	T=313.15	T=333.15	T=353.15	T=373.15
n-pentane	0.960	0.978	0.990	1.002
n-hexane	1.096	1.111	1.124	1.130
n-heptane	1.151	1.253	1.312	1.423
n-octane	1.404	1.441	1.461	1.493
n-nonane	1.600	1.670	1.773	1.869
Pent-1-ene	0.806	0.824	0.842	0.850
Hex-1-ene	0.907	0.921	0.930	0.942
Hept-1-ene	1.032	1.065	1.101	1.122
Oct-1-ene	1.161	1.383	1.608	1.903
Pent-1-yne	0.613	0.636	0.663	0.699
Hex-1-yne	0.693	0.709	0.720	0.732
Hept-1-yne	0.726	0.749	0.762	0.782
Oct-1-yne	0.836	0.865	0.886	0.899
Non-1-yne	0.853	0.915	0.956	0.979
Cyclopentane	0.687	0.698	0.713	0.721
Cyclohexane	0.795	0.797	0.798	0.800
Cycloheptane	0.870	0.881	0.891	0.905
Cyclooctane	0.963	0.998	1.069	1.120
Methanol	1.083	1.026	0.922	0.863
Ethanol	1.269	1.095	0.951	0.882
Propan-1-ol	1.280	1.152	1.072	0.953
Butan-1-ol	1.423	1.191	1.085	0.954
Benzene	0.391	0.405	0.417	0.437
Toluene	0.452	0.472	0.486	0.510
Acetone	0.297	0.327	0.332	0.334
Butan-2-one	0.321	0.328	0.324	0.331

Table 5-5: Partial molar excess enthalpies at infinite dilution $\Delta H_1^{E,\infty}$ for organic solutes in the ionic liquid trihexyltetradecylphosphonium bis (trifluoromethylsulfonyl) imide, calculated from the Gibbs-Helmholtz equation.

SOLUTE	Linear regression using Eq.(2-11)			$\Delta H_1^{E,\infty}$
	B/1000K	A	R^2	kJ.mol^{-1}
n-pentane	-0.083	0.223	0.995	-0.69
n-hexane	-0.061	0.286	0.982	-0.51
n-heptane	-0.398	1.413	0.987	-3.31
n-octane	-0.116	0.710	0.990	-0.96
n-nonane	-0.306	1.440	0.988	-2.54
Pent-1-ene	-0.107	0.126	0.985	-0.89
Hex-1-ene	-0.072	0.132	0.995	-0.60
Hept-1-ene	-0.166	0.563	0.994	-1.38
Oct-1-ene	-0.953	3.186	0.997	-7.92
Pent-1-yne	-0.253	0.312	0.981	-2.10
Hex-1-yne	-0.105	-0.029	0.997	-0.87
Hept-1-yne	-0.140	0.129	0.991	-1.17
Oct-1-yne	-0.142	0.278	0.984	-1.18
Nony-1-ne	-0.270	0.710	0.970	-2.24
Cyclopentane	-0.097	-0.065	0.990	-0.81
Cyclohexane	-0.011	-0.192	0.982	-0.10
Cycloheptane	-0.075	0.100	0.987	-0.63
Cyclooctane	-0.303	0.923	0.978	-2.52
Methanol	0.459	-1.372	0.978	3.81
Ethanol	0.723	-2.078	0.991	6.02
Propan-1-ol	0.557	-1.528	0.987	4.63
Butan-1-ol	0.757	-2.075	0.990	6.30
Benzene	-0.211	-0.269	0.980	-1.75
Toluene	-0.228	-0.067	0.986	-1.90
Acetone	-0.079	-0.880	0.994	-0.66
Butan-2-one	-0.218	-0.514	0.998	-1.81

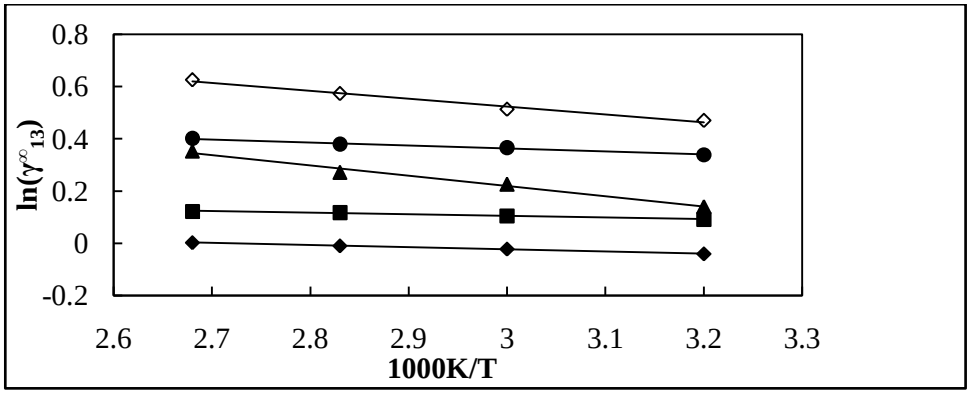

Figure 5-1: Plots of $\ln \gamma_{13}^{\infty}$ versus $1/T$ for alkanes in [$3C_6C_{14}P$] [Tf_2N] together with a linear correlation of the data using the Gibbs-Helmholtz equation; (♦) n-pentane, (■) n-hexane, (▲) n-heptane and (●) n-octane, (◊) n-nonane.

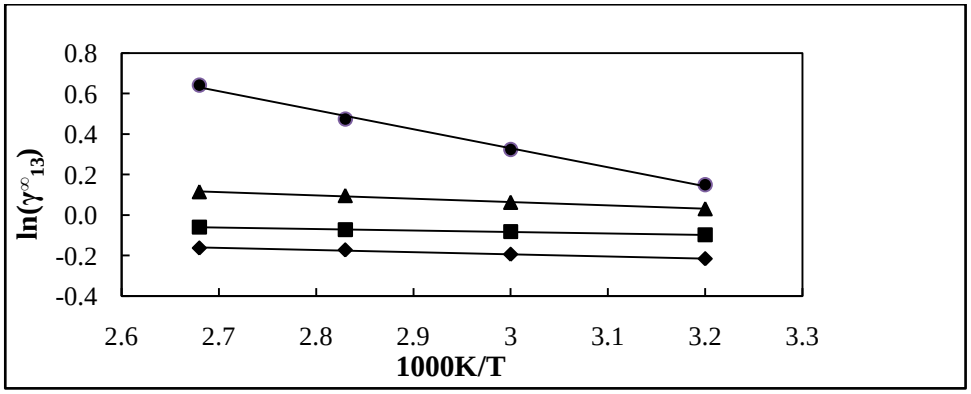

Figure 5-2: Plots of $\ln \gamma_{13}^{\infty}$ versus $1/T$ for alk-1-enes in [$3C_6C_{14}P$] [Tf_2N] together with a linear correlation of the data using the Gibbs-Helmholtz equation; (♦) pent-1-ene, (■) hex-1-ene, (▲) hept-1-ene and (●) oct-1-ene.

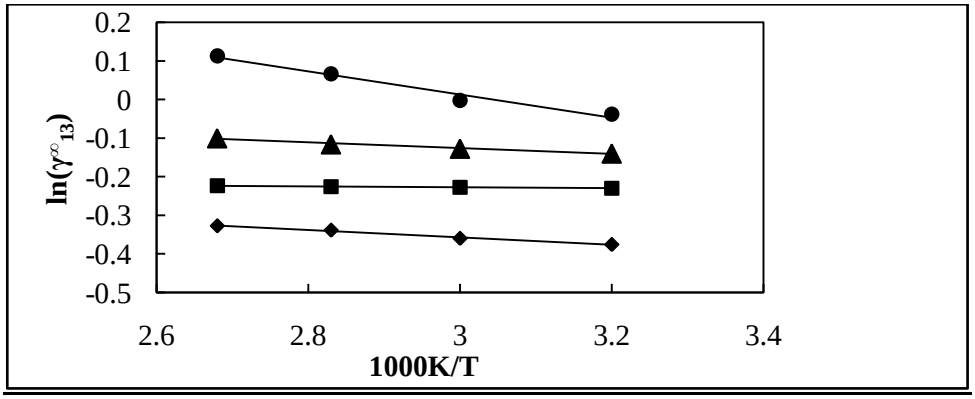

Figure 5-3: Plots of $\ln \gamma_{13}^{\infty}$ versus $1/T$ for cycloalkanes in [$3C_6C_{14}P$] [Tf_2N] together with a linear correlation of the data using the Gibbs-Helmholtz equation; (♦) cyclopentane, (■) cyclohexane, (▲) cycloheptane and (●) Cyclooctane.

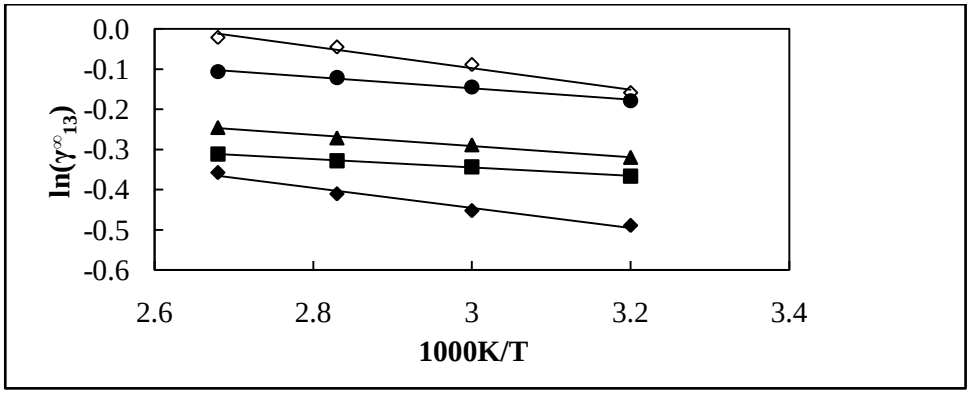

Figure 5-4: Plots of $\ln \gamma_{13}^{\infty}$ versus $1/T$ for alk-1-ynes in $[3C_6C_{14}P]$ $[Tf_2N]$ together with a linear correlation of the data using the Gibbs-Helmholtz equation; (♦)pent-1-yne, (■) hex-1-yne, (▲) hept-1-yne, (●) oct-1-yne and (◊) n-nonyne.

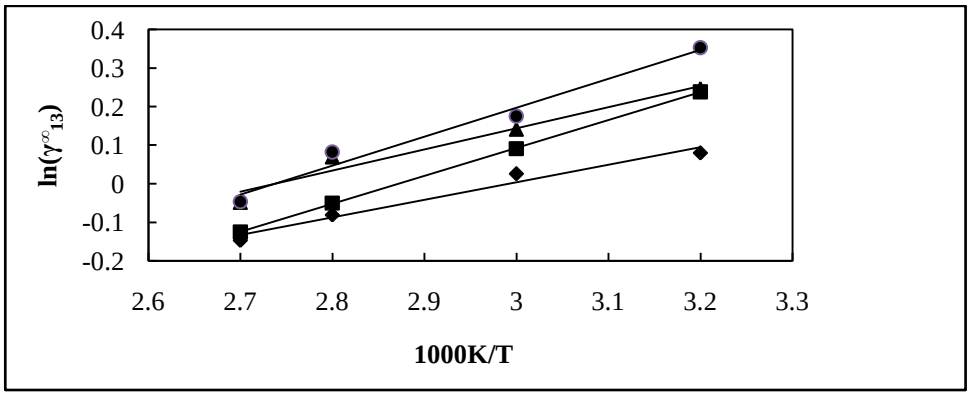

Figure 5-5: Plots of $\ln \gamma_{13}^{\infty}$ versus $1/T$ for alkanols in $[3C_6C_{14}P]$ $[Tf_2N]$ together with a linear correlation of the data using the Gibbs-Helmholtz equation; (♦) methanol, (■) ethanol, (▲) propan-1-ol and (●) butan-1-ol.

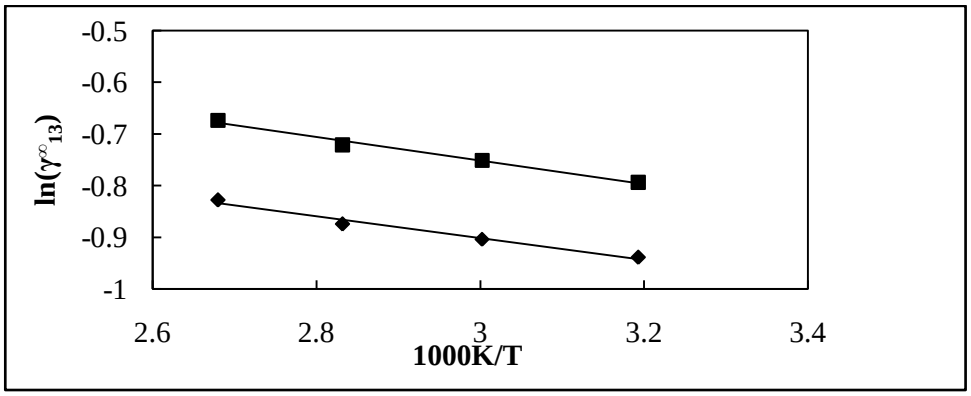

Figure 5-6: Plots of $\ln \gamma_{13}^{\infty}$ versus $1/T$ for alkylbenzenes in $[3C_6C_{14}P]$ $[Tf_2N]$ together with a linear correlation of the data using the Gibbs-Helmholtz equation; (♦) benzene and (■) toluene.

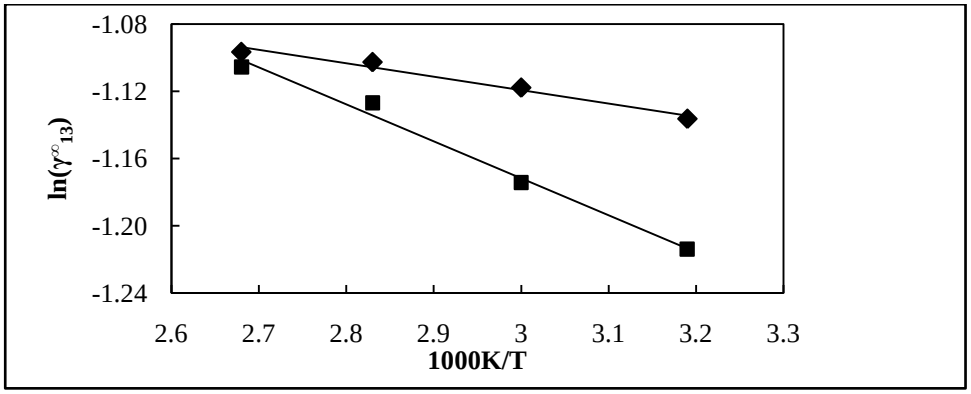

Figure 5-7: Plots of $\ln \gamma_{13}^{\infty}$ versus $1/T$ for ketones in $[3C_6C_{14}P]$ $[Tf_2N]$ together with a linear correlation of the data using the Gibbs-Helmholtz equation; (♦) acetone and (■) butan-2-one.

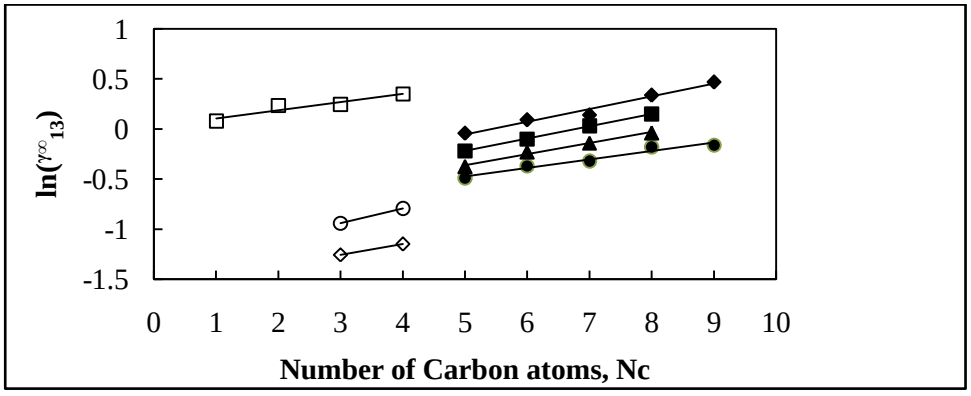

Figure 5-8: Plots of $\ln \gamma_{13}^{\infty}$ versus the carbon number of the solute at 313.15 K for (♦) n-alkanes, (■) alk-1-enes, (▲) cycloalkanes, (●) alk-1-ynes (◊) ketones, (□) alkanols and (○) alkylbenzenes in $[3C_6C_{14}P]$ $[Tf_2N]$.

5.1.3. Trihexyltetradecylphosphonium tetrafluoroborate, [$3C_6C_{14}P$] [BF_4]

Table 5-6: Activity coefficients at infinite dilution γ_{13}^{∞} of organic solutes in trihexyltetradecylphosphonium tetrafluoroborate with solvent column loading n_3 = 2.395 mmol (25.09 %) at T = (313.15, 333.15, 353.15 and 373.15) K.

Experimental γ_{13}^{∞} at T /K					
Solute	n_3/ mmol	T=313.15	T=333.15	T=353.15	T=373.15
n-pentane.	2.395	1.231	1.211	1.208	1.199
n-hexane	2.395	1.392	1.368	1.362	1.353
n-heptane	2.395	1.579	1.538	1.525	1.516
n-octane	2.395	1.792	1.769	1.711	1.697
n-nonane	2.395	2.053	1.965	1.936	1.912
n-decane	2.395	2.400	2.236	2.184	2.125
Pent-1-ene	2.395	0.971	0.984	0.992	1.017
Hex-1-ene	2.395	1.117	1.120	1.125	1.131
Hept-1-ene	2.395	1.247	1.250	1.254	1.262
Oct-1-ene	2.395	1.403	1.412	1.413	1.419
Non-1-ene	2.395	1.630	1.589	1.568	1.596
Pent-1-yne	2.395	0.569	0.591	0.624	0.690
Hex-1-yne	2.395	0.610	0.646	0.682	0.705
Hept-1-yne	2.395	0.670	0.697	0.749	0.820
Octy-1-ne	2.395	0.760	0.818	0.870	0.923
Non-1-yne	2.395	0.784	0.871	0.950	1.025
Cyclopentane	2.395	0.841	0.816	0.813	0.802
Cyclohexane	2.395	0.970	0.935	0.919	0.905
Cycloheptane	2.395	1.047	1.007	0.982	0.965
Cyclooctane	2.395	1.112	1.088	1.073	1.063
Methanol	2.395	0.548	0.500	0.466	0.453
Ethanol	2.395	0.611	0.553	0.507	0.479
Benzene	2.395	0.432	0.440	0.447	0.464
Toluene	2.395	0.524	0.539	0.546	0.564
Ethylbenzene	2.395	0.659	0.665	0.682	0.696
Acetone	2.395	0.436	0.437	0.438	0.439
Butan-2-one	2.395	0.450	0.452	0.455	0.457

Table 5-7: Activity coefficients at infinite dilution γ_{13}^{∞} of organic solutes in trihexyltetradecylphosphonium tetrafluoroborate with solvent column loading n_3 = 2.236 mmol (30.97 %) at T = (313.15, 333.15, 353.15 and 373.15) K.

Experimental γ_{13}^{∞} at T /K					
Solute	n_3/ mmol	T=313.15	T=333.15	T=353.15	T=373.15
n-pentane	2.694	1.285	1.269	1.230	1.193
n-hexane	2.694	1.408	1.400	1.358	1.311
n-heptane	2.694	1.577	1.590	1.527	1.458
n-octane	2.694	1.788	1.729	1.701	1.623
n-nonane	2.694	2.069	1.991	1.912	1.812
n-decane	2.694	2.360	2.290	2.172	2.069
Pent-1-ene	2.694	1.017	0.990	0.958	0.929
Hex-1-ene	2.694	1.101	1.090	1.083	1.073
Hept-1-ene	2.694	1.273	1.248	1.234	1.192
Oct-1-ene	2.694	1.449	1.402	1.393	1.345
Non-1-ene	2.694	1.640	1.607	1.580	1.476
Pent-1-yne	2.694	0.599	0.611	0.638	0.594
Hex-1-yne	2.694	0.596	0.650	0.668	0.697
Hept-1-yne	2.694	0.806	0.789	0.793	0.746
Oct-1-yne	2.694	0.738	0.820	0.838	0.839
Non-1-yne	2.694	0.862	0.871	0.894	0.931
Cyclopentane	2.694	0.845	0.838	0.809	0.812
Cyclohexane	2.694	0.980	0.947	0.887	0.883
Cycloheptane	2.694	0.993	0.965	0.952	0.931
Cyclooctane	2.694	1.248	1.160	1.077	1.011
Methanol	2.694	0.526	0.482	0.446	0.381
Ethanol	2.694	0.547	0.513	0.495	0.423
Benzene	2.694	0.388	0.410	0.437	0.432
Toluene	2.694	0.528	0.523	0.574	0.584
Ethylbenzene	2.694	0.661	0.677	0.686	0.734
Acetone	2.694	0.426	0.427	0.428	0.431
Butan-2-one	2.694	0.438	0.442	0.447	0.451

Table 5-8: Average activity coefficients at infinite dilution γ_{13}^{∞} of organic solutes in trihexyltetradecylphosphonium tetrafluoroborate at T = (313.15, 333.15, 353.15 and 373.15) K.

	Experimental γ_{13}^{∞} at T /K			
Solute	T=313.15	T=333.15	T=353.15	T=373.15
n-pentane.	1.258	1.240	1.219	1.196
n-hexane	1.400	1.384	1.360	1.332
n-heptane	1.578	1.564	1.526	1.487
n-octane	1.790	1.749	1.706	1.660
n-nonane	2.061	1.978	1.924	1.862
n-decane	2.380	2.263	2.178	2.097
Pent-1-ene	0.994	0.987	0.975	0.973
Hex-1-ene	1.109	1.105	1.104	1.102
Hept-1-ene	1.260	1.249	1.244	1.227
Oct-1-ene	1.426	1.407	1.403	1.382
Non-1-ene	1.635	1.598	1.574	1.536
Pent-1-yne	0.584	0.601	0.631	0.642
Hex-1-yne	0.603	0.648	0.675	0.701
Hept-1-yne	0.738	0.743	0.771	0.783
Oct-1-yne	0.749	0.819	0.854	0.881
Non-1-yne	0.823	0.871	0.922	0.978
Cyclopentane	0.843	0.827	0.811	0.807
Cyclohexane	0.975	0.941	0.903	0.894
Cycloheptane	1.020	0.986	0.967	0.948
Cyclooctane	1.180	1.124	1.075	1.037
Methanol	0.537	0.491	0.456	0.417
Ethanol	0.579	0.533	0.501	0.451
Benzene	0.410	0.425	0.442	0.448
Toluene	0.526	0.531	0.560	0.574
Ethylbenzene	0.660	0.671	0.684	0.715
Acetone	0.431	0.432	0.433	0.435
Butan-2-one	0.444	0.447	0.451	0.454

Table 5-9: Partial molar excess enthalpies at infinite dilution $\Delta H_1^{E,\infty}$ for organic solutes in the ionic liquid trihexyltetradecylphosphonium tetrafluoroborate, calculated from the Gibbs-Helmholtz equation.

SOLUTE	Linear regression using Eq.(2-11)			$\Delta H_1^{E,\infty}$
	B/1000K	A	R^2	kJ.mol^{-1}
n-pentane.	0.096	-0.077	0.984	0.80
n-hexane	0.095	0.035	0.964	0.79
n-heptane	0.115	0.093	0.933	0.96
n-octane	0.144	0.123	0.989	1.20
n-nonane	0.192	0.108	0.997	1.60
n-decane	0.241	0.093	0.999	2.00
Pent-1-ene	0.044	-0.149	0.952	0.37
Hex-1-ene	0.018	0.065	0.949	0.10
Hept-1-ene	0.048	0.077	0.939	0.40
Oct-1-ene	0.056	0.174	0.940	0.47
Non-1-ene	0.118	0.115	0.988	0.98
Pent-1-yne	-0.195	0.082	0.975	-1.62
Hex-1-yne	-0.290	0.425	0.986	-2.40
Hept-1-yne	-0.124	0.087	0.925	-1.03
Oct-1-yne	-0.312	0.720	0.960	-2.60
Non-1-yne	-0.335	0.870	0.996	-2.78
Cyclopentane	0.088	-0.455	0.966	0.74
Cyclohexane	0.177	-0.594	0.967	1.48
Cycloheptane	0.140	-0.431	0.990	1.17
Cyclooctane	0.253	-0.642	0.999	2.10
Methanol	0.486	-2.169	0.996	4.04
Ethanol	0.472	-2.046	0.981	3.92
Benzene	-0.179	-0.316	0.978	-1.49
Toluene	-0.183	-0.068	0.925	-1.52
Ethylbenzene	-0.149	0.054	0.913	-1.24
Acetone	-0.017	-0.786	0.946	-0.14
Butan-2-one	-0.044	-0.671	0.993	-0.37

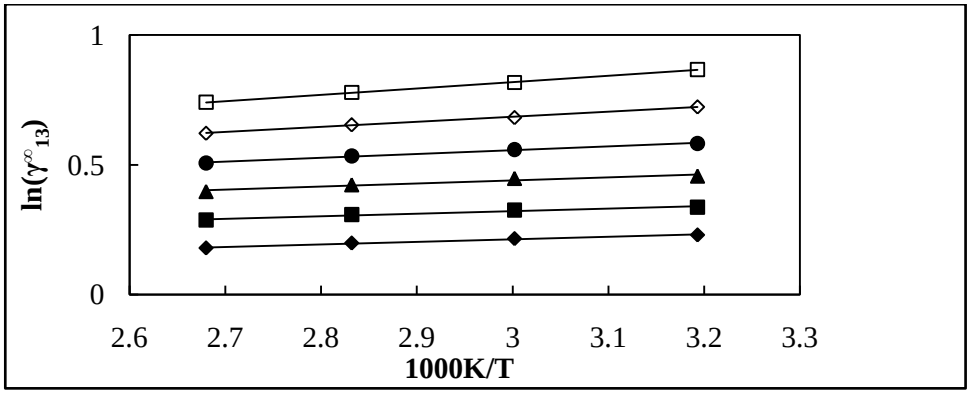

Figure 5-9: Plots of $\ln \gamma_{13}^{\infty}$ versus $1/T$ for n-alkanes in [$3C_6C_{14}P$] [BF_4] together with a linear correlation of the data using the Gibbs-Helmholtz equation; (♦) n-pentane, (■) n-hexane, (▲) n-heptane, (●) n-octane, (◊) n-nonane and (□) n-decane.

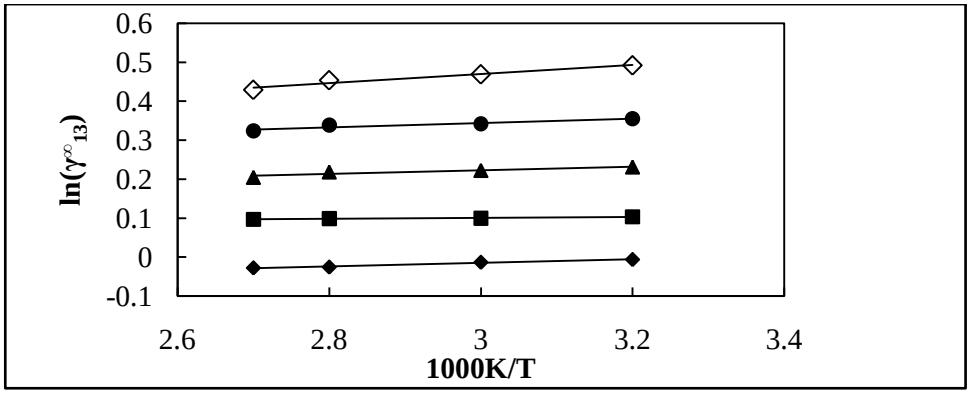

Figure 5-10: Plots of $\ln \gamma_{13}^{\infty}$ versus $1/T$ for alk-1-enes in [$3C_6C_{14}P$] [BF_4] together with a linear correlation of the data using the Gibbs-Helmholtz equation; (♦) pent-1-ene, (■) hex-1-ene, (▲) hept-1ene, (●) oct-1-ene and (◊) non-1-ene.

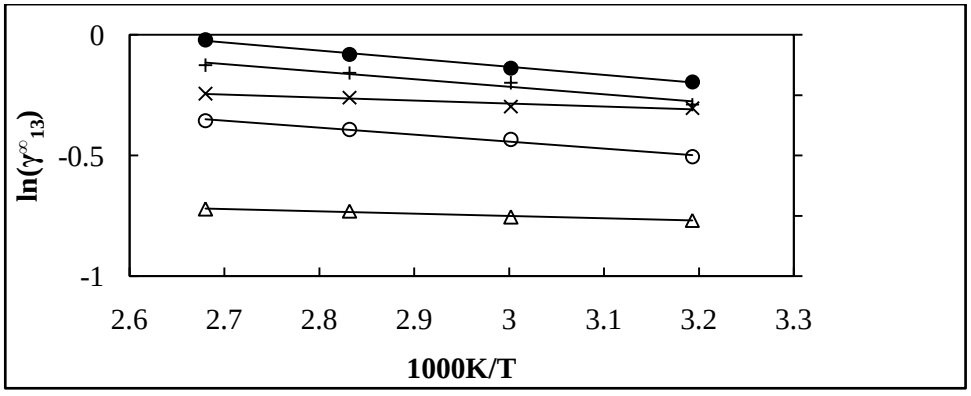

Figure 5-11: Plots of $\ln \gamma_{13}^{\infty}$ versus $1/T$ for alk-1-ynes in [$3C_6C_{14}P$] [BF_4] together with a linear correlation of the data using the Gibbs-Helmholtz equation; (Δ) pent-1-yne, (○) hex-1-yne, (x) hept-1-yne, (+) oct-1-yne and (●) non-1-yne.

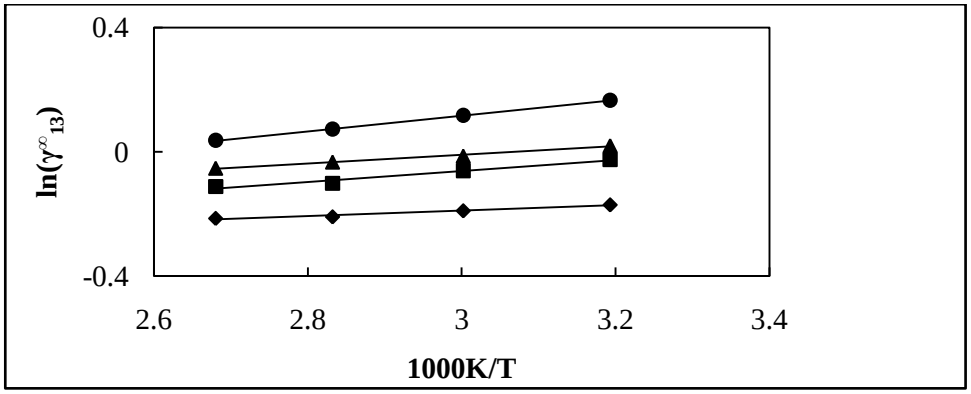

Figure 5-12: Plots of $\ln \gamma_{13}^{\infty}$ versus $1/T$ for cycloalkanes in [$3C_6C_{14}P$] [BF_4] together with a linear correlation of the data using the Gibbs-Helmholtz equation; (♦) cyclopentane, (■) cyclohexane, (▲) cycloheptane and (●) cyclooctane.

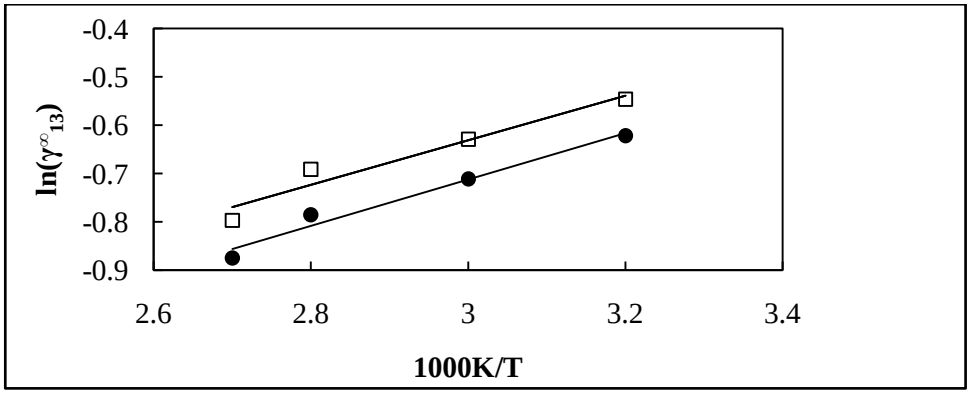

Figure 5-13: Plots of $\ln \gamma_{13}^{\infty}$ versus $1/T$ for alkanols in [$3C_6C_{14}P$] [BF_4] together with a linear correlation of the data using the Gibbs-Helmholtz equation; (●) methanol and (□) ethanol.

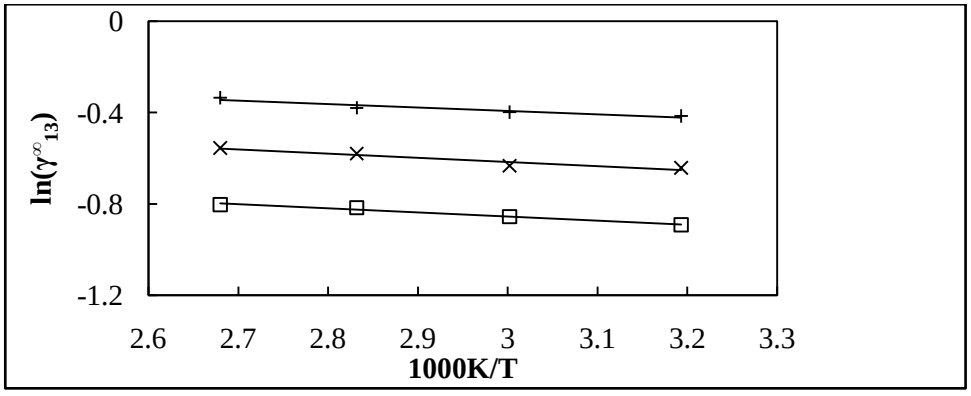

Figure 5-14: Plots of $\ln \gamma_{13}^{\infty}$ versus $1/T$ for alkylbenzenes in [$3C_6C_{14}P$] [BF_4] together with a linear correlation of the data using the Gibbs-Helmholtz equation; (□) benzene, (x) toluene and (+) ethylbenzene.

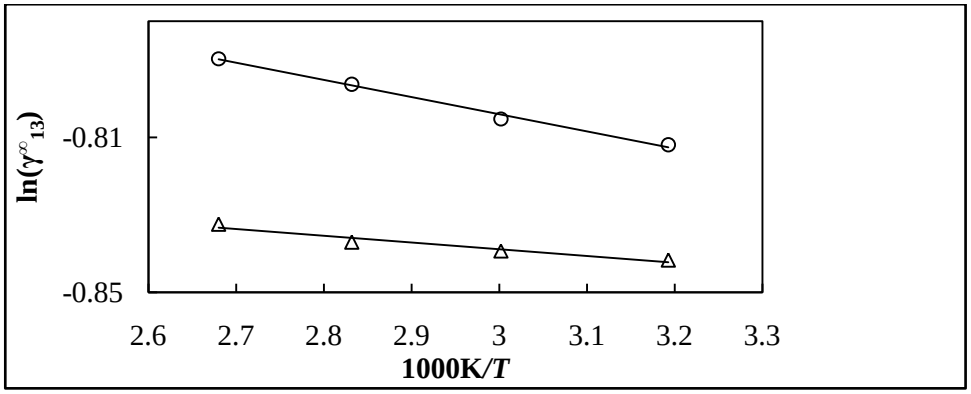

Figure 5-15: Plots of $\ln \gamma_{13}^{\infty}$ versus $1/T$ for ketones in [$3C_6C_{14}P$] [BF_4] together with a linear correlation of the data using the Gibbs-Helmholtz equation; (Δ) acetone and (○) butan-2-one.

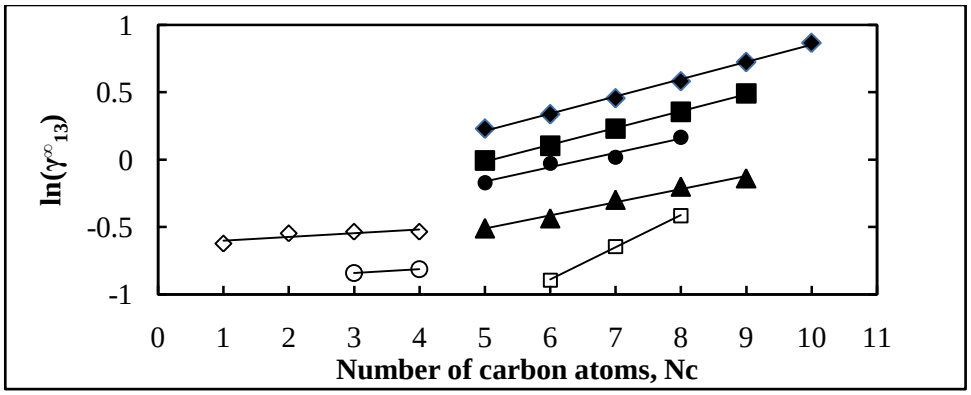

Figure 5-16: Plots of $\ln \gamma_{13}^{\infty}$ versus the number of carbon atoms at 313.15 K for (♦) n-alkanes, (■) alk-1-enes, (▲) alk-1-ynes, (●) cycloalkanes, (◊) alkanols, (□) alkylbenzenes and (○) ketones in [$3C_6C_{14}P$] [BF_4].

5.1.4. Trihexyltetradecylphosphonium hexafluorophosphate, [$3C_6C_{14}P$] [PF_6]

Table 5-10: Activity coefficients at infinite dilution γ_{13}^{∞} of organic solutes in trihexyltetradecylphosphonium hexafluorophosphate with n_3 = 1.615 mmol (25.1 %) at T = (313.15, 333.15, 353.15 and 363.15) K.

Experimental γ_{13}^{∞} at T /K					
Solute	n_3/mmol	T=313.15	T=333.15	T=353.15	T=363.15
n-pentane.	1.615	1.773	1.517	1.268	1.193
n-hexane	1.615	1.960	1.687	1.482	1.430
n-heptane	1.615	2.246	1.806	1.648	1.555
n-octane	1.615	2.528	2.120	1.869	1.812
n-nonane	1.615	2.774	2.426	2.088	1.984
n-decane	1.615	3.278	2.620	2.295	2.186
Pent-1-ene	1.615	1.421	1.236	1.066	1.049
Hex-1-ene	1.615	1.665	1.410	1.138	1.128
Hept-1-ene	1.615	1.857	1.581	1.321	1.269
Oct-1-ene	1.615	2.023	1.752	1.514	1.437
Non-1-ene	1.615	2.400	2.013	1.617	1.539
Dec-1-ene	1.615	2.788	2.276	1.827	1.750
Pent-1-yne	1.615	1.025	0.549	0.697	0.668
Hex-1-yne	1.615	1.145	0.649	0.780	0.732
Hept-1-yne	1.615	1.216	0.630	0.833	0.798
Oct-1-yne	1.615	1.369	0.754	0.962	0.928
Non-1-yne	1.615	1.476	0.827	1.063	0.978
Dec-1-yne	1.615	1.595	0.865	1.117	1.031
Cyclopentane	1.615	1.348	1.079	0.901	0.883
Cyclohexane	1.615	1.475	1.212	0.969	0.951
Cycloheptane	1.615	1.574	1.299	1.084	1.035
Cyclooctane	1.615	1.643	1.402	1.171	1.115
Cyclononane	1.615	1.883	1.567	1.319	1.234
Methanol	1.615	2.115	1.412	0.938	0.855
Ethanol	1.615	2.215	1.515	0.989	0.893
Benzene	1.615	0.659	0.543	0.438	0.415
Toluene	1.615	0.772	0.671	0.535	0.506
Ethylbenzene	1.615	0.961	0.783	0.630	0.626
Propylbenzene	1.615	1.103	0.949	0.779	0.735
Acetone	1.615	0.648	0.517	0.388	0.371
Butan-2-one	1.615	0.677	0.524	0.396	0.375

Table 5-11: Activity coefficients at infinite dilution γ_{13}^{∞} of organic solutes in trihexyltetradecylphosphonium hexafluorophosphate with n_3 = 2.659 mmol (29.4 %) at T = (313.15, 333.15, 353.15 and 363.15) K.

Experimental γ_{13}^{∞} at T /K					
Solute	n_3/mmol	T=313.15	T=333.15	T=353.15	T=363.15
n-pentane.	2.659	1.921	1.553	1.288	1.251
n-hexane	2.659	2.072	1.795	1.496	1.472
n-heptane	2.659	2.194	2.004	1.668	1.651
n-octane	2.659	2.492	2.184	1.831	1.742
n-nonane	2.659	3.040	2.468	2.054	2.004
n-decane	2.659	3.324	2.896	2.309	2.236
Pent-1-ene	2.659	1.541	1.368	1.134	1.069
Hex-1-ene	2.659	1.701	1.436	1.264	1.174
Hept-1-ene	2.659	1.903	1.591	1.361	1.299
Oct-1-ene	2.659	2.199	1.794	1.484	1.433
Non-1-ene	2.659	2.496	1.975	1.627	1.549
Dec-1-ene	2.659	2.810	2.290	1.851	1.740
Pent-1-yne	2.659	1.061	0.861	0.713	0.654
Hex-1-yne	2.659	1.125	0.889	0.758	0.714
Hept-1-yne	2.659	1.250	1.034	0.831	0.822
Oct-1-yne	2.659	1.333	1.160	0.952	0.942
Non-1-yne	2.659	1.498	1.247	1.011	0.966
Dec-1-yne	2.659	1.615	1.315	1.063	1.009
Cyclopentane	2.659	1.344	1.141	0.941	0.871
Cyclohexane	2.659	1.459	1.234	1.049	0.991
Cycloheptane	2.659	1.602	1.335	1.100	1.049
Cyclooctane	2.659	1.799	1.442	1.199	1.143
Cyclononane	2.659	1.891	1.601	1.333	1.304
Methanol	2.659	2.139	1.444	0.984	0.881
Ethanol	2.659	2.315	1.491	1.015	0.911
Benzene	2.659	0.705	0.553	0.448	0.419
Toluene	2.659	0.814	0.639	0.541	0.516
Ethylbenzene	2.659	1.005	0.835	0.694	0.642
Propylbenzene	2.659	1.139	0.939	0.799	0.777
Acetone	2.659	0.694	0.507	0.404	0.381
Butan-2-one	2.659	0.735	0.542	0.410	0.373

Table 5-12: Average activity coefficients at infinite dilution γ_{13}^{∞} of organic solutes in trihexyltetradecylphosphonium hexafluorophosphate at T = (313.15, 333.15, 353.15 and 363.15) K.

	Experimental γ_{13}^{∞} at T /K			
Solute	T=313.15	T=333.15	T=353.15	T=363.15
n-pentane.	1.847	1.535	1.278	1.222
n-hexane	2.016	1.741	1.489	1.451
n-heptane	2.220	1.905	1.658	1.603
n-octane	2.510	2.152	1.850	1.777
n-nonane	2.907	2.447	2.071	1.994
n-decane	3.301	2.758	2.302	2.211
Pent-1-ene	1.481	1.302	1.100	1.059
Hex-1-ene	1.683	1.423	1.201	1.151
Hept-1-ene	1.880	1.586	1.341	1.284
Oct-1-ene	2.111	1.773	1.499	1.435
Non-1-ene	2.448	1.994	1.622	1.544
Dec-1-ene	2.799	2.283	1.839	1.745
Pent-1-yne	1.043	0.852	0.705	0.661
Hex-1-yne	1.135	0.898	0.769	0.723
Hept-1-yne	1.233	1.003	0.832	0.810
Oct-1-yne	1.351	1.161	0.957	0.935
Non-1-yne	1.487	1.250	1.037	0.972
Dec-1-yne	1.605	1.354	1.090	1.020
Cyclopentane	1.346	1.110	0.921	0.877
Cyclohexane	1.467	1.223	1.009	0.971
Cycloheptane	1.588	1.317	1.092	1.042
Cyclooctane	1.721	1.422	1.185	1.129
Cyclononane	1.887	1.584	1.326	1.269
Methanol	2.127	1.428	0.961	0.868
Ethanol	2.265	1.503	1.002	0.902
Benzene	0.682	0.548	0.443	0.417
Toluene	0.793	0.655	0.538	0.511
Ethylbenzene	0.983	0.809	0.662	0.634
Propylbenzene	1.121	0.944	0.789	0.756
Acetone	0.671	0.512	0.396	0.376
Butan-2-one	0.706	0.533	0.403	0.374

Table 5-13: Partial molar excess enthalpies at infinite dilution $\Delta H_1^{E,\infty}$ for organic solutes in the ionic liquid trihexyltetradecylphosphonium hexafluorophosphate calculated from the Gibbs-equation.

SOLUTE	Linear regression using Eq.(2-11)			$\Delta H_1^{E,\infty}$
	B/1000K	*A*	R^2	kJ.mol^{-1}
n-pentane.	0.918	-2.325	0.999	7.63
n-hexane	0.742	-1.673	0.999	6.17
n-heptane	0.722	-1.516	0.999	6.00
n-octane	0.765	-1.528	0.999	6.36
n-nonane	0.839	-1.621	0.999	6.98
n-decane	0.894	-1.668	0.999	7.43
Pent-1-ene	0.754	-2.014	0.999	6.27
Hex-1-ene	0.844	-2.181	0.999	7.02
Hept-1-ene	0.845	-2.075	0.999	7.03
Oct-1-ene	0.855	-1.991	0.999	7.11
Non-1-ene	1.026	-2.388	0.999	8.53
Dec-1-ene	1.053	-2.338	0.999	8.76
Pent-1-yne	0.741	-1.979	0.999	6.16
Hex-1-yne	0.845	-2.183	0.999	7.03
Hept-1-yne	0.850	-2.087	0.999	7.07
Oct-1-yne	0.857	-1.998	0.999	7.13
Non-1-yne	1.028	-2.396	0.999	8.55
Dec-1-yne	1.093	-2.445	0.982	9.09
Cyclopentane	0.949	-2.741	0.999	7.89
Cyclohexane	0.925	-2.578	0.999	7.69
Cycloheptane	0.936	-2.533	0.999	7.78
Cyclooctane	0.933	-2.445	0.999	7.76
Cyclononane	0.882	-2.188	0.999	7.33
Methanol	1.989	-5.611	0.999	16.54
Ethanol	2.042	-5.718	0.999	16.98
Benzene	1.086	-3.860	0.999	9.03
Toluene	0.975	-3.352	0.999	8.11
Ethylbenzene	0.980	-3.154	0.999	8.15
Propylbenzene	0.878	-2.694	0.999	7.30
Acetone	1.294	-4.545	0.999	10.76
Butan-2-one	1.408	-4.853	0.999	11.71

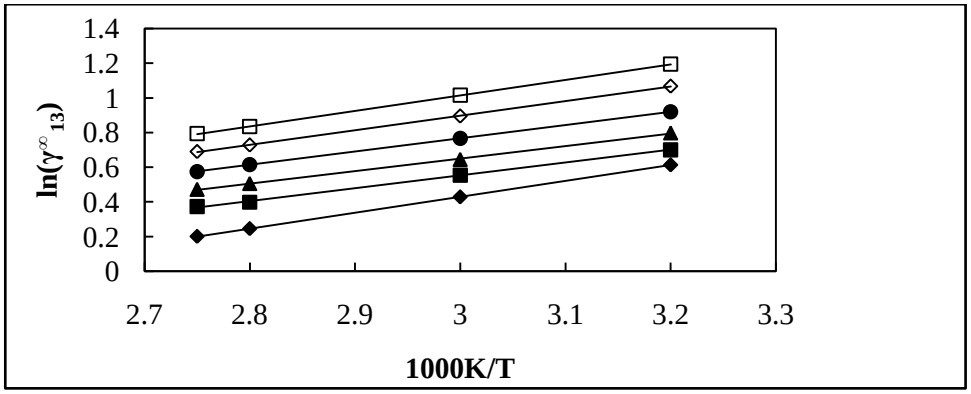

Figure 5-17: Plots of $\ln \gamma_{13}^{\infty}$ versus $1/T$ for alkanes in $[3C_6C_{14}P]$ $[PF_6]$ together with a linear correlation of the data using the Gibbs-Helmholtz equation; (♦) n-pentane, (■) n-hexane, (▲) n-heptane, (●) n-octane, (◊) n-nonane and (□) n-decane.

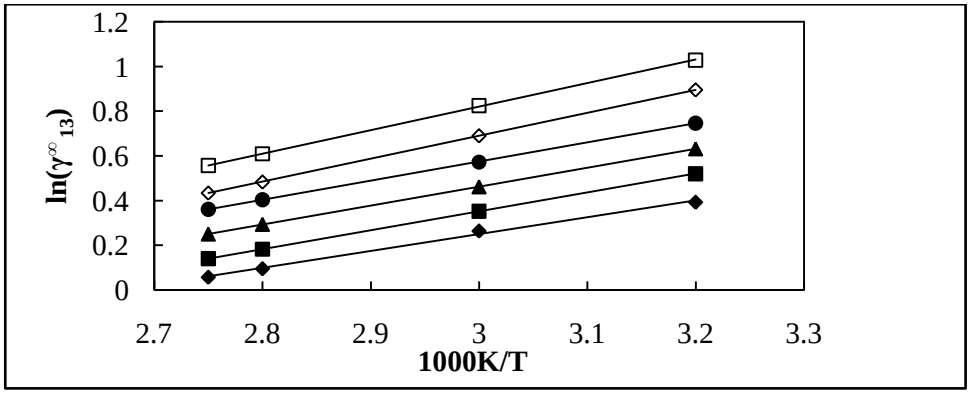

Figure 5-18: Plots of $\ln \gamma_{13}^{\infty}$ versus $1/T$ for alk-1-enes in $[3C_6C_{14}P]$ $[PF_6]$ together with a linear correlation of the data using the Gibbs-Helmholtz equation; (♦) pent-1-ene, (■) hex-1-ene, (▲) hept-1-ene, (●) oct-1-ene and (◊) non-1-ene.

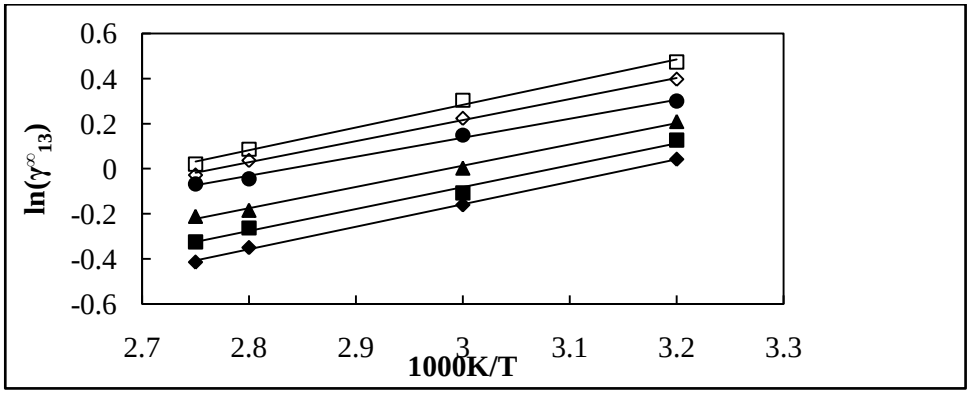

Figure 5-19: Plots of $\ln \gamma_{13}^{\infty}$ versus $1/T$ for alk-1-ynes in $[3C_6C_{14}P]$ $[PF_6]$ together with a linear correlation of the data using the Gibbs-Helmholtz equation; (♦) pent-1-yne, (■) hex-1-yne, (▲) hept-1-yne and (●) oct-1-yne.

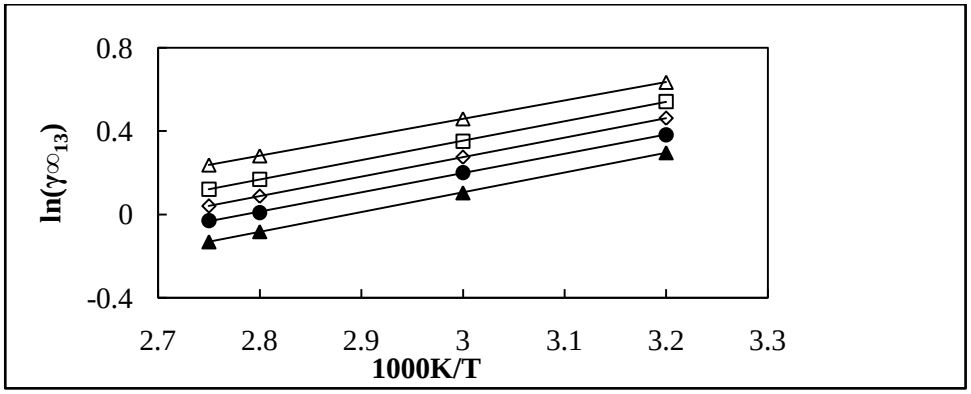

Figure 5-20: Plots of $\ln \gamma_{13}^{\infty}$ versus $1/T$ for cycloalkanes in [$3C_6C_{14}P$] [PF_6] together with a linear correlation of the data using the Gibbs-Helmholtz equation; (▲) cyclopentane, (●) cyclohexane, (◊) cycloheptane, (□) cyclooctane and (Δ) Cyclononane.

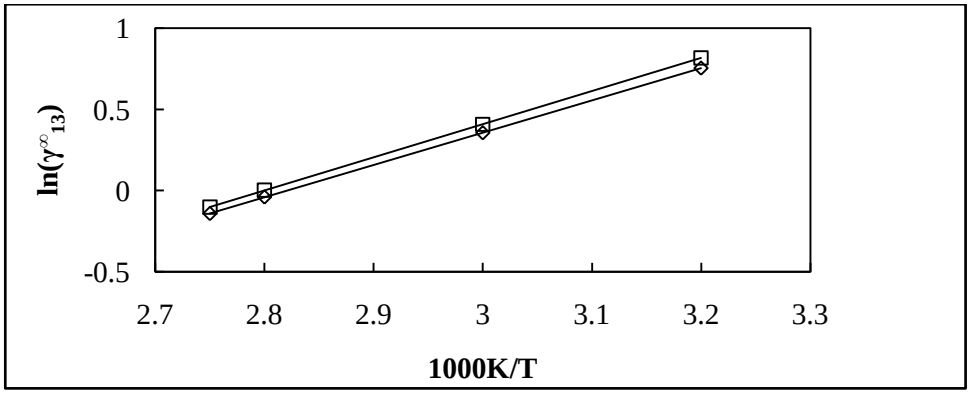

Figure 5-21: Plots of $\ln \gamma_{13}^{\infty}$ versus $1/T$ for alkanols in [$3C_6C_{14}P$] [PF_6] together with a linear correlation of the data using the Gibbs-Helmholtz equation; (◊) methanol and (□) ethanol

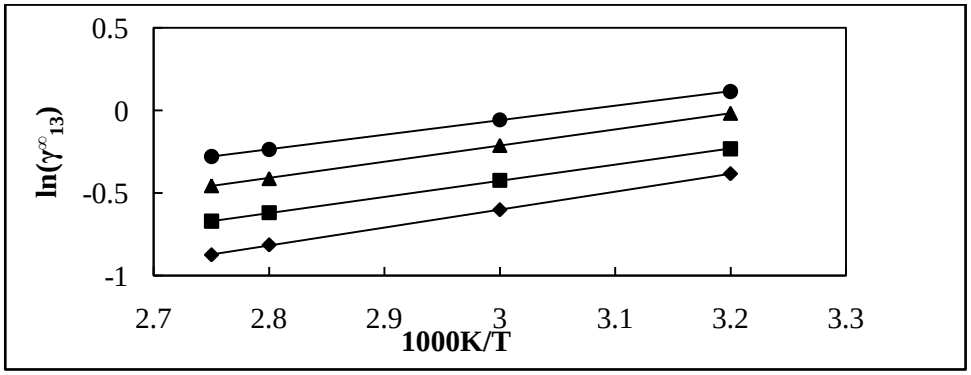

Figure 5-22: Plots of $\ln \gamma_{13}^{\infty}$ versus $1/T$ for alkylbenzenes in [$3C_6C_{14}P$] [PF_6] together with a linear correlation of the data using the Gibbs-Helmholtz equation; (♦) benzene, (■) toluene, (▲) ethylbenzene and (●) propylbenzene.

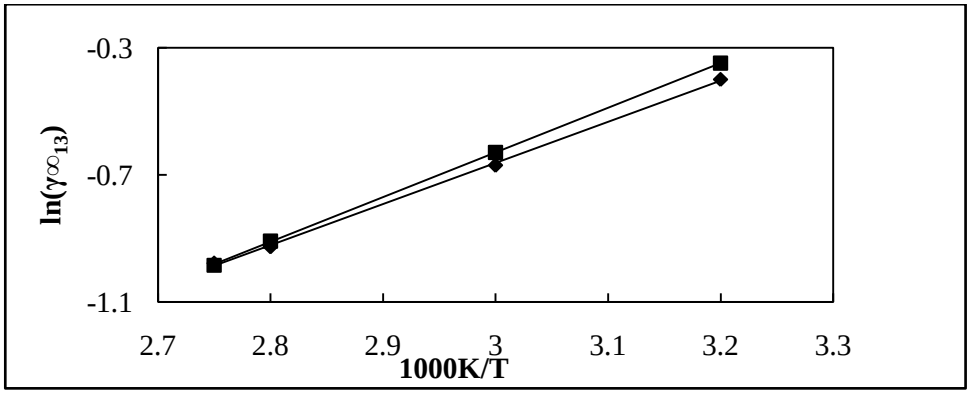

Figure 5-23: Plots of $\ln \gamma_{13}^{\infty}$ versus $1/T$ for ketones in $[3C_6C_{14}P]$ $[PF_6]$ together with a linear correlation of the data using the Gibbs-Helmholtz equation; (♦) acetone and (■) butan-2-one.

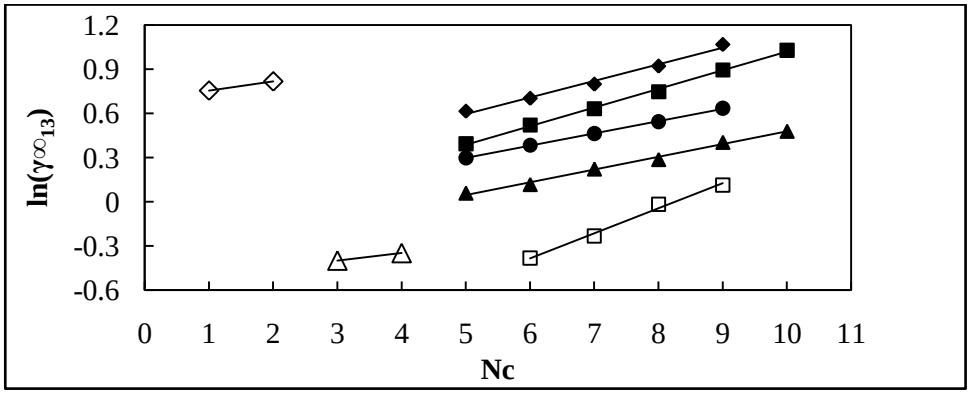

Figure 5-24: Plots of $\ln \gamma_{13}^{\infty}$ versus the number of carbon atoms at 313.15 K for (♦)n-alkanes, (■) alk-1-enes, (▲) alk-1-ynes, (●) cycloalkanes, (◊) alkanols, (□) alkylbenzenes and (Δ) ketones in $[3C_6C_{14}P]$ $[PF_6]$.

5.1.5. Methyltrioctylammonium bis (trifluoromethylsulfonyl) imide, [$C_1 3C_8 N$] [$Tf_2 N$].

Table 5-14: Activity coefficients at infinite dilution γ_{13}^{∞} of organic solutes in methyltrioctylammonium bis (trifluoromethylsulfonyl) imide with n_3 = 1.77 mmol (25.33 %) at T = (303.15, 313.15 and 323.15) K.

Experimental γ_{13}^{∞} at T /K				
Solute	n_3/mmol	T=303.15	T=313.15	T=323.15
n-pentane	1.77	1.47	1.44	1.42
n-hexane	1.77	1.70	1.72	1.69
n-heptane	1.77	1.85	1.83	1.83
n-octane	1.77	2.17	2.06	2.04
n-nonane	1.77	2.57	2.39	2.21
n-decane	1.77	3.20	2.72	2.50
Pent-1-ene	1.77	1.16	1.17	1.14
Hex-1-ene	1.77	1.22	1.21	1.21
Hept-1-ene	1.77	1.44	1.43	1.42
Oct-1-ene	1.77	1.69	1.67	1.66
Non-1-ene	1.77	1.99	1.91	1.85
Dec-1-ene	1.77	2.22	2.11	2.05
Pent-1-yne	1.77	0.72	0.74	0.75
Hex-1-yne	1.77	0.83	0.86	0.87
Hept-1-yne	1.77	0.89	0.91	0.92
Oct-1-yne	1.77	1.05	1.06	1.08
Non-1-yne	1.77	1.15	1.17	1.18
Dec-1-yne	1.77	1.30	1.31	1.34
Cyclopentane	1.77	0.90	0.98	0.97
Cyclohexane	1.77	1.18	1.19	1.16
Cycloheptane	1.77	1.32	1.31	1.26
Cyclooctane	1.77	1.54	1.47	1.43
Cyclononane	1.77	1.74	1.68	1.61
Methanol	1.77	1.26	1.19	1.11
Ethanol	1.77	1.32	1.24	1.13
Benzene	1.77	0.45	0.43	0.43
Toluene	1.77	0.51	0.52	0.53
Acetone	1.77	0.35	0.38	0.44
Butan-2-one	1.77	0.34	0.35	0.39

Table 5-15: Activity coefficients at infinite dilution γ_{13}^{∞} of organic solutes in methyltrioctylammonium bis (trifluoromethylsulfonyl) imide with n_3 = 2.044 mmol (29.63 %) at T = (303.15, 313.15 and 323.15) K.

Experimental γ_{13}^{∞} at T /K				
Solute	n_3/mmol	T=303.15	T=313.15	T=323.15
n-pentane	2.044	1.43	1.44	1.44
n-hexane	2.044	1.68	1.60	1.61
n-heptane	2.044	1.83	1.81	1.79
n-octane	2.044	2.23	2.16	2.10
n-nonane	2.044	2.59	2.39	2.21
n-decane	2.044	3.00	2.72	2.50
Pent-1-ene	2.044	1.14	1.11	1.12
Hex-1-ene	2.044	1.30	1.29	1.27
Hept-1-ene	2.044	1.44	1.43	1.42
Oct-1-ene	2.044	1.69	1.67	1.66
Non-1-ene	2.044	1.99	1.91	1.85
Dec-1-ene	2.044	2.22	2.11	2.05
Pent-1-yne	2.044	0.74	0.74	0.77
Hex-1-yne	2.044	0.83	0.84	0.85
Hept-1-yne	2.044	0.89	0.91	0.92
Oct-1-yne	2.044	1.05	1.06	1.08
Non-1-yne	2.044	1.15	1.17	1.18
Dec-1-yne	2.044	1.30	1.31	1.34
Cyclopentane	2.044	1.10	1.00	0.99
Cyclohexane	2.044	1.20	1.15	1.14
Cycloheptane	2.044	1.34	1.29	1.28
Cyclooctane	2.044	1.52	1.47	1.43
Cyclononane	2.044	1.74	1.68	1.61
Methanol	2.044	1.24	1.17	1.15
Ethanol	2.044	1.34	1.24	1.17
Benzene	2.044	0.43	0.45	0.47
Toluene	2.044	0.51	0.52	0.53
Acetone	2.044	0.35	0.38	0.44
Butan-2-one	2.044	0.34	0.37	0.41

Table 5-16: Average activity coefficients at infinite dilution γ_{13}^{∞} of organic solutes in methyltrioctylammonium bis (trifluoromethylsulfonyl) imide at T = (303.15, 313.15 and 323.15) K.

Experimental γ_{13}^{∞} at T /K			
Solute	T=303.15	T=313.15	T=323.15
n-pentane	1.45	1.44	1.43
n-hexane	1.69	1.66	1.65
n-heptane	1.84	1.82	1.81
n-octane	2.20	2.11	2.07
n-nonane	2.58	2.39	2.21
n-decane	3.10	2.72	2.50
Pent-1-ene	1.15	1.14	1.13
Hex-1-ene	1.26	1.25	1.24
Hept-1-ene	1.44	1.43	1.42
Oct-1-ene	1.69	1.67	1.66
Non-1-ene	1.99	1.91	1.85
Dec-1-ene	2.22	2.11	2.05
Pent-1-yne	0.73	0.74	0.76
Hex-1-yne	0.83	0.85	0.86
Hept-1-yne	0.89	0.91	0.92
Oct-1-yne	1.05	1.06	1.08
Non-1-yne	1.15	1.17	1.18
Dec-1-yne	1.30	1.31	1.34
Cyclopentane	1.00	0.99	0.98
Cyclohexane	1.19	1.17	1.15
Cycloheptane	1.33	1.30	1.27
Cyclooctane	1.53	1.47	1.43
Cyclononane	1.74	1.68	1.61
Methanol	1.25	1.18	1.13
Ethanol	1.33	1.24	1.15
Benzene	0.44	0.44	0.45
Toluene	0.51	0.52	0.53
Acetone	0.35	0.38	0.44
Butan-2-one	0.34	0.36	0.40

Table 5-17: Excess molar enthalpies at infinite dilution $\Delta H_1^{E,\infty}$ of organic solutes in the ionic liquid methyltrioctylammonium bis (trifluoromethylsulfonyl) imide, calculated using the Gibbs-Helmholtz equation.

SOLUTE	Linear regression using Eq.(2-11)			$\Delta H_1^{E,\infty}$
	B/1000K	*A*	R^2	*kJ.mol*$^{-1}$
n-pentane	0.694	0.142	1.00	5.77
n-hexane	0.120	0.128	0.92	1.00
n-heptane	0.082	0.338	0.97	0.68
n-octane	0.305	-0.220	0.96	2.53
n-nonane	0.774	-1.606	1.00	6.44
n-decane	1.075	-2.425	0.99	8.93
Pent-1-ene	0.088	-0.150	1.00	0.73
Hex-1-ene	0.080	-0.033	1.00	0.67
Hept-1-ene	0.105	0.028	0.96	0.87
Oct-1-ene	0.120	0.128	0.92	1.00
Non-1-ene	0.419	-0.698	0.98	3.48
Dec-1-ene	0.419	-0.580	0.97	3.48
Pent-1-yne	-0.201	0.348	0.97	-1.67
Hex-1-yne	-0.178	0.402	0.96	-1.48
Hept-1-yne	-0.111	0.250	1.00	-0.92
Oct-1-yne	-0.140	0.517	0.97	-1.16
Non-1-yne	-0.129	0.563	0.97	-1.07
Dec-1-yne	-0.114	0.640	0.96	-0.95
Cyclopentane	0.101	-3.333	1.00	0.84
Cyclohexane	0.171	-0.390	1.00	1.42
Cycloheptane	0.231	-0.476	1.00	1.92
Cyclooctane	0.338	-0.692	0.99	2.81
Cyclononane	0.386	-0.715	1.00	3.21
Methanol	0.505	-1.445	0.99	4.20
Ethanol	0.727	-2.113	1.00	6.05
Benzene	-0.112	-0.454	0.75	-0.93
Toluene	-0.286	0.267	0.97	-2.38
Acetone	-0.962	2.062	0.98	-8.00
Butan-2-one	-1.029	2.349	1.00	-8.56

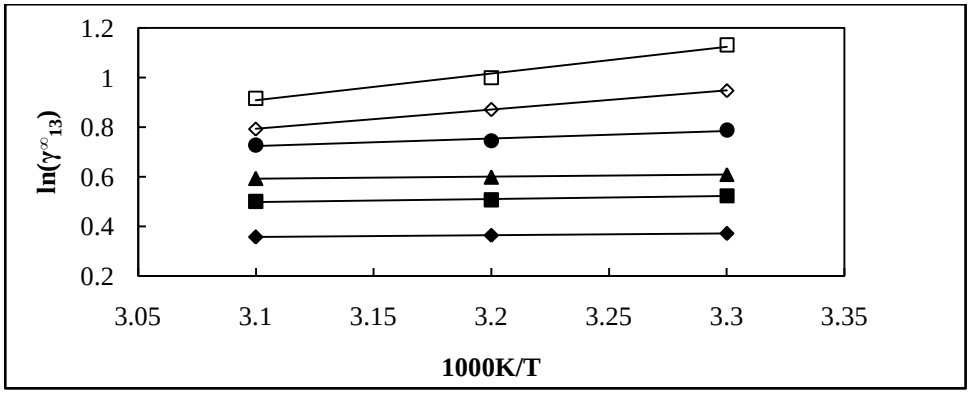

Figure 5-25: Plots of $\ln \gamma_{13}^{\infty}$ versus $1/T$ for alkanes in [$C_1$3C_8N] [Tf_2N] together with a linear correlation of the data using the Gibbs-Helmholtz equation; (♦) n-pentane, (■) n-hexane, (▲) n-heptane, (●) n-octane, (◊) n-nonane and (□) n-decane.

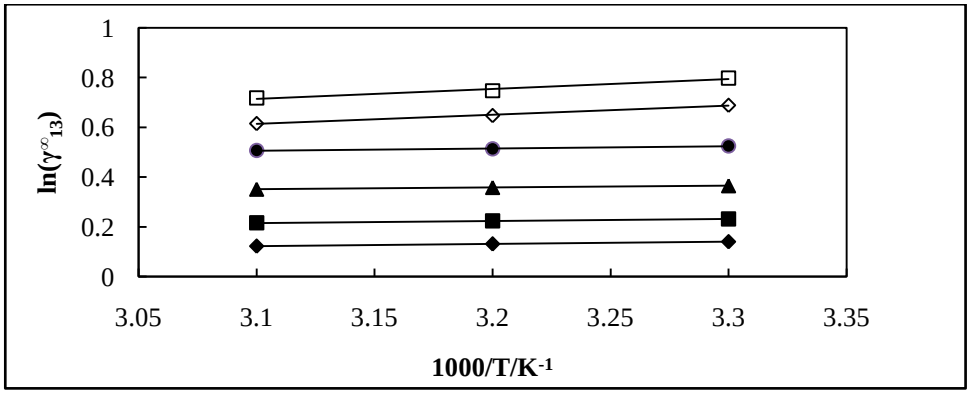

Figure 5-26: Plots of $\ln \gamma_{13}^{\infty}$ versus $1/T$ for alk-1-enes in [$C_1$3C_8N] [Tf_2N] together with a linear correlation of the data using the Gibbs-Helmholtz equation; (♦) pent-1-ene, (■) hex-1-ene, (▲) hept-1-ene, (●) oct-1-ene, (◊) non-1-ene and (□) dec-1-ene.

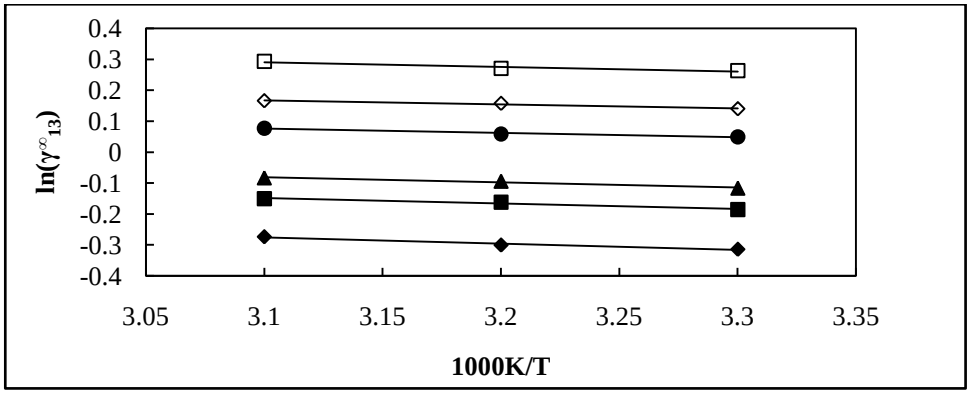

Figure 5-27: Plots of $\ln \gamma_{13}^{\infty}$ versus $1/T$ for alk-1-ynes in [$C_1$3C_8N] [Tf_2N] together with a linear correlation of the data using the Gibbs-Helmholtz equation; (♦) pent-1-y-ne, (■) hex-1-yne, (▲) hept-1-yne, (●) oct-1-yne, (◊) non-1-yne and (□) dec-1-yne.

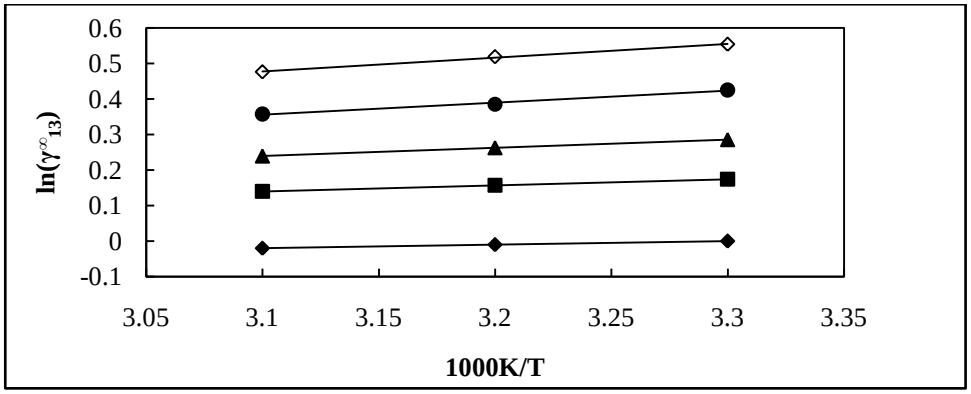

Figure 5-28: Plots of $\ln \gamma_{13}^{\infty}$ versus $1/T$ for cycloalkanes in [$C_1$3C_8N] [Tf_2N] together with a linear correlation of the data using the Gibbs-Helmholtz equation; (♦) cyclopentane, (■) cyclohexane, (▲) cycloheptane, (●) cyclooctane and (◊) cyclononane.

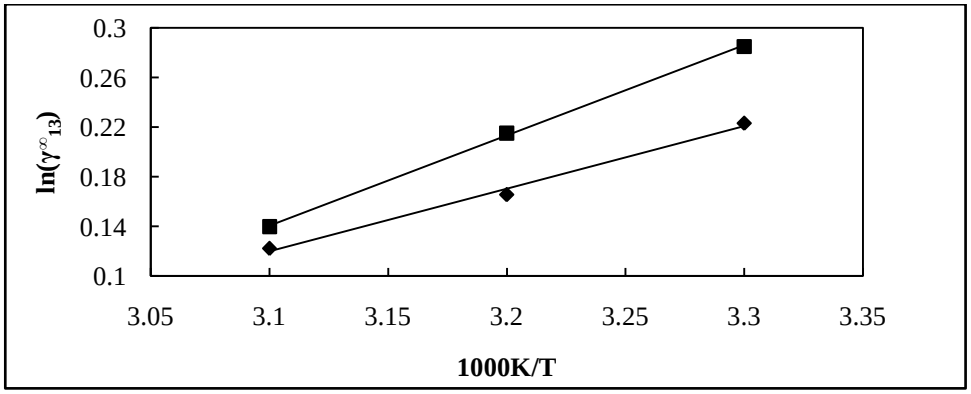

Figure 5-29: Plots of $\ln \gamma_{13}^{\infty}$ versus $1/T$ for alkanols in [$C_1$3C_8N] [Tf_2N] together with a linear correlation of the data using the Gibbs-Helmholtz equation; (♦) methanol and (■) ethanol.

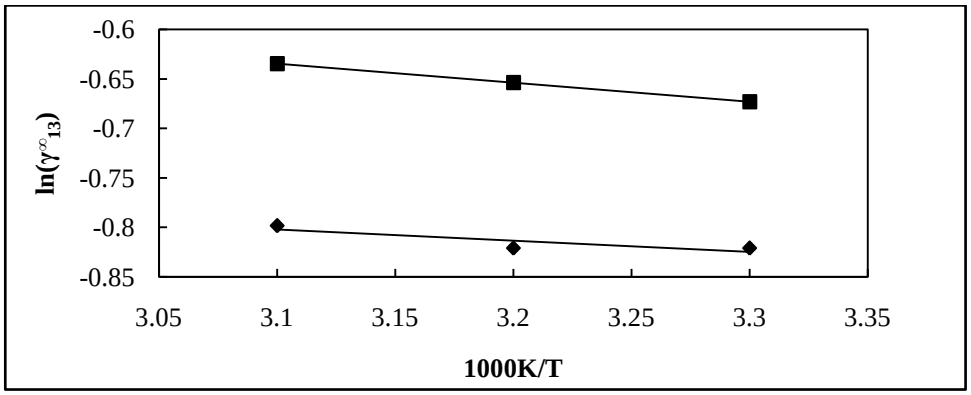

Figure 5-30: Plots of $\ln \gamma_{13}^{\infty}$ versus $1/T$ for alkylbenzenes in [$C_1$3C_8N] [Tf_2N] together with a linear correlation of the data using the Gibbs-Helmholtz equation; (♦) benzene and (■) toluene.

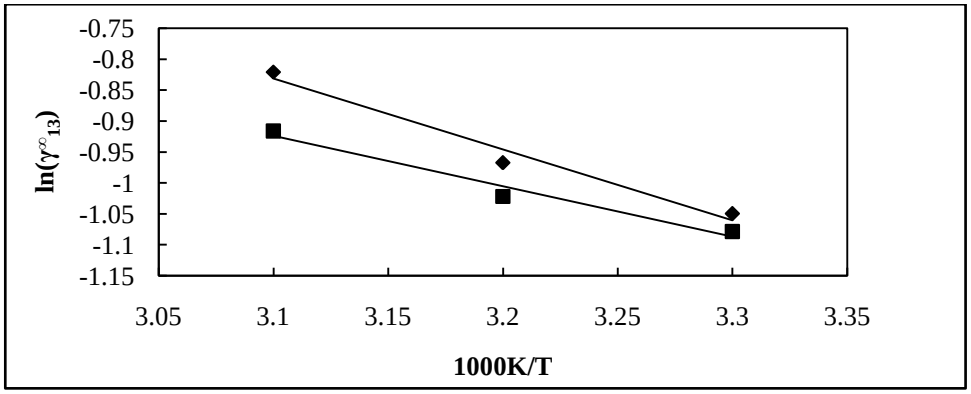

Figure 5-31: Plots of $\ln \gamma_{13}^{\infty}$ versus $1/T$ for ketones in [$C_1$3C_8N] [Tf_2N] together with a linear correlation of the data using the Gibbs-Helmholtz equation; (♦) acetone and (■) butan-2-one.

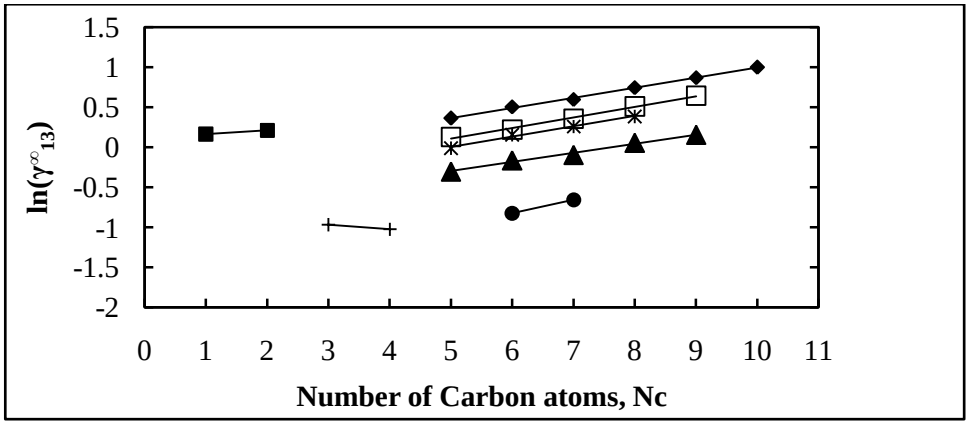

Figure 5-32: Plots of $\ln \gamma_{13}^{\infty}$ versus the number of carbon atoms at 313.15 K for (♦) n-alkanes, (□) alk-1-enes, and (▲) alk-1-ynes, (*) cycloalkanes, (■) alkanols, and (●) alkylbenzenes and (+) ketones in [$C_1$3C_8N] [Tf_2N].

5.1.6. 1-Butyl-3-methylimidazolium hexafluoroantimonate, [BMIM] [SbF_6]

Table 5-18: Activity coefficients at infinite dilution γ_{13}^{∞} of organic solutes in 1-butyl-3-methylimidazolium hexafluoroantimonate with n_3 = 3.312 mmol (26.90 %) at T = (313.15, 323.15 and 333.15) K.

Experimental γ_{13}^{∞} at T /K				
Solute	n_3/mmol	T=313.15	T=323.15	T=333.15
n-pentane.	3.312	19.611	17.552	16.962
n-hexane	3.312	28.627	26.428	25.994
n-heptane	3.312	37.066	34.182	31.424
n-octane	3.312	40.437	39.454	39.176
n-nonane	3.312	47.704	44.947	44.137
Pent-1-ene	3.312	9.956	10.168	9.938
Hex-1-ene	3.312	14.006	13.017	13.356
Hept-1-ene	3.312	19.291	17.762	15.857
Oct-1-ene	3.312	25.680	24.604	24.205
Non-1-ene	3.312	32.427	30.780	30.800
Pent-1-yne	3.312	2.817	2.885	2.933
Hex-1-yne	3.312	4.256	4.108	4.102
Hept-1-yne	3.312	5.741	5.816	5.739
Oct-1-yne	3.312	8.678	8.820	8.558
Non-1-yne	3.312	11.426	10.934	10.894
Cyclopentane	3.312	11.379	10.560	10.193
Cyclohexane	3.312	16.409	11.044	14.132
Cycloheptane	3.312	19.954	15.745	17.295
Cyclooctane	3.312	22.852	17.172	20.433
Methanol	3.312	1.701	1.639	1.565
Ethanol	3.312	2.334	2.144	2.005
Propan-1-ol	3.312	3.128	2.819	2.513
Benzene	3.312	1.229	1.276	1.314
Toluene	3.312	1.866	1.876	1.916
Ethylbenzene	3.312	3.113	3.085	3.176
Acetone	3.312	0.403	0.445	0.463
Butan-2-one	3.312	0.648	0.681	0.702

Table 5-19: Activity coefficients at infinite dilution γ_{13}^{∞} of organic solutes in 1-butyl-3-methylimidazolium hexafluoroantimonate with n_3 = 4.578 mmol (31.98 %) at T = (313.15, 323.15 and 333.15) K.

Experimental γ_{13}^{∞} at T /K				
Solute	n_3/mmol	T=313.15	T=323.15	T=333.15
n-pentane.	4.578	21.459	18.268	18.088
n-hexane	4.578	27.893	28.232	26.626
n-heptane	4.578	38.734	35.798	34.386
n-octane	4.578	44.603	42.656	42.714
n-nonane	4.578	48.766	49.123	47.263
Pent-1-ene	4.578	10.474	10.232	10.442
Hex-1-ene	4.578	13.134	14.103	13.754
Hept-1-ene	4.578	21.109	19.698	16.623
Oct-1-ene	4.578	25.700	25.696	24.915
Non-1-ene	4.578	32.573	33.420	32.620
Pent-1-yne	4.578	2.883	2.885	3.027
Hex-1-yne	4.578	4.054	4.232	4.318
Hept-1-yne	4.578	6.109	6.084	6.231
Oct-1-yne	4.578	9.402	9.080	8.992
Non-1-yne	4.578	11.634	11.846	11.646
Cyclopentane	4.578	11.881	10.860	10.657
Cyclohexane	4.578	15.391	18.626	14.558
Cycloheptane	4.578	18.666	21.075	18.175
Cyclooctane	4.578	23.418	27.128	21.467
Methanol	4.578	1.880	1.711	1.565
Ethanol	4.578	2.456	2.296	2.065
Propan-1-ol	4.578	3.222	2.961	2.747
Benzene	4.578	1.311	1.374	1.370
Toluene	4.578	1.784	1.944	1.972
Ethylbenzene	4.578	2.917	3.225	3.450
Acetone	4.578	0.437	0.459	0.487
Butan-2-one	4.578	0.632	0.681	0.718

Table 5-20: Average activity coefficients at infinite dilution γ_{13}^{∞} of organic solutes in 1-butyl-3-methylimidazolium hexafluoroantimonate at T = (313.15, 323.15 and 333.15) K.

Experimental γ_{13}^{∞} at T /K			
Solute	T=313.15	T=323.15	T=333.15
n-pentane.	20.535	17.910	17.525
n-hexane	28.260	27.330	26.310
n-heptane	37.900	34.990	32.905
n-octane	42.520	41.055	40.945
n-nonane	48.235	47.035	45.700
Pent-1-ene	10.215	10.200	10.190
Hex-1-ene	13.570	13.560	13.555
Hept-1-ene	20.200	18.730	16.240
Oct-1-ene	25.690	25.150	24.560
Non-1-ene	32.500	32.100	31.710
Pent-1-yne	2.850	2.885	2.980
Hex-1-yne	4.155	4.170	4.210
Hept-1-yne	5.925	5.950	5.985
Oct-1-yne	9.040	8.950	8.775
Non-1-yne	11.530	11.390	11.270
Cyclopentane	11.630	10.710	10.425
Cyclohexane	15.900	14.835	14.345
Cycloheptane	19.310	18.410	17.735
Cyclooctane	23.135	22.150	20.950
Methanol	1.790	1.675	1.565
Ethanol	2.395	2.220	2.035
Propan-1-ol	3.175	2.890	2.630
Benzene	1.270	1.325	1.342
Toluene	1.825	1.910	1.944
Ethylbenzene	3.015	3.155	3.313
Acetone	0.420	0.452	0.475
Butan-2-one	0.640	0.681	0.710

Table 5-21: Excess molar enthalpies at infinite dilution $\Delta H_1^{E,\infty}$ of organic solutes in the ionic liquid 1-butyl-3-methylimidazolium hexafluoroantimonate calculated using the Gibbs-Helmholtz equation.

Solute	Linear regression using Eq.(2-21)			$\Delta H_1^{E,\infty}$
	B/1000K	*A*	R^2	*kJ.mol*$^{-1}$
n-pentane.	0.793	0.467	0.851	6.59
n-hexane	0.357	2.198	0.999	2.97
n-heptane	0.707	1.371	0.994	5.88
n-octane	0.189	3.141	0.803	1.57
n-nonane	0.270	3.013	0.999	2.25
Pent-1-ene	0.012	2.285	0.987	0.10
Hex-1-ene	0.006	2.590	0.964	0.05
Hept-1-ene	1.091	-0.474	0.969	9.07
Oct-1-ene	0.225	2.527	0.999	1.87
Non-1-ene	0.123	3.088	1.000	1.02
Pent-1-yne	-0.223	1.758	0.936	-1.85
Hex-1-yne	-0.066	1.634	0.936	-0.55
Hept-1-yne	-0.050	1.940	0.991	-0.42
Oct-1-yne	0.149	1.727	0.966	1.24
Non-1-yne	0.114	2.080	0.998	0.95
Cyclopentane	0.547	0.694	0.921	4.55
Cyclohexane	0.515	1.114	0.961	4.28
Cycloheptane	0.425	1.598	0.995	3.53
Cyclooctane	0.496	1.556	0.995	4.12
Methanol	0.672	-1.567	1.000	5.59
Ethanol	0.814	-1.731	0.998	6.77
Propan-1-ol	0.942	-1.858	1.000	7.83
Benzene	-0.276	1.126	0.912	-2.30
Toluene	-0.316	1.617	0.939	-2.63
Ethylbenzene	-0.471	2.611	0.999	-3.92
Acetone	-0.615	1.105	0.998	-5.11
Butan-2-one	-0.519	1.218	0.987	-4.32

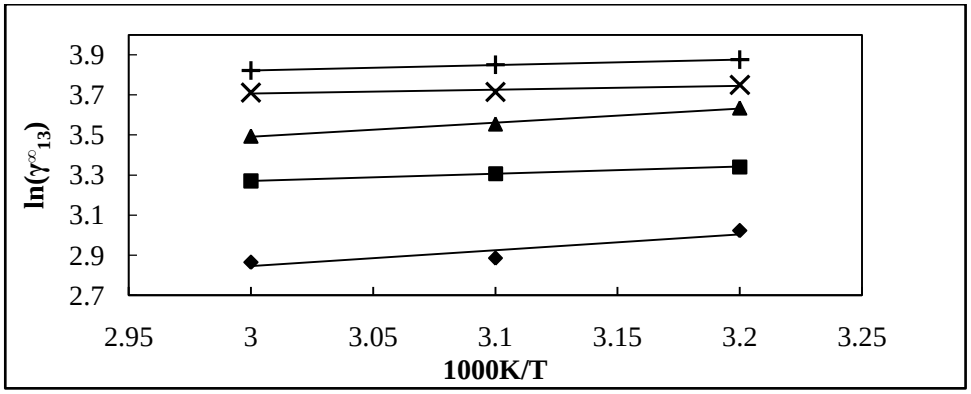

Figure 5-33: Plots of $\ln \gamma_{13}^{\infty}$ versus $1/T$ for alkanes in [BMIM] [SbF_6] together with a linear correlation of the data using the Gibbs-Helmholtz equation; (♦) n-pentane, (■) n-hexane, (▲) n-heptane, (x) n-octane, (+) n-nonane.

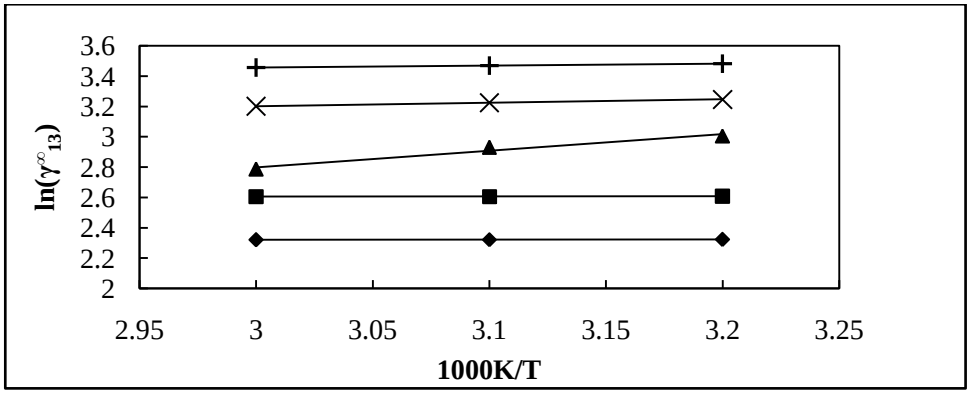

Figure 5-34: Plots of $\ln \gamma_{13}^{\infty}$ versus $1/T$ for alk-1-enes in [BMIM] [SbF_6] together with a linear correlation of the data using the Gibbs-Helmholtz equation; (♦) pent-1-ene, (■) hex-1-ene, (▲) hept-1-ene, (x) oct-1-ene and (+) non-1-ene

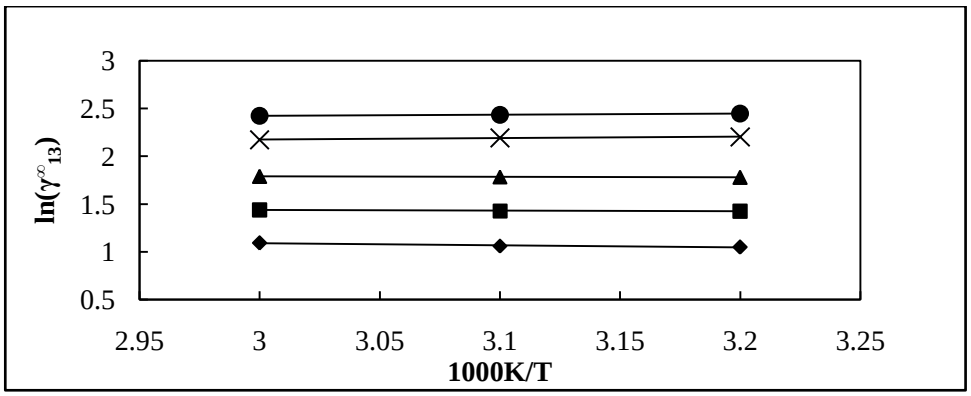

Figure 5-35: Plots of $\ln \gamma_{13}^{\infty}$ versus $1/T$ for alk-1-ynes in [BMIM] [SbF_6] together with a linear correlation of the data using the Gibbs-Helmholtz equation; (♦) pent-1-yne, (■) hex-1-yne, (▲) hept-1-yne, (x) oct-1-yne and (●) non-1-yne.

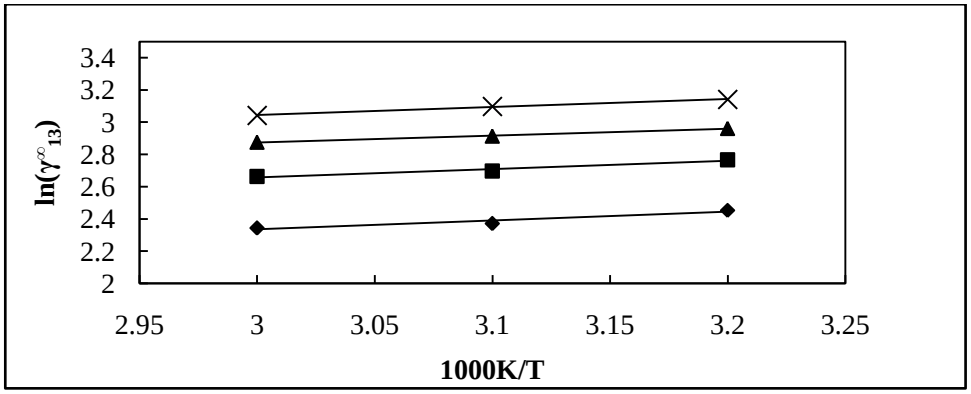

Figure 5-36: Plots of $\ln \gamma_{13}^{\infty}$ versus $1/T$ for cycloalkanes in [BMIM] [SbF_6] together with a linear correlation of the data using the Gibbs-Helmholtz equation; (♦) cyclopentane, (■) cyclohexane, (▲) cycloheptane and (x) cyclooctane.

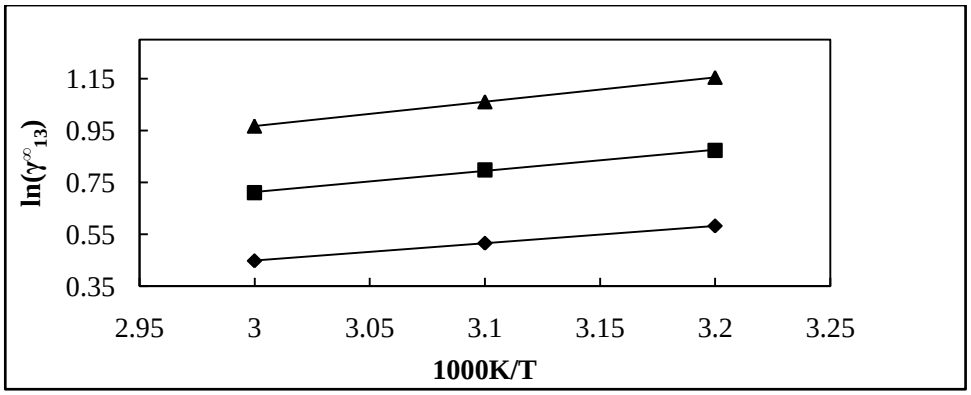

Figure 5-37: Plots of $\ln \gamma_{13}^{\infty}$ versus $1/T$ for alkanols in [BMIM] [SbF_6] together with a linear correlation of the data using the Gibbs-Helmholtz equation; (♦) methanol, (■) ethanol and (▲) propan-1-ol.

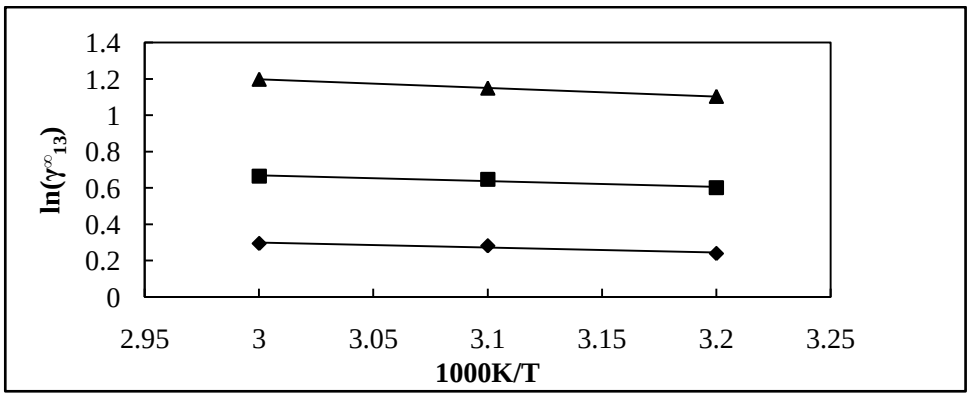

Figure 5-38: Plots of $\ln \gamma_{13}^{\infty}$ versus $1/T$ for alkylbenzenes in [BMIM] [SbF_6] together with a linear correlation of the data using the Gibbs-Helmholtz equation; (♦) benzene, (■) toluene and (▲) ethylbenzene.

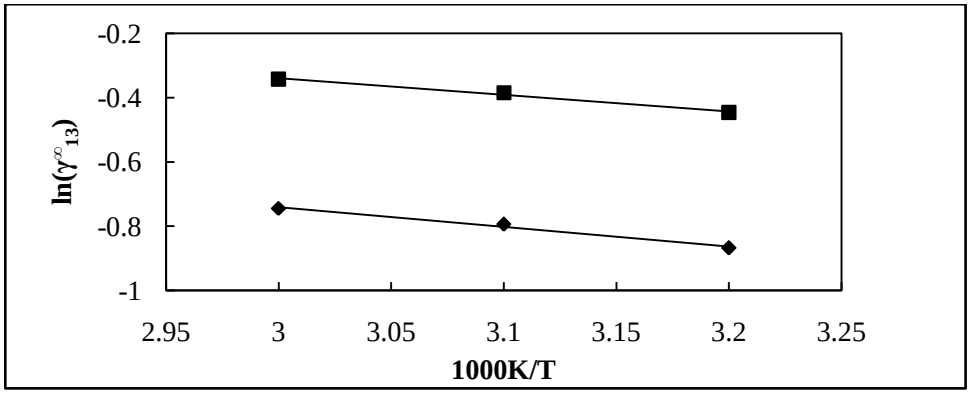

Figure 5-39: Plots of $\ln \gamma_{13}^{\infty}$ versus $1/T$ for ketones in [BMIM] [SbF_6] together with a linear correlation of the data using the Gibbs-Helmholtz equation; (♦) acetone and (■) butan-2-one.

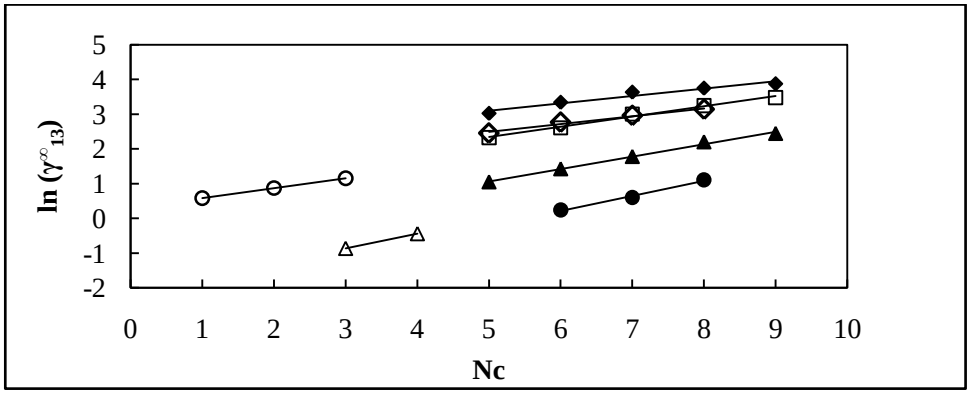

Figure 5-40: Plots of $\ln \gamma_{13}^{\infty}$ versus the number of carbon atoms at 313.15 K for (♦) n-alkanes, (□) alk-1-enes, (▲) alk-1-ynes, and (◊) cycloalkanes, (o) alkanols, (●) alkylbenzenes and (Δ) ketones in [BMIM] [SbF_6].

5.1.7.1-ethyl-3-methylimidazolium trifluoromethanesulfonate, [EMIM] [TfO]

Table 5-22: Activity coefficients at infinite dilution γ_{13}^{∞} of organic solutes in 1-ethyl-3-methylimidazolium trifluoromethanesulfonate with n_3 = 8.01 mmol (29.3 %) at T = (313.15, 323.15 and 333.15) K.

Experimental γ_{13}^{∞} at T /K				
Solute	n_3/mmol	T=313.15	T=323.15	T=333.15
n-pentane	8.01	40.74	38.62	36.57
n-hexane	8.01	66.98	63.11	60.16
n-heptane	8.01	107.28	99.46	93.32
n-octane	8.01	170.38	154.86	143.78
Hex-1-ene	8.01	28.60	27.68	26.72
Hept-1-ene	8.01	47.01	44.82	42.87
Oct-1-ene	8.01	75.66	70.99	67.26
Non-1-ene	8.01	122.18	113.25	105.70
Dec-1-ene	8.01	171.88	162.96	154.72
Undec-1-ene	8.01	315.79	283.50	257.07
Pent-1-yne	8.01	3.95	4.02	4.08
Hex-1-yne	8.01	6.35	6.43	6.47
Hept-1-yne	8.01	9.83	9.79	9.78
Oct-1-yne	8.01	16.32	16.24	16.07
Non-1-yne	8.01	23.77	24.07	24.14
Cyclopentane	8.01	20.92	20.00	18.99
Cyclohexane	8.01	33.30	31.24	29.29
Cycloheptane	8.01	46.87	43.29	40.23
Cyclooctane	8.01	67.24	61.17	56.18
Methanol	8.01	0.73	0.70	0.67
Ethanol	8.01	1.19	1.12	1.06
Benzene	8.01	2.23	2.25	2.26
Toluene	8.01	3.62	3.65	3.67
Ethylbenzene	8.01	6.37	6.32	6.28

Table 5-23: Activity coefficients at infinite dilution γ_{13}^{∞} of organic solutes in 1-ethyl-3-methylimidazolium trifluoromethanesulfonate with n_3 = 6.23 mmol (32.88 %) at T = (313.15, 323.15 and 333.15) K.

Experimental γ_{13}^{∞} at T /K				
Solute	n_3/mmol	T=313.15	T=323.15	T=333.15
n-pentane	6.23	42.50	39.52	36.94
n-hexane	6.23	67.09	65.82	61.25
n-heptane	6.23	102.33	94.91	90.16
n-octane	6.23	162.50	159.27	145.47
Hex-1-ene	6.23	29.47	27.76	27.84
Hept-1-ene	6.23	45.57	43.07	43.57
Oct-1-ene	6.23	74.91	68.50	64.18
Non-1-ene	6.23	126.58	117.25	106.34
Dec-1-ene	6.23	179.20	166.94	160.49
Undec-1-ene	6.23	320.33	288.38	260.50
Pent-1-yne	6.23	4.01	4.00	3.98
Hex-1-yne	6.23	6.36	6.51	6.76
Hept-1-yne	6.23	9.59	9.75	9.87
Oct-1-yne	6.23	15.56	16.56	17.03
Non-1-yne	6.23	24.02	24.13	24.36
Cyclopentane	6.23	21.22	20.92	19.50
Cyclohexane	6.23	34.13	32.13	30.31
Cycloheptane	6.23	45.37	43.95	38.46
Cyclooctane	6.23	69.71	62.49	55.74
Methanol	6.23	0.72	0.69	0.68
Ethanol	6.23	1.15	1.09	1.07
Benzene	6.23	2.21	2.23	2.28
Toluene	6.23	3.51	3.53	3.64
Ethylbenzene	6.23	6.03	6.22	6.46

Table 5-24: Average activity coefficients at infinite dilution γ_{13}^{∞} of organic solutes in 1-ethyl-3-methylimidazolium trifluoromethanesulfonate at T = (313.15, 323.15 and 333.15) K.

Experimental γ_{13}^{∞} at T /K			
Solute	T=313.15	T=323.15	T=333.15
n-pentane	41.62	39.07	36.76
n-hexane	67.04	64.47	60.71
n-heptane	104.81	97.19	91.74
n-octane	166.44	157.07	144.63
Hex-1-ene	29.04	27.72	27.28
Hept-1-ene	46.29	43.95	43.22
Oct-1-ene	75.29	69.75	65.72
Non-1-ene	124.38	115.25	106.02
Dec-1-ene	175.54	164.95	157.61
Undec-1-ene	318.06	285.94	258.79
Pent-1-yne	3.98	4.01	4.03
Hex-1-yne	6.36	6.47	6.62
Hept-1-yne	9.71	9.77	9.83
Oct-1-yne	15.94	16.40	16.55
Non-1-yne	23.81	24.10	24.25
Cyclopentane	21.07	20.46	19.25
Cyclohexane	33.72	31.69	29.80
Cycloheptane	46.12	43.62	39.35
Cyclooctane	68.48	61.83	55.96
Methanol	0.73	0.70	0.68
Ethanol	1.17	1.11	1.07
Benzene	2.22	2.24	2.27
Toluene	3.57	3.59	3.66
Ethylbenzene	6.20	6.27	6.37

Table 5-25: Excess molar enthalpies at infinite dilution $\Delta H_1^{E,\infty}$ of organic solutes for the ionic liquid 1-ethyl-3-methylimidazolium trifluoromethanesulfonate, calculated using the Gibbs-Helmholtz equation.

SOLUTE	Linear regression using Eq.(2-11)			$\Delta H_1^{E,\infty}$
	B/1000K	*A*	R^2	*kJ.mol*$^{-1}$
n-pentane	0.648	1.659	0.999	5.39
n-hexane	0.516	2.561	0.981	4.29
n-heptane	0.695	2.430	0.997	5.78
n-octane	0.731	2.784	0.986	6.08
Hex-1-ene	0.327	2.321	0.936	2.72
Hept-1-ene	0.360	2.681	0.928	2.99
Oct-1-ene	0.709	2.054	0.997	5.90
Non-1-ene	0.832	2.167	0.998	6.92
Dec-1-ene	0.563	3.368	0.994	4.68
Undec-1-ene	1.076	2.327	1.000	8.94
Pent-1-yne	-0.065	1.590	0.990	-0.54
Hex-1-yne	-0.209	2.515	0.994	-1.74
Hept-1-yne	-0.061	2.469	0.999	-0.51
Oct-1-yne	-0.197	3.401	0.928	-1.64
Non-1-yne	-0.096	3.477	0.973	-0.80
Cyclopentane	0.471	1.550	0.953	3.91
Cyclohexane	0.644	1.463	0.999	5.35
Cycloheptane	0.826	1.202	0.965	6.87
Cyclooctane	1.053	0.866	0.999	8.75
Methanol	0.373	-1.516	0.992	3.10
Ethanol	0.491	-1.415	0.989	4.09
Benzene	-0.116	1.668	0.983	-0.96
Toluene	-0.129	1.683	0.931	-1.08
Ethylbenzene	-0.141	2.273	0.987	-1.17

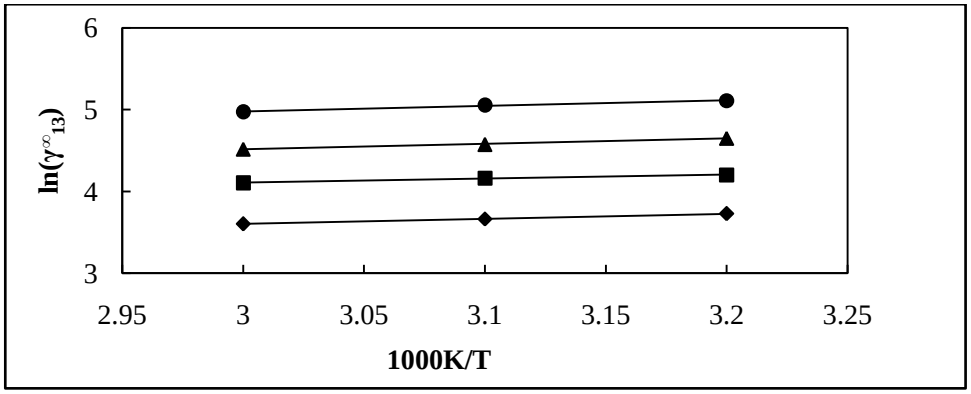

Figure 5-41: Plots of $\ln \gamma_{13}^{\infty}$ versus $1/T$ for alkanes in [EMIM] [TfO] together with a linear correlation of the data using the Gibbs-Helmholtz equation; (♦) n-pentane, (■) n-hexane, (▲) n-heptane and (●) n-octane.

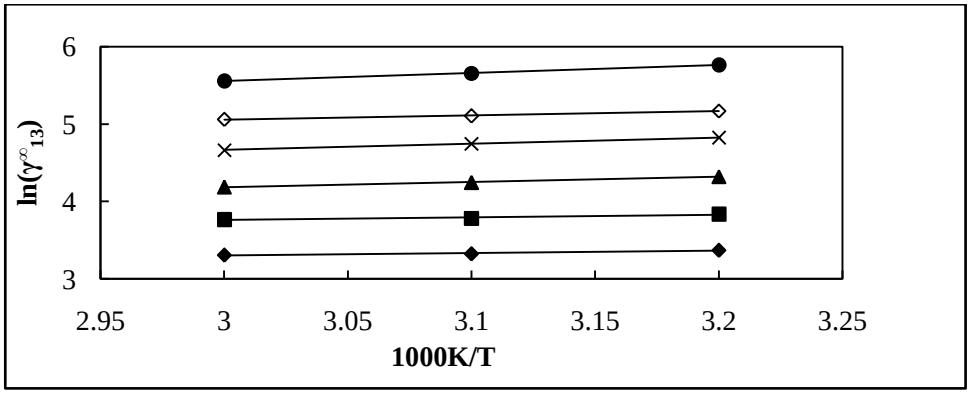

Figure 5-42: Plots of $\ln \gamma_{13}^{\infty}$ versus $1/T$ for alk-1-nes in [EMIM] [TfO] together with a linear correlation of the data using the Gibbs-Helmholtz equation; (♦) hex-1-ene, (■) hept-1-ene, (▲) oct-1-ene, (x) non-1-ene, (◊) dec-1-ene and (●) undec-1-ene.

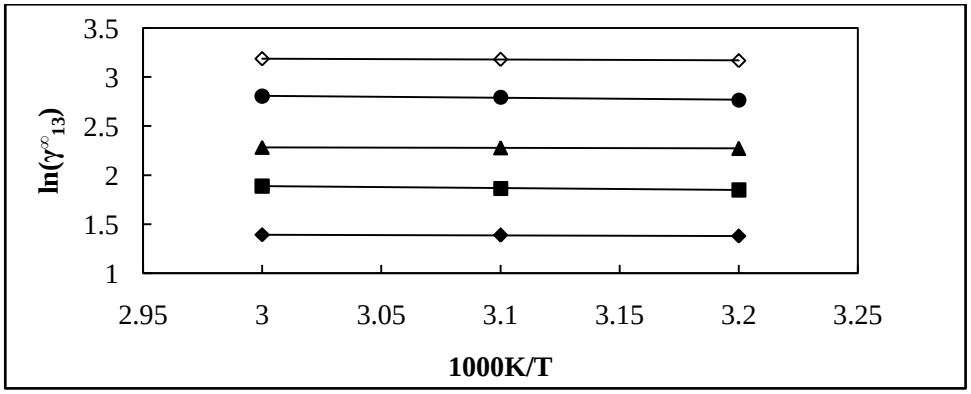

Figure 5-43: Plots of $\ln \gamma_{13}^{\infty}$ versus $1/T$ for alk-1-ynes in [EMIM] [TfO] together with a linear correlation of the data using the Gibbs-Helmholtz equation; (♦) pent-1-yne, (■) hex-1-yne, (▲) hept-1-yne, (●) oct-1-yne and (◊) non-1-yne.

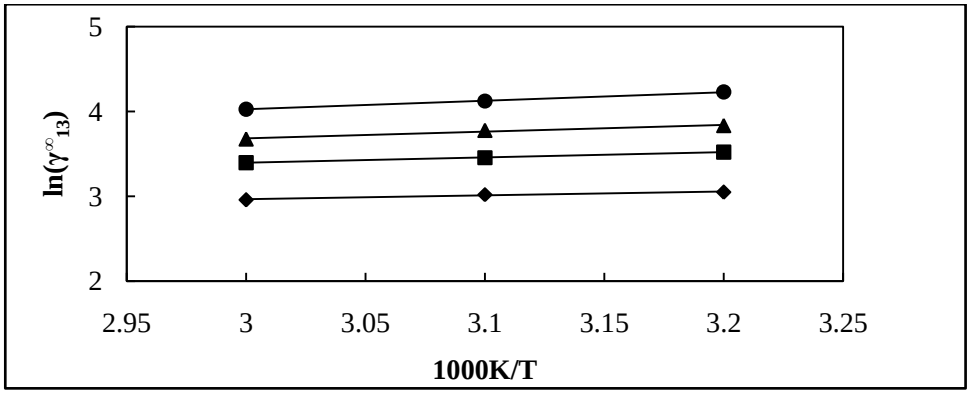

Figure 5-44: Plots of $\ln \gamma_{13}^{\infty}$ versus $1/T$ for cycloalkanes in [EMIM] [TfO] together with a linear correlation of the data using the Gibbs-Helmholtz equation; (♦) cyclopentane, (■) cyclohexane, (▲) cycloheptane and (●) cyclooctane.

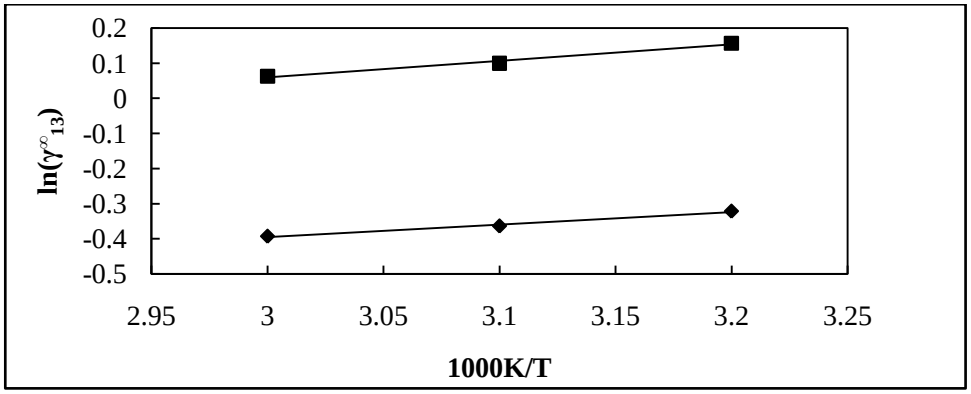

Figure 5-45: Plots of $\ln \gamma_{13}^{\infty}$ versus $1/T$ for alkanols in [EMIM] [TfO] together with a linear correlation of the data using the Gibbs-Helmholtz equation; (♦) methanol and (■) ethanol.

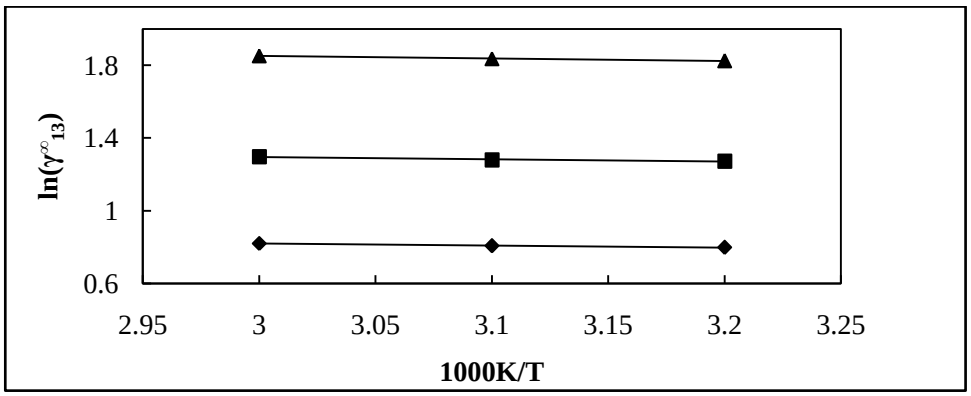

Figure 5-46: Plots of $\ln \gamma_{13}^{\infty}$ versus $1/T$ for alkylbenzenes in [EMIM] [TfO] together with a linear correlation of the data using the Gibbs-Helmholtz equation; (♦) benzene, (■) toluene and (▲) ethylbenzene.

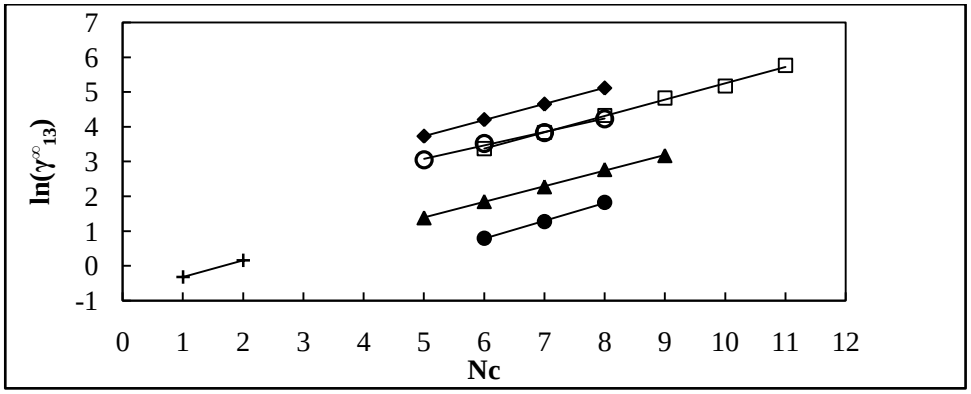

Figure 5-47: Plots of $\ln \gamma_{13}^{\infty}$ versus the number of carbon atoms at 313.15 K for (♦) n-alkanes, (□) alk-1-enes, (▲) alk-1-ynes, and (○) cycloalkanes, (+) alkanols and (●) alkylbenzenes in [EMIM] [TfO].

5.1.8. 1-methyl-3-octylimidazolium hexafluorophosphate, [MOIM][PF_6]

Table 5-26: Activity coefficients at infinite dilution γ_{13}^{∞} of organic solutes in 1-methyl-3-octylimidazolium hexafluorophosphate with n_3 = 6.69 mmol (28.55 %) at T = (313.15, 323.15 and 333.15) K.

Experimental γ_{13}^{∞} at T /K				
Solute	n_3/mmol	T=313.15	T=323.15	T=333.15
n-pentane	6.69	8.21	8.06	7.83
n-hexane	6.69	10.75	10.56	10.20
n-heptane	6.69	14.07	13.78	13.24
n-octane	6.69	18.34	17.87	17.04
n-decane	6.69	31.75	30.25	28.23
n-undecane	6.69	42.06	39.62	36.52
Hex-1-ene	6.69	6.17	6.15	6.06
Hept-1-ene	6.69	8.23	8.18	8.02
Oct-1-ene	6.69	10.77	10.66	10.39
Non-1-ene	6.69	14.16	13.93	13.50
Dec-1-ene	6.69	16.32	16.52	16.34
Undec-1-ene	6.69	25.10	24.01	22.75
Pent-1-yne	6.69	1.70	1.75	1.78
Hex-1-yne	6.69	2.24	2.30	2.34
Hept-1-yne	6.69	2.81	2.87	2.93
Oct-1-yne	6.69	3.77	3.87	3.94
Non-1-yne	6.69	4.38	4.65	4.83
Cyclopentane	6.69	5.02	4.92	4.77
Cyclohexane	6.69	6.74	6.56	6.29
Cycloheptane	6.69	8.24	7.97	7.63
Cyclooctane	6.69	10.21	9.85	9.39
Methanol	6.69	1.77	1.61	1.46
Ethanol	6.69	2.22	2.00	1.79
Benzene	6.69	0.96	0.99	1.00
Toluene	6.69	1.31	1.35	1.37
Ethylbenzene	6.69	1.95	1.98	1.99

Table 5-27: Activity coefficients at infinite dilution γ_{13}^{∞} of organic solutes in 1-methyl-3-octylimidazolium hexafluorophosphate with n_3 = 5.135 mmol (33.26 %) at T = (313.15, 323.15 and 333.15) K.

Experimental γ_{13}^{∞} at T /K				
Solute	n_3/mmol	T=313.15	T=323.15	T=333.15
n-pentane	5.14	8.32	8.11	7.99
n-hexane	5.14	11.01	10.68	10.41
n-heptane	5.14	14.30	13.59	13.21
n-octane	5.14	17.64	17.09	16.93
n-decane	5.14	31.68	30.80	28.98
n-undecane	5.14	41.33	40.13	36.99
Hex-1-ene	5.14	6.45	6.29	6.15
Hept-1-ene	5.14	8.19	8.12	8.14
Oct-1-ene	5.14	10.30	10.23	10.34
Non-1-ene	5.14	13.48	13.25	13.28
Dec-1-ene	5.14	16.66	16.30	16.36
Undec-1-ene	5.14	25.24	24.79	22.52
Pent-1-yne	5.14	1.72	1.79	1.84
Hex-1-yne	5.14	2.33	2.38	2.43
Hept-1-yne	5.14	2.93	2.98	3.04
Oct-1-yne	5.14	3.90	3.94	4.03
Non-1-yne	5.14	4.47	4.71	4.91
Cyclopentane	5.14	5.06	4.95	4.79
Cyclohexane	5.14	6.82	6.61	6.30
Cycloheptane	5.14	8.02	7.74	7.75
Cyclooctane	5.14	9.92	9.51	9.37
Methanol	5.14	1.85	1.65	1.50
Ethanol	5.14	2.32	2.05	1.82
Benzene	5.14	0.97	0.99	1.03
Toluene	5.14	1.36	1.37	1.41
Ethylbenzene	5.14	1.95	1.98	2.02

Table 5-28: Average activity coefficients at infinite dilution γ_{13}^{∞} of organic solutes in 1-methyl-3-octylimidazolium hexafluorophosphate at T = (313.15, 323.15 and 333.15) K.

Experimental γ_{13}^{∞} at T /K			
Solute	T=313.15	T=323.15	T=333.15
n-pentane	8.27	8.09	7.91
n-hexane	10.88	10.62	10.31
n-heptane	14.19	13.69	13.23
n-octane	17.99	17.48	16.99
n-decane	31.72	30.53	28.61
n-undecane	41.70	39.88	36.76
Hex-1-ene	6.31	6.22	6.11
Hept-1-ene	8.21	8.15	8.08
Oct-1-ene	10.54	10.45	10.37
Non-1-ene	13.82	13.59	13.39
Dec-1-ene	16.49	16.41	16.35
Undec-1-ene	25.17	24.40	22.64
Pent-1-yne	1.71	1.77	1.81
Hex-1-yne	2.29	2.34	2.39
Hept-1-yne	2.87	2.93	2.99
Oct-1-yne	3.84	3.91	3.99
Non-1-yne	4.43	4.68	4.87
Cyclopentane	5.04	4.94	4.78
Cyclohexane	6.78	6.59	6.30
Cycloheptane	8.13	7.86	7.69
Cyclooctane	10.07	9.68	9.38
Methanol	1.81	1.63	1.48
Ethanol	2.27	2.03	1.81
Benzene	0.97	0.99	1.02
Toluene	1.34	1.36	1.39
Ethylbenzene	1.95	1.98	2.01

Table 5-29: Excess molar enthalpies at infinite dilution $\Delta H_1^{E,\infty}$ of organic solutes for the ionic liquid 1-methyl-3-octylimidazolium hexafluorophosphate, calculated using the Gibbs-Helmholtz equation.

SOLUTE	Linear regression using Eq.(2-11)			$\Delta H_1^{E,\infty}$
	B/1000K	*A*	R^2	*kJ.mol*$^{-1}$
n-pentane	0.229	1.381	0.999	1.90
n-hexane	0.283	1.485	0.994	2.35
n-heptane	0.366	1.485	1.000	3.04
n-octane	0.300	1.933	0.999	2.49
n-decane	0.537	1.748	0.973	4.46
n-undecane	0.656	1.643	0.966	5.45
Hex-1-ene	0.172	1.294	0.991	1.43
Hept-1-ene	0.083	1.840	0.996	0.69
Oct-1-ene	0.085	2.084	0.999	0.71
Non-1-ene	0.165	2.099	0.999	1.37
Dec-1-ene	0.045	2.660	0.996	0.37
Undec-1-ene	0.551	1.473	0.937	4.58
Pent-1-yne	-0.297	1.487	0.989	-2.47
Hex-1-yne	-0.224	1.541	0.998	-1.86
Hept-1-yne	-0.205	1.708	0.999	-1.70
Oct-1-yne	-0.200	1.982	0.997	-1.66
Non-1-yne	-0.501	3.088	0.994	-4.16
Cyclopentane	0.276	0.739	0.982	2.29
Cyclohexane	0.386	0.684	0.980	3.21
Cycloheptane	0.291	1.165	0.986	2.42
Cyclooctane	0.368	1.133	0.998	3.06
Methanol	1.050	-2.760	1.000	8.73
Ethanol	1.195	-2.996	0.999	9.94
Benzene	-0.263	0.806	0.999	-2.19
Toluene	-0.210	0.960	0.996	-1.75
Ethylbenzene	-0.145	1.132	0.999	-1.21

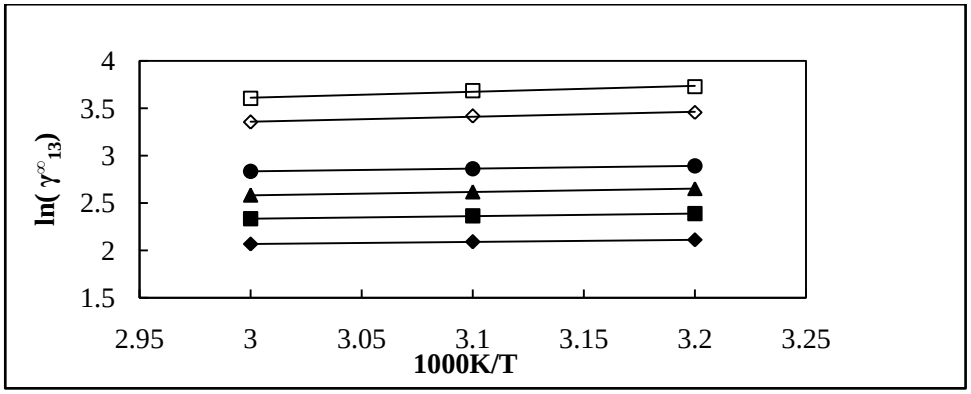

Figure 5-48: Plots of $\ln \gamma_{13}^{\infty}$ versus $1/T$ for n-alkanes in [MOIM] [PF_6] together with a linear correlation of the data using the Gibbs-Helmholtz equation; (♦) n-pentane, (■) n-hexane, (▲) n-heptane, (●) n-octane, (◊) n-decane and (□) n-undecane.

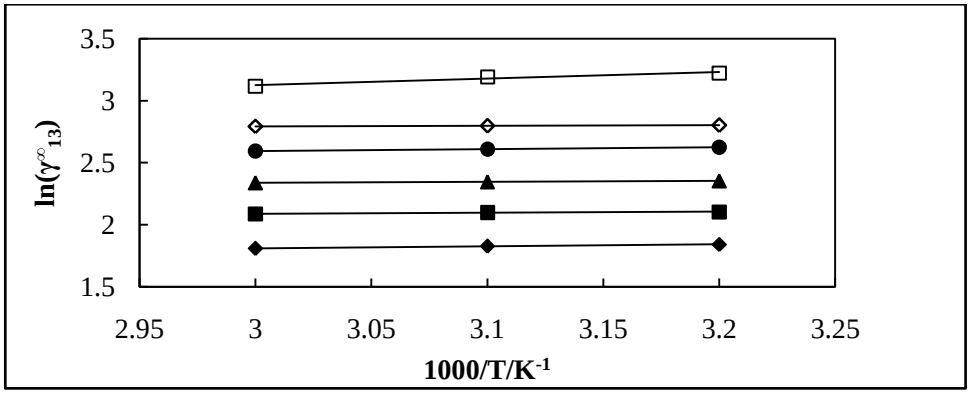

Figure 5-49: Plots of $\ln \gamma_{13}^{\infty}$ versus $1/T$ for alk-1-enes in [MOIM] [PF_6] together with a linear correlation of the data using the Gibbs-Helmholtz equation; (♦) hex-1-ene, (■) hept-1-ene, (▲) oct-1-ene, (●) non-1-ene, (◊) dec-1-ene and (□) undec-1-ene.

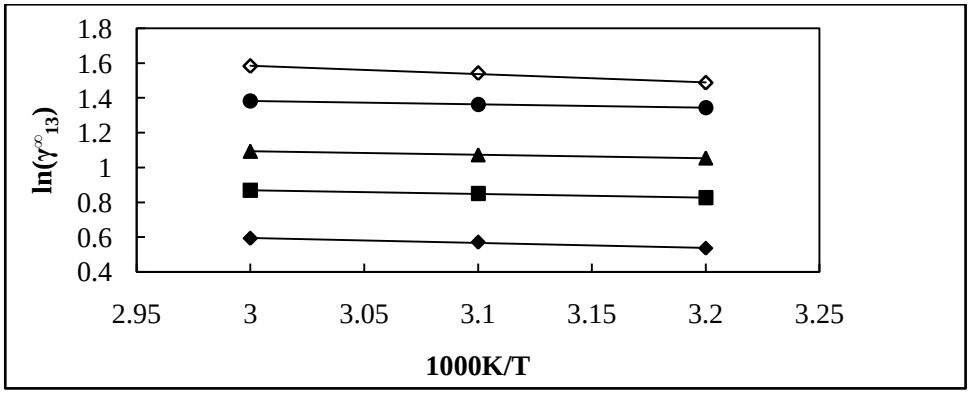

Figure 5-50: Plots of $\ln \gamma_{13}^{\infty}$ versus $1/T$ for alk-1-ynes in [MOIM] [PF_6] together with a linear correlation of the data using the Gibbs-Helmholtz equation; (♦) pent-1-yne, (■) hex-1-yne, (▲) hept-1-yne, (●) oct-1-yne and (◊) non-1-yne.

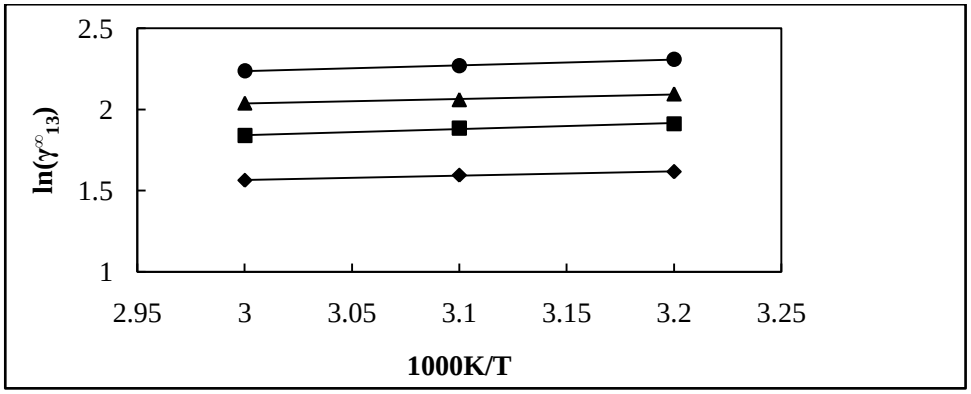

Figure 5-51: Plots of $\ln \gamma_{13}^{\infty}$ versus $1/T$ for cycloalkanes in [MOIM] [PF_6] together with a linear correlation of the data using the Gibbs-Helmholtz equation; (♦) cyclopentane, (■) cyclohexane, (▲) cycloheptane and (●) cyclooctane.

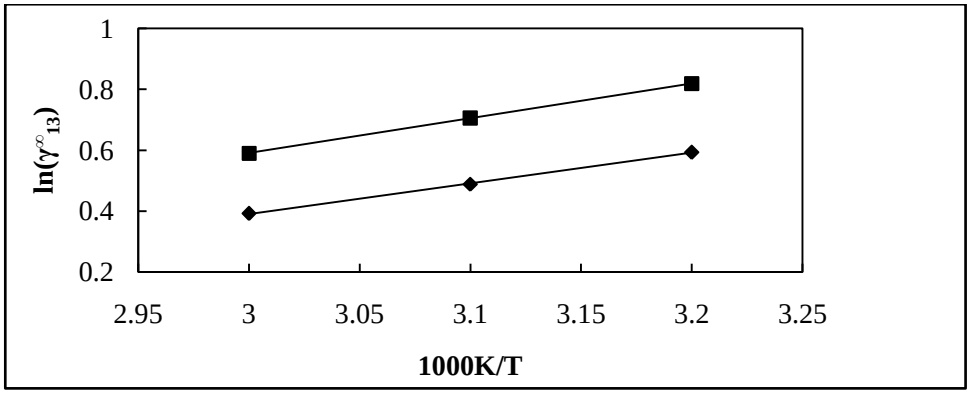

Figure 5-52: Plots of $\ln \gamma_{13}^{\infty}$ versus $1/T$ for alkanols in [MOIM] [PF_6] together with a linear correlation of the data using the Gibbs-Helmholtz equation; (♦) methanol and (■) ethanol.

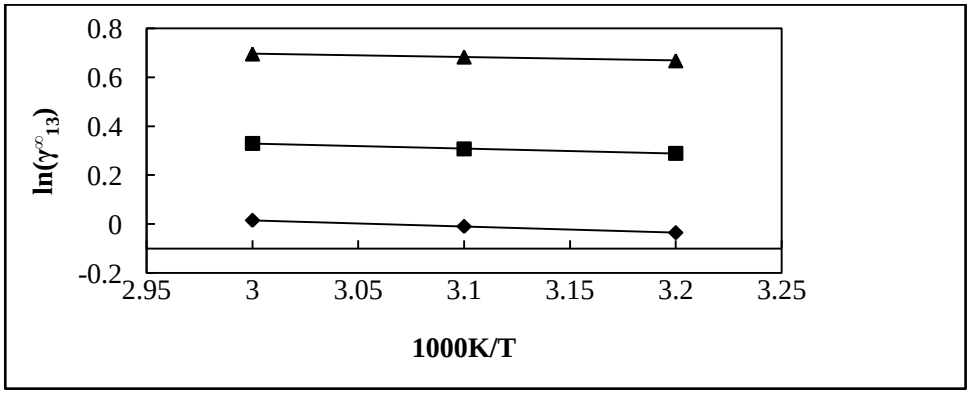

Figure 5-53: Plots of $\ln \gamma_{13}^{\infty}$ versus $1/T$ for alkylbenzenes in [MOIM] [PF_6] together with a linear correlation of the data using the Gibbs-Helmholtz equation; (♦) benzene, (■) toluene and (▲) ethylbenzene.

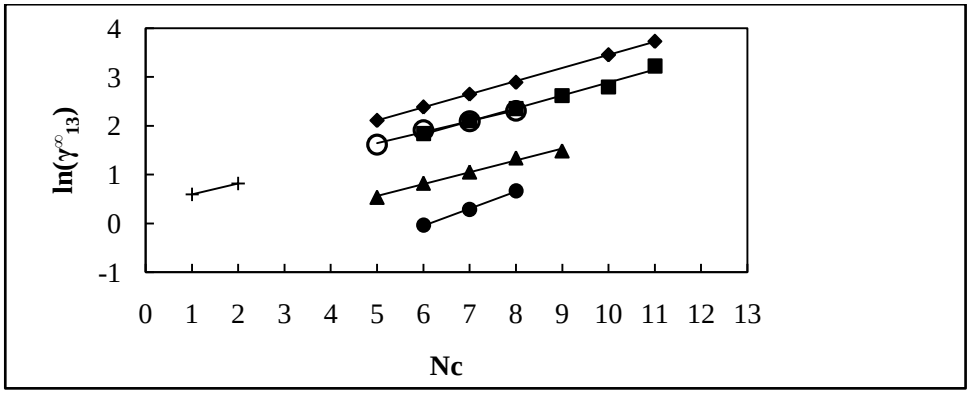

Figure 5-54: Plots of $\ln \gamma_{13}^{\infty}$ versus the number of carbon atoms at 313.15 K for (♦) n-alkanes, (■) alk-1-enes, (▲) alk-1-ynes, and (○) cycloalkanes, (+) alkanols and (●) alkylbenzenes in [MOIM] [PF_6]

5.2. Results from the inert gas stripping technique

5.2.1. N-methyl-2-pyrrolidone, NMP

Table 5-30: Experimental infinite dilution activity coefficients of n-hexane as well as cyclohexane in NMP obtained by the dilutor method and comparison with literature data taken from Gruber et al. (1999). Experimental values were determined using equation (3-90).

T / *K*	Experimental data		Literature data		Deviation[#] / %
	D/ $cm^3.min^{-1}$	γ_{13}^{∞}	D/ $cm^3.min^{-1}$	γ_{13}^{∞}	
n-hexane					
303.15	7.550	13.278	21.4 -35.4	13.10	1.359
303.15	14.96	13.28	21.4 -35.4	13.10	1.374
303.15	20.23	13.271	21.4 -35.4	13.10	1.305
313.15	7.480	11.561	21.4 -35.4	11.80	-2.025
313.15	15.21	11.568	21.4 -35.4	11.80	-1.966
313.15	19.94	11.549	21.4 -35.4	11.80	-2.127
323.15	7.620	10.992	21.4 -35.4	10.90	0.844
323.15	15.09	11.009	21.4 -35.4	10.90	1.000
323.15	19.85	10.983	21.4 -35.4	10.90	0.761
Cyclohexane					
303.15	7.510	8.199	21.4 -35.4	8.06	1.725
303.15	15.07	8.213	21.4 -35.4	8.06	1.898
303.15	21.53	8.184	21.4 -35.4	8.06	1.538
313.15	7.660	7.546	21.4 -35.4	7.40	1.973
313.15	15.14	7.539	21.4 -35.4	7.40	1.878
313.15	20.39	7.541	21.4 -35.4	7.40	1.905
323.15	7.480	6.836	21.4 -35.4	6.80	0.529
323.15	14.98	6.841	21.4 -35.4	6.80	0.603
323.15	21.43	6.839	21.4 -35.4	6.80	0.574

Relative deviation, R.D., given by $\frac{\left(\gamma_{13}^{\infty,\exp} - \gamma_{13}^{\infty,lit}\right)}{\gamma_{13}^{\infty,lit}} \times 100$

5.2.2. Trihexyltetradecylphosphonium bis (trifluoromethylsulfonyl) imide

Table 5-31: Experimental infinite dilution activity coefficients obtained by the inert gas stripping method (IGSM) for six different organic solutes in the ionic liquid Trihexyltetradecylphosphonium bis (trifluoromethylsulfonyl) imide, and comparison with similar data obtained by the GLC method.

	Results from the IGST						Results from GLC		
T	D		D		D				Deviation#
K	cm^3/min	γ_{13}^{∞}	cm^3/min	γ_{13}^{∞}	cm^3/min	γ_{13}^{∞}	γ_{13}^{∞} (Average)	γ_{13}^{∞}	%
				n-hexane					
303.15	7.55	1.087	15.05	1.084	20.98	1.083	1.085	1.089	-0.367
313.15	7.48	1.101	14.91	1.109	-	-	1.105	1.096	0.821
323.15	7.52	1.116	15.65	1.121	-	-	1.119	1.103	1.451
				Hex-1-ene					
303.15	7.51	0.895	15.32	0.899	19.87	0.890	0.895	0.900	-0.556
313.15	7.72	0.911	15.45	0.916	-	-	0.914	0.907	0.772
323.15	7.43	0.924	15.50	0.918	-	-	0.921	0.913	0.876
				Cyclohexane					
303.15	7.53	0.801	15.29	0.815	21.52	0.803	0.806	0.794	1.511
313.15	7.52	0.813	14.82	0.821	-	-	0.817	0.795	2.767
323.15	7.59	0.825	14.93	0.821	-	-	0.823	0.796	3.392
				Methanol					
303.15	7.64	1.140	14.48	1.111	20.06	1.136	1.129	1.151	-1.911
313.15	7.62	1.105	15.08	1.094	-	-	1.100	1.083	1.570
323.15	7.57	1.033	15.86	1.058	-	-	1.046	1.048	-0.191
				Benzene					
303.15	7.61	0.391	15.11	0.399	20.15	0.387	0.392	0.381	2.887
313.15	7.55	0.406	15.72	0.400	-	-	0.403	0.391	3.069
323.15	7.52	0.409	14.98	0.413	-	-	0.411	0.398	3.266
				Acetone					
303.15	7.54	0.285	15.64	0.287	21.33	0.289	0.287	0.297	-3.367
313.15	7.66	0.303	14.89	0.308	-	-	0.306	0.297	3.030
323.15	7.46	0.318	15.41	0.323	-	-	0.321	0.311	3.215

Relative deviation given by $\frac{\left(\gamma_{13}^{\infty,IGST} - \gamma_{13}^{\infty,GLC}\right)}{\gamma_{13}^{\infty,GLC}} \times 100$

5.3.Separation potential of the investigated ionic liquids

From experimental data, equations (2-3) and (2-4) were used to calculate selectivities, S_{ij}^{∞} and capacities, k_j^* at infinite dilution for seven different separation problems. Table 5-32 gives an insight into the effectiveness of the ionic liquids investigated in this work as a separation solvent, as compared to other ionic liquids and some industrial molecular solvents such as sulfolane, NMP, dimethylsulfoxide and chlorobenzene.

Table 5-32: Selectivity and capacity at infinite dilution at T = 313.15 K of the ionic liquids investigated in this work for different separation problems and comparison with industrial separation agents as well as other ionic liquids

	Selectivity at infinite dilution, S_{12}^{∞}							Limiting Capacity, k_2^{∞}			
	n-hexane/ benzene	Methanol/ benzene	Ethanol/ benzene	Butan-2-one /benzene	Hexane/ hex-1-ene	Methanol/ acetone	Ethanol / butan-2-one	Benzene	Hex-1-ene	Methanol	Butan-2-one
[EMIM][BF_4][a]	38.65	0.17	0.31	0.65	2.02	0.39	0.47	0.41	0.02	2.33	0.62
[C_{16}MIM][BF_4][b]	3.10	1.52	1.94	1.32	1.35	1.28	1.47	1.27	0.55	0.83	0.96
[$3C_6C_{14}$P][BF_4][c]	3.41	1.31	1.41	1.08	1.26	1.25	1.30	2.44	0.90	1.86	2.25
[$3C_6C_{14}$P][Tf_2N][c]	2.80	2.77	3.25	0.81	1.21	3.85	4.00	2.56	1.10	0.92	3.15
[$3C_6C_{14}$P][PF_6][c]	2.96	3.12	3.32	1.04	1.20	3.13	3.21	1.47	0.59	0.32	1.42
[$3C_6C_{14}$P][$(C_2F_5)_3PF_3$][d]	3.25	5.83	5.87	-	1.23		-	5.00	1.89	0.86	-
[$3C_1C_4$N][Tf_2N][e]	13.94	1.07	1.38	-	1.89	3.33	-	0.75	0.10	0.70	-
[BMPyrr][Tf_2N][f]	15.47	-	2.01	0.62	1.92		3.26	1.16	0.14	-	1.89
[C_13C_8N] [Tf_2N][c]	3.77	2.68	2.82	0.82	1.33	3.13	3.44	2.27	0.80	0.85	2.78
[EMIM][TfO][c,j]	30.20	0.33	0.53	-	2.31		-	0.45	0.03	1.38	-
[MOIM][PF_6][c]	11.27	1.88	2.35	-	1.72		-	1.04	0.16	0.55	-
[BMIM][SbF_6][c]	22.25	1.41	1.89	0.50	2.08	4.35	3.74	0.79	0.07	0.56	1.56
Sulfolane[g]	18.17	0.91	1.26	0.83	-	1.37	1.52	0.43	-	0.47	0.51
NMP[h]	11.24	-	-	-	0.53		-	0.95	0.16	-	-
Chlorobenzene[i,k]	-	-	-	-	-	0.17*	8.29	-	-	-	0.47
Dimethylsulfoxide[k]	-	-	-	-	-	0.35*	0.20*	-	-	2.00*	0.35*

[a]Foco et al. (2006), [b]Mutelet and Jaubert (2007), [c]This work, [d] Letcher et al. (2008, [e] Heintz et al (2006b), [f] Kato and Gmehling (2005), [g]Möllmann and Gmehling (1997),[h]Krummen et al. (2000), [i]Kossack et al.(2008), [j]Olivier et al.(2010a); [k]Dortmund Data Bank, DDB, [*] Data obtained at 298.15 K.

CHAPTER SIX: DISCUSSION

6.1. Fluorinated Ionic Liquids investigated in this work

6.1.1. Gas-Liquid Chromatography

6.1.1.1. Phosphonium-based Ionic Liquids

Infinite dilution activity coefficients of various organic solutes in the ionic liquids $[3C_6C_{14}P]$ $[Tf_2N]$, $[3C_6C_{14}P]$ $[BF_4]$, $[3C_6C_{14}P]$ $[PF_6]$ are listed in tables 5-2 through 5-4, 5-6 through 5-8 and 5-10 through 5-12. For two different solvent loadings IDAC values obtained with the same solutes generally remained close to each other. It is an indication that no adsorption took place onto the column packing, even for polar solutes such as ketones and alcohols. For all the three phosphonium-based ionic liquids, infinite dilution activity coefficients decrease in the order: n-alkanes ≅ alk-1-enes ≅ alcohols > cycloalkanes > alk-1-ynes > alkylbenzenes > ketones. IDAC values for ketones were the smallest for all the investigated solutes, an indication of strong solute-solvent interactions. This can be attributed to the interaction between the two pairs of electrons on the oxygen atom of the ketone with the cation of the IL, as well as between the positive pole of the ketone and the ionic liquid's anion. Banerjee and Khanna (2006), Letcher et al. (2008) and Revelli et al. (2009) reported infinite dilution activity coefficients of various organic solutes in $[3C_6C_{14}P]$ $[Tf_2N]$ and/or $[3C_6C_{14}P]$ $[BF_4]$. In this work, a larger number of solutes have been considered. Additionally, IDAC data of organics in the ionic liquid $[3C_6C_{14}P][Tf_2N]$ obtained from the inert gas stripping technique are presented. Tables 6-1 and 6-2 allow a quick comparison of experimental infinite dilution activity coefficient data obtained in this work to literature data. Results from this study are in good agreement with those published by Letcher et al. (2008) and Revelli et al. (2009). However, there are large discrepancies between data reported in this work and those obtained by Banerjee and Khanna (2006). This may be due to different purities as far as ionic liquids samples are concerned. Moreover, the methodological approach used by Banerjee and coworkers is different from the one used in this study.

During experiments, it was observed that alcohols led to very long retention times. Resulting peaks were so broad that a very accurate determination of the retention time was not possible. This is the reason why the linear regression of experimental data shown in Figures 5-5 and 5-13 was not convincingly successful.

Table 6-1: Comparison of experimental IDACs in the ionic liquid [$3C_6C_{14}P$] [Tf_2N] at 313.15 K from this work to literature data;*Interpolated data.

Solute	*Banerjee and Khanna (2006)	Letcher et al. (2008)	*Revelli et al. (2009)	This work
n-Hexane	0.759	1.130	1.064	1.096
Hex-1-ene	0.498	0.920	0.889	0.907
Cyclohexane	0.611	0.830	0.802	0.795
Methanol	0.951	1.230	1.128	1.083
Benzene	0.405	0.400	0.392	0.391
Butan-2-one	-	-	0.270	0.321

Table 6-2: Comparison of experimental IDACs in the ionic liquid [$3C_6C_{14}P$] [BF_4] at 313.15 K from this work to literature data; * Interpolated data.

Solute	*Banerjee and Khanna (2006)	This work
n-Hexane	0.956	1.400
Hex-1-ene	0.565	1.109
Cyclohexane	0.725	0.975
Methanol	6.524	0.537
Benzene	0.369	0.410

Partial molar excess enthalpies at infinite dilution $\Delta H_1^{E,\infty}$ were calculated from the plots of $\ln \gamma_i^{\infty}$ as a function of $\frac{1}{T}$ provided in Figures 5-1 through 5-7, 5-9 through 5-15 and 5-17 through 5-23, using the Gibbs-Helmholtz equation:

$$\frac{\partial \ln \gamma_i^{\infty}}{\partial (1/T)} = \frac{\Delta H_1^{E,\infty}}{R} \qquad (2\text{-}11)$$

Tables 5-5, 5-9 and 5-13 show that partial molar excess enthalpies at infinite dilution are generally small. Thus, limiting activity coefficients values vary little with temperature. (The greatest γ_{13}^{∞} variation was 0.023 K^{-1}). Positive values of partial molar excess enthalpies imply that infinite dilution activity coefficients decrease with increasing temperature. In addition, positive infinite dilution partial molar excess enthalpies indicate that dissociation effects outweigh association effects in very dilute mixtures involving the ionic liquid and the solute under consideration. Negative infinite dilution partial molar excess enthalpies indicate that association effects outweigh dissociation effects. Figures 5-8, 5-16 and 5-24 show that extending the solute alkyl chain weakens its interaction with the ionic liquid as γ_{13}^{∞} values increase when the number of carbon atoms is increased.

Table 5-32 shows selectivities and capacities at infinite dilution for selected ionic liquids and some industrial solvents in relation with n-hexane/benzene, n-hexane/hex-1-ene and methanol/acetone separation problems. It appears that the studied phosphonium-based fluorinated ionic liquids are poor solvents for separating aromatics from aliphatics. However, they are fairly more selective when it comes to the methanol/benzene and methanol/acetone separation problems. For example, the limiting selectivity value of the ionic liquid [$3C_6C_{14}P$] [Tf_2N] for the methanol/ acetone mixture was calculated as 3.85 at 313.15 K, with the limiting capacity found to be 2.3. These values lead to one of the best selectivity-capacity combinations at infinite dilution for ionic liquids reported in the open literature.

6.1.1.2. Ammonium–based Ionic Liquid.

Experimental limiting activity coefficients of the investigated solutes in the ionic liquid [C_13C_8N] [Tf_2N] are listed in Tables 5-14 through 5-16. They decrease in the following order: n-alkanes > alk-1-enes > alcohols > cycloalkanes > alk-1-ynes > alkylbenzenes > ketones. Alk-1-ynes, alkylbenzenes and ketones have low IDAC values in the ionic liquid. This is due to the interaction between the π electrons of these unsaturated inorganics and the cation of the ionic liquid [C_13C_8N] [Tf_2N].

From Figure 5-32, it can be seen that for all classes of solutes, except ketones, IDAC values increase with the increasing number of carbon atoms in the structure of the solutes. The magnitude of solute-solvent interactions which is related to the infinite dilution activity coefficient is determined by the solute polarity. The more polar the solute, the stronger the interaction and the smaller the limiting activity of the solute in the ionic liquid.

Temperature-dependence of IDAC values is depicted by Table 5-17 obtained from Figures 5-25 through 5-31. IDACs of unsaturated organic solutes, except alk-1-enes increase with increasing temperature. Thus, they exhibit negative partial molar excess enthalpies. Limiting selectivities and capacities displayed in Table 5-32 reveal that similar to the three phosphonium ionic liquids discussed in the previous section, [C_13C_8N] [Tf_2N] exhibits poor separation performance for the n-hexane/benzene system. It is likely to represent a fair separation agent for ketones/alcohols and aromatic compounds/alcohols mixtures.

6.1.1.3. Imidazolium–based Ionic Liquids.

Infinite dilution activity coefficients and partial molar excess enthalpies of different organic solutes are provided in tables 5-18 through 5-21 for [BMIM] [SbF_6], 5-22 through 5-25 for [EMIM] [TfO], 5-26 through 5-29 for [MOIM] [PF_6]. Polar solutes have strong interaction with

the investigated imidazolium-based ionic liquids. The following hierarchies in the variation of IDAC values have been observed:

- [BMIM] [SbF_6]: n-alkanes > cycloalkanes ≅ alk-1-enes > alcohols > alk-1-ynes > alkylbenzenes > ketones;
- [EMIM] [TfO]: n-alkanes > cycloalkanes ≅ alk-1-enes > alk-1-ynes > alkylbenzenes > alcohols;
- [MOIM] [PF_6]: n-alkanes > alk-1-enes ≅ cycloalkanes > alcohols ≅ alk-1-ynes > alkylbenzenes.

For all three imidazolium–based ionic liquids, infinite dilution activity coefficients increase with increasing number of carbon atoms as shown in Figures 5-40, 5-47 and 5-54.
From the plots presented in Figures 5-33 through 5-39 for [BMIM] [SbF_6], 5-41 through 5-46 for [EMIM] [TfO] and 5-48 through 5-53 for [MOIM] [PF_6], the partial molar excess enthalpy at infinite dilution of all investigated unsaturated solutes, except alk-1-enes was found to be negative.

These three ionic liquids are potentially effective separation agents for aromatic/aliphatic compounds mixtures (Table 5-32). Their limiting selectivity and capacity data are high compared to NMP and sulfolane.

6.1.2. The inert gas stripping technique

Mixtures of n-hexane and cyclohexane as solutes in NMP were used as test systems. Measurements were carried out in the temperature range from 303.15 K and 323.15 K at three different stripping gas flow rates. Experimental results presented in table 5-30 were within 2 % of published literature data. Good agreement was also observed between data obtained from the gas-liquid chromatography and the dilutor method. Table 5-31 lists infinite dilution activity coefficients of six solutes, each one representing a functional group, in the ionic liquid [$3C_6C_{14}P$] [Tf_2N]. A comparison, in term of relative deviations was made to assess the extent of the agreement between the two experimental techniques used in this work with exactly the same systems. It was found that experimental results agreed within approximately 3.4 %. This is significant as not only the reliability of the newly constructed gas stripping set up was confirmed but also doubts on the validity of the GG experimental procedure were dispelled. In effect, the open literature (Mutelet and Jaubert 2006) warns of large experimental errors in the GC method when polar solutes are investigated due to adsorption of the latter onto the column packing and probably onto the inner walls of the GC column. To minimize adsorption effects, large mass fractions of the ionic liquids were used during the column packing stage. This

strategy was effective since even for methanol and acetone results from the GC and the dilutor techniques are not very different, and are within experimental errors.

Table 6-4 suggests that the uncertainty in determining the flow rate was the largest contributor to the overall error of infinite dilution activity coefficient data. Apart from the inability of the flow regulator to stabilize the inert gas flow rate over a long period of time, no major difficulties were encountered. All minor problems were sorted out as soon as they had arisen. Using the dilutor technique, a typical run with flow rates around 15 cm^3. $min.^{-1}$ could last three and eight hours for results displayed in tables 5-30 and 5-31 respectively. An experiment was terminated when, according to Krummen et al. (2000), around 15 % of the solute was stripped out of the system. It took a month and half to generate these data when, for the same systems and number of runs, the GLC equipment used in this study would require only a single day. The inert gas stripping technique is known as a more time consuming technique than GLC. These durations are not particularly longer than those reported by other authors. In order to decrease the experimental time, the first attempt consisted of increasing the inert gas flow rate. The best compromise between thermodynamics and kinetics of the stripping process was observed in the neighborhoods of flow rates about 23 $cm^3.min^{-1}$. Beyond this value, infinite dilution activity coefficient values tended to depend on the stripping gas flow rate, an indication that thermodynamic equilibrium was not achieved in the cell. For similar systems involving NMP, Krummen et al. (2000) took only 90 minutes to achieve a run. They used a dilutor cell with larger volume and probably higher height than the one constructed for this study, and flow rates as high as 20 to 40 $cm^3.min^{-1}$.

6.1.3. Error estimation

Uncertainties in determining the various quantities required to calculate activity coefficients at infinite dilution are provided in tables 6-3 and 6-4. The presented values were obtained by taking into account the accuracy of sensors as stated by suppliers, the stability of experimental parameters and deviations of parameters under different experimental conditions. The procedures described by George (2008) were used in this work to assign errors to mass, gas flow rate, as well as temperature measurements. As suggested by Harris (2000), the relative standard deviation of experimental variables were calculated according to the method presented by Skoog et al. (1996). Table 6-5 gives the overall relative errors calculated using the law of error propagation applied to equations (2-3), (2-4), (2-11), (3-9) and (3-88). Additional details are provided by the experimental procedures given in Chapter four.

Table 6-3: Uncertainties on experimental parameters for the GLC method.

Number of moles for the solvent,	±0.03 %
Oven temperature,	±0.35 %
Inlet pressure	±0.50 %
Outlet pressure	±0.30 %
Carrier gas flow rate	±0.20 %
Saturation vapour pressures	±0.30 %
Net retention volume	±3.00%
Difference of retention times (Solute - inert gas)	±0.20 %

Table 6-4: Uncertainties on experimental parameters for the dilutor method.

Number of moles for the solvent,	±0.03 %
System temperature,	±0.10 %
Dilutor cell pressure	±0.03 %
Stripping gas flow rate	±3.33 %
Saturation vapour pressures	±0.30 %
Saturation fugacity coefficients	±0.50 %
Flow-meter pressure	±0.03 %

Table 6-5: Overall uncertainties on experimental data and derived quantities.

Infinite dilution activity coefficient (GLG method)	±3.68 %
Infinite dilution activity coefficient (Dilutor method)	±4.26 %
Molar excess enthalpy at infinite dilution	±7.66 %
Selectivity at infinite dilution	±7.36 %
Capacity at infinite dilution	±3.68 %

6.2. Limiting activity coefficients of fluorinated ionic liquids

It was found, after an extensive literature survey, up to October 2009, experimental infinite dilution activity coefficients of 37 fluorinated ionic liquids, including the ones studied in this thesis, were available (See Table 6-6). In this section, experimental data, others than those generated in this work, were taken from various research papers published in the following journals:

- The Journal of Chemical Thermodynamics
- The Journal of Chemical and Engineering Data
- Fluid Phase Equilibria
- The Journal of Physical Chemistry B
- The Journal of Chromatography A

Numbers which are assigned to ionic liquids in table 6-6 are used as *x*-coordinates in the plots presented in Figures 6-1 through 6-3. The fluorinated ionic liquids 1-butyronitrile-3-methylimidazolium bis (trifluoromethylsulfonyl) imide ([CpMIM] [Tf_2N]), 1-butyronitrile-2, 3-dimethylimidazolium bis(trifluoromethylsulfonyl) imide ([CpMMIM][Tf_2N]),

1-hexyloxymethyl-3-methylimidazolium bis (trifluoromethylsulfonyl) imide ([H-O-MIM] [Tf_2N]) (Domańska and Marciniak, 2009b) and 1,3-dihexyloxymethyl-imidazolium bis(trifluoromethylsulfonyl)-imide ([DH-O-MIM] [Tf_2N]) (Domańska and Marciniak, 2009b) are not discussed in this dissertation due to insufficient database for comparison.

Table 6-6: List of fluorinated ionic liquids investigated in the literature and assigned numbers.

No.	Ionic Liquid	No.	Ionic Liquid	No.	Ionic Liquid
1	[EMIM][BF_4]	14	[C_{16}MIM][BF_4]	27	[BMIM][SbF_6]
2	[EMIM] [Tf_2N]	15	[$3C_6C_{14}P$][BF_4]	28	[BMIM][PF_6]
3	[MMIM][Tf_2N]	16	[$3C_6C_{14}P$][Tf_2N]	29	[EMIM][TFA]
4	[BMIM][BF_4]	17	[$3C_6C_{14}P$][$(C_2F_5)_3PF_3$]	30	[HMIM][TfO]
5	[BMIM][Tf_2N]	18	[$3C_1C_4N$][Tf_2N]	31	[BMPyrr][TfO]
6	[BMIM][TfO]	19	[BMPy][BF_4]	32	[HMPyrr][Tf_2N]
7	[MMPIM][BF_4]	20	[BMPyrr][Tf_2N]	33	[OMPyrr][Tf_2N]
8	[EMMIM][Tf_2N]	21	[Et_3S][Tf_2N]	34	[CpMIM][Tf_2N]
9	[HMIM][BF_4]	22	[Epy][Tf_2N]	35	[CpMMIM][Tf_2N]
10	[HMIM][PF_6]	23	[$3C_6C_{14}P$][PF_6]	36	[H-O-MIM][Tf_2N]
11	[HMIM][Tf_2N]	25	[EMIM][TfO]	37	[DH-O-MIM][Tf_2N]
13	[MOIM][Tf_2N]	26	[MOIM][PF_6]		
12	[MOIM][BF_4]	24	[$3C_8C_1N$][Tf_2N]		

6.2.1. Hierarchy of IDACs values

Figures 6-1 to 6-3 shows a comparison of limiting activity coefficients of six solutes, each one representing a homologous series, in fluorinated ionic liquids.

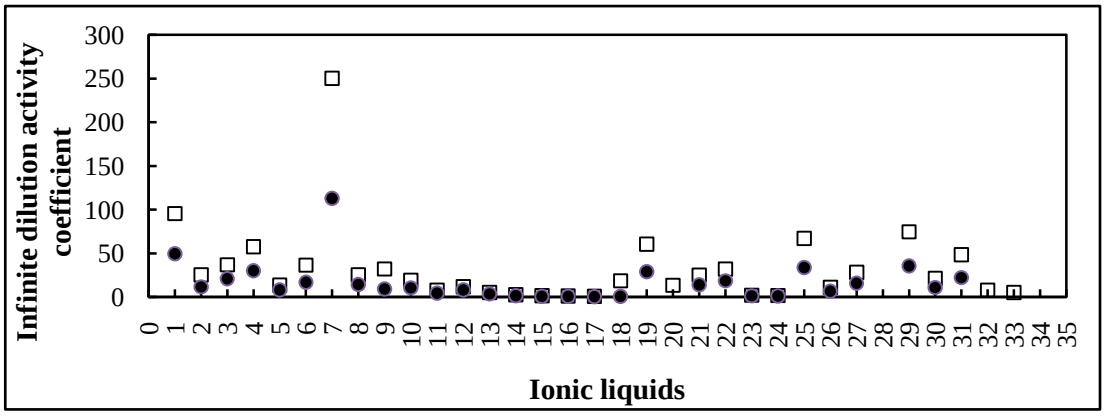

Figure 6-1: Experimental infinite dilution activity coefficients of (□) n-hexane and (●) cyclohexane in various fluorinated ionic liquids at 313.15 K.;1, [EMIM][BF_4][1][2]; 2, [EMIM] [Tf_2N] [3][5]; 3, [MMIM] [Tf_2N] [4] ; 4, [BMIM][BF_4] [6] ; 5, [BMIM] [Tf_2N] [4] ; 6, [BMIM][TfO] [9] ; 7, [MMPIM][BF_4] [10] ; 8, [EMMIM] [Tf_2N] [3] ; 9, [HMIM][BF_4] [12] ; 10, [HMIM][PF_6] [13] ; 11, [HMIM] [Tf_2N] [14][15] ; 12, [MOIM][BF_4] [17] ; 13, [MOIM] [Tf_2N] [16] ; 14, [C_{16}MIM][BF_4] [18] ; 15, [$3C_6C_{14}P$][BF_4] [19] ; 16, [$3C_6C_{14}P$] [Tf_2N] [19] ; 17, [$3C_6C_{14}P$][$(C_2F_5)_3PF_3$] [20] ; 18, [$3C_1C_4N$] [Tf_2N] [21] ; 19, [BMPy][BF_4] [22] ; 20, [BMPyrr] [Tf_2N] [16] ; 21, [Et_3S] [Tf_2N] [24] ; 22, [Epy] [Tf_2N] [25] ; 23, [$3C_6C_{14}P$][PF_6] [19] ; 24, [$3C_8C_1N$] [Tf_2N] [27]; 25, [EMIM][TfO] [28]; 26, [MOIM][PF_6] [29]; 27, [BMIM][SbF_6] [30] ; 28, [BMIM][PF_6] [31] ; 29, [EMIM][TFA] [32] ; 30, [HMIM][TfO] [33] ; 31, [BMPyrr][TfO] [34] ; 32, [HMPyrr] [Tf_2N] [35] ; 33 , [OMPyrr] [Tf_2N] [35]

Superscripts on ionic liquids' abbreviations in this section, as well as, in appendices F, G, H and I correspond to the following publications used as references: [1] Ge et al. (2008a); [2] Foco et al. (2006); [3] Heintz et al. (2002); [4] Krummen et al. (2002); [5] Deenadayalu et al. (2005); [6] Zhou and Wang (2006); [7] Zhou et al. (2007) ; [8]Heintz et al. (2005) ; [9]Domańska, U. and Marciniak, A., (2008a) ; [10]Wang et al. (2008) ; [11] Ge et al. (2008b); [12]Letcher et al. (2003b) [13]Letcher et al. (2003a) [14]Heintz et al. (2006a); [15]Letcher et al. (2005); [16]Kato et al. (2005) [17]Heintz et al. (2005b) [18]Mutelet et al. (2007); [19]Domańska et al. (2009); [20]Letcher and Reddy (2005); [21]Heintz et al. (2006b); [22]Heintz et al. (2001); [23]Heintz et al. (2002); [24]Domańska and Marciniak (2009); [25] Kato and Gmehling (2004); [26]Kato and Gmehling (2005); [27]Gwala et al. (2010), [28]Olivier et al (2010a); [29]Olivier et al (2010b); [30]Olivier et al. (2009c) ; [31]Shimoyama et al. (2008); [32]Domańska, U. and Marciniak, A., (2007) [33]Yang et al. (2008) [35]Nebig et al. (2009); [36] Möllmann and

Gmehling (1997); [37] Krummen et al. (2000); [38]Kossack et al.(2008); [39]Dortmund Data Bank, DDB.

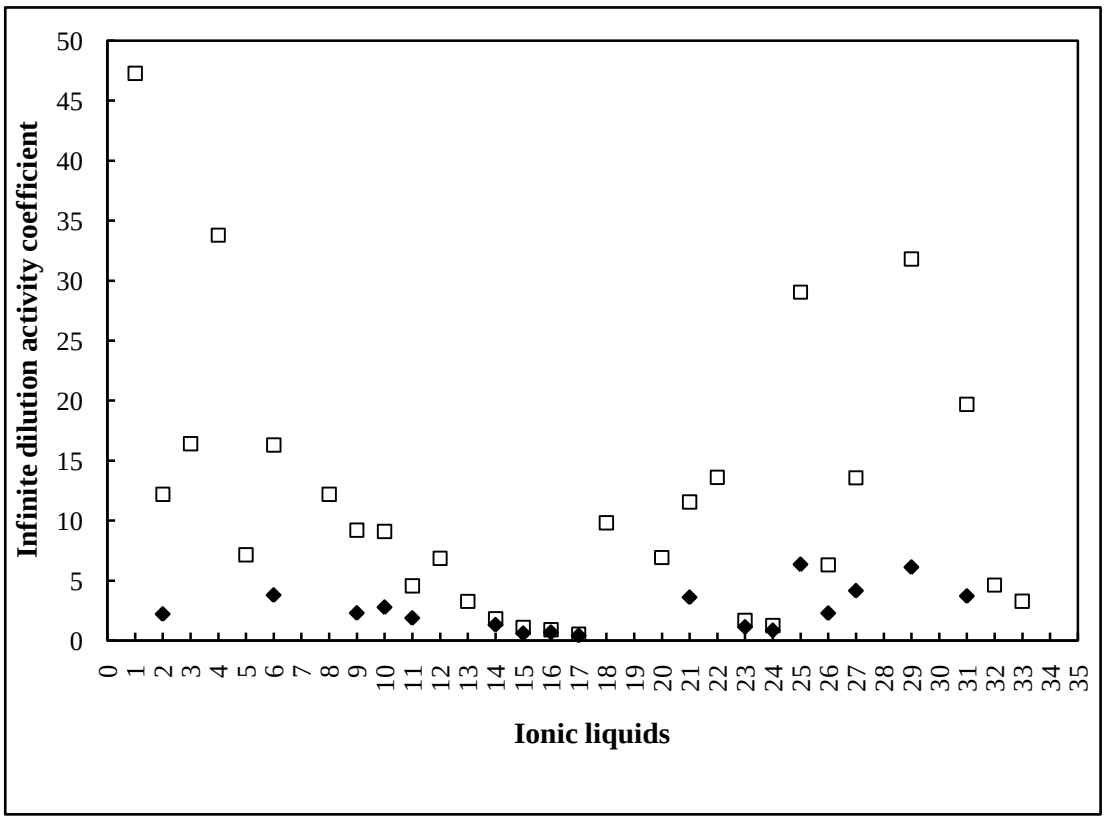

Figure 6-2: Experimental infinite dilution activity coefficients of (□) hex-1-ene and (♦) hex-1-yne in various fluorinated ionic liquids at 313.15 K; 1, [EMIM][BF_4] [2]; 2, [EMIM][Tf_2N] [4][5]; 3, [MMIM][Tf_2N] [4] ; 4, [BMIM][BF_4] [2][6] ; 5, [BMIM][Tf_2N] [4] ; 6, [BMIM][TfO] [9]; 8, [EMMIM][Tf_2N] [3] ; 9, [HMIM][BF_4] [12] ; 10, [HMIM][PF_6] [13] ; 11, [HMIM][Tf_2N] [14][15] ; 12, [MOIM][BF_4] [17] ; 13, [MOIM][Tf_2N] [16] ; 14, [C_{16}MIM][BF_4] [18] ; 15, [$3C_6C_{14}P$][BF_4] [19] ; 16, [$3C_6C_{14}P$][Tf_2N] [19] ; 17, [$3C_6C_{14}P$][$(C_2F_5)_3PF_3$] [20] ; 18, [$3C_1C_4N$][Tf_2N] [21] ; 20, [BMPyrr][Tf_2N] [16] ; 21, [Et_3S][Tf_2N] [24] ; 22, [Epy][Tf_2N] [25] ; 23, [$3C_6C_{14}P$][PF_6] [19] ; 24, [$3C_8C_1N$][Tf_2N] [27]; 25, [EMIM][TfO] [28]; 26, [MOIM][PF_6] [29]; 27, [BMIM][SbF_6] [30] ; 29, [EMIM][TFA] [32] ; 31, [BMPyrr][TfO] [34] ; 32, [HMPyrr][Tf_2N] [35] ; 33 , [OMPyrr][Tf_2N] [35]

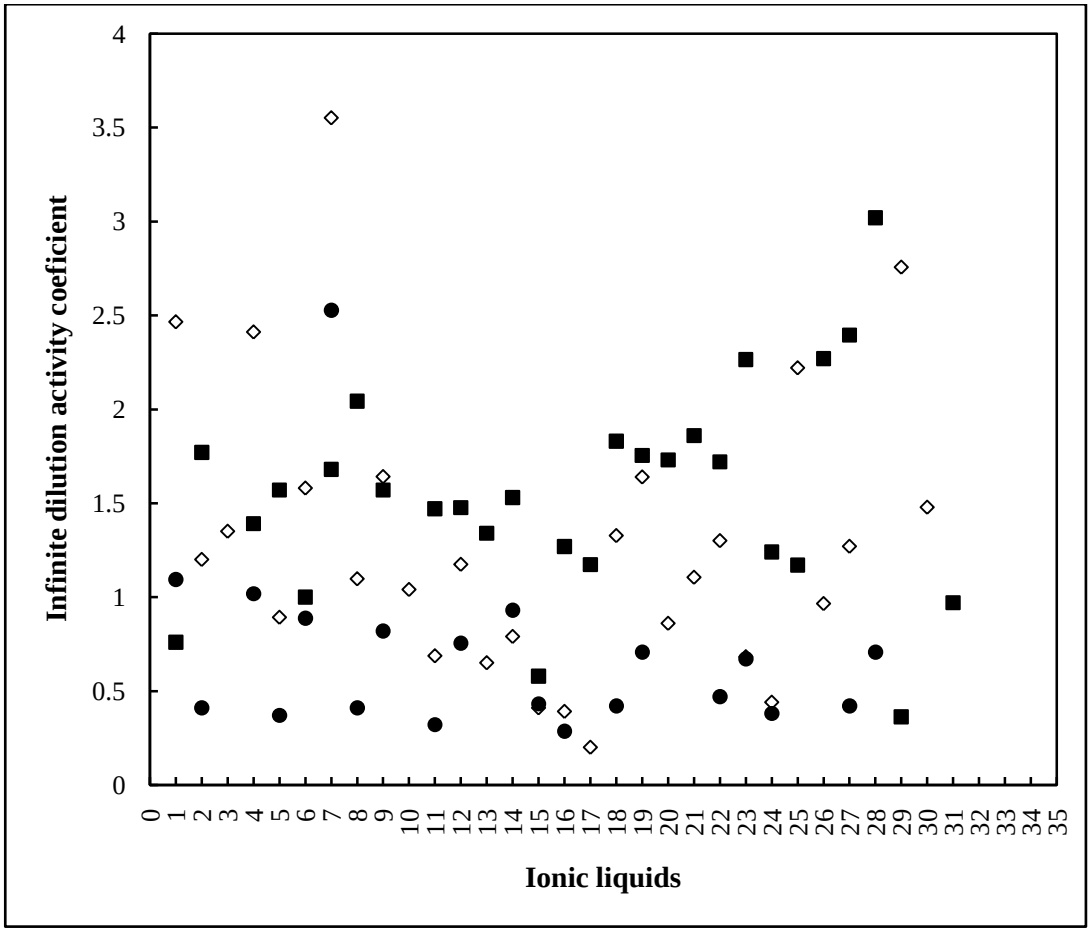

Figure 6-3: Experimental infinite dilution activity coefficients of (■) ethanol, (◊) benzene and (●) acetone in various fluorinated ionic liquids at 313.15 K.; 1, [EMIM][BF_4] [2]; 2, [EMIM][Tf_2N] [4]; 3, [MMIM][Tf_2N] [4] ; 4, [BMIM][BF_4] [6][7] ; 5, [BMIM][Tf_2N] [8] ; 6, [BMIM][TfO] [9] ; 7, [MMPIM][BF_4] [10][11] ; 8, [EMMIM][Tf_2N] [3] ; 9, [HMIM][BF_4] [2] ; 10, [HMIM][PF_6] [13] ; 11, [HMIM][Tf_2N] [16] ; 12, [MOIM][BF_4] [17] ; 13, [MOIM][Tf_2N] [16] ; 14, [C_{16}MIM][BF_4] [18] ; 15, [$3C_6C_{14}P$][BF_4] [19] ; 16, [$3C_6C_{14}P$][Tf_2N] [19] ; 17, [$3C_6C_{14}P$][$(C_2F_5)_3PF_3$] [20] ; 18, [$3C_1C_4N$][Tf_2N] [21] ; 19, [BMPy][BF_4] [22][23] ; 20, [BMPyrr] [Tf_2N] [16] ; 21, [Et_3S][Tf_2N] [24] ; 22, [Epy][Tf_2N] [25][26] ; 23, [$3C_6C_{14}P$][PF_6] [19] ; 24, [$3C_8C_1N$][Tf_2N] [27]; 25, [EMIM][TfO] [28]; 26, [MOIM][PF_6] [29]; 27, [BMIM][SbF_6] [30] ; 28, [BMIM][PF_6] [31] ; 29, [EMIM][TFA] [32] ; 30, [HMIM][TfO] [33] ; 31, [BMPyrr][TfO] [34] ; 32, [HMPyrr][Tf_2N] [35] ; 33 , [OMPyrr] [Tf_2N] [35]

According to the above plots, activity coefficient values for organic solutes in FILs follow the following patterns:

- Imidazolium, pyridinium, pyrrolidinium and sulfonium-based fluorinated ionic liquids: n-alkanes > cycloalkanes > alk-1-enes > alk-1-ynes > alcohols > alkylbenzenes > ketones

- Phosphonium-based fluorinated ionic liquids:
  n-alkanes ≅ alk-1-enes ≅ alcohols > cycloalkanes > alk-1-ynes > alkylbenzenes > ketones
- Ammonium-based fluorinated ionic liquids:
  No clear hierarchy is observable.

6.2.2. Effect of structure on IDACs of organic solutes in Fluorinated Ionic Liquids, FILs

It would be misleading to conclude that the stated hierarchies fully translate the behavior of all mixtures of fluorinated ionic liquids and the solutes under consideration. These are merely general trends. However, the only constant for all systems is that alkanes and ketones lead to the largest and the smallest experimental infinite dilution activity coefficient values respectively.

Linear alkanes are non-polar organic compounds. They interact with ILs mostly through small range van der Waals forces which are weaker than induced dipole-dipole interactions appearing in systems involving corresponding alk-1-enes, alk-1-ynes and aromatic compounds. These compounds have delocalized electrons that enhance polarisability. Increasing polarisability leads naturally to smaller limiting activity coefficients. Infinite dilution activity coefficient values of alcohols are even smaller due to their polar nature and the presence of an electronegative oxygen atom which is likely to interact more strongly with the positive charge of the ionic liquid cation. Infinite dilution activity coefficients values for ketones are the smallest, an indication of strong solute-solvent interactions. This can be attributed to the interaction between the two pairs of electrons on the oxygen atom of the ketone with the cation of the IL, as well as, between its positive pole and the ionic liquid anion.

There are strong cation-anion coulombic interactions in imidazolium and pyridinium-based ionic liquids due to the polarisability of their molecules. Conversely, no delocalized electrons exist in phosphonium, ammonium and sulfonium-based fluorinated ionic liquids. Association with organic solutes is likely to be stronger with these solvents in comparison with imidazolium and pyridinium-based ionic liquids as accommodating a solute will not require overcoming the strong coulombic interactions and probably hydrogen bonds. It follows that for the same solute, the limiting activity coefficient value increases with the introduction of a polarisable ring in the cation of the ionic liquid. Extending the alkyl chain of the solute generally weakens the interactions between organic solutes and ionic liquids as infinite dilution activity coefficients increase with increasing solute carbon number. This is visible in Figures G-1 through G-83 of Appendix G which relate the infinite dilution activity coefficient at 313.15 K to the carbon number of various solutes in all investigated fluorinated ionic liquids. In the presence of hydrogen bonds and coulombic forces that are common in ionic liquids, long-chained ionic

liquids are probably too large and closely packed to accommodate solutes. Exceptions include the following systems: alkan-1-ols + [BMIM] [Tf_2N], alkan-1-ols + [$3C_6C_{14}P$] [$(C_2F_5)_3PF_3$] and ket-2-ones + [C_13C_8N][Tf_2N] . Their corresponding plots of the natural logarithm of γ_i^{∞} versus carbon number are found in Figures G-56, G-59 and G-81 respectively. It is possible that lengthening the alkyl chain of an alcohol or a ketone to a certain extent in these particular cases favours additional attractive forces between the alkyl chain of the solute and the one of the solvent through van der Waals interactions.

As far as the effect of the ionic liquid anion is concerned, shape, polarity and size have to be taken into account to interpret infinite dilution activity coefficient experimental results. Most polar ionic liquids i.e. those containing [BF_4] $^-$ and [TFA] $^-$ do not generally interact strongly with the solutes due probably to strong intrinsic anion-cation coulombic forces, as well as hydrogen bonds.

6.2.2.1. Infinite dilution activity coefficients in imidazolium-based FILs

An examination of figures in Appendix G gives an insight into how IDACs values are affected by the presence of a particular cation in the structure of the imidazolium-based FILs . It appears that for the same anion, limiting activity coefficients of n-alkanes (Figures G-1 to G-4), alk-1-enes (Figures G-15 to G-18), alk-1-ynes (Figures G-29 to G-32), cycloalkanes (Figures G-38 to G-41), alkan-1-ols (Figures G-51 to G-54), alkylbenzenes (Figures G-64 to G-66) and ket-2-ones (Figures G-75 to G-76) decrease with increasing alkyl chain length of the IL cation.

It is observed that for n-alkanes (Figures G-5 to G-8), alk-1-enes (Figures G-19 to G-22), cycloalkanes (Figures G-42 to G-45) and ket-2-ones (Figures G-77 to G-79), infinite dilution activity coefficients decrease when the anion is changed in the following order: $[BF_4]^-$ > $[TFA]^-$ > $[TfO]^-$ > $[SbF_6]^-$; $[PF_6]^-$ > [Tf_2N] $^-$. This is the general trend as in some cases this is not true (Figures G-44 and G-78)

No such clear hierarchy is displayed by mixtures involving alk-1-ynes (Figures G-33 to G-35) and alkan-1-ols (Figures G-55 to G-58). However, for all investigated FILs, the smallest activity coefficient values are obtained with [Tf_2N] $^-$ anion.

6.2.2.2. Infinite dilution activity coefficients in phosphonium-based FILs

The available experimental data allow examination of the effects of the anion only, since all the phosphonium-based fluorinated ionic liquids studied so far have in common the [$3C_6C_{14}P$] $^+$ cation**.** According to the plots represented in Figures G-9, G-23 and G-46, G-71 and G-80, the infinite dilution activity coefficients of all classes of solutes, except alcohols and alk-1-ynes,

decrease when anions are changed in the following order: $[PF_6]^-$ > $[BF_4]^-$ > $[Tf_2N]^-$ > $[(C_2F_5)_3PF_3]^-$. The following hierarchy is observed for alcohols: $[PF_6]^-$ > $[Tf_2N]^-$; $[(C_2F_5)_3PF_3]^-$ > $[BF_4]^-$ (See Figure G-59). And for alk-1-ynes: $[PF_6]^-$ > $[Tf_2N]^-$ > $[BF_4]^-$ > $[(C_2F_5)_3PF_3]^-$. (Figure G-36)

6.2.2.3. Infinite dilution activity coefficients in ammonium-based FILs

There are no data for a reliable description of the effect of the anion as only two ammonium-based fluorinated ionic liquids have been investigated in the literature. They have in common the $[Tf_2N]^-$ anion. For n-alkanes (Figure G-10), alkan-1-ols (Figure G-60), alkylbenzenes (Figure G-72) and ket-2-ones (Figure G-81), limiting activity coefficients decrease with increasing alkyl chain length of the ammonium-based FILs. The opposite trend is observed only for cycloalkanes (Figure G-47).

6.2.2.4. Infinite dilution activity coefficients in pyrrolidinium-based FILs

Under the same anion, the limiting activity coefficients of n-alkanes (Figure G-12) and alk-1-enes (Figure G-26) decrease with the increasing alkyl chain length of pyrrolidinium-based fluorinated ionic liquids. There are no literature data related to alk-1-ynes, cycloalkanes, alkan-1-ols and alkylbenzenes. Limiting activity coefficients of n-alkanes (Figure G-13), alk-1-enes (Figure G-27) and cycloalkanes (Figure G-49) decrease when the anion is changed from $[TfO]^-$ to $[Tf_2N]^-$. The reverse is observed for alkan-1-ols. (Figure G-62). Data for other classes of solutes are not available.

6.3. Limiting selectivity and capacity of fluorinated ionic liquids

The theory of Prausnitz and Anderson (1961) explains the separation mechanism of a mixture of hydrocarbons using a polar separation agent. It is also true for ionic liquids. To act as an effective entrainer or extractant, an ionic liquid has to interact differently with the mixed components. This occurs when one of the components is saturated whereas the other is not. The ionic liquid solvent polarises the non-saturated component. The former interacts more strongly with the solvent and is carried along as the bottom product. Selectivity values depend on the relative polarisability of the two components to be separated. This explains in part the trends of selectivity and capacity values described in this section and depicted by Figures H-1through H-21 in Appendix H. Solvent capacity is, the numerical amount of solute removed from the mixture by the extracting solvent. Selectivity normally decreases with temperature and often follows a different trend from solvent capacity. The compromise between selectivity and capacity is quantified as the Performance Index, P.I., which is the arithmetic product of these two properties. For each separation problem discussed in this work, the effect of structure on the

separation ability of ionic liquids is reflected by the hierarchies given in each of the following sections. When analyzing the trends of selectivity and capacity, it is essential to incorporate in addition to polarisability, the shape and the size of species, as well as hydrogen bonding potential within ionic liquids.

6.3.1. n-Hexane (1)/Benzene (2) separation problem

Limiting selectivities of the experimentally investigated fluorinated ionic liquids follow this pattern:

[EMIM][BF_4] > [BMPy][BF_4] > [EMIM][TfO] > [MMIM][Tf_2N] > [EMIM][TFA] > [BMIM][BF_4] > [BMIM][TfO] > [Et_3S][Tf_2N] > [BMIM][SbF_6] > [EMIM][Tf_2N] > [HMIM][BF_4] > [HMIM][PF_6] > Sulfolane > [BMPyrr][Tf_2N] > [BMIM][Tf_2N] > [HMIM][TfO] > [$3C_1C_4N$] [Tf_2N] > [MOIM][PF_6] > NMP > [HMIM] [Tf_2N] > [MOIM][BF_4] > [MOIM][Tf_2N] > [$3C_8C_1N$][Tf_2N] > [$3C_6C_{14}P$][BF_4] > [$3C_6C_{14}P$][$(C_2F_5)_3PF_3$] > [C_{16}MIM][BF_4] > [$3C_6C_{14}P$][PF_6] >[$3C_6C_{14}P$] [Tf_2N]

In terms of good compromise between selectivity and capacity, FILs are arranged in decreasing order of limiting performance index values, PI^{∞} as follows:

[BMPy][BF_4] > [Et_3S][Tf_2N] > [MMIM][Tf_2N] > [Epy][Tf_2N] > [BMPyrr][Tf_2N] > [HMIM][PF_6] > [EMIM][Tf_2N] > [BMIM][SbF_6] > [BMIM][Tf_2N] > [HMIM][Tf_2N] > [$3C_6C_{14}P$][$(C_2F_5)_3PF_3$] > [EMIM][BF_4] > [BMIM][TfO] > [EMIM][TfO] > [MOIM][Tf_2N] > [HMIM][BF_4] > [MOIM][PF_6] > NMP > [$3C_1C_4N$][Tf_2N] > [BMIM][BF_4] > [EMIM][TFA] > [HMIM][TfO] > [$3C_8C_1N$] [Tf_2N] > [MOIM][BF_4] > [$3C_6C_{14}P$][BF_4] > Sulfolane > [$3C_6C_{14}P$][Tf_2N] > [$3C_6C_{14}P$][PF_6] > [C_{16}MIM][BF_4]

The best selectivity is obtained with [EMIM] [BF_4]. The ionic liquid [BMPy] [BF_4] presents the best compromise between selectivity and capacity at infinite dilution. It is a remarkable fact that a great deal of FILs would potentially perform better than industrial molecular solvents NMP and Sulfolane, as separation agents. At 313.15 K [EMIM] [BF_4] is twice as selective as Sulfolane. The infinite dilution performance index of [BMPy] [BF_4] is three times higher than the one obtained with the same industrial molecular solvent.

6.3.1.1. Imidazolium-based fluorinated ionic liquids

According to Figures H-1 and H-2 in Appendix H, favorable structures of FILs for separating aromatic/aliphatic compounds mixtures are that the alkyl chain of the cation is short and the anion is small with sterical shielding around its charge centre. For the same anion, selectivity at infinite dilution decreases with alkyl chain extension. For the same cation, the smaller the anion,

the higher the limiting selectivity. In all cases, limiting capacity and limiting selectivity for the n-hexane (1)/benzene (2) system vary in inverse orders.
Extending the alkyl chain of the IL cation accentuates the steric hindrance on the imidazolium ring. This results in poorer ability to polarize the benzene molecule and thus, lower selectivity whereas interactions with n-hexane do not vary notably. Capacity increases with increasing alkyl chain length because greater van der Waals volume weakens the intrinsic hydrogen bond within the IL.

Under the same anion, it is observed that selectivities of pyrrolidinium and pyridinium-based FILs which have six-membered rings exhibit higher selectivities of n-hexane to benzene in comparison with the corresponding imidazolium-based ones. The similarity of their rings to benzene explains this. It is one of the reasons why investigated phosphonium and ammonium-based FILs manifest poor potential for separating aliphatic/aromatic compounds mixtures. Kumar and Banerjee (2009) came up with a similar interpretation when studying thiophene separation from diesel. They pointed out that thiophene with its five-membered ring preferentially attaches more to an imidazolium-based cation provided with a five-membered ring, in comparison with a pyridinium or quinolinium (six-membered) cation.

In the absence of sterical shielding effect, the anion tends to approach the positive center of the cation leading to a closed shape for the molecule. Interactions between the positive charge centers of the IL cation and the delocalized electrons of benzene are hindered since the polarity of the IL is reduced. This is why anions with sterical shielding effect around the charge center lead to higher selectivities. Moreover, the increase in the volume of the cation results in a greater solvent ability to remove benzene.
These explanations are consistent with the recent publication by Kumar and Banerjee (2009), as well as, the findings related to olefin/aliphatic separation reported by Lei et al. (2006, 2007b) and hold for non-polar systems discussed in the following sections as well. Concerning polar systems, the overall effect of structure on selectivity and capacity is a result of the relative magnitude of polarity and molecular volume of entities composing the ionic liquid.

To understand the trends described hereafter, one should bear in mind that, depending on anions comprising FILs , polarity together with intrinsic strength of hydrogen bonding varies in the order:
$[TFA]^- \cong [TfO]^- > [BF_4]^- > [PF_6]^- > [Tf_2N]^-$. Volume increases as follows: $[BF_4]^- < [TFA]^- < [PF_6]^- < [TfO]^- < [Tf_2N]^-$.

6.3.1.2. Phosphonium-based fluorinated ionic liquids

As indicated by Figure H-3 in Appendix H, S_{12}^{∞} for the n-hexane (1)/benzene (2) system decreases with the increasing anion volume. Selectivity values remain very small as compared to Sulfolane, a commonly used industrial solvent for aliphatic/aromatic compounds mixtures. Smaller anions lead to higher selectivities. The S_{12}^{∞} value for $[3C_6C_{14}P]$ $[(C_2F_5)_3PF_3]$ is an outlier, probably due to differences in experimental conditions. Limiting capacity tends to increase with increasing anion volume. In the absence of data related to the ionic liquid $[3C_6C_{14}P]$ $[PF_6]$ which were provided by this thesis, it would be difficult to reliably derive these hierarchies of limiting capacity and selectivity values with only the previously published experimental results. This emphasizes the contribution of the present study to the expansion of knowledge in relation of FILs.

6.3.1.3. Ammonium-based fluorinated ionic liquids

Only the effect of the cation can be discussed in the light of available data. Extending the alkyl chain of the ionic liquid leads to lower selectivities and higher capacities. This is observed in Figure H-4 in Appendix H.

6.3.2. Methanol (1)/benzene (2) separation problem

Infinite dilution selectivities of the experimentally investigated fluorinated ionic liquids for the Methanol (1)/benzene (2) system decrease in this order:

$[3C_6C_{14}P][(C_2F_5)_3PF_3]$ > $[3C_6C_{14}P][PF_6]$ > $[3C_6C_{14}P]$ $[Tf_2N]$ > $[3C_8C_1N]$ $[Tf_2N]$ > $[MOIM][PF_6]$ > $[MOIM]$ $[Tf_2N]$ > $[HMIM]$ $[Tf_2N]$ > $[HMIM][PF_6]$ > $[C_{16}MIM][BF_4]$ > $[BMIM][SbF_6]$ > $[3C_6C_{14}P][BF_4]$ > $[Et_3S]$ $[Tf_2N]$ > $[BMIM]$ $[Tf_2N]$ > $[EMIM]$ $[Tf_2N]$ > $[3C_1C_4N]$ $[Tf_2N]$ > $[Epy]$ $[Tf_2N]$ > $[MOIM][BF_4]$ > $[BMPy][BF_4]$ > $[BMIM][BF_4]$ > $[BMIM][TfO]$ > $[HMIM][BF_4]$ > $[EMIM][TfO]$ > $[DMPIM][BF_4]$ > $[EMIM][BF_4]$ > [EMIM][TFA]

Performance indices follow the sequence below:

$[3C_6C_{14}P][(C_2F_5)_3PF_3]$ > $[3C_6C_{14}P]$ $[Tf_2N]$ > $[3C_8C_1N]$ $[Tf_2N]$ > $[3C_6C_{14}P][PF_6]$ > $[3C_6C_{14}P][BF_4]$ > $[MOIM]$ $[Tf_2N]$ > $[HMIM]$ $[Tf_2N]$ > $[MOIM][PF_6]$ > $[C_{16}MIM][BF_4]$ > $[HMIM][PF_6]$ > $[BMIM]$ $[Tf_2N]$ > $[EDMIM]$ $[Tf_2N]$ > $[Et_3S]$ $[Tf_2N]$ > $[BMIM][SbF_6]$ > $[EMIM]$ $[Tf_2N]$ > $[3C_1C_4N]$ $[Tf_2N]$ > $[Epy]$ $[Tf_2N]$ > $[MOIM][BF_4]$ > $[BMPy][BF_4]$ > $[BMIM][TfO]$ > $[HMIM][BF_4]$ > $[BMIM][BF_4]$ > $[EMIM][TfO]$ > $[EMIM][BF_4]$ > [EMIM][TFA]

Depending on whether methanol is collected as part of the bottom or overhead stream, [EMIM] [TFA] and [$3C_6C_{14}P$] [$(C_2F_5)_3PF_3$] are found to be the best solvents for this separation problem. Due to the absence of the required data, no comparison with industrial molecular solvent is attempted.

6.3.2.1. Imidazolium-based fluorinated ionic liquids

For the same anion, it is observed in Figures H-2 and H-5 that infinite dilution selectivity and capacity for the methanol (1)/benzene (2) decrease when the alkyl chain is shortened. Figure H-2 is applicable to both methanol/benzene and hexane/benzene capacity values. Experimental data do not totally agree on a common pattern as far as the effect of the anion is concerned. However, according to Figure H-5, it seems that imidazolium-based fluorinated ionic liquids with low selectivity are the ones containing anions such as $[BF_4]^-$, $[TFA]^-$ and $[TfO]^-$, characterized by small volume and a sterical shielding effect around the anion charge centre. As far as limiting capacity is concerned, it is found to increase with increasing anion volume.

6.3.2.2. Phosphonium-based fluorinated ionic liquids

Limiting selectivity values of phosphonium-based FILs containing the common cation $[3C_6C_{14}P]^+$ are observed to decrease when the anion is changed in this order (Figure H-6):

$$[(C_2F_5)_3PF_3]^- > [PF_6]^- > [Tf_2N]^- > [BF_4]^-$$

The general trend is that limiting selectivity and limiting capacity increase with increasing anion volume and decreasing polarity of the ionic liquid, [$3C_6C_{14}P$] [PF_6] being an outlier.

6.3.2.3. Ammonium-based fluorinated ionic liquids

Figure H-7 in Appendix H suggests that lengthening the ionic liquid alkyl chain leads to higher values of infinite dilution selectivity and capacity for the methanol (1)/benzene (2) system.

6.3.3. Methanol (1)/acetone (2) separation problem

For the methanol (1)/acetone (2) system, the hierarchy of selectivity values is:

[BMIM][SbF_6] > [$3C_6C_{14}P$][Tf_2N] > [HMIM][Tf_2N] > [$3C_1C_4N$][Tf_2N] > [EMIM][Tf_2N] > [$3C_6C_{14}P$][PF_6] > [$3C_8C_1N$][Tf_2N] > [BMIM][PF_6] > [BMIM][Tf_2N] > [Epy][Tf_2N] > [BMPy][BF_4] > [C_{16}MIM][BF_4] > [MOIM][BF_4] > [$3C_6C_{14}P$][BF_4] > [BMIM][BF_4] > [HMIM][BF_4] > [BMIM][TfO] > [EMIM][BF_4] > Dimethylsulfoxide

Infinite dilution performance indices for the methanol (1)/acetone (2) system can be arranged in this order:

Dimethylsulfoxide > $[3C_6C_{14}P]$ $[Tf_2N]$ > [HMIM] $[Tf_2N]$ > [BMIM] $[Tf_2N]$ > $[3C_8C_1N]$ $[Tf_2N]$ > [EMIM] $[Tf_2N]$ > $[BMIM][SbF_6]$ > $[3C_1C_4N]$ $[Tf_2N]$ > $[3C_6C_{14}P][BF_4]$ > [Epy] $[Tf_2N]$ > $[3C_6C_{14}P][PF_6]$ > $[BMPy][BF_4]$ > $[BMIM][PF_6]$ > $[MOIM][BF_4]$ > $[HMIM][BF_4]$ > $[BMIM][TfO]$ > $[C_{16}MIM][BF_4]$ > $[BMIM][BF_4]$ > $[EMIM][BF_4]$.

$[BMIM][SbF_6]$ and $[3C_6C_{14}P]$ $[Tf_2N]$ lead to the highest selectivity and performance index respectively. No FIL is potentially better than dimethylsulfoxide, one of the most suitable molecular solvents for this separation problem. The limiting selectivity of $[BMIM][SbF_6]$ is 19 % smaller than the one given by dimethylsulfoxide. Compared with $[3C_6C_{14}P]$ $[Tf_2N]$, the infinite dilution performance index of DMSO is three times higher.

6.3.3.1. Imidazolium-based fluorinated ionic liquids

Data represented in Figure H-8 show that under the same anion, selectivity and capacity tend to increase with increasing alkyl chain length of the FIL cation. Both properties increase with increasing anion volume. It can be noted that $[BMIM]^+$-containing ionic liquids do not rigorously comply with trends possibly due to experimental uncertainties. More data are required for a more accurate description of the influence of structure on the separation performance of imidazolium-based FILs for the methanol (1)/acetone (2) system.

6.3.3.2. Phosphonium-based fluorinated ionic liquids

An examination of Figure H-10 in Appendix H reveals that infinite dilution selectivity for the methanol (1)/acetone (2) system increases with increasing anion volume. No regular variation trend regarding capacity emerges.

6.3.3.3. Ammonium-based fluorinated ionic liquids

Infinite dilution selectivity of ammonium-based FILs for the methanol (1)/acetone (2) system reduces when the alkyl chain is extended as shown by Figure H-11. The reverse is true for limiting capacity.

6.3.4. n-hexane (1)/ hex-1-ene (2) separation problem

Selectivity of n-Hexane to Hex-1-ene decreases according to this order:
[BMPyrr][TfO] > [EMIM][TFA] > [Epy] $[Tf_2N]$ > [EMIM][TfO] > [MMIM]$[Tf_2N]$> [BMIM][TfO] > $[Et_3S]$ $[Tf_2N]$ > $[HMIM][PF_6]$ > $[BMIM][SbF_6]$ > [EMIM] $[Tf_2N]$ > [EDMIM] $[Tf_2N]$ > $[EMIM][BF_4]$ > $[HMIM][BF_4]$ > [BMPyrr] $[Tf_2N]$ > [BMIM] $[Tf_2N]$ > $[3C_1C_4N]$ $[Tf_2N]$ > $[MOIM][PF_6]$ > $[MOIM][BF_4]$ > $[BMIM][BF_4]$ > [HMPyrr] $[Tf_2N]$ >

[HMIM] [Tf_2N] > [MOIM] [Tf_2N] > [OMPyrr] [Tf_2N] > [$C_{16}MIM$][BF_4] > [$3C_8C_1N$] [Tf_2N] > [$3C_6C_{14}P$][BF_4] > [$3C_6C_{14}P$][$(C_2F_5)_3PF_3$] > [$3C_6C_{14}P$] [Tf_2N] > [$3C_6C_{14}P$][PF_6] > NMP.

Performance indices follow this trend:
[$3C_6C_{14}P$][$(C_2F_5)_3PF_3$] > [$3C_6C_{14}P$] [Tf_2N] > [$3C_6C_{14}P$][BF_4] > [$3C_8C_1N$] [Tf_2N] > [$C_{16}MIM$][BF_4] > [$3C_6C_{14}P$][PF_6] > [MOIM] [Tf_2N] > [OMPyrr] [Tf_2N] > [HMIM] [Tf_2N] > [HMPyrr] [Tf_2N] > [BMPyrr] [Tf_2N] > [MOIM][PF_6] > [BMIM] [Tf_2N] > [MOIM][BF_4] > [HMIM][PF_6] > [HMIM][BF_4] > [$3C_1C_4N$] [Tf_2N] > [Et_3S] [Tf_2N] > [Epy] [Tf_2N] > [EMIM] [Tf_2N] > [EDMIM] [Tf_2N] > [BMIM][SbF_6] > [BMIM][TfO] > [MMIM] [Tf_2N] > [BMPyrr][TfO] > NMP > [EMIM][TfO] > [EMIM][TFA] > [BMIM][BF_4] > EMIM][BF_4].

On the basis of experimental data, the best selectivity is obtained with the ionic liquid [BMPyrr] [TfO]. It amounts to an increase of 30 % when compared to NMP. It can be seen that the ionic liquid [$3C_6C_{14}P$] [$(C_2F_5)_3PF_3$] leads to the best compromise between selectivity and capacity. The calculated value of its limiting performance index is 29 times higher than NMP. Where comparison is possible, the above hierarchies are consistent with the findings of Lei and co-workers (Lei et al. 2006, 2007) in their study related to n-hexane (1)/ hex-1-ene (2) separation using the quantum approach. In relation to the effect of the anion, their finding is that higher selectivities are obtained with smaller anions with sterical shielding effect around the anion charge centre. Additionally, they predicted that the best ionic liquid for this separation problem is 1-octylquinolinium bis (trifluoromethylsulfonyl) imide. However, the present study could not confirm this result due to the lack of experimental infinite dilution activity coefficient data in the ionic liquid 1-octylquinolinium bis (trifluoromethylsulfonyl) imide.

6.3.4.1. Imidazolium-based Fluorinated ionic liquids

For the same anion, selectivity at infinite dilution decreases with increasing alkyl chain length (Figure H-12). A look at Figure H-12, as well as the hierarchy of selectivities provided in the previous section reveals that small anions with sterical shielding effect around the charge center are essential to achieve high selectivities. Capacity increases with increasing alkyl chain length, as well as, increasing anion volume, as illustrated by Figure H-13.

6.3.4.2. Phosphonium-based fluorinated ionic liquids

For phosphonium-based FILs containing the $[3C_6C_{14}P]^+$ cation, selectivity at infinite dilution for the n-hexane (1)/ hex-1-ene (2) system decreases slightly with increasing anion size (Figure H-14) whereas capacity at infinite dilution for this system and this class of FILs seems to be constant.

6.3.4.3. Ammonium-based Fluorinated ionic liquids

With increasing alkyl chain length the limiting selectivity of ammonium-based FILs decreases and limiting capacity increases, as can be seen in Figure H-15.

6.3.4.4. Pyrrolidinium-based Fluorinated ionic liquids

The available experimental data used in Figure H-16, Appendix H, suggest that for the same cation, limiting selectivity of pyrrolidinium-based FILs reduces when the anion size increases, whereas limiting capacity follows the opposite trend.; and for the same anion, the longer the alkyl chain of the ionic liquid cation, the smaller the selectivity and the higher the capacity (Figure H-16).

6.3.5. Benzene (1)/ butan-2-one (2) separation problem

Limiting selectivities of the experimentally investigated fluorinated ionic liquids follow this pattern:

[EMIM] [Tf_2N] > [Epy][Tf2N] > [BMIM][SbF_6] > [BMPy][BF_4] > [HMIM][Tf_2N] > [BMPyrr][Tf_2N]> [EMIM][BF_4] > [BMIM][BF_4] > [HMIM][BF_4] > [$3C_6C_{14}P$][Tf_2N] > [$3C_8C_1N$][Tf_2N] > [MOIM][BF_4] > [$3C_6C_{14}P$][PF_6] > [$3C_6C_{14}P$][BF_4] > [C_{16}MIM][BF_4]

In terms of good compromise between selectivity and capacity, FILs are arranged in decreasing order of limiting performance index values as follows:

[EMIM][Tf_2N] > [HMIM][Tf_2N] > [$3C_6C_{14}P$][Tf_2N] > [$3C_8C_1N$][Tf_2N] > [BMIM][SbF_6] > [Epy][Tf_2N] > [BMPyrr][Tf_2N]> [$3C_6C_{14}P$][BF_4] > [BMPy][BF_4] > [$3C_6C_{14}P$][PF_6] > [HMIM][BF_4] > [MOIM][BF_4] > [EMIM][BF_4] > [BMIM][BF_4] > [C_{16}MIM][BF_4].

The best selectivity and the best performance index are obtained with [EMIM] [Tf_2N]. No comparison with industrial solvents is possible due to lack of required experimental data.

6.3.5.1. Imidazolium-based fluorinated ionic liquids

Figures H-17 and H-18 show that with increasing anion volume, the limiting selectivity and the limiting capacity of imidazolium-based FILs for the benzene (1)/butan-2-one (2) system increase. And the longer the alkyl chain of the FIL cation, the smaller the selectivity and the higher the capacity at infinite dilution.

6.3.5.2. Phosphonium-based fluorinated ionic liquids

Due to a very limited database, it is not possible to reliably derive the effect of structure on selectivity or capacity in this case using Figure H-19. Only three ionic liquids having a common

cation are considered and the obtained selectivity and capacity plots do not allow any derivation of the effect of the anion on these two properties.

6.3.6. Ethanol (1)/ butan-2-one (2) separation problem

Infinite dilution selectivities of the experimentally investigated fluorinated ionic liquids for the ethanol (1)/butan-2-one (2) system decrease in this order:
Chlorobenzene > $[3C_6C_{14}P]$ $[Tf_2N]$ > [BMIM][SbF_6] > [EMIM] $[Tf_2N]$ > [HMIM] $[Tf_2N]$ > $[3C_8C_1N]$ $[Tf_2N]$ > [BMPyrr] $[Tf_2N]$ > $[3C_6C_{14}P][PF_6]$ > [BMIM][PF_6] > [Epy] $[Tf_2N]$ > [BMPy][BF_4] > [MOIM][BF_4] > $[C_{16}MIM][BF_4]$ > [HMIM][BF_4] > $[3C_6C_{14}P][BF_4]$ > [BMIM][BF_4] > [EMIM][BF_4].

Performance indices follow the sequence below:
$[3C_6C_{14}P]$ $[Tf_2N]$ > $[3C_8C_1N]$ $[Tf_2N]$ > [HMIM] $[Tf_2N]$ > [EMIM] $[Tf_2N]$ > [BMPyrr] $[Tf_2N]$ > [BMIM][SbF_6] > $[3C_6C_{14}P][PF_6]$ > [Epy] $[Tf_2N]$ > Chlorobenzene > [BMIM][PF_6] > $[3C_6C_{14}P][BF_4]$ > [BMPy][BF_4] > [MOIM][BF_4] > $[C_{16}MIM][BF_4]$ > [HMIM][BF_4] > [BMIM][BF_4] > [EMIM][BF_4].

On the basis of selectivity and performance index at infinite dilution, the best potential solvent for this separation problem is $[3C_6C_{14}P]$ $[Tf_2N]$. Chlorobenzene, a commonly used industrial molecular solvent is twice as selective as $[3C_6C_{14}P]$ $[Tf_2N]$. However its limiting performance index is 3.25 times smaller than the one achieved with the same ionic liquid.

6.3.6.1. Imidazolium-based fluorinated ionic liquids

According to Figure H-20 and H-18 (Since the capacity value at a given temperature for the ethanol/ butan-2-one is the same as for the benzene/butan-2-one system), high limiting selectivity and capacity are achieved with imidazolium-based fluorinated ionic liquids consisting of long-chained cations and big-sized anions.

6.3.6.2. Phosphonium-based fluorinated ionic liquids

It can be seen in Figure H-21 that the limiting selectivity of phosphonium-based fluorinated ionic liquids for the ethanol (1)/ butan-2-one (2) system increases with increasing anion volume. It is impossible to derive a reliable trend for capacity variation.

6.4. Correlation of limiting activity coefficient and selectivity with the FIL alkyl chain

It is the outcome of this study that a simple model can correlate γ_i^{∞} with the alkyl chain length of the pyrrolidinium and imidazolium-based FILs at constant temperature. As shown in the plots

presented in Figures I-1 through I-4 in Appendix I, obtained from experimental data published by different groups under different conditions, the natural logarithm of γ_{13}^{∞} of n-hexane, hex-1-ene, cyclohexane, ethanol, benzene and acetone is a linear function of the carbon number of the alkyl chain attached to the imidazolium or pyrrolidinium moiety. The quality of correlation is good except for ketones and alkan-1-ols in $[BF_4]^-$-containing FILs. Available data allowed to examine imidazolium-based FILs containing $[BF_4]^-$ (Figure I-1), $[Tf_2N]^-$.
(Figure I-2) and $[TfO]^-$ (Figure I-3) anions as well as a few systems involving pyrrolidinium–based fluorinated ionic liquids (Figure I-4) The correlating equation is:

$$\ln \gamma_i^{\infty} = aNc + b \tag{6.1}$$

where *a* and *b* are parameters related to the nature of the anion, as well as, the solute under consideration. γ_i^{∞} is obviously always greater than zero. Consequently, it can be stated that the natural logarithm of both limiting selectivity and capacity of imidazolium-based FILs for different systems are also linear functions of the carbon number of the alkyl chain attached to the methylimidazolium as well as the methylpyrrolidinium. A similar equation to (6-1) can be used to relate selectivity to the alkyl chain length as follows:

$$\ln S_{ij}^{\infty} = a_{ij} Nc + b_{ij} \tag{6.2}$$

Figures I-5 and I-6 in Appendix D show a good quality of the linear regression used to approximate experimental selectivity data. Systems referred to include n-hexane/benzene (Figure I-5) and n-hexane/hex-1-ene (Figure I-6).

CHAPTER SEVEN: CONCLUSION AND RECOMMENDATIONS

The objective of this study was to investigate the effect of structure on fluorinated ionic liquids ability to separate organic mixtures. To assess the effectiveness of FILs as separation agents, limiting experimental selectivities and capacities were calculated from experimental infinite dilution activity coefficient data.

Infinite dilution activity coefficients of various organic solutes have been measured by gas-liquid chromatography over a wide temperature range in seven fluorinated ionic liquids:

- Trihexyltetradecylphosphonium tetrafluoroborate, $[3C_6C_{14}P]$ $[BF_4]$;
- Trihexyltetradecylphosphonium bis(trifluoromethylsulfonyl) imide, $[3C_6C_{14}P]$ $[Tf_2N]$;
- Trihexyltetradecylphosphonium hexafluorophosphate, $[3C_6C_{14}P]$ $[PF_6]$;
- Methyltrioctylammonium bis (trifluoromethylsulfonyl) imide, $[C_13C_8N]$ $[Tf_2N]$;
- 1-ethyl-3-methylimidazolium trifluoromethanesulfonate, [EMIM] [TfO];
- 1-butyl-3-methylimidazolium hexafluoroantimonate, [BMIM] $[SbF_6]$;
- 1-methyl-3-octylimidazoliumhexafluorophosphate. $[MOIM][PF_6]$.

Two of these FILs ($[3C_6C_{14}P]$ $[BF_4]$ and $[3C_6C_{14}P]$ $[Tf_2N]$) have been investigated previously with a smaller number of solutes and a narrower temperature range than in this study. Most of the reported measurements are new. For each solvent, the Gibbs-Helmholtz equation was used to derive molar excess enthalpies of solutes at infinite dilution. This was important as the property provides information on the tendency of the solvent to associate with a solute of interest. The large number of newly generated infinite dilution activity coefficient values expanded the database used for examining the effect of structure on the separation ability of FILs. If these additional data were not produced, some of the useful evidences exploited herein would not have emerged.

A simple empirical correlation was also proposed for limiting activity coefficient as a function of the alkyl chain length. This is significant since in previous work, the description of γ_i^{∞} change with the alkyl chain length has been merely qualitative. As a matter of fact, the natural logarithm of γ_i^{∞} was found to vary linearly with the carbon number of the alkyl chain attached to the methylpyrrolidinium or methylimidazolium group. The same applied to limiting selectivity. The model correlated well γ_i^{∞} and limiting selectivity with the cation alkyl chain length for systems involving non-polar components as solutes. Poor correlation coefficients were however observed for polar solutes. This outcome can be exploited when developing a priori predictive thermodynamic models.

A detailed analysis of infinite dilution activity coefficient, selectivity and capacity data obtained from this work and the literature, allowed to derive the following trends, in relation to six separation problems selected among the most interesting ones for the chemical industry:

- **n-hexane (1)/benzene (2) system:** Pyridinium and imidazolium-based FILs were potentially the best suitable solvents for this separation problem. The best selectivity was obtained with [EMIM] [BF_4]. The ionic liquid [BMPy] [BF_4] presented the best compromise between selectivity and capacity at infinite dilution. Higher selectivities were obtained with short-chained cations and small anion volumes.

- **Methanol (1)/benzene (2):** [EMIM] [TFA] and [$3C_6C_{14}P$] [$(C_2F_5)_3PF_3$] were found to be the best solvents for this separation problem, depending on the stream in which methanol was to be collected i.e. overhead or bottom stream. Phosphonium-based fluorinated ionic liquids with large anion volume and an appropriate cation would be more selective. FILs with short alkyl chain length for the cation and a small anion volume were generally the least favorable ones.

- **Methanol (1)/acetone (2):** Limiting capacity and selectivity varied in the same manner as for the previous system except in case of ammonium-based FILs. [BMIM][SbF_6] and [$3C_6C_{14}P$] [Tf_2N] lead to the highest selectivity and performance index respectively.

- **n-Hexane (1)/ hex-1-ene (2):** Regardless of the class of the ionic liquid, higher selectivities were obtained with longer alkyl chains attached to the cation and smaller anions with sterical shielding effect around the anion charge centre. The best selectivity was displayed by the ionic liquid [BMPyrr] [TfO]. It was seen that the ionic liquid [$3C_6C_{14}P$] [$(C_2F_5)_3PF_3$] lead to the best compromise between selectivity and capacity.

- **Benzene (1)/ butan-2-one (2):** The best selectivity as well as the best performance index was obtained with [EMIM] [Tf_2N]. With increasing anion volume, the limiting selectivity was found to increase. And the longer the alkyl chain of the cation, the smaller the selectivity. Due to insufficient database, no reliable conclusion could be reached for phosphonium-based FILs.

- **Ethanol (1)/ butan-2-one (2):** $[3C_6C_{14}P]$ $[Tf_2N]$ was found to be the best potential solvent for this separation problem on the basis of both selectivity and performance index. It was found that fluorinated ionic liquids consisting of long-chained cations and big-sized anions were potentially the best separation agents for this system.

Judging from performance index values it was observed that the ionic liquid $[3C_6C_{14}P]$ $[Tf_2N]$ would be a reasonable separation solvent for all the investigated mixtures, except the n-Hexane/ Benzene system. In some cases, no comprehensive conclusion could be made due to insufficient or incoherent data. Nevertheless, where comparison was possible, the findings were consistent with previously published results derived from COSMO-RS (Kumar and Banerjee, 2009 and Lei et al. 2006, 2007). It is an indication that the approach consisting of using experimental data was at once economic, less time consuming and qualitatively effective.

These results emphasize the important role played by the nature of ions comprising the ionic liquid in determining the magnitude of activity coefficient values and consequently its effectiveness as separation solvent. Chances to have a FIL which would act as a "universal separation agent" are very slim. For a given separation problem, there is a specific profile for appropriate ionic liquid solvents.

The importance of this study lies in its contribution to the understanding of how structure influences ionic liquids selectivity and capacity in different separation problems. It expands the knowledge about FILs which are potentially green separation agents. Additionally, the reported infinite dilution activity coefficient data can be used to extend the applicability range of predictive thermodynamic models. Such are UNIFAC, and modified UNIFAC models which are already incorporated in some chemical engineering process simulators.

Due to the limited nature of the data set used in this work, the following was not addressed:

- The effect of the cation for phosphonium-based FILs on limiting activity coefficient, selectivity and capacity;
- The effect of the anion for ammonium -based FILs;
- The effect of both cation and anion in other types of ILs such as quinolinium, guadinium, sulfonium, piperidinium and thiazolium-based FILs (though they are less popular in separation-related studies);
- The effect of introducing functional groups other than n-alkyl in the cation of different FILs.

These topics are worthy of interest for future work. They will require more experimental data or the use of the quantum approach.

The calculated relative error on γ_i^{∞} data obtained by the IGST was larger than most values reported in the literature, due to high uncertainties in determining the flow-rate. Its stability left much to desire. Replacing the flow-regulator is to be considered for more accurate measurements.

REFERENCES

Alessi, P., Fermeglia, M. and Kikic, I., (1986), "A Differential Static Apparatus for the Investigation of the Infinitely Dilute Region", *Fluid Phase Equilibr.*, 29, 249-256.

Alessi, P., Fermeglia, M. and Kikic, I., (1991), "Significance of Dilute Regions", *Fluid Phase Equilibr.*, 70, 239-250.

Appleby, D., Hussey, C. L., Seddon, K. R. and Turp, J. E., (1986), " Room-temperature ionic liquids as solvents for electronic absorption spectroscopy of halide complexes", *Nature*, 323, 614-615.

Arlt, W., Seiler, M., Jork, C. and Schneider, T., (2002), "Ionic liquids as selective additives for the separation of close-boiling or azeotropic mixtures", *Patent*; Basf Aktiengesellschaft, Germany. 2002-EP2824 (2002074718), 29, 3-14-2002, WO.

Banerjee, T. and Khanna, A., (2006), "Infinite Dilution Activity Coefficients for Trihexyltetradecylphosphonium Ionic Liquids: Measurements and COSMO-RS Prediction", *Journ. Chem. Thermodyn.*, 51, 2170–2177.

Banerjee, T., (2008), "Liquid–Liquid Equilibrium for Ionic Liquid Systems Using COSMO-RS: Effect of Cation and Anion Dissociation", AIChE *J.*, 54, 1874-1885.

Bao J. B., Hang L. L., Ling Y-P., Chen, G-H. and Han S-J., (1993a), "Studies on the determination of infinite dilution activity coefficients of acetone-cycloalkanes systems by gas stripping method", *Chem. J. Chin. Univ.*, 14, 1280-1283.

Bao, J. B., Huang, Q., Chen, G-H and Han, S-J, (1993b), "Determination of large value activity coefficients at infinite dilution", Acta *Phys. Chem.*, 9, 724-727.

Bao, J. B., Hang L. L. and Han S-J., (1994), "Infinite Dilution Activity Coefficients of (propanone + an n-alkanes) by Gas Stripping", *Journ. Chem. Thermodyn.*, 26, 673-680.

Bao, J-B and Han, S-J, (1995), "Infinite Dilution Activity Coefficients for Various Types of Systems", *Fluid Phase Equilibr.*, 112, 307-316.

Bonhôte, P., Dias, A. P., Papageorgiou, N., Kalyanasundaram, K. and Grätzel, M., (1996), "Hydrophobic, Highly Conductive Ambient-Temperature Molten Salts", *Inorg. Chem., 35*, 1168-1178.

Boudreau, L. C., Driver, M.S., Munson, C.L. and Schinski, W. L., (2001), "Separation of dienes from olefins using ionic liquids and metal salt complexing agents", *Patent;* USA. 2001-37044(2003125599), 15 12-31-2001, US.

Castells R. C., Arancibia, E. L., Nardillo A. M. and Castells C., (1990), "Thermodynamics of Hydrocarbon solutions using GLC, n-Hexane, n-Heptane, Benzene and Toluene as solute, each at infinite dilution, in n-Hexadecane, n-Octadecane and n-Eicosane", *Journ. Chem. Thermodyn.*, 22, 969-977.

Castells, C. B. and Carr P. W., (1999), "A Comparative Study of Semi-theoretical models for Predicting Infinite Dilution Activity Coefficients of Alkanes in Organic Solvents", *Ind. Eng. Chem. Res.*, 38, 4104-4109.

Cheong W. J., (2003), "A critical examination of the limiting activity coefficients of normal alkanes in common organic liquids", *Bull. Kor. Chem. Soc.*, 24, 1708-1710.

Chien, C. F., Kopecni, M. M., Laub R. J. and Smith C. A., (1981), "Solute Liquid-Gas Activity and Partition Coefficients with Mixtures of n-Octadecane with N, N-Dibutyl-2-EthylHexylamine Solvents", *Journ. Phys. Chem.*, 85, 1864-1871.

Chum, H. L., Koch, V. R., Miller, L. L. and Osteryoung, R. A., (1975), "Electrochemical scrutiny of organometallic iron complexes and hexamethylbenzene in a room temperature molten salt", *J. Am. Chem. Soc.*, 97, 3264-3265.

Condor, J. R. and Young, C. L., (1979), "Physico-chemical Measurement by Gas Chromatography", John Willey and Sons, U.S.A.

Cooper, E. I. and O'Sullivan, E. J. M., (1992), "Proceedings of the Eighth International Symposium of Molten Salts, Physical and High Temperature Materials Division Proceedings ", 92-16.

Coquelet, C. and Richon, D., (2005), " Measurement of Henry's Law Constants and Infinite Dilution Activity Coefficients of Propyl Mercaptan, Butyl Mercaptan, and Dimethyl Sulfide in Methyldiethanolamine (1) + Water (2) with w_1=0.5 Using a Gas Stripping Technique", *J. Chem. Eng. Data*, 50, 2053-2057.

CRC Handbook of Chemistry and Physics, (2005), 86th ed., Taylor & Francis, London.

Cruickshank, A. J. B., Windsor M. L., and Young C. L., (1966a), "Prediction of Second Virial Coefficients of Mixtures from the principles of Corresponding states", *Trans. Faraday Soc.*, 62, 2341-2355.

Cruickshank, A. J. B., Windsor, M. L., and Young, C. L., (1966b), "The Use of Gas-Liquid Chromatography to Determine Activity Coefficients and Second Virial Coefficients of Mixtures; II Experimental studies on hydrocarbon solutes'', *Proc. R. Soc. London, Ser. A,* 295-271.

Cruickshank, A. J. B., Gainey, B. W., Hicks, C. P., Letcher, T.M., Moody, R. W. and Young, C. L., (1969), "Gas-Liquid Chromatographic Determination of Cross-Term Second Virial Coefficients Using Glycerol", *Trans. Faraday Soc*., 65,1014-1031.

David W., Letcher, T.M. and Ramjugernath, D., (2003), "Activity Coefficients of Hydrocarbon Solutes at Infinite Dilution in the Ionic Liquid 1-methyl-3-octylimidazolium chloride from Gas-liquid chromatography", *Journ. Chem. Thermodyn.*, 35, 1335-1341.

David, W., (2004), "Ionic liquids as solvents in separation processes" MSc Thesis, University of KwaZulu-Natal, South Africa.

Deenadayalu, N., Letcher, T. M. and Reddy, P., (2005), "Determination of Activity Coefficients at Infinite Dilution of Polar and Nonpolar Solutes in the Ionic Liquid 1-Ethyl-3-methylimidazolium Bis(trifluoromethylsulfonyl) Imide Using Gas-Liquid Chromatography at the Temperature 303.15 K or 318.15 K.", *J. Chem. Eng. Data*, 50, 105-108.

Deenadayalu, N., Thango, S. H., Letcher, T. M. and Ramjugernath, D., (2006a), "Measurement of activity coefficients at infinite dilution using polar and non-polar solutes in the ionic liquid 1-methyl-3-octyl-imidazolium diethyleneglycolmonomethylethersulfate at T = (288.15, 298.15, and 313.15) K", *Journ. Chem. Thermodyn.*, 38, 542–546.

Deenadayalu, N., Ngcongo C. N., Letcher, T. M. and Ramjugernath, D., (2006b), "Liquid-liquid equilibria for ternary mixtures (an ionic liquid + benzene + heptane or hexadecane at T= 298.15 K and atmospheric pressure", *J. Chem. Eng. Data*, 51, 988–991.

Derr E. L. and Deal C. H., (1969), "Analytical Solutions of Groups: correlation of activity coefficients through structural group parameters", *Inst. Chemical. Eng, Sympos. Ser.* London., 32, 3:44-3:51.

Dobryakov, Y. G. and Vitenberg, A. G., (2006), "Determination of distribution coefficients of volatile sulfur-containing compounds among aqueous solutions and gas phase by continuous gas extraction", *Russ. J. Appl. Chem.*, 79, 1244–1250.

Dobryakov, Y. G., Tuma, D. and Maurer, G., (2008), "Activity Coefficients at Infinite Dilution of Alkanols in the Ionic Liquids 1-Butyl-3-methylimidazolium Hexafluorophosphate, 1-Butyl-3-methylimidazoliumMethyl Sulfate, and 1-Hexyl-3-methylimidazolium Bis(trifluoromethylsulfonyl) Amide Using the Dilutor Technique*.", J. Chem. Eng. Data*, 53, 2154–2162.

Dohnal V. and Horakova I., (1991), "A New Variant of the Rayleigh Distillation Method for the Determination of Limiting Activity Coefficients", *Fluid Phase Equilibr.*, 68, 173-185.

Doležal, B., Popl, M. and Holub, R., (1981), "Determination of activity coefficients at very low concentrations by the inert gas stripping method", *J. Chromatogr.,* 207: 193-201.

Doležal, B. and Holub, R., (1985), "Approximate relations for determining the activity coefficients at very low concentration by the method of variation of solute concentration", Coil. *Czech. Chem. Commun.,* 50, 704-711.

Domańska, U. and Marciniak, A., (2007), "Activity Coefficients at Infinite Dilution Measurements for Organic Solutes and Water in the Ionic Liquid 1-Ethyl-3-methylimidazolium Trifluoroacetate", *J. Phys. Chem. B,* 111, 11984-11988.

Domańska, U. and Marciniak, A., (2008a), "Activity Coefficients at Infinite Dilution Measurements for Organic Solutes and Water in the Ionic Liquid 1-Butyl-3-methylimidazolium Trifluoromethanesulfonate", *J. Phys. Chem. B,* 2008, 112 (35), 11100-11105.

Domańska, U. and Marciniak, A., (2008b), "Measurements of activity coefficients at infinite dilution of aromatic and aliphatic hydrocarbons, alcohols and water in the new ionic liquid [EMIM] [SCN] using GLC", *Journ. Chem. Thermodyn.,* 40, 860–866.

Domańska, U. and Laskowska, M., (2009), "Measurements of activity coefficients at infinite dilution of aliphatic and aromatic hydrocarbons, alcohols, thiophene, tetrahydrofurane, MTBE and water in ionic liquid [BMIM] [SCN] Using GLC", *J. Chem. Thermodyn.,* 41, 645–650.

Domańska, U. and Marciniak, A., (2009a), "Activity coefficients at infinite dilution measurements for organic solutes and water in the ionic liquid triethylsulphonium bis (trifluoromethylsulfonyl) imide", *Journ. Chem. Thermodyn.,* 41, 754–758.

Domańska, U. and Marciniak, A., (2009b), "Activity coefficients at infinite dilution measurements for organic solutes and water in the 1-hexyloxymethyl-3-methyl-imidazolium and 1,3-dihexyloxymethyl-imidazolium bis(trifluoromethylsulfonyl)-imide ionic liquids—The cation influence", *Fluid Phase Equilibr.*, 286, 154-161.

Domańska, U., Redhi, G.G. and Marciniak, A., (2009), "Activity coefficients at infinite dilution measurements for organic solutes and water in the ionic liquid 1-butyl-1-methylpyrrolidinium trifluoromethanesulfonate using GLC", *Fluid Phase Equilibr.,* 278, 97–102.

Dortmund Data Bank, DDB, www.ddbst.com. Accessed 15 October 2009.

Duhem, P. and Vidal, J., (1978), "Extension of the Dilutor Method to Measurement of High Activity Coefficients at Infinite Dilution", *Fluid Phase Equilibr.* 2, 231-235.

Dupont, J., (2004), "On the Solid, Liquid and Solution Structural Organization of Imidazolium Ionic Liquids", *J. Braz. Chem. Soc*., 15, 341-350.

Earle, M. J., Esperança, J. M. S. S., Gilea, M. A., Lopes, J. N. C., Rebelo, L. P. N., Magee, J. W., Seddon, K. R. and Widegren, J. A., (2006), "The distillation and volatility of ionic liquids", *Nature*, 439, 831-834.

Eckert, C. A. and Sherman, S. R., (1996), "Measurement and Predictions of Limiting Activity Coefficients", *Fluid Phase Equilibr.*, 116, 333-342.

Eckert F, and Klamt A., (2003), "Prediction of halocarbon thermodynamics with COSMO-RS", *Fluid Phase Equilibr.*, 210, 117-141.

Eike D.M., Brennecke, J.F., and Maginn, E.J., (2004) "Predicting Infinite-Dilution Activity Coefficients of organic solutes in ionic liquids" *Ind. Eng. Chem. Res.*, 43, 1039-1048.

Ellis, S.R.M. and Jonah, D.A., (1962) "Prediction of Activity Coefficients at Infinite Dilution." *Chem. Eng. Sci.*, 17, 971-976.

Endres, F. and El Abedin, S.Z., (2006), "Air and water stable ionic liquids in physical chemistry" *Phys. Chem. Chem. Phys.*, 8, 2101-2116.

Everett, D. H., (1965), "Effect of Gas Imperfection on Gas-Liquid Chromatography Measurements: a Refined Method for Determining Activity Coefficients and Second Virial Coefficients", *Trans. Faraday Soc.* 61, 1637-1645.

Foco, G. M., Bottini, S. B., Quezada, N., De la Fuente, J.C. and Peters, C.J., (2006), "Activity Coefficients at Infinite Dilution in 1-Alkyl-3-methylimidazolium Tetrafluoroborate Ionic Liquids", *J. Chem. Eng. Data*, 51, 1088-1091.

Ford, E., DePaoli, D., Miller, J., Kanel, J. and Tiley, R., (2004), "Accelerating Ionic Liquid Commercialization; Research Needs to Advance New Technology", Workshop Results, BCS, Incorporated.

Fox, D. M., Gilman, J. W., Morgan, A. B., Shields, J. R., Maupin, P. H., Lyon, R. E., De Long, H. C. and Trulove, P. C., (2008), "Flammability and Thermal Analysis Characterization of Imidazolium-Based Ionic Liquids", *Ind. Eng. Chem. Res.*, 47, 6327–6332.

Fredenslund, A., Jones, R. L. and Prausnitz, J. M., (1975), "Group Contribution Estimation of Activity Coefficients in Nonideal Liquid Mixtures", *AIChE J.*, 21, 1086-1099.

Gainey B. W., and Young C. L., (1968), "Activity coefficients of benzene in solution of n-alkanes and the second virial coefficients of benzene + nitrogen mixtures; Gas-chromatographic investigation", *J. Chem. Soc., Faraday Trans.* 64, 349-358.

Gautreaux, M. F., Jr. and Coates, J., (1955), "Activity Coefficients at Infinite Dilution", *AIChE J.*, 1, 406-500.

Ge, M-L., Wang, L-S. Li, M-Y. and Wu, J-S., (2007), "Activity Coefficients at Infinite Dilution of Alkanes, Alkenes, and Alkyl Benzenes in 1-Butyl-3-methylimidazolium Trifluoromethanesulfonate Using Gas-Liquid Chromatography", *J. Chem. Eng. Data*, 52, 2257-2260.

Ge, M-L. and Wang, L-S., (2008), "Activity Coefficients at Infinite Dilution of Polar Solutes in 1-Butyl-3-methylimidazolium Trifluoromethanesulfonate Using Gas–Liquid Chromatography", *J. Chem. Eng. Data*, *53*, 846–849.

Ge, M-L., Wang, L-S., Wu, J-S., and Zhou, Q., (2008a), "Activity Coefficients at Infinite Dilution of Organic Solutes in 1-Ethyl-3-methylimidazolium Tetrafluoroborate Using Gas-Liquid Chromatography", *J. Chem. Eng. Data*, 53, 1970-1974.

Ge, M-L., Wu, J-S., Wang, M-H. and Wang, L-S., (2008b), "Activity Coefficients at Infinite Dilution of Polar Solutes in 1-Propyl-2, 3-dimethylimidazolium Tetrafluoroborate Using Gas–Liquid Chromatography" *J. Chem. Eng. Data*, *53*, 871–873.

George, S., (2008), "Determination of activity coefficients at infinite dilution using the inert gas stripping technique", MSc Thesis, University of KwaZulu-Natal, South Africa.

Gmehling, J., Li, J. and Schiller, M., (1993), "A Modified UNIFAC Model 2. Present parameters Matrix and Results for Different Thermodynamic Properties", *Ind. Eng. Chem. Res.*, 32, 178-193.

Gmehling, J., (1995), "From UNIFAC to Modified UNIFAC to PSRK with the help of DDB", *Fluid Phase Equilibr.*., 107, 1-29.

Gmehling J., and Möllmann, C., (1998), "Synthesis of Distillation processes using thermodynamic models and the Dortmund Data Bank", *Ind. Eng. Chem. Res.*, 37, 3112-3123.

Gmehling J., Lohmann J., Jakob A., Li, J. and Joh, R., (1998), "A Modified UNIFAC Model 3: Revision and Extension*", Ind. Eng. Chem. Res*., 37, 4876-4882.

Gmehling, J., Krummen, M. and Carl, V., (2001), "Use of ionic liquids as entraining agents and selective solvents for separation of aromatic hydrocarbons in aromatic petroleum streams", *Patent*; Ossietzky Universitaet Oldenburg, 2001-10154052(10154052), 14, 11-2-2001, DE.

Gmehling, J., Wittig, R., Lohmann, J. and Joh, R., (2002), "A Modified UNIFAC (Dortmund) Model 4: Revision and Extension", *Ind. Eng. Chem. Res.*, 41, 1678-1688.

Gmehling, J., (2003), "Potential of thermodynamic tools (group contribution methods, factual data banks) for the development of chemical processes", *Fluid Phase Equilibr.*, 210, 161–173.

Gmehling, J., (2009), "Present status and potential of group contribution methods for process development", *Journ. Chem. Thermodyn.,* 41, 731-747.

Go, I, Yoshio, I., Munehiro, Y., Katsumi, H. and Yasuhiko, A., (2007), " Measurement of infinite dilution activity coefficients of n-alkanes in 4-methyl-n-butylpyridinium tetrafluoroborate using gas–liquid chromatography ", *Fluid Phase Equilibr.,* 251, 17–23.

Grensemann, H. and Gmehling, J., (2005), "Performance of A Conductor-Like Screening Model for Real Solvents Model in Comparison to Classical Group Contribution Methods", *Ind. Eng. Chem. Res.,* 44, 1610-1624.

Gruber, D., Krummen, M. and Gmehling, J., (1999), "The Determination of Activity Coefficients at Infinite Dilution with the Help of the Dilutor Technique (Inert Gas Stripping)", *Chem. Eng. Technol., 22,* 827-831.

Gwala, N.V., Deenandayalu, N., Tumba, K. and Ramjugernath, D., (2010), "Activity Coefficients at Infinite Dilution for Different Solutes in an Ammonium Ionic Liquid Using Gas Liquid Chromatography at T = (303 or 313 or 323) K", *J. Chem. Thermodyn*., 42, 256-261.

Hagiwara, R. and Ito, Y., (2000), "Room temperature ionic liquids of alkylimidazolium cations and fluoroanions", *Journ.Fluor. Chem.,* 105, 221-227.

Hansen H.K., Schiller, M., Fredenslund A., Gmehling J. and Rasmussen P., (1991), "Vapour-Liquid Equilibria by UNIFAC Group Contribution Method: Revision and Extension 5" *Ind. Eng. Chem. Res.,* 30, 2352-2355.

Harris, R. A., (2000), "Monoethanolamine: suitability as an extractive solvent", MSc Thesis, University of KwaZulu-Natal, South Africa.

Heintz, A., Kulikov, D.V. and Verevkin, S.P., (2001), "Thermodynamic Properties of Mixtures Containing Ionic Liquids. 1. Activity Coefficients at Infinite Dilution of Alkanes, Alkenes, and Alkylbenzenes in 4-Methyl-n-butylpyridinium Tetrafluoroborate Using Gas-Liquid Chromatography" *J. Chem. Eng. Data,* 46, 1526-1529.

Heintz, A., Kulikov, D. V. and Verevkin, S. P., (2002a), "Thermodynamic properties of mixtures containing ionic liquids. Activity coefficients at infinite dilution of polar solutes in 4-methyl-*N*-butyl-pyridinium tetrafluoroborate using gas–liquid chromatography", *Journ. Chem. Thermodyn.,* 34, 1341–1347.

Heintz, A., Kulikov, D. V. and Verevkin, S. P., (2002b), "Thermodynamic Properties of Mixtures Containing Ionic Liquids. 2. Activity Coefficients at Infinite Dilution of Hydrocarbons and Polar Solutes in 1-Methyl-3-ethyl-imidazolium Bis(trifluoromethyl-sulfonyl) Amide and in 1,2-Dimethyl-3-ethyl-imidazolium Bis(trifluoromethyl-sulfonyl) Amide Using Gas-Liquid Chromatography", *J. Chem. Eng. Data* , 47, 894-899.

Heintz, A., (2005), "Recent developments in Thermodynamics and Thermo physics of non-aqueous mixtures containing ionic liquids", *Journ. Chem. Thermodyn.*, 37, 525-535.

Heintz, A., and Verevkin, S. P., (2005), "Thermodynamic Properties of Mixtures Containing Ionic Liquids. 6. Activity Coefficients at Infinite Dilution of Hydrocarbons, Alcohols, Esters, and Aldehydes in 1-Methyl-3-octyl-imidazolium Tetrafluoroborate Using Gas-Liquid Chromatography", *J. Chem. Eng. Data,* 50, 1515-1519.

Heintz, A., Casa´s, L. M., Nesterov, I. A., Emel'yanenko, V. N. and Verevkin, S. P., (2005), "Thermodynamic Properties of Mixtures Containing Ionic Liquids 5.Activity Coefficients at Infinite Dilution of Hydrocarbons, Alcohols, Esters, and Aldehydes in 1-Methyl-3-butyl-imidazolium Bis(trifluoromethyl-sulfonyl) Imide Using Gas-Liquid Chromatography", *J. Chem. Eng. Data, 50,* 1510-1514.

Heintz, A., Verevkin, S.P. and Ondo, D., (2006a), "Thermodynamic Properties of Mixtures Containing Ionic Liquids. 8. Activity Coefficients at Infinite Dilution of Hydrocarbons, Alcohols, Esters, and Aldehydes in 1-Hexyl-3-methylimidazolium Bis-(trifluoromethylsulfonyl) Imide Using Gas-Liquid Chromatography", *J. Chem. Eng. Data, 51,* 434-437.

Heintz, A., Vasiltsova, T. V., Safarov, J., Bich, E. and Verevkin, S. P., **(**2006b), "Thermodynamic properties of mixtures containing ionic liquids; 9. Activity coefficients at infinite dilution of hydrocarbons, alcohols, esters, and aldehydes in trimethylbutylammonium bis (trifluoromethylsulfonyl) imide using gas-liquid chromatography and static method", *J. Chem. Eng. Data*, *51*, 648-655.

Heintz, A., Verevkin, S. P., Lehmann, J. K., Vasiltsova, T. V. and Ondo, D., (2007), "Activity coefficients at infinite dilution and enthalpies of solution of methanol, 1-butanol, and 1-hexanol in 1-hexyl-3-methyl-imidazolium bis (trifluoromethyl-sulfonyl) imide", *Journ. Chem. Thermodyn.*, 39, 268–274.

Heitzman, H., Young, B. A., Rausch, D. J., Rickert, P., Stepinski, D. C. and Dietz, M. L., (2006), "Fluorous ionic liquids as solvents for the liquid–liquid extraction of metal ions by macrocyclic polyethers", *Talanta,* 69, 527–531.

Hovorka S. H. and Dohnal V., (1997), "Determination of Air-Water Partitioning of Volatile Halogenated Hydrocarbons by Inert Gas Stripping Method", *J. Chem. Eng. Data*, 42, 924-933.

Hradetzky, G., Wobst, M., Vopel, H. and Bittrich H. J., (1990), "Measurement of activity coefficients in highly dilute solutions part I", *Fluid Phase Equilibr.*, 54, 133-145.

Huddleston, J. G, Visser, A. E., Reichert, W. M., Willauer, H. D., Broker, G. A. and Rogers, R.D., (2001), "Characterization and comparison of hydrophilic and hydrophobic room temperature ionic liquids incorporating the imidazolium cation", *Green Chem.*, 3, 156-164.

Hudson, G. H. and McCoubrey, J. C., (1960), "Intermolecular Forces Between Unlike Molecules; A More Complete Form of the Combining Rules", *Trans. Faraday Soc*. 56, 761-766.

Hurley, F. H. and Weir, T. P., (1951), "The Electrodeposition of Aluminum from Nonaqueous Solutions at Room Temperature" *J. Electrochem Soc.*, 98, 207-212.

Hussam, A. and Carr, P. W., (1985) "A Study of Rapid and Precise Methodology for the Measurement of Vapor/Liquid Equilibria by Headspace Gas Chromatography", *Anal. Chem.*, 57, 793-801.

Jakob A, Grensemann H., Lohmann J. and Gmehling J., (2006), "Further Development of Modified UNIFAC (Do): Revision and Extension 5", *Ind. Eng. Chem. Res.*, 45, 7924-7933.

Jork, C., Kristen, C., Pieraccini, D., Stark, A., Chiappe, C., Beste, Y.A. and Arlt, W., (2005), "Tailor-made ionic liquids", *Journ. Chem. Thermodyn.*, 37, 537–558.

Kato, R. and Gmehling, J., (2004), "Activity coefficients at infinite dilution of various solutes in the ionic Liquids $[MMIM]^+[CH_3SO_4]^-$, $[MMIM]^+[CH_3OC_2H_4SO_4]^-$, $[MMIM]^+[(CH_3)_2PO_4]^-$, $[C_5H_5NC_2H_5]^+[(CF_3SO_2)_2N]^-$ and $[C_5H_5NH]^+[C_2H_5OC_2H_4OSO_3]^-$", *Fluid Phase Equilibr.*, 226, 37–44.

Kato, R. and Gmehling, J., (2005a), "Systems with ionic liquids: Measurement of VLE and γ^∞ data and prediction of their thermodynamic behaviour using original UNIFAC, mod. UNIFAC (Do) and COSMO-RS (Ol)", *Journ. Chem. Thermodyn.*, 37, 603–619.

Kato, R. and Gmehling, J., (2005b), "Measurement and correlation of vapor–liquid equilibria of binary systems containing the ionic liquids [EMIM] $[(CF_3SO_2)_2N]$, [BMIM] $[(CF_3SO_2)_2N]$, [MMIM] $[(CH_3)_2PO_4]$ and oxygenated organic compounds respectively water", *Fluid Phase Equilibr.*, 231, 38–43.

Kato, R. and Gmehling, J., (2005c), "Erratum to "Activity coefficients at infinite dilution of various solutes in the ionic liquids [MMIM]+[CH_3SO_4]−, [MMIM]+[$CH_3OC_2H_4SO_4$]−, [MMIM]+[$(CH_3)_2PO_4$]−, [$C_5H_5NC_2H_5$]+[$(CF_3SO_2)_2N$]− and [C_5H_5NH]+[$C_2H_5OC_2H_4OSO_3$]−"[Fluid Phase Equilib. 226 (2004) 37–44]", *Fluid Phase Equilibr.*, 235, 124.

Khasanshin, T. S., Samuilov, V. S. and Shchemelev, A. P., (2009), "Determination of the thermodynamic properties of liquid *n*-hexadecane from the measurements of the velocity of sound", *Journ. Eng. Phys. Thermophys.*, 82,149-156.

Klamt A., (1995), "Conductor-Like Screening Model for Real-Solvents (COSMO-RS): A New Approach the Quantitative Calculation of Solvation Phenomena", *Journ. Phys. Chem.*, 99, 2224-2235.

Klamt A. (2005), "Comments on "Performance of a Conductor-Like Screening Model for Real Solvents Model in Comparison to Classical Group Contribution Methods", *Ind. Eng. Chem. Res.*, 44, 7042

Klamt A. and Eckert F., (2008), "Comments on "Refining of COSMO-SAC and the Applications", *Ind. Eng. Chem. Res.*. 47, 1351-1352.

Klamt A., Jones, V., Burger, T. and Lohrenz, J. C. W., (1998), "Refinement and Parameterization of COSMO-RS", *Journ. Phys. Chem. A.*, 102, 5074-5085.

Klamt, A. and Eckert F., (2000), "COSMO-RS: A Novel and Efficient Method for the A Priori Prediction of Thermophysical Data of Liquids" *Fluid Phase Equilibr.*, 172, 43-72.

Kneisl, P. and Zondlo, J. W., (1987), "Vapor Pressure, Liquid Density, and the Latent Heat of Vaporization as Functions of Temperature for Four Dipolar Aprotic Solvents", *J. Chem. Eng. Data*, 32, 11-13.

Kojima K and Tochigi K., (1979), Prediction of Vapor-Liquid Equilibria by the ASOG Method; Elsevier :Tokyo.

Kojima, K., Zhang, S. and Hiaki, T., (1997), "Measuring methods of infinite dilution activity coefficients and a database for systems including water" *Fluid Phase Equilibr.*, 131, 145-179.

Kossack, S., Kraemer, K., Gani, R. and Marquardt, W. (2008), "A systematic synthesis framework for extractive distillation processes", *Chem. Eng. Res. and Des.*, 86, 781-792.

Kozlova, S.A., Verevkin, S.P., Heintz, A., Peppel, T. and Köckerling, M., (2009), "Activity coefficients at infinite dilution of hydrocarbons, alkylbenzenes, and alcohols in the paramagnetic ionic liquid 1-butyl-3-methyl-imidazolium tetrachloridoferrate (III) using gas–liquid chromatography", *Journ. Chem. Thermodyn.*, 41, 330–333.

Krummen M., Gruber D. and Gmehling J., (2000), "Measurement of Activity Coefficients at Infinite Dilution in Solvent Mixtures using the Dilutor Technique", *Ind. Eng. Chem. Res*., 39, 2114-2123.

Krummen, M. and Gmehling, J., (2004), "Measurement of activity coefficients at infinite dilution in N-methyl-2-pyrrolidone and N-formylmorpholine and their mixtures with water using the dilutor technique", *Fluid Phase Equilibr*., 215, 283–294.

Krummen, M., Wasserscheid, P. and Gmehling, J., (2002), "Measurement of Activity Coefficients at Infinite Dilution in Ionic Liquids Using the Dilutor Technique", *J. Chem. Eng. Data*, 47, 1411-1417.

Kumar, A.A.P. and Banerjee, T., (2009), "Thiophene separation with ionic liquids for Desulphurization: A Quantum Chemical Approach", *Fluid Phase Equilibr.*, 278, 1–8.

Kutsuna, S. and Hori, H., (2008), "Experimental determination of Henry's law constant of perfluorooctanoic acid (PFOA) at 298 K by means of an inert-gas stripping method with a helical plate", *Atm. Environ.*, 42, 8883–88920.

Larsen B.L, Rasmussen P and A. Fredenslund., (1987), "A Modified UNIFAC Group Contribution Method for Prediction of Phase Equilibria and Heats of Mixing", *Ind. Eng. Chem. Res.*, 26, 2274-2286.

Laub, R. J. and Peacsok, R. L., (1978), "Physico-chemical Applications of Gas Chromatography", John Willey and Sons, U.S.A.

Lebert, A. and Richon, D., (1984a), "Infinite dilution activity coefficients of n-alcohols as a function of dextrin concentration in water-dextrin systems", *J. Agric. Food Chem*., 32: 1156-1161.

Lebert, A. and Richon, D., (1984b), "Study of the influence of solute (n-alcohols and n-alkanes) chain length on their retention by purified olive oil", *J. Food Sci*., 49, 1301-1304.

Legret, D., Desteve, J., Richon D. and Renon H., (1983), "Vapor-liquid equilibrium constants at infinite dilution determined by a gas stripping method: Ethane, propane, n-butane, n-pentane in the methane-n-decane system", *AIChE J.*, 29, 137-144.

Lei, Z., Arlt, W. and Wasserscheid, P., (2006), "Separation of 1-hexene and *n*-hexane with ionic liquids", *Fluid Phase Equilibr.*, 241 290–299.

Lei, Y.D., Shunthirasingham, C. and Wania, F., (2007a), "Comparison of headspace and gas-stripping techniques for measuring the air-water partitioning of normal alkanols (C4 to C10): effect of temperature, chain length, and adsorption to the water surface", *J. Chem. Eng. Data*, 52, 168–179.

Lei, Z., Arlt, W. and Wasserscheid, P., (2007b), "Selection of entrainers in the 1-hexene/n-hexane system with a limited solubility", *Fluid Phase Equilibr*. 260, 29–35.

Lei, Z., Chen, B., Li, C., and Liu, H., (2008), "Predictive Molecular Thermodynamic Models for Liquid Solvents, Solid Salts, Polymers, and Ionic Liquids", *Chem. Rev.*, 108, 1419-1455.

Leroi, J. C., Masson, J. C., Renon, H., Fabries, J. F. and Sannier H., (1977), "Accurate Measurement of Activity Coefficients at Infinite Dilution by Inert Gas Stripping and Gas Chromatography", *Ind. Eng. Chem. Process Des. Dev*, 16, 139-144.

Letcher, T. M., (1980), "Activity Coefficients at Infinite Dilution from Gas-Liquid Chromatography", *Faraday symposium*, 15, 103-111.

Letcher, T. M., Soko, B., Ramjugernath, D., Deenadayalu, N., Nevines, A. and Naicker, P. K., (2003a), "Activity Coefficients at Infinite Dilution of Organic Solutes in 1-Hexyl-3-methylimidazolium Hexafluorophosphate from Gas-Liquid Chromatography", *J. Chem. Eng. Data*, 48, 708-711.

Letcher, T. M., Soko, B., Reddy, P. and Deenadayalu, N., (2003b), "Determination of Activity Coefficients at Infinite Dilution of Solutes in the Ionic Liquid 1-Hexyl-3-methylimidazolium Tetrafluoroborate Using Gas-Liquid Chromatography at the Temperatures 298.15 K and 323.15 K", *J. Chem. Eng. Data*, 48, 1587-1590.

Letcher, T. M., Domańska, U., Marciniak, M., and Marciniak, A., (2005a), "Activity coefficients at infinite dilution measurements for organic solutes in the ionic liquid 1-butyl-3-methyl-imidazolium2-(2-methoxyethoxy) ethylsulfate using g.l.c. at T = (298.15, 303.15, and 308.15) K", *Journ. Chem. Thermodyn.*, 37, 587–593.

Letcher, T. M., Marciniak, A. and Marciniak, M., (2005b), "Determination of Activity Coefficients at Infinite Dilution of Solutes in the Ionic Liquid 1-Butyl-3-methylimidazolium Octyl Sulfate Using Gas-Liquid Chromatography at a Temperature of 298.15 K, 313.15K, or 328.15 K", *J. Chem. Eng. Data*, 50, 1294-1298.

Letcher, T. M., Marciniak, A., Marciniak, M. and Domańska, U., (2005c), "Activity coefficients at infinite dilution measurements for organic solutes in the ionic liquid 1-hexyl-3-methyl-imidazolium bis (trifluoromethylsulfonyl)-imide using g.l.c. at T = (298.15, 313.15, and 333.15) K", *J. Chem. Thermodyn.* 37, 1327–1331.

Letcher, T. M. and Reddy, P., (2005), "Determination of activity coefficients at infinite dilution of organic solutes in the ionic liquid, Trihexyltetradecylphosphonium tris (pentafluoroethyl) trifluorophosphate, by gas–liquid chromatography", *Fluid Phase Equilibr.*, 235, 11–17.

Letcher, T. M. and Reddy, P., (2007), "Determination of activity coefficients at infinite dilution of organic solutes in the ionic liquid, tributylmethylphosphonium methylsulphate by gas–liquid chromatography", *Fluid Phase Equilibr.*, 260, 23–28.

Letcher T. M., (2007), in "Thermodynamics, Solubility and environmental issues", T.M. Letcher (Ed.) Elsevier B.V., Amsterdam, First edition.

Letcher, T. M., Ramjugernath, D., Laskowska, M., Królikowski, M., Naidoo, P. and Domańska, U., (2008a), "Determination of activity coefficients at infinite dilution of solutes in the ionic liquid, trihexyltetradecylphosphonium bis (trifluoromethylsulfonyl) imide, using gas-liquid chromatography at *T* (303.15, 308.15, 313.15 and 318.15) K", *J. Chem. Eng. Data*, *53*, 2044–2049.

Letcher, T.M., Ramjugernath, D., Laskowska, M., Królikowski, M., Naidoo, P. and Domańska, U., (2008b), "Activity coefficients at infinite dilution measurements for organic solutes in the ionic liquid trihexyltetradecylphosphonium-bis-(2, 4, 4-trimethylpentyl) - phosphinate using g.l.c. at T = (303.15, 308.15, 313.15, and 318.15) K", *Journ. Chem. Thermodyn.*, 40, 1243–1247.

Letcher, T. M., Ramjugernath, D., Królikowski, M., Laskowska, M., Naidoo, P. and Domańska, U., (2009), "Activity coefficients at infinite dilution measurements for organic solutes in the ionic liquid N-butyl-4-methylpyridinium tosylate using GLC at T = (328.15, 333.15, 338.15, and 343.15) K", *Fluid Phase Equilibr.*, 276, 31–36.

Li, J. and Carr, P.W., (1993), "Measurement of water-hexadecane partition coefficients by headspace gas chromatography and calculation of limiting activity coefficients in water", *Anal. Chem.*, *65*, 1443–1450.

Li, J., Dallas, A. J., Eikens, D. I. and Carr, P. W., (1993), "Measurement of Large Infinite Dilution Activity Coefficients of Nonelectrolytes in Water by Inert Gas Stripping and Gas Chromatography", *Anal. Chem*., 65, 3212-3218.

Liebert, V., Nebig, S. and Gmehling, J., (2008), "Experimental and predicted phase equilibria and excess properties for systems with ionic liquids", *Fluid Phase Equilibr.*, 268, 14–20.

Lin, S. and Sandler, I., (2002), "A Priori Phase Equilibrium Prediction from a Segment Contribution Solvation Model", *Ind. Eng. Chem. Res.* 41, 899-913.

Lohmann J. and Gmehling J., (2001), "Modified UNIFAC (Dortmund): reliable model for the development of Thermal Separation processes", *J. Chem. Eng. Japan*, 24, 43-54.

Lydersen A.L. Mass transfer in Engineering Practice. (1983) John Willey& sons.

McGlashan, M. L. and Potter, D. J. B., (1962), "The Second Virial Coefficients" *Proc. Roy. Soc*., 267, 487-500.

McMillan, W.G. and Mayer, J.E., (1945), "The Statistical Thermodynamics of Multicomponent Systems", *J. Chem. Phys.*, 13, 276-305.

Mehra, R, (2003), "Application of refractive index mixing rules in binary systems of hexadecane and heptadecane with *n*-alkanols at different temperatures", *Proc. Indian Acad. Sci.* (*Chem. Sci.*), 115, 147–154.

Meindersma, G.W., Podt, A. and Haan, A.B. (2006) "Ternary liquid-liquid Equilibria for mixtures of an aromatic + an aliphatic hydrocarbon + 4-methyl-N-butylpyridinium tetrafluoroborate" *J. Chem. Eng Data*, 51, 1814–1819.

Meshri, D.T., (2000), in "advanced inorganic fluorides: Synthesis, Characterization and applications", Elsevier, 661-682.

Miyano Y., Nakanishi K. and Kukuchi K., (2003), "Henry's constants of butane, isobutene, 1-butene and isobutene in methanol at 255-320K", *Fluid Phase Equilibr.*, 208, 223-238.

Möllmann, C. and Gmehling, J., (1997), "Measurement of Activity Coefficients at Infinite Dilution Using Gas-Liquid Chromatography 5. Results for N-Methylacetamide, N, N-Dimethylacetamide, N, N-Dibutylformamide, and Sulfolane as Stationary Phases", *J. Chem. Eng. Data*, 42, 35–40.

Moutiers G. and Isabelle Billard, (2003), "Des solvents plus propres", *Nature*, 311, 45-49.

Mutelet, F. and Jaubert, J-N., (2006), "Accurate measurements of thermodynamic properties of solutes in ionic liquids using inverse gas chromatography", *Journ. Chromatograph. A*, 1102, 256–267.

Mutelet, F., Jaubert, J-N., Rogalski, M., Boukherissa, M. and Dicko, A., (2006), "Thermodynamic Properties of Mixtures Containing Ionic Liquids: Activity Coefficients at Infinite Dilution of Organic Compounds in 1-Propyl Boronic Acid-3-Alkylimidazolium Bromide and 1-Propenyl-3-alkylimidazolium Bromide Using Inverse Gas Chromatography", *J. Chem. Eng. Data*, *51*, 1274-1279.

Mutelet, F. and Jaubert, J-N, (2007), "Measurement of activity coefficients at infinite dilution in 1-hexadecyl-3 methylimidazolium tetrafluoroborate ionic liquid", *Journ. Chem. Thermodyn.*, 39, 1144–1150.

Nebig, S., Bölts, R. and Gmehling, J., (2007), "Measurement of vapor–liquid equilibria (VLE) and excess enthalpies (H^E) of binary systems with 1-alkyl-3-methylimidazolium Bis (trifluoromethylsulfonyl)imide and prediction of these properties and $\gamma\infty$ using modified UNIFAC (Dortmund)", *Fluid Phase Equilibr.*, 258, 168–178.

Nebig, S., Liebert, V. and Gmehling, J., (2009), "Measurement and prediction of activity coefficients at infinite dilution (γ^{∞}), vapor–liquid equilibria (VLE) and excess enthalpies (H^E) of binary systems with 1, 1-dialkyl-pyrrolidinium bis (trifluoromethylsulfonyl) imide using mod UNIFAC (Dortmund)", *Fluid Phase Equilibr.*, 277, 61–67.

Novak, J. P. and Matous, J.; Pick, J., (1987), "Liquid-Liquid Equilibria", Elsevier: Amsterdam,

Olivier, E., Letcher, T.M., Naidoo, P. and Ramjugernath, D., (2010a), "Activity coefficients at infinite dilution of organic solutes in the ionic liquid 1-ethyl-3-methylimidazolium trifluoromethanesulfonate using gas–liquid chromatography at T = (313.15, 323.15, and 333.15) K", *Journ. Chem. Thermodyn.*, 42, 78-83.

Olivier, E., Letcher, T.M., Naidoo, P. and Ramjugernath, D., (2010b), "Activity coefficients at infinite dilution of organic solutes in the ionic liquid1-Octyl-3-methylimidazolium hexafluorophosphate using gas–liquid chromatography at T = (313.15, 323.15, and 333.15) K", *Journ. Chem. Thermodyn.*, doi:10.1016/j.jct.2009.12.004.

Olivier, E., Letcher, T.M., Naidoo, P. and Ramjugernath, D., (2010c), "Activity coefficients at infinite dilution of organic solutes in the ionic liquid 1-Butyl-3-methylimidazolium hexafluoroantimonate using gas–liquid chromatography at T = (313.15, 323.15, and 333.15) K", Unpublished manuscript.

O'Rear, D. J., Boudreau, L. C., Driver, M. S., and Munson, C. L., (2001), "Removal of mercaptans from hydrocarbon streams using ionic liquids", *Patent*; Chevron U.S. 2001-US32211 (2002034863), 19, 10-16-2001.

Pereiro, A. B., Legido, J. L. and Rodriguez, A., (2007), "Physical properties of ionic liquids based on 1-alkyl-3-methylimidazolium cation and hexafluorophosphate as anion and temperature dependence", *J. Chem. Thermodyn.* 39 , 1168-1175.

Plechkova, N. V. and Seddon, K. R., (2008), "Applications of ionic liquids in the chemical industry", *Chem. Soc. Rev*., 37, 123–150.

Poling, B.E, Prausnitz, J.M. and O'Connell, J.P., (2001), "The Properties of Liquids and Gases", Fifth ed., McGraw-Hill, New York.

Porter, P. E., Deal, C. H. and Stross, F. H., (1956), "The Determination of Partition Coefficients from Gas-Liquid Partition Chromatography", *J. Am. Chem. Soc*., 78, 2999-3006.

Prausnitz, J. M. and Anderson, R., (1961), "Thermodynamics of Solvent Selectivity in Extractive Distillation of Hydrocarbons", *AIChE J*., 7, 96-101.

Putnam R.; Taylor R.; Klamt A.; Eckert F. and Schiller M., (2004), "Prediction of Infinite Dilution Activity Coefficients using COSMO-R", *Ind. Eng. Chem. Res.* 42, 3635-3641.

Raal, JD and Mühlbauer, A.L, (1998), "Phase Equilibria: Measurement and Computation", Taylor and Francis, Bristol P.A.

Revelli, A-L., Sprunger, L.M., Gibbs, J., Acree Jr., W.E., Baker, G.A. and Mutelet, F., (2009) "Activity Coefficients at Infinite Dilution of Organic Compounds in Trihexyl(tetradecyl)phosphonium Bis(trifluoromethylsulfonyl)imide Using Inverse Gas Chromatography", *J. Chem. Eng. Data*, 54, 977-985.

Richon D., Antoine P. and Renon H., (1980), "Infinite Dilution Activity Coefficients of Linear and Branched Alkanes from C_1 to C_9 in n-Hexadecane by Inert Gas Stripping", *Ind. Eng. Chem. Process Des. Dev.*, 19, 144-147.

Richon, D. and Renon, H., (1980), "Infinite dilution Henry's constants of light hydrocarbons in n-hexadecane, n-octadecane, and 2, 2, 4, 4, 6, 8, 8-heptamethylnonane by inert gas stripping", *J. Chem. Eng. Data*, 25, 59-60.

Richon, D., Antoine, P. and Renon, H., (1980), "Infinite dilution activity coefficients of linear and branched alkanes from C 1 and C 9 in n-hexadecane by inert gas stripping." *Ind. Eng. Chem. Process Des. Dev.*, 19, 144-147.

Richon D., Sorrentino F. and Voilley A., (1985), "Infinite Dilution Activity Coefficients by Inert Gas Stripping Method: Extension to the Study of Viscous and Foaming Mixtures", *Ind. Eng. Chem. Process Des. Dev.*, 24, 1160-1165.

Robinson, J. and Osteryoung, R.A., (1979), "An electrochemical and spectroscopic study of some aromatic hydrocarbons in the room temperature molten salt system Aluminum Chloride-n-Butylpyridinium Chloride", *J. Am. Chem. Soc*., 101,323-327.

Rodriguez, A. and Brennecke, J. F., (2006), "Temperature and Composition Dependence of the Density and Viscosity of Binary Mixtures of Water + Ionic Liquid", *J.Chem. Eng. Data*, 51, 2145-2155.

Roettger, D., Nierlich, F., Krissmann, J., Wasserscheid, P. and Keim, W., (2003), "Method for separating organic compounds by extracting or washing them with ionic liquids", *Patent*; Oxeno, Olefinchemie G. 2003-EP430 (2003070667), 16. 1-17-2003. WO.

Rogers, R. D. and Seddon, K. R., (2003), "Ionic Liquids-Solvents of the Future?", *Science*, 302, 792-793.

Sandler, S.I., (1996), "Infinite Dilution Activity Coefficients in Chemical, Environmental and Biological engineering", *Fluid Phase Equilibr.* 116, 343-353.

Schult C. J., Neely B. J., Robinson Jr R. L., Gasema, K. A. M. and Todd, B. A., (2001), "Infinite Dilution Activity Coefficients for several solutes in Hexadecane and in n-Methyl-2-Pyrrolidone (NMP): Experimental Measurements and UNIFAC Predictions", *Fluid Phase Equilibr.*, 179, 117-129.

Seddon, K. R., Scheffler, T. B., Hussey, C. L., Kear, C. M. and Armitage, P. D., (1983) "Molybdenum Chloro Complexes in Room-Temperature Chloroaluminate Ionic Liquids: Stabilization of $[MoCl_6]^{2-}$ and $[MoCl_6]^{3-}$", *Inorg. Chem.*, 22, 2099-2100.

Shimoyama, Y., Hirayama, T. and Iwai, Y., (2008), "Measurement of Infinite Dilution Activity Coefficients of Alcohols, Ketones, and Aromatic Hydrocarbons in 4-Methyl-*N*-butylpyridinium Tetrafluoroborate and 1-Butyl-3-methylimidazolium Hexafluorophosphate by Gas- Liquid Chromatography", *J. Chem. Eng. Data*, 53 , 2106-2111.

Shröder, U., Wadhawan, J. D., Compton, R. G., Marken, F., Suarez, P. A. Z., Consorti, C. S., De Souza, R. F. and Dupont, J., (2000), "Water-induced accelerated ion diffusion : voltammetric studies in 1-methyl-3- **[** 2,6-(**S**)-dimethylocten-2-yl **]**imidazolium tetrafluoroborate, 1-butyl-3 methylimidazolium tetrafluoroborate and hexafluorophosphate ionic liquids", *New J. Chem.*, 24, 1009-1015.

Shunthirasingham, C., Lei, Y.D., Wania, F., (2007), "Evidence of bias in air water Henry's law constants for semivolatile organic compounds measured by inert gas stripping", *Environ. Sci. Technol.* 41, 3807–3814.

Skoog, D. A., West D. M. and Holler, F. J., (1996), "Fundamentals of Analytical Chemistry", 7th Edition, Saunders College Publishing, Philadelphia.

Smiglak, M., Reichert, W.M., Holbrey, J.D., Wilkes, J.S., Sun, L., Thrasher, J.S., Kirichenko, K., Singh, S., Katritzkyc, A.R. and Rogers, R.D., (2006), "Combustible ionic liquids by design: is laboratory safety another ionic liquid myth?", *Chem. Commun.*, 2554–2556.

Smith, J.M., Van Ness, H.C. and Abbott, M.M., (2005), "Introduction to Chemical Engineering Thermodynamics", McGraw Hill, 7th Ed.

Sumartschenkowa, I. A., Verevkin, S. P., Vasiltsova, T. V., Bich, E., Heintz, A., Shevelyova, M. P. and Kabo, G. J., (2006), "Experimental Study of Thermodynamic Properties of Mixtures Containing Ionic Liquid 1-Ethyl-3-methylimidazolium Ethyl Sulfate Using Gas-Liquid Chromatography and Transpiration Method", *J. Chem. Eng. Data*, 51, 2138-2144.

Sumon, K.Z., (2005), "Extraction of aromatics using green solvents based on ionic liquids", MSc thesis, King Fahd University of Petroleum and minerals, Dhahran, Saudi, Arabia.

Tiegs, D.G., Medina, A., Soares, M., Bastos, J., Alessi, P., Kikic, I., (1986), "Activity Coefficients at Infinite Dilution", Vol. 9, Part 1, *Dechema Chemistry Data Series*, Dechema, Frankfurt.

Trulove, P.C. and Mantz, R.A., (2003), in "Ionic Liquids in Synthesis", ed. P. Wasserscheid and T.Welton, Wiley-VCH, Weinheim, 103–126.

Vitenberg, A. G., (2003), "Equilibrium model in the description of gas extraction and headspace analysis", *J. Anal, Chem*., 58, 2–15.

Walden, P., (1914), "Ueber die Moleculargrösse und elektrisehe Leitfähigkeit einiger gesehmolzenen salze", *Bull. Acad. Imper. Sci.* (St. Petersburg), 1800-1801.

Wang, M-H., Wu, J-S., Wang, L-S. and Li, M-Y., (2007), "Activity Coefficients at Infinite Dilution of Alkanes, Alkenes, and Alkyl Benzenes in 1-Propyl-2,3-dimethylimidazolium Tetrafluoroborate Using Gas-Liquid Chromatography", *J. Chem. Eng. Data*, *52*, 1488-1491.

Wasserscheid, P. and Keim, W., (2000), "Ionic liquids-New "Solutions" For Transition Metal Catalysis", Angew., Chem. Int. Ed., 39, 3772-3789.

Wasserscheid, P., Boesmann, A., Jess, A., Datsevitch, L., Schmitz, C., and Lauter, A., (2002) "Extractive method for eliminating polarizable impurities from hydrocarbons and hydrocarbon mixtures using ionic liquids as the extractants", *Patent* ; Solvent, Innovation G. 2002-EP12239(2003037835), 18. 11-2-2002. WO.

Weidlich, U. and Gmehling, J., (1987), "A modified UNIFAC model, 1: Prediction of VLE, H^E, and gamma infinity", *Ind. Eng. Chem. Res*., 26, 1372-1381.

Welton T., (1999), "Room temperature ionic liquids. Solvents for synthesis and catalysis", *Chem. Rev*., 99, 2071-2083.

Wilkes, J. S., Levisky, J. A., Wilson, R. A. and Hussey, C. L., **(**1982), "Dialkylimidazolium chloroaluminate melts: a new class of room-temperature ionic liquids for electrochemistry, spectroscopy and synthesis", *Inorg. Chem.*, 21, 1263–1264.

Wilson G.M. and Deal C.H, (1962), "Activity Coefficient and Molecular Structure. Activity coefficients in changing environments-solutions of groups", *Industrial Engineering Chemistry Fundamentals*, 1, 20-23.

Wittig R.; Lohmann J.; Joh R; Horstmann S, Gmehling J., (2001), "Vapour-Liquid Equilibria and Enthalpies of Mixing in a Temperature Range from 298.15 to 413.15 K for the Further Development of Modified UNIFAC (Dortmund)", *Ind. Eng. Chem. Res.*, 40, 5831-5838.

Xue, H., Verma, R. and Shreeve, J.M., (2006), "Review of the IL's with fluorine-containing anions", *Journ. Fluor. Chem.*, 127, 159-176.

Yang, X-J., Wu, J-S., Ge, M-L., Wang, L-S. and Li, M-Y, (2008), "Activity Coefficients at Infinite Dilution of Alkanes, Alkenes, and Alkyl Benzenes in 1-Hexyl-3-methylimidazolium Trifluoromethanesulfonate Using Gas-Liquid Chromatography", *J. Chem. Eng. Data*, 53, 1220-1222.

Zaworotko, M. J. and Wilkes, J. S., (1992), "Air and Water Stable 1-Ethyl-3-methylimidazolium Based Ionic Liquids", *J. Chem. Soc., Chem. Comm.***,** 13, 965-967.

Zhang, J., Zhang, Q., Qiao, B. and Deng, Y., (2007), "Solubilities of the Gaseous and Liquid Solutes and Their Thermodynamics of Solubilization in the Novel Room-Temperature Ionic Liquids at Infinite Dilution by Gas Chromatography", *J. Chem. Eng. Data*, 52, 2277-2283.

Zhang, L., Qiao, B., Ge, Y., Deng, D. and Ji, J., (2009), "Effect of ionic liquids on (vapor + liquid) equilibrium behavior of (water + 2-methyl-2-propanol)", *Journ. Chem. Thermodyn.*, 41, 138-143.

Zhao, J., Cong-Cong, D., Chun-Xi, L., Meng, H. and Zi-Hao, W., (2006), "Isobaric vapor-liquid equilibria for ethanol-water system containing different ionic liquids at atmospheric pressure", *Fluid Phase Equilibr.*, 242, 147-153.

Zhou, Q. and Wang, L-S., (2006), "Activity Coefficients at Infinite Dilution of Alkanes, Alkenes, and Alkyl Benzenes in 1-Butyl-3-methylimidazolium Tetrafluoroborate Using Gas-Liquid Chromatography", *J. Chem. Eng. Data*, 51, 1698-1701.

Zhou, Q., Wang, L-S, Wu, J-S. and Li, M-Y., (2007), "Activity Coefficients at Infinite Dilution of Polar Solutes in 1-Butyl-3-methylimidazolium Tetrafluoroborate Using Gas-Liquid Chromatography", *J. Chem. Eng. Data*, 52, 131-134.

APPENDIX A: SOURCES OF IDACs LITERATURE DATA

Table A-1: Literature data for γ_i^{∞} in imidazolium–based fluorinated ionic liquids.

Ionic liquids	References	No. of Solutes	Data Points	Temp. Range (K)	Method
[EMIM][Tf_2N]	Deenadayalu et al. (2005)	15	30	303.15-318.15	GLC
	Heintz et al. (2002b)	19	76	313.15-343.15	GC
	Kato and Gmehling (2005a,b)	4	4	353.15	VLE
	Krummen et al. (2002)	20	80	293.15-323.15	GST
[BMIM][PF_6]	Dobryakov et al. (2008)	8	32	293.15-353.15	GST
	Shimoyama et al. (2008)	18	54	315.9-334.8	GLC
[HMIM][Tf_2N]	Dobryakov et al. (2008)	8	32	293.15-353.15	GST
	Heintz et al. (2007)	3	18	301-396	GLC
	Kato and Gmehling (2005a)	26	148	303.15-333.15	GLC/GST
	Letcher et al. (2005c)	15	45	298.15-333.15	GC
	Heintz et al. (2006a)	52	52	301-396	GLC
[MOIM][BF_4]	Jork et al. (2005)	4	4	363.15	GLC
	Foco et al. (2006)	20	46	303-343	GLC
	Heintz and Verevkin (2005)	51	51	302-396	GLC
	Zhang et al. (2007)	14	28	298-323	GLC
[EMIM] [TFA]	Domańska and Marciniak (2007)	29	185	298.15-368.15	GLC
[BMIM][TfO]	Domańska and Marciniak (2008a)	32	242	298.15-368.15	GLC
	Ge et al. (2007)	17	119	303.15-363.15	GLC
	Ge and Wang (2008)	17	115	303.15-363.15	GLC
[EMIM][BF_4]	Foco et al. (2006)	18	41	303-343	GLC
	Ge et al. (2008a)	25	175	303.15-363.15	GLC
	Jork et al. (2005)	4	4	363.15	GLC
[BMIM][BF_4]	Foco et al. (2006)	20	46	303-343	GLC
	Jork et al. (2005)	4	4	363.15	GLC
	Zhang et al. (2007)	14	28	298-323	GLC
	Zhou and Wang (2006)	17	85	303.15-343.15	GLC
	Zhou et al. (2007)	17	85	303.15-343.15	GLC
[BMIM][Tf_2N]	Heintz et al. (2005)	53	53	302-385	GLC
	Kato and Gmehling (2005b)	3	3	353.15	VLE
	Krummen et al. (2002)	13	52	293.15-323.15	IGST
	Zhang et al. (2007)	15	15	323	GLC
[PDMIM][BF_4]	Ge et al. (2008b)	17	119	303.15-363.15	GLC
	Wang et al. (2007)	17	119	303.15-363.15	GC

Table A-1: Literature data for γ_i^{∞} in imidazolium–based fluorinated ionic liquids (Continued).

Ionic liquids	References	No. of Solutes	Data Points	Temp. Range(K)	Method
[HMIM][BF_4]	Foco et al. (2006)	20	42	303-343	GLC
	Letcher et al. (2003b)	15	26	298.15-323.15	GLC
[MOIM][Tf_2N]	Kato and Gmehling (2005a)	21	119	303.15-333.15	GLC/GST
EMIM][Tf_2N]+ [BMIM][Tf_2N]	Kato and Gmehling (2005b)	7	28	293.15-353.15	IGST
[MMIM][Tf_2N]	Krummen et al. (2002)	13	54	293.15-333.15	IGST
[HMIM][PF_6]	Letcher et al. (2003a)	16	43	298.15-323.15	GLC
[C_{16}MIM][BF_4]	Mutelet and Jaubert (2007)	31	93	323.15-343.15	GLC
[HMIM][TfO]	Yang et al. (2008)	17	119	303.15-363.15	GLC
[CpMIM][Tf_2N]	Zhang et al. (2007)	15	29	303-323	GLC
[CpMMIM][Tf_2N]	Zhang et al. (2007)	15	29	303-323	GLC
[EDMIM][Tf_2N]	Heintz et al (2002b)	19	76	313.15-343.15	GLC
[H-O-MIM] [Tf_2N]	Domańska and Marciniak (2009b)	35	280	298.15–368.15	GLC
[DH-O-MIM][Tf_2N]	Domańska and Marciniak (2009b)	35	280	298.15–368.15	GLC

Table A-2: literature data for γ_i^{∞} in phosphonium-based fluorinated ionic liquids.

Ionic liquids	References	No. of Solutes	Data Points	Temp. Range (K)	Method
[$3C_6C_{14}P$][BF_4]	Banerjee and Khanna (2006)	16	48	308.15-328.15	GLC
[$3C_6C_{14}P$][Tf_2N]	Banerjee and Khanna (2006)	16	48	308.15-328.15	GLC
	Letcher et al. (2008a)	18	72	303.15-318.15	GLC
	Revelli et al. (2009)	39	117	302.15-322.35	GLC
[$3C_6C_{14}P$][$(C_2F_5)_3PF_3$]	Letcher and Reddy (2005)	17	51	308.15-328.15	GLC

Table A-3: Literature data for γ_i^{∞} in pyridinium and pyrrolidinium-based fluorinated ionic liquids

Ionic liquids	References	No. of Solutes	Data Points	Temp. Range (K)	Method
[BMPy][BF_4]	Heintz et al. (2002a)	19	76	313.15-343.15	GLC
	Heintz et al. (2001)	19	76	313.1-363.1	GLC
	Go et al. (2007)	3	18	297-344	GLC
	Shimoyama et al. (2008)	4	12	306.6-325.3	GLC
[EPy][Tf_2N]	Kato and Gmehling (2004)	31	122	303.15-333.15	GLC/GST
[BMPyrr][TfO]	Domańska et al. (2009)	32	245	298.15-368.15	GLC
[BMPyrr][Tf_2N]	Kato and Gmehling (2005a)	15	60	303.15-333.15	IGST
[HMPyrr][Tf_2N]	Nebig et al. (2009)	11	44	303.15-333.15	IGST
[OMPyrr][Tf_2N]	Nebig et al. (2009)	7	28	303.15-343.15	IGST

Table A-4: Literature data for γ_i^{∞} in ammonium and sulfonium-based fluorinated ionic liquids.

Ionic liquids	References	No. of Solutes	Data Points	Temp. Range (K)	Method
[Et_3S][Tf_2N]	Domańska and Marciniak (2009a)	32	250	298.15-368.15	GLC
[$3C_1C_4N$][Tf_2N]	Heintz et al. (2006b)	54	54	302-393	GLC/SM

Table A-5: Literature data for γ_i^{∞} in non-fluorinated ionic liquids

Ionic liquids	References	No. of Solutes	Data Points	Temp. Range(K)	Method
[MOIM][Cl]	David et al. (2003)	15	45	298.15-318.15	GLC
[MOIM][$MDEGSO_4$]	Deenadayalu et al. (2006a)	23	45	288.15-313.15	GLC
[BMIM][$MeSO_4$]	Dobryakov et al. (2008)	8	32	293.15-353.15	IGST
[EMIM][SCN]	Domańska and Marciniak (2008b)	29	203	298.15-368.15	GLC
[BMIM][SCN]	Domańska and Laskowska (2009)	32	231	298.15-368.15	GLC
[BMIM][Cl]	Jork et al. (2005)	4	4	363.15	GLC
[MMIM][Me_2PO_4]	Kato and Gmehling (2005c)	5	5	353.15	VLE
	Kato and Gmehling (2004)	15	59	303.15-383.15	IGST
[MMIM][$C_1OC_2SO_4$]	Kato and Gmehling (2004)	15	60	303.15-343.15	IGST
[MMIM][$MeSO_4$]	Kato and Gmehling (2004)	14	56	303.15-333.15	GLC IGST
	Kato and Gmehling (2005c)	2	8	303.15-333.15	IGST
[BMIM][$FeCl_4$]	Kozlova et al. (2009)	19	19	303-403	GLC
[EMIM][Et-SO_4]	Krummen et al. (2002)	10	42	293.15-333.15	IGST
	Summartschenkowa et al.(2006)	46	46	301-427.15	GLC TM
[BMIM][$MDEGSO_4$]	Letcher et al (2005a)	16	48	298.15-328.15	GLC
[BMIM][Oc-SO_4]	Letcher et al (2005b)	16	47	298.15-328.15	GLC
	Mutelet and Jaubert (2006)	29	87	323.15-343.15	GLC

Table A-5: Literature data for γ_i^{∞} in non-fluorinated ionic liquids (Continued)

Ionic liquids	References	No. of Solutes	Data Points	Temp. Range(K)	Method
[EMIM][TOS]	Mutelet and Jaubert (2006)	29	29	323.15	GLC
[PropMIM][Br]	Mutelet et al. (2006)	28	28	323.15	GLC
[PropOMIM][Br]	Mutelet et al. (2006)	28	28	323.15	GLC
[PropC_{10}MIM][Br]	Mutelet et al. (2006)	28	28	323.15	GLC
[PropC_{12}MIM][Br]	Mutelet et al. (2006)	28	28	323.15	GLC
[PBA-MIM][Br]	Mutelet et al. (2006)	21	21	323.15	GLC
[PBA-OMIM][Br]	Mutelet et al. (2006)	23	23	323.15	GLC
[PBA-C_{10}MIM][Br]	Mutelet et al. (2006)	23	23	323.15	GLC
[PBA-C_{12}MIM][Br]	Mutelet et al. (2006)	23	23	323.15	GLC
[BMIM][n-$C_{16}H_{31}OO$]	Zhang et al. (2007)	14	14	333	GLC
[BMIM][n-$C_{18}H_{35}OO$]	Zhang et al. (2007)	14	28	323-333	GLC
[CpMIM][$N(CN)_2$]	Zhang et al. (2007)	14	28	323-333	GLC
[CpMMIM][$N(CN)_2$]	Zhang et al. (2007)	14	28	323-333	GLC
[$3C_6C_{14}P$][Cl]	Banerjee and Khanna (2006)	16	48	308.15-328.15	GLC
[$3C_6C_{14}P$] [$(C_8H_{17})_2PO_2$]	Letcher et al. (2008b)	14	70	298.15-318.15	GLC
[$3C_4C_1P$][$MeSO_4$]	Letcher and Reddy (2007)	12	36	308.15-318.15	GLC
[Py][$C_1OC_2SO_4$]	Kato and Gmehling (2004)	14	56	303-333.15	IGST
[BMPy][TOS]	Letcher et al. (2009)	19	76	328.15-343.15	GLC

APPENDIX B: STRUCTURE OF IONIC LIQUIDS

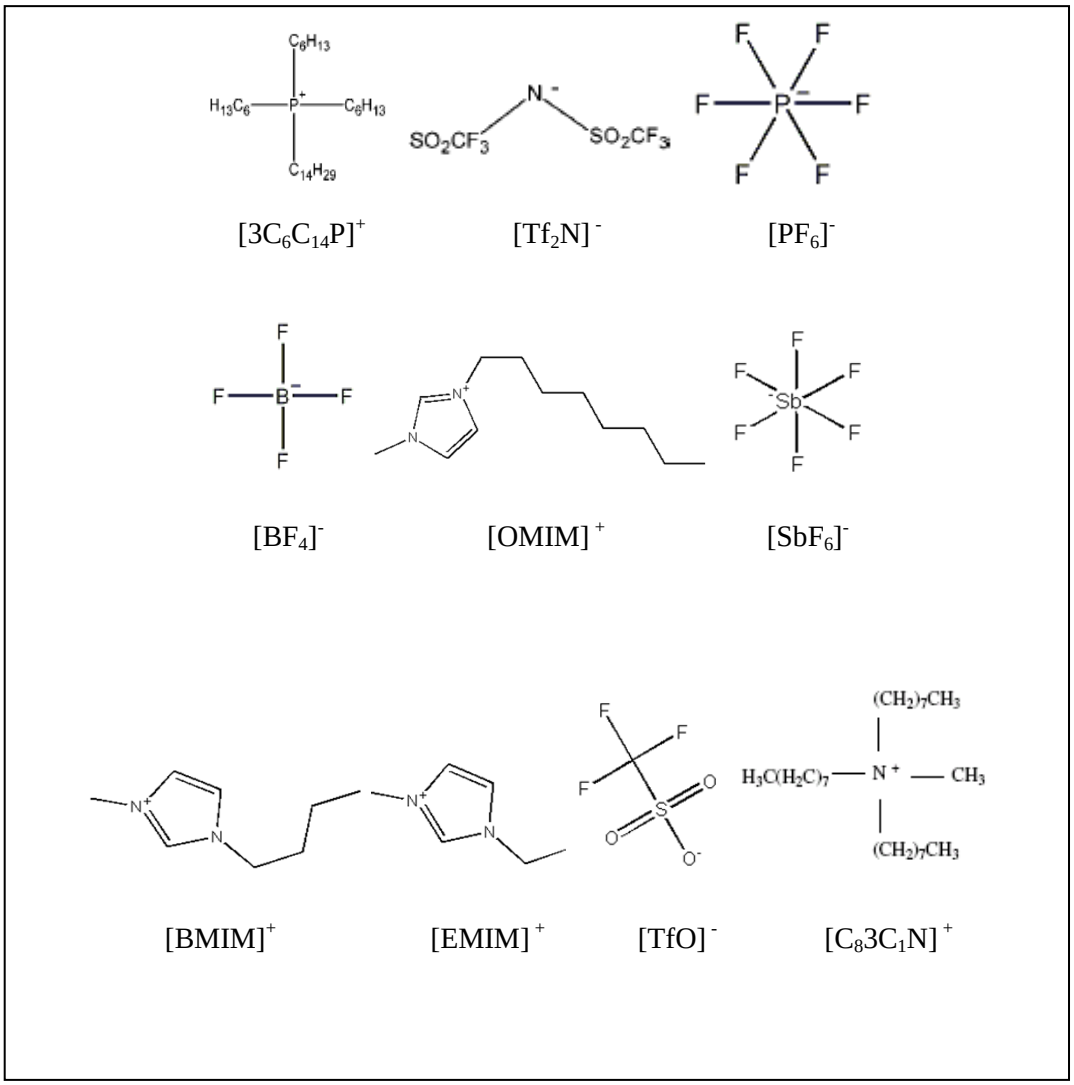

Figure B-1: Ions present in the structure of ionic liquids used in this work.

APPENDIX C: ORIGIN AND PURITY OF CHEMICALS

Table C-1: Origin and Stated purity of solutes and solvents.

Compound	Origin	Stated purity (Mass %)
$[3C_6C_{14}P]$ $[Tf_2N]$	Cytec	≥ 0.98
$[3C_6C_{14}P]$ $[BF_4]$	Cytec	≥ 0.98
$[3C_6C_{14}P]$ $[PF_6]$	Cytec	≥ 0.98
$[3C_8C_1N]$ $[Tf_2N]$	Solvent innovation	0.98
[BMIM] $[SbF_6]$	Capital Lab	≥ 0.98
[EMIM] TfO]	Capital Lab	≥ 0.98
[MOIM] $[PF_6]$	Capital Lab	≥ 0.95
NMP	Merck	≥ 0.98
n-hexadecane	Acros	0.99
n-alkanes (C_5 to C_{12})	Capital Lab	≥ 0.98
Alk-1-enes (C_5 to C_{12})	Capital Lab	≥ 0.98
Alk-1-ynes (C_5 to C_{12})	Capital Lab	≥ 0.98
Cycloalkanes (C_5 to C_{10})	Capital Lab	≥ 0.98
n-alkanols (C_1 to C_4)	Capital Lab	≥ 0.98
Alkylbenzenes (C_6 to C_9)	Capital Lab	≥ 0.98
Ket-2-ones (C_3 to C_4)	Capital Lab	≥ 0.98

Table C-2: Densities of solvents after purification at different temperatures-Accuracy: ± 0.4 %.;*Interpolated value;[#] Extrapolated data [a]From Rodriguez and Brennecke (2006); [b] From Pereiro et al. (2007); [c] From Kneisl and Zondlo, (1987); [d] From Khasanshin et al (2009).

Solvents	293.15 K	303.15 K	313.15 K	323.15 K	333.15 K	Literature Data at 293.15 K
$[3C_6C_{14}P]$ $[Tf_2N]$	1.068870	1.062387	1.056497	1.051422	1.047132	
$[3C_6C_{14}P]$ $[BF_4]$	-	-	-	0.925100	-	
$[3C_6C_{14}P]$ $[PF_6]$	-	-	-	0.987150	-	
$[3C_8C_1N]$ $[Tf_2N]$	1.112700	-	-	-	-	
[BMIM] $[SbF_6]$	1.694300	-	-	-	-	
[EMIM] TfO]	1.387070	1.375511	1.369032	1.363705	1.359564	1.387392[a*]
[MOIM] $[PF_6]$	1.238510	-	-	-	-	1.23957[b]
NMP	-	1.025173	1.017633	1.010888	1.004919	1.032313[c#]
n-hexadecane	0.770522	-	-	-	-	0.77418[d#]

Table C-3: Refractive indices of solvents after purification at 293.15 K. [#]Extrapolated data; [a]Mehra, (2003); [b]From "www.haochem.com"; [c]From Pereiro et al. (2007).

Solvents	Refractive index	Literature Data
$[3C_6C_{14}P]$ $[Tf_2N]$	1.45069	
$[3C_8C_1N]$ $[Tf_2N]$	-	
[BMIM] $[SbF_6]$	1.41568	
[EMIM] TfO]	1.43434	
[MOIM] $[PF_6]$	1.42430	1.42440[c]
NMP	1.47047	1.465-1.470[b]
n-Hexadecane	1.43463	1.4356[a#]

APPENDIX D: FUGACITIES, CRITICAL DATA AND IONIZATION ENERGIES

Table D-1: Saturation fugacity coefficients of selected solutes at different temperatures determined from second virial coefficients (Smith et al (2005).

Solutes	303.15 K	313.15 K	323.15 K
n-hexane	0.982	0.977	0.970
Hex-1-ene	0.981	0.974	0.967
Cyclohexane	0.988	0.983	0.978
Methanol	0.997	0.995	0.993
Benzene	0.989	0.986	0.981
Acetone	0.988	0.984	0.980

Table D-2: Critical volumes, V_C critical temperatures, T_C and ionization energies, I_C of the solutes and the carrier gas used in the calculation of the virial coefficients. (Reference: CRC Handbook of Chemistry and Physics).

Solute	T_C /K	V_C/ cm^3.mol^{-1}	I_C/ kJ.mol^{-1}
n-pentane	469.7	304	998.62
n-hexane	507.4	370	977.39
n-heptane	540.3	432	957.13
n-octane	568.8	492	947.48
n-nonane	594.7	555.2	937.83
Pent-1-ene	464.7	300	917.57
Hex-1-ene	504	350	910.82
Hept-1-ene	537.2	405	910.82
Oct-1-ene	566.6	464	909.85
Pent-1-yne	493.4	278	969.67
Hex-1-yne	539.29	331	960.02
Hept-1-yne	551.621	376.53	960.02
Oct-1-yne	598.46	441	960.02
Nony-1-ne	611	513.3	955.20
Cyclopentane	511.7	259	1014.05
Cyclohexane	553.8	308	951.34
Cycloheptane	604.2	353	961.95
Cyclooctane	647.2	410	941.69
Methanol	512.6	118	1046.86
Ethanol	516.2	167	1010.20
Propan-1-ol	536.7	218.5	986.07
Butan-1-ol	562.9	274	970.64
Benzene	562.1	259	892.10
Toluene	591.7	316	851.00
Acetone	508.1	209	935.90
Butan-2-one	535.6	267	918.54
Helium	5.2	57.5	2372.56

APPENDIX E: CALIBRATION DATA

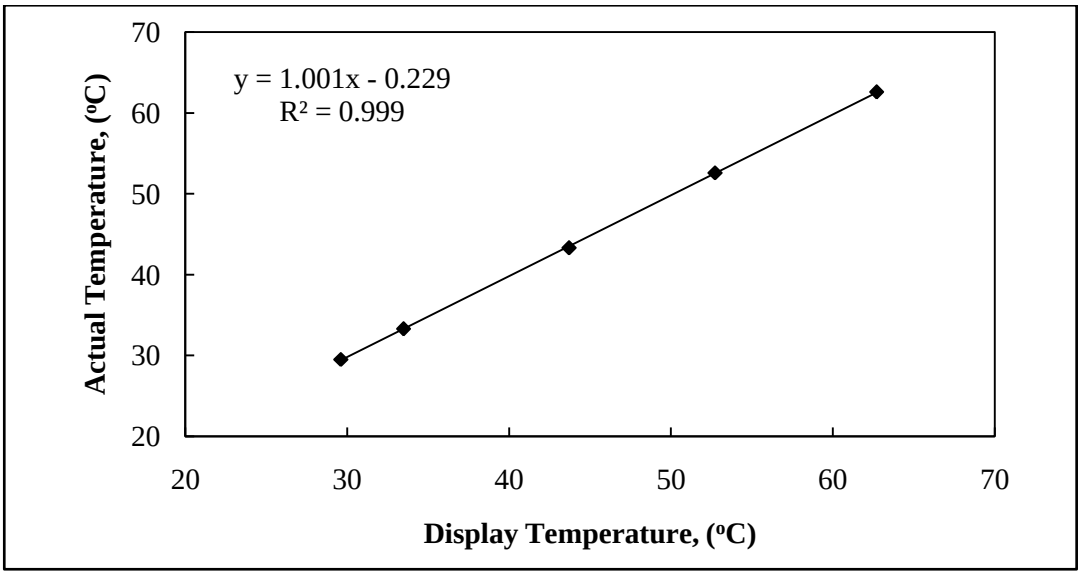

Figure E-1: Temperature calibration curve for the dilutor cell Pt 100.

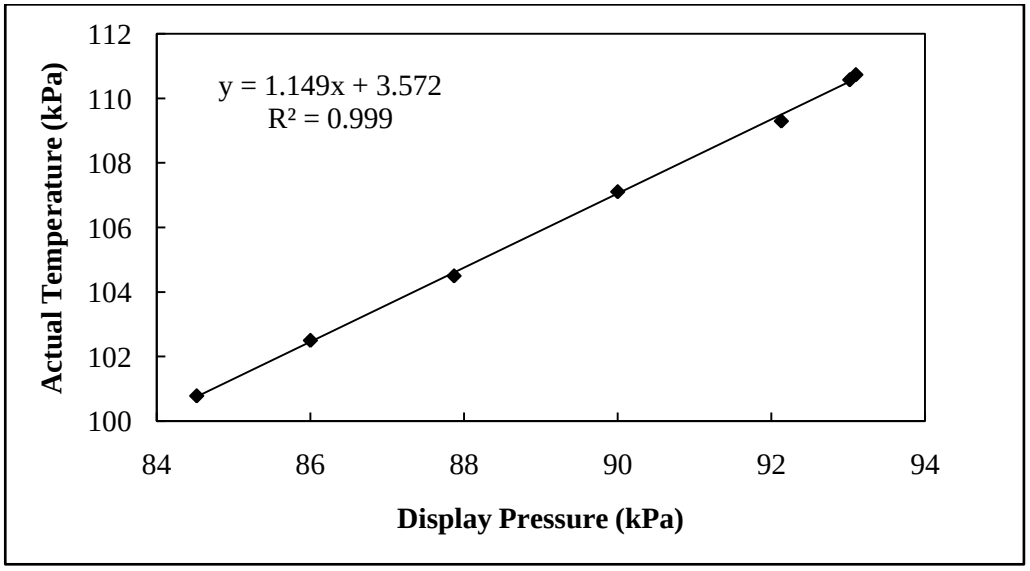

Figure E-2: Pressure calibration curve for the dilutor cell pressure transducer.

APPENDIX F: SELECTIVITIES AND CAPACITIES

Table F-1: Infinite dilution selectivity and capacity data at 313.15 K for FIL's and selected industrial solvents investigated in the literature (Subscripts are references given in Chapter 6) as well as in this work*; *#Data obtained at 298.15 K.*

	Limiting Selectivity S_{12}^{∞}							Limiting Capacity k_2^{∞}			
	Hexane (1) /benzene (2)	Cyclohexane (1)/benzene (2)	Methanol (1) /benzene (2)	Benzene (1) /butan-2-one (2)	Hexane (1) /hex-1-ene (2)	Methanol (1) /acetone (2)	Ethanol (1) /butan-2-one (2)	Benzene (2)	Hex-1-ene (2)	Acetone (2)	Butan-2-one (2)
[EMIM][BF_4][1][2]	38.65	20.06	0.17	1.54	2.02	0.39	0.47	0.41	0.02	0.91	0.62
[EMIM] [Tf_2N] [3][4][5]	21.12	9.75	1.08	2.40	2.08	3.17	3.54	0.83	0.08	2.44	2.00
[MMIM] [Tf_2N] [4]	27.26	15.48	-	-	2.24	-	-	0.74	0.06	-	-
[BMIM][BF_4][2][6][7]	23.84	12.53	0.52	1.51	1.70	1.23	0.87	0.41	0.03	0.98	0.63
[BMIM] [Tf_2N] [4][8]	15.13	9.16	1.23	-	1.89	2.97	-	1.12	0.14	2.70	-
[BMIM][TfO][9]	23.04	10.66	0.44	-	2.23	0.79	-	0.63	0.06	1.13	-
[DMPIM][BF_4][10][11]	70.40	31.77	0.24	-	-	0.34	-	0.28	-	0.40	-
[EDMIM] [Tf_2N] [3]	23.03	13.22	1.33	1.92	2.07	3.56	3.58	0.91	0.08	2.44	1.75
[HMIM][BF_4][2][12]	19.53	5.61	0.41	1.49	2.00	0.82	1.42	0.61	0.11	1.22	0.91
[HMIM][PF_6][13]	18.46	10.19	1.54	-	2.11	-	-	0.96	0.11	-	-
[HMIM] [Tf_2N] [14][15][16]	11.22	6.70	1.65	1.64	1.69	3.54	3.50	1.46	0.22	3.13	2.38
[MOIM][BF_4][17]	10.01	7.04	0.83	1.17	1.71	1.29	1.48	0.85	0.15	1.33	1.00
[MOIM] [Tf_2N] [16]	7.89	5.52	1.75	-	1.57	-	-	1.54	0.31	-	-
[C_{16}MIM][BF_4][18]	3.10	2.13	1.52	0.76	1.35	1.29	1.47	1.27	0.55	1.08	0.96
[$3C_6C_{14}$P][BF_4]*	3.41	2.38	1.31	0.92	1.26	1.25	1.30	2.44	0.90	2.32	2.25
[$3C_6C_{14}$P] [Tf_2N]*	2.80	2.03	2.77	1.23	1.21	3.80	4.00	2.56	1.10	3.51	3.15
[$3C_6C_{14}$P][$(C_2F_5)_3PF_3$][20]	3.25	2.40	5.83	-	1.23	-	-	5.00	1.89	-	-
[$3C_1C_4$N] [Tf_2N] [21]	13.94	0.58	1.07	-	1.89	3.38	-	0.75	0.10	2.38	-
[BMPy][BF_4][22][23]	36.88	17.71	0.66	1.66	-	1.52	1.78	0.61	-	1.41	1.01
[BMPyrr] [Tf_2N] [16]	15.47	-	-	1.62	1.92	-	3.26	1.16	0.14	-	1.89
[Et_3S] [Tf_2N] [24]	22.71	12.76	1.28	-	2.17	-	-	0.90	0.09	-	-
[Epy] [Tf_2N] [25][26]	24.38	14.31	0.95	2.00	2.33	2.62	2.65	0.77	0.07	2.13	1.54
[$3C_6C_{14}$P][PF_6]*	2.96	2.15	3.12	0.97	1.20	3.17	3.21	1.47	0.59	1.49	1.42
[$C_1$3C_8N] [Tf_2N] [27]*	3.77	2.70	2.68	1.22	1.33	3.11	3.44	2.27	0.80	2.63	2.78
[EMIM][TfO][28]*	30.20	15.19	0.33	-	2.31	-	-	0.45	0.03	-	-
[MOIM][PF_6][29]*	11.27	7.03	1.88	-	1.72	-	-	1.04	0.16	-	-
[BMIM][SbF_6][30]*	22.25	12.52	1.41	1.98	2.08	4.26	3.74	0.79	0.07	2.38	1.56
[BMIM][PF_6][31]	-	-	-	-	3.06	3.06	-	-	-	1.41	1.01
[EMIM][TFA][32]	27.03	12.97	0.08	-	2.34	-	-	0.36	0.03	-	-
[HMIM][TfO][33]	14.37	7.37	-	-	-	-	-	0.68	-	-	-
[BMPyrr][TfO][34]	-	-	-	2.45	-	-	-	-	0.05	-	-
[HMPyrr] [Tf_2N] [35]	-	-	-	1.70	-	-	-	-	0.22	-	-
[OMPyrr] [Tf_2N] [35]	-	-	-	1.53	-	-	-	-	0.30	-	-
Sulfolane[36]	18.17	9.81	0.91	1.20	-	1.38	1.52	0.43	-	0.64	0.51
NMP[37]	11.24	7.05	-	-	0.53	-	-	0.95	0.16	-	-
Chlorobenzene[38][39]	-	-	-	-	-	0.17*	8.29	-	-	-	0.47
Dimethylsulfoxide[38][39]	-	-	-	-	-	0.35*	0.20*	-	-	0.38*	0.35*

APPENDIX G: EFFECT OF STRUCTURE ON IDAC VALUES

1. Infinite dilution activity coefficients of alkanes in fluorinated ionic liquids.

1.1. Infinite dilution activity coefficients of alkanes in imidazolium-based fluorinated ionic liquids.

1.1.1. Effect of the cation

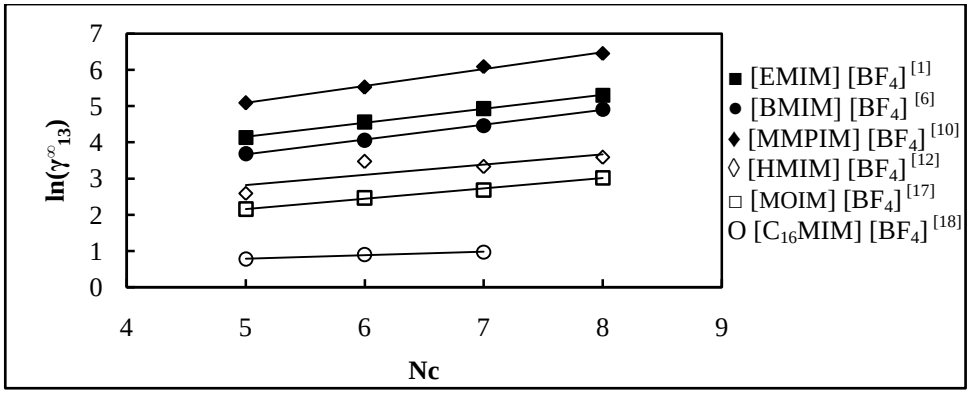

Figure G-1: Plots of $\ln \gamma_{13}^{\infty}$ versus Nc for alkanes in imidazolium-based FILs comprising $[BF_4]^-$ ion.

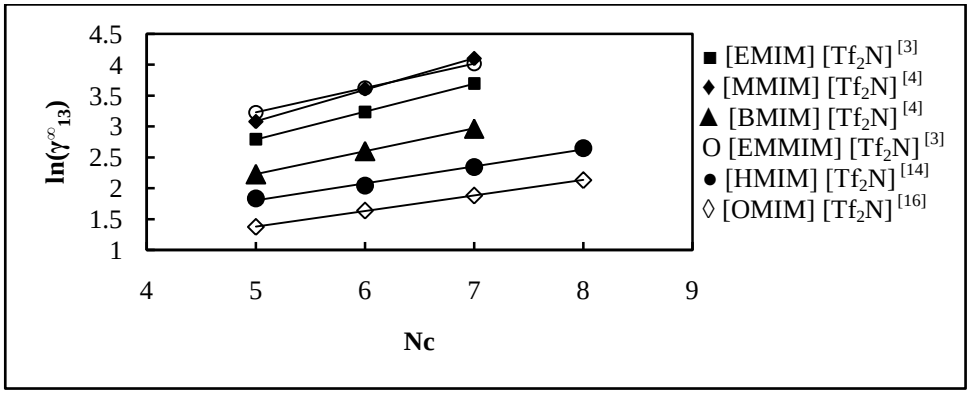

Figure G-2: Plots of $\ln \gamma_{13}^{\infty}$ versus Nc for alkanes in imidazolium-based FILs comprising $[Tf_2N]^-$ ion.

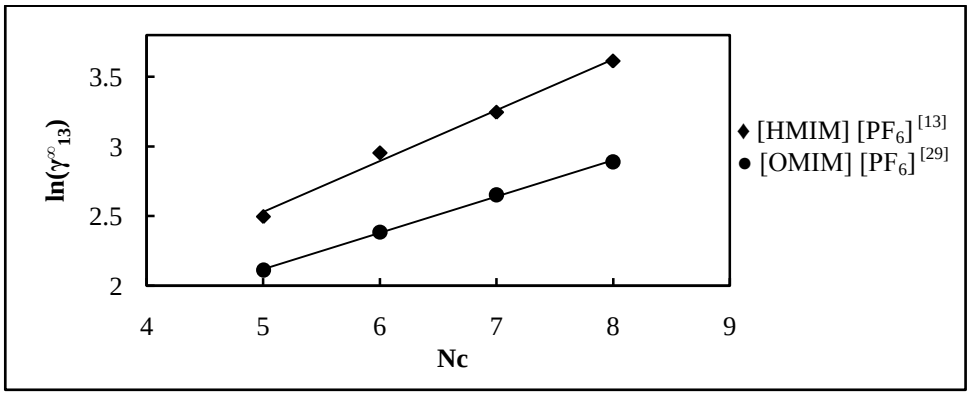

Figure G-3: Plots of $\ln \gamma_{13}^{\infty}$ versus Nc for alkanes in imidazolium-based FILs comprising $[PF_6]^-$ ion.

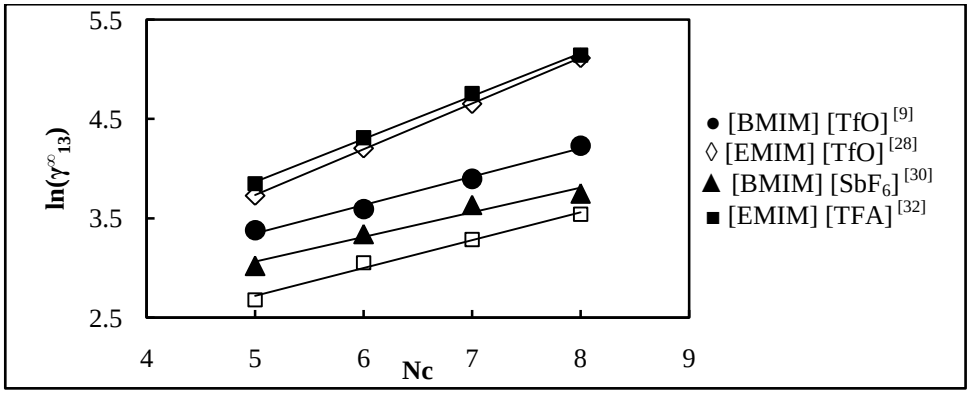

Figure G4: Plots of $\ln \gamma_{13}^{\infty}$ versus Nc for alkanes in imidazolium-based FILs comprising $[TfO]^-$, $[SbF_6]^-$ and $[TFA]^-$ ions.

1.1.2. Effect of the anion

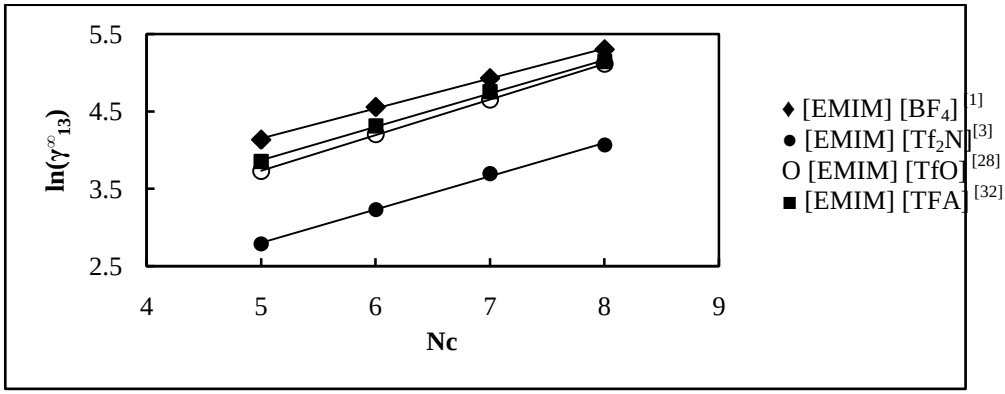

Figure G-5: Plots of $\ln \gamma_{13}^{\infty}$ versus Nc for alkanes in imidazolium-based FILs comprising $[EMIM]^+$ ion.

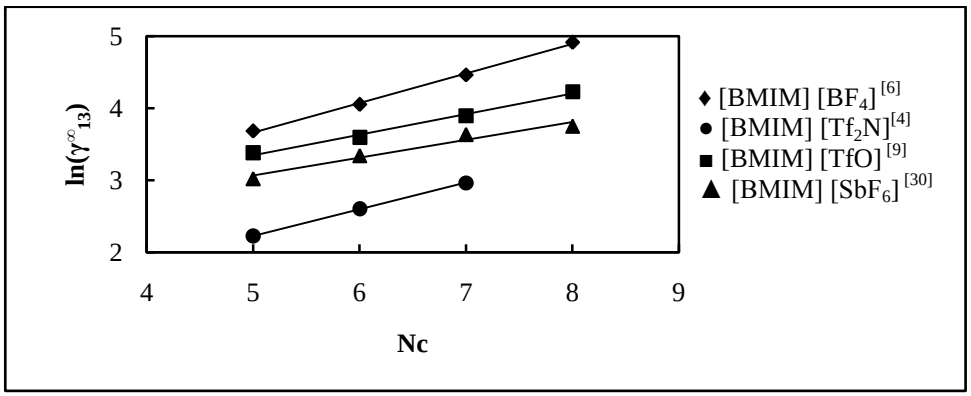

Figure G-6: Plots of $\ln \gamma_{13}^{\infty}$ versus Nc for alkanes in imidazolium-based FILs comprising $[BMIM]^+$ ion.

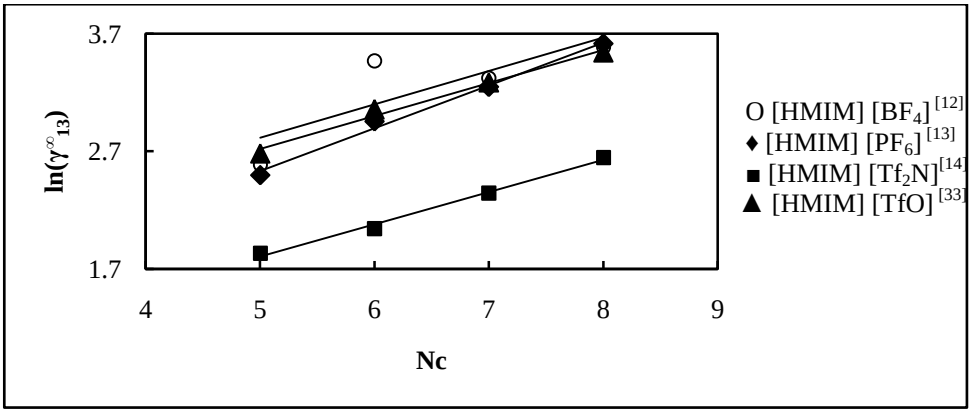

Figure G-7: Plots of $\ln \gamma_{13}^{\infty}$ versus Nc for alkanes in imidazolium-based FILs comprising $[HMIM]^+$ ion.

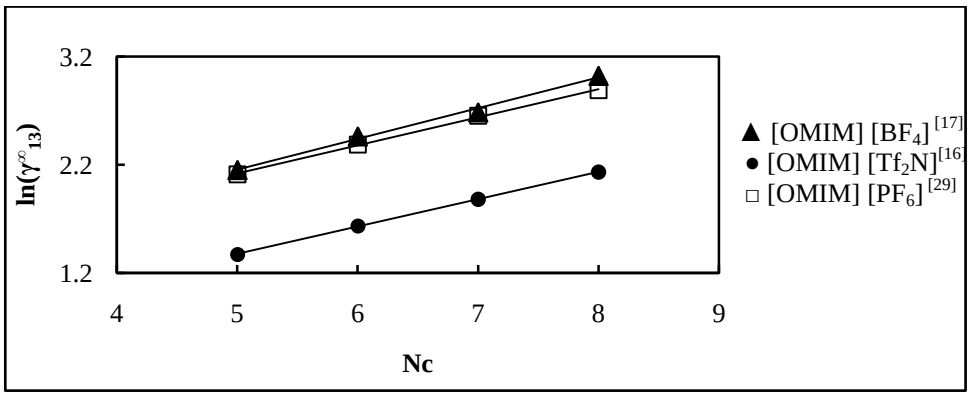

Figure G-8: Plots of $\ln \gamma_{13}^{\infty}$ versus Nc for alkanes in imidazolium-based FILs comprising $[MOIM]^+$ ion.

1.2. Infinite dilution activity coefficients of alkanes in phosphonium-based FILs

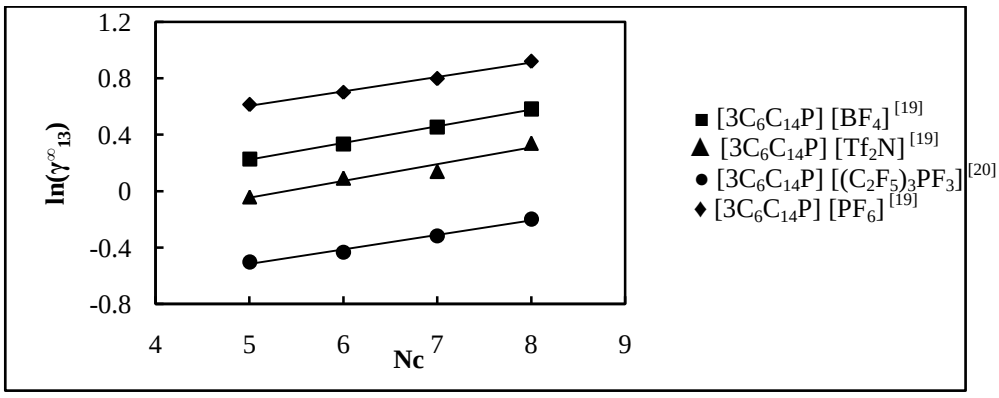

Figure G-9: Plots of $\ln \gamma_{13}^{\infty}$ versus Nc for alkanes in phosphonium-based FILs comprising $[3C_6C_{14}P]^+$ ion.

1.3. Infinite dilution activity coefficients of alkanes in ammonium-based FILs

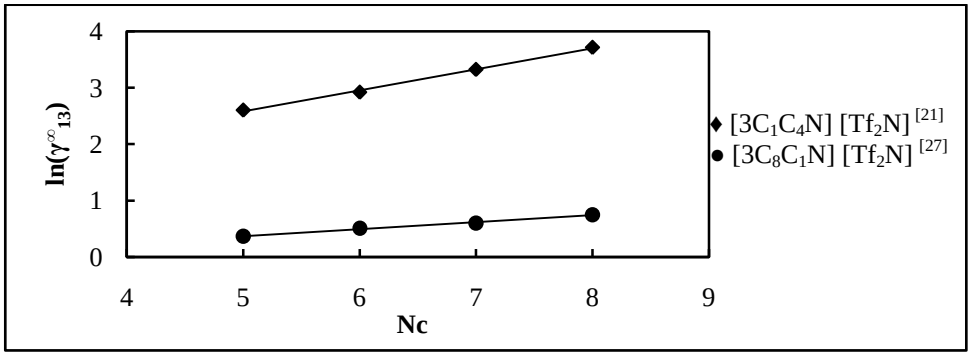

Figure G-10: Plots of $\ln \gamma_{13}^{\infty}$ versus Nc for alkanes in ammonium-based FILs comprising $[Tf_2N]^-$ ion.

1.4. Infinite dilution activity coefficients of alkanes in pyridinium-based FILs

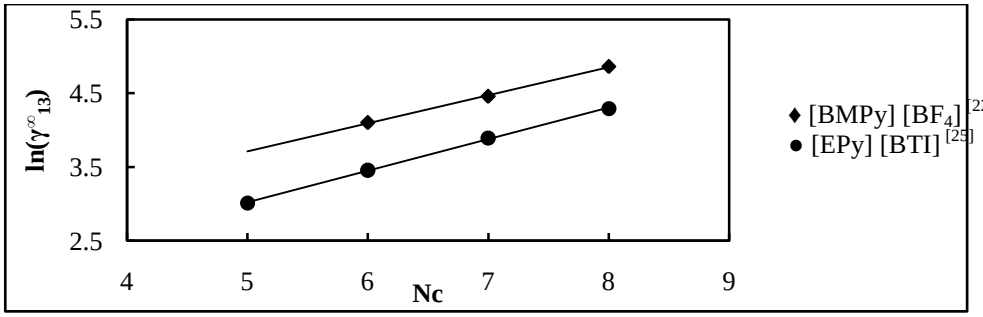

Figure G-11: Plots of $\ln \gamma_{13}^{\infty}$ versus Nc for alkanes in pyridinium-based FILs.

1.5. Infinite dilution activity coefficients of alkanes in pyrrolidinium-based FILs

1.5.1. Effect of the cation

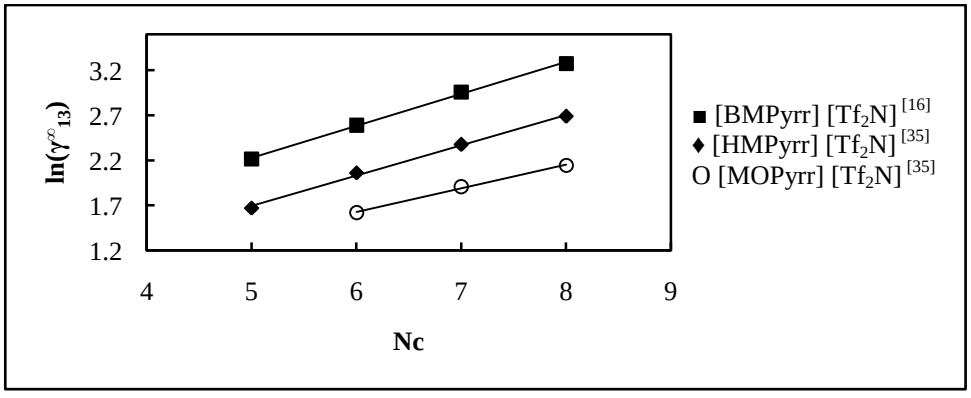

Figure G-12: Plots of $\ln \gamma_{13}^{\infty}$ versus Nc for alkanes in pyrrolidinium-based FILs comprising $[Tf_2N]^-$ ion.

1.5.2. Effect of the anion

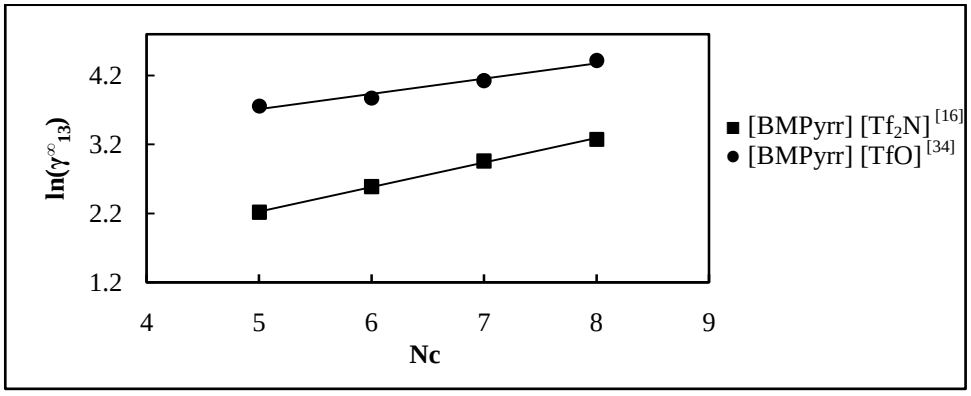

Figure G-13: Plots of $\ln \gamma_{13}^{\infty}$ versus Nc for alkanes in pyrrolidinium-based FILs comprising $[BMPyrr]^+$ ion.

1.6. Infinite dilution activity coefficients of alkanes in sulfonium-based FILs

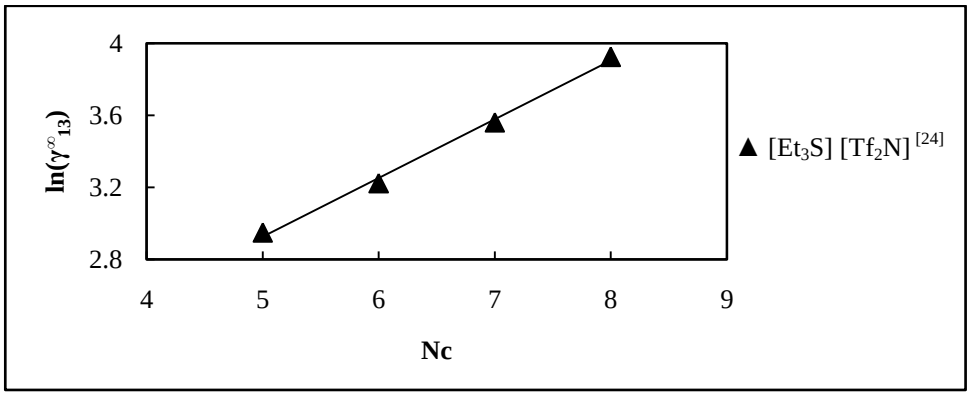

Figure G-14: Plot of $\ln \gamma_{13}^{\infty}$ versus Nc for alkanes in the sulfonium-based FIL $[Et_3S][Tf_2N]$.

2. Infinite dilution activity coefficients of alk-1-enes in fluorinated ionic liquids.

2.1. Infinite dilution activity coefficients of alk-1-enes in imidazolium-based FILs

2.1.1. Effect of the cation

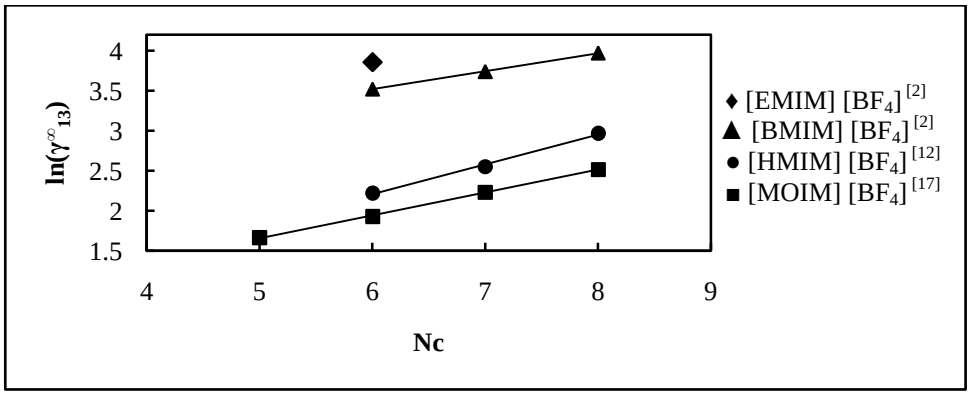

Figure G-15: Plots of $\ln \gamma_{13}^{\infty}$ versus Nc for alk-1-enes in imidazolium-based FILs comprising $[BF_4]^-$ ion.

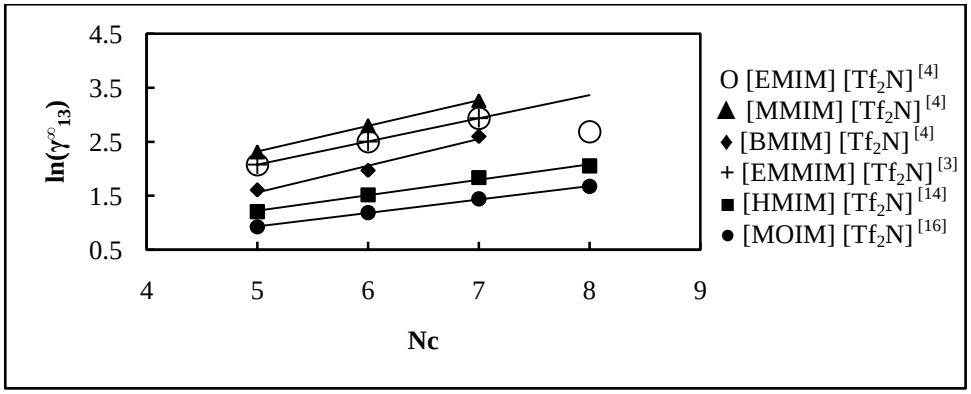

Figure G-16: Plots of $\ln \gamma_{13}^{\infty}$ versus Nc for alk-1-enes in imidazolium-based FILs comprising $[Tf_2N]^-$ ion.

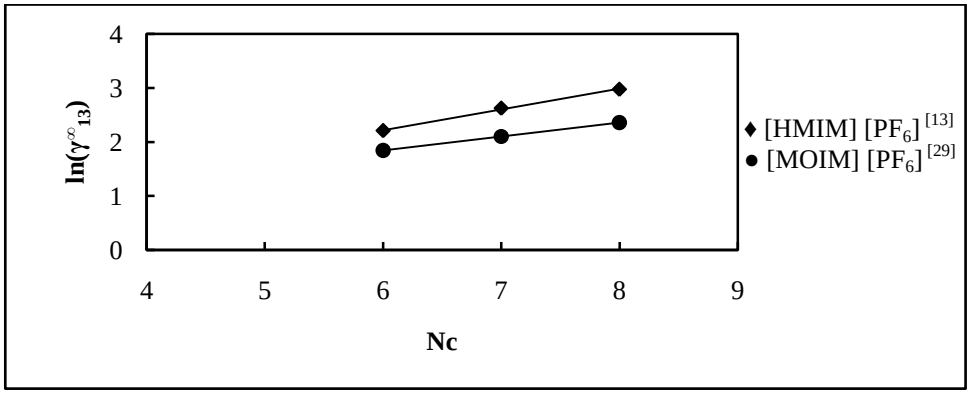

Figure G-17: Plots of $\ln \gamma_{13}^{\infty}$ versus Nc for alk-1-enes in imidazolium-based FILs comprising $[PF_6]^-$ ion.

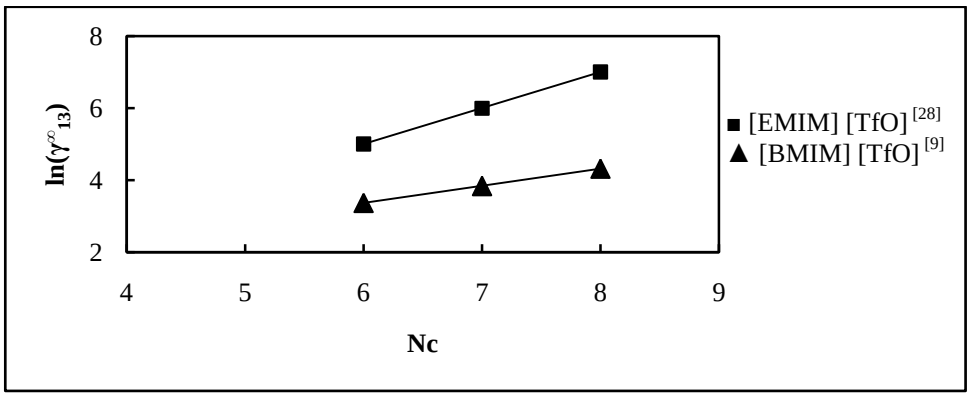

Figure G-18: Plots of $\ln \gamma_{13}^{\infty}$ versus Nc for alk-1-enes in imidazolium-based FILs comprising $[TfO]^-$ ion.

2.1.2. Effect of the anion

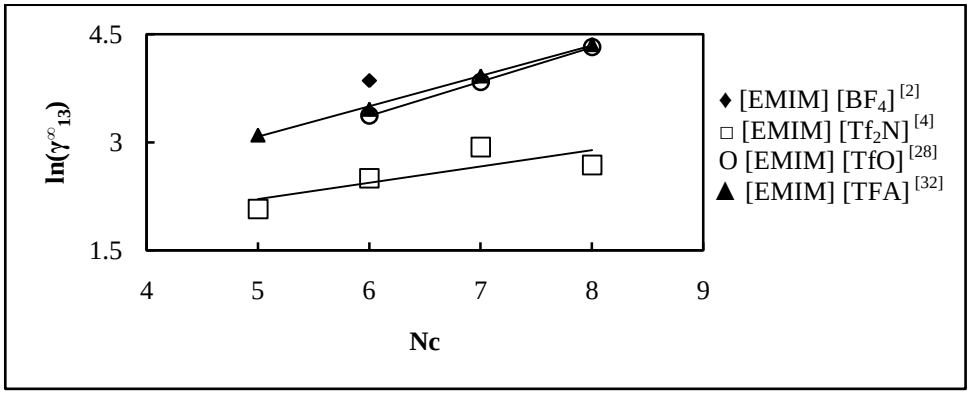

Figure G-19: Plots of $\ln \gamma_{13}^{\infty}$ versus Nc for alk-1-enes in imidazolium-based FILs comprising $[EMIM]^+$ ion.

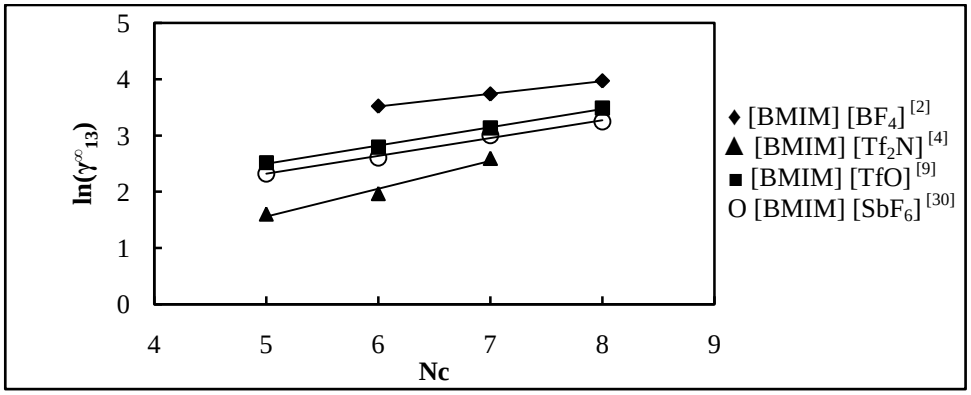

Figure G-20: Plots of $\ln \gamma_{13}^{\infty}$ versus Nc for alk-1-enes in imidazolium-based FILs comprising $[BMIM]^+$ ion.

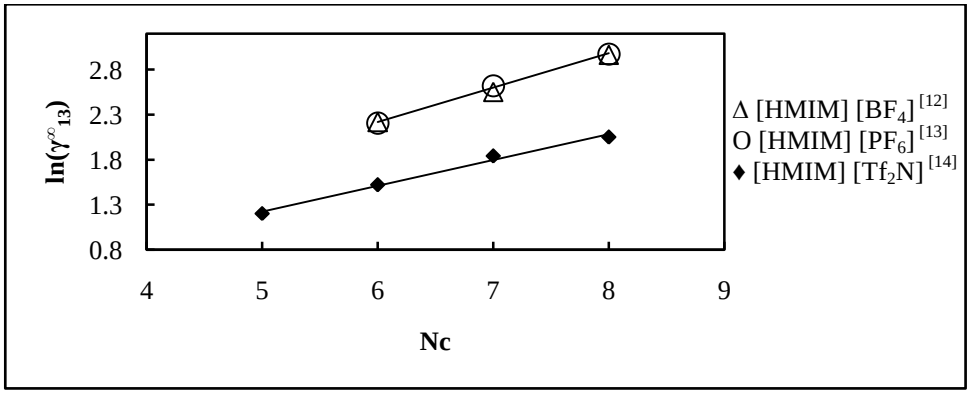

Figure G-21: Plots of $\ln \gamma_{13}^{\infty}$ versus Nc for alk-1-enes in imidazolium-based FILs comprising $[HMIM]^+$ ion.

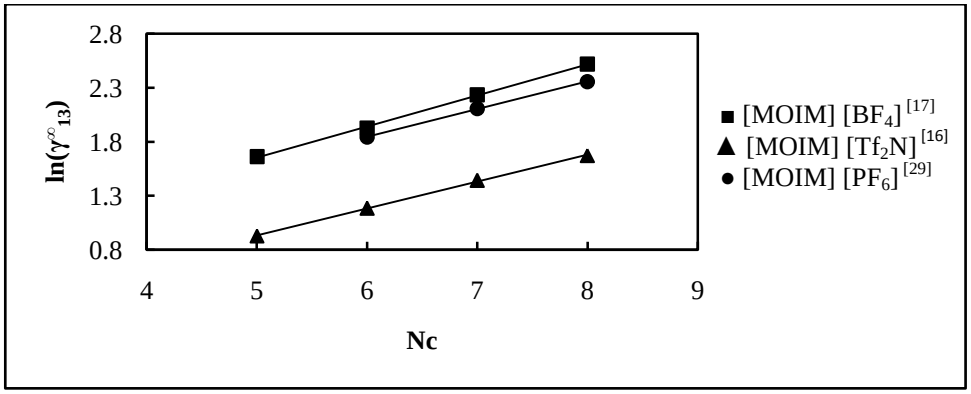

Figure G-22: Plots of $\ln \gamma_{13}^{\infty}$ versus Nc for alk-1-enes in imidazolium-based FILs comprising $[MOIM]^+$ ion.

2.2. Infinite dilution activity coefficients of alk-1-enes in phosphonium-based FILs

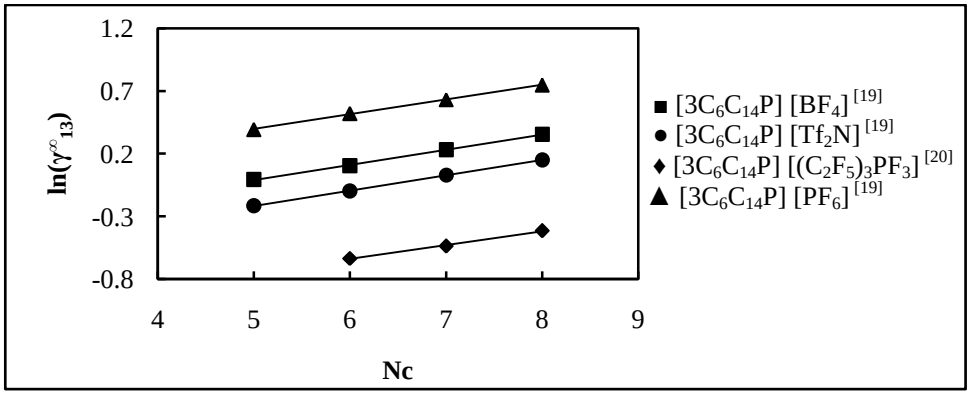

Figure G-23: Plots of $\ln \gamma_{13}^{\infty}$ versus Nc for alk-1-enes in phosphonium-based FILs comprising $[3C_6C_{14}P]^+$ ion.

2.3. Infinite dilution activity coefficients of alk-1-enes in ammonium-based FILs

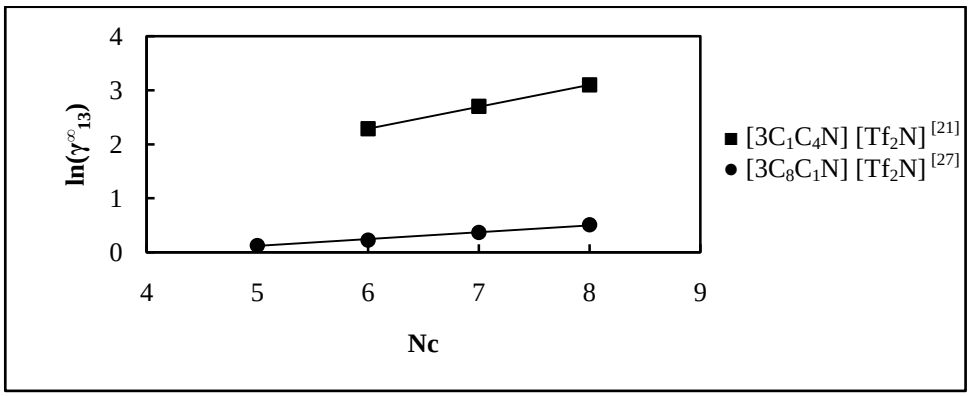

Figure G-24: Plots of $\ln \gamma_{13}^{\infty}$ versus Nc for alk-1-enes in ammonium-based FILs comprising $[Tf_2N]^-$ ion.

2.4. Infinite dilution activity coefficients of alk-1-enes in pyridinium-based FILs

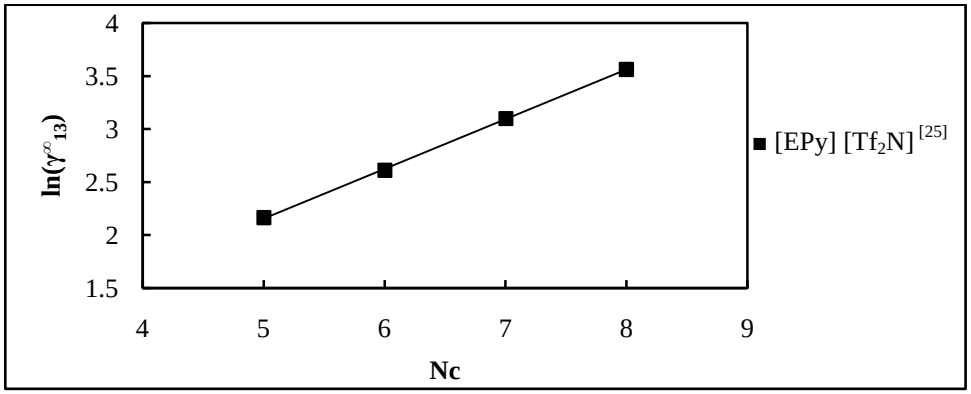

Figure G-25: Plot of $\ln \gamma_{13}^{\infty}$ versus Nc for alk-1-enes in the pyridinium-based FIL [Epy] [Tf_2N].

2.5. Infinite dilution activity coefficients of alk-1-enes in pyrrolidinium-based FILs

2.5.1. Effect of the cation

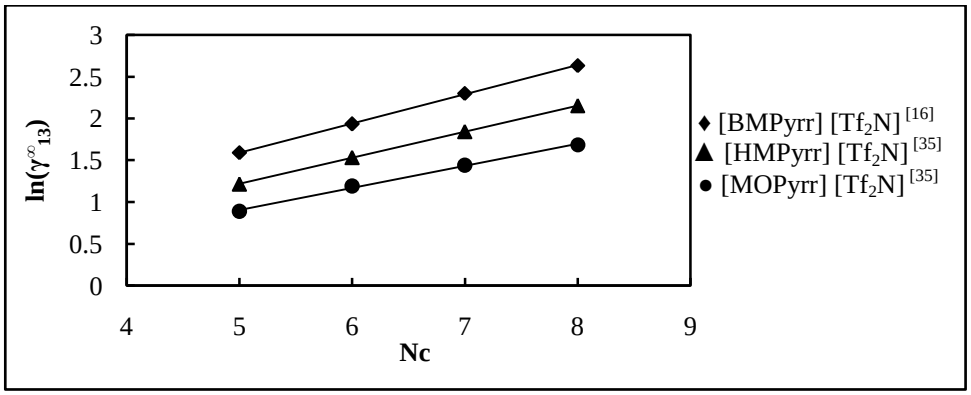

Figure G-26: Plots of $\ln \gamma_{13}^{\infty}$ versus Nc for alk-1-enes in pyrrolidinium-based FILs comprising $[Tf_2N]^-$ ion.

2.5.2. Effect of the anion

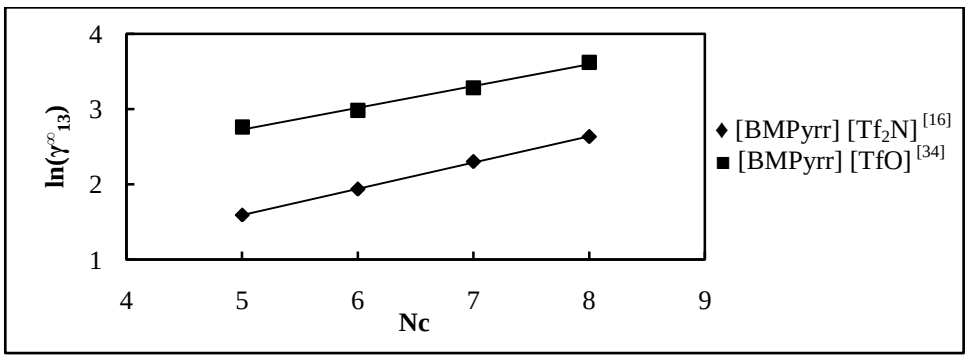

Figure G-27: Plots of $\ln \gamma_{13}^{\infty}$ versus Nc for alk-1-enes in pyrrolidinium-based FILs comprising $[BMPyrr]^+$ ion.

1.2.7. Infinite dilution activity coefficients of alk-1-enes in sulfonium-based FILs

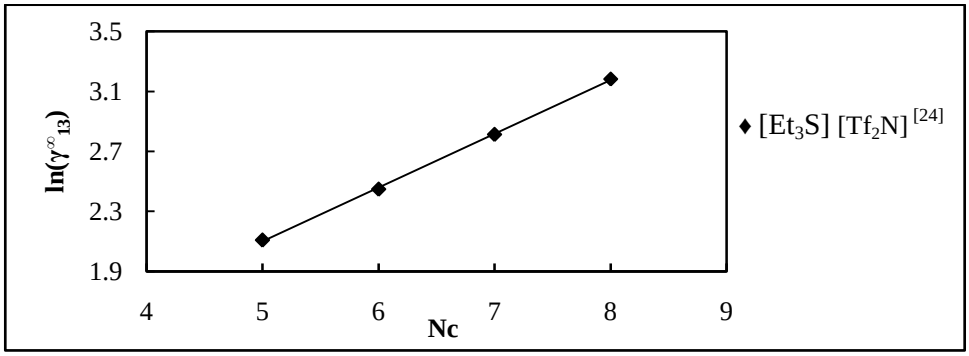

Figure G-28: Plot of $\ln \gamma_{13}^{\infty}$ versus Nc for alk-1-enes in the sulfonium-based FIL [Et_3S] [Tf_2N].

3. Infinite dilution activity coefficients of alk-1-ynes in fluorinated ionic liquids.
3.1. Infinite dilution activity coefficients of alk-1-ynes in imidazolium-based FILs
3.1.1. Effect of the cation

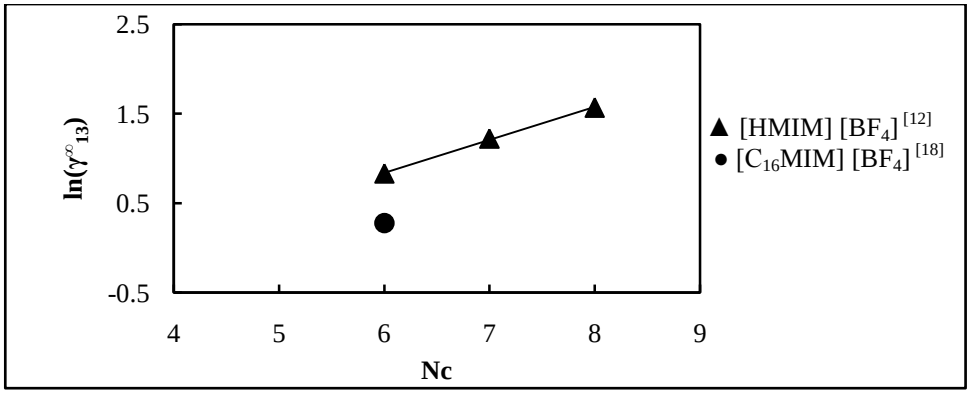

Figure G-29: Plots of $\ln \gamma_{13}^{\infty}$ versus Nc for alk-1-ynes in imidazolium-based FILs comprising $[BF_4]^-$ ion.

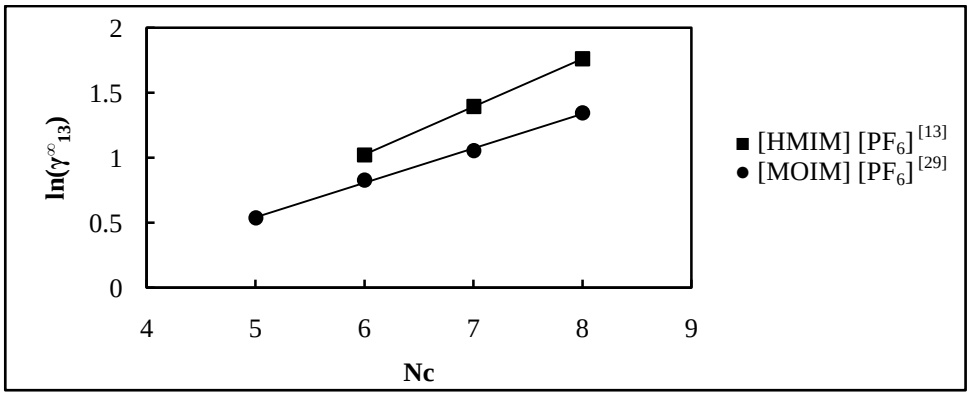

Figure G-30: Plots of $\ln \gamma_{13}^{\infty}$ versus Nc for alk-1-ynes in imidazolium-based FILs comprising $[PF_6]^-$ ion.

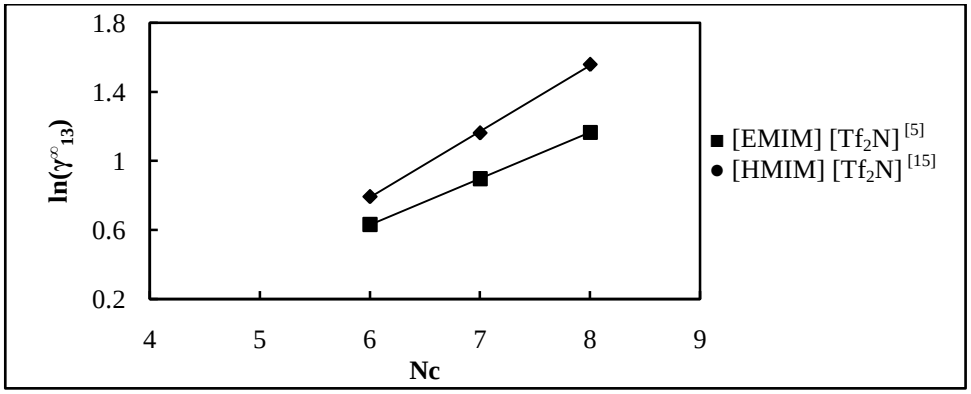

Figure G-31: Plots of $\ln \gamma_{13}^{\infty}$ versus Nc for alk-1-ynes in imidazolium-based FILs comprising $[Tf_2N]^-$ ion.

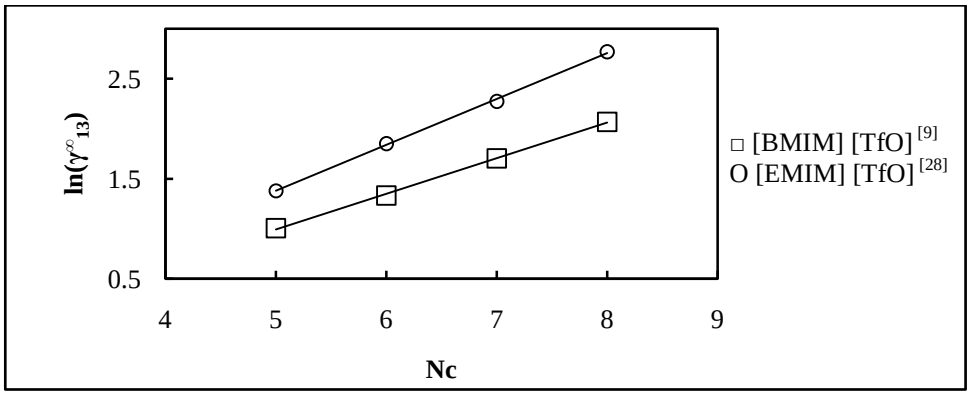

Figure G-32: Plots of $\ln \gamma_{13}^{\infty}$ versus Nc for alk-1-ynes in imidazolium-based FILs comprising $[TfO]^-$ ion.

3.1.2. Effect of the anion

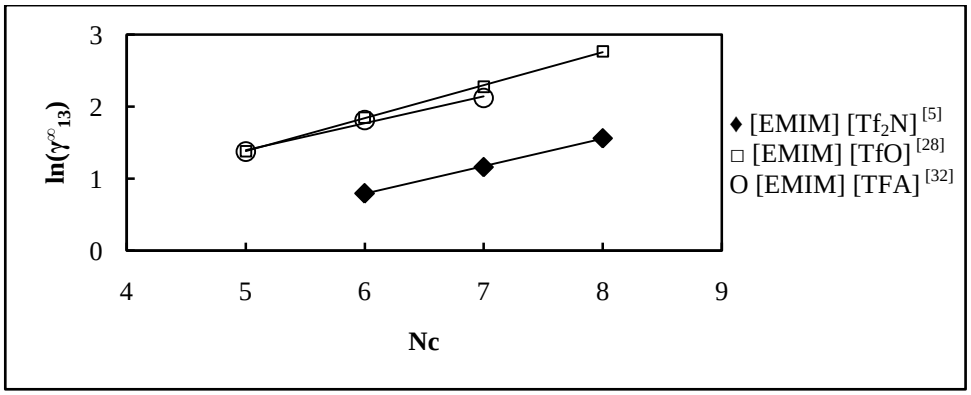

Figure G-33: Plots of $\ln \gamma_{13}^{\infty}$ versus Nc for alk-1-ynes in imidazolium-based FILs comprising $[EMIM]^+$ ion.

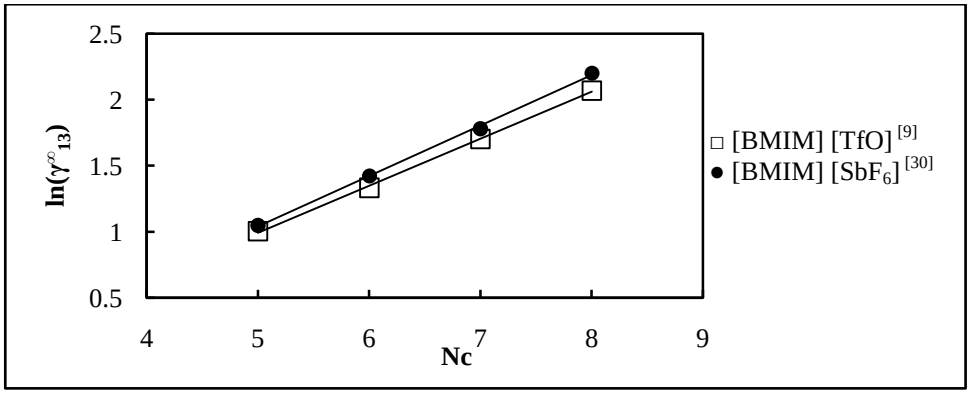

Figure G-34: Plots of $\ln \gamma_{13}^{\infty}$ versus Nc for alk-1-ynes in imidazolium-based FILs comprising $[BMIM]^+$ ion.

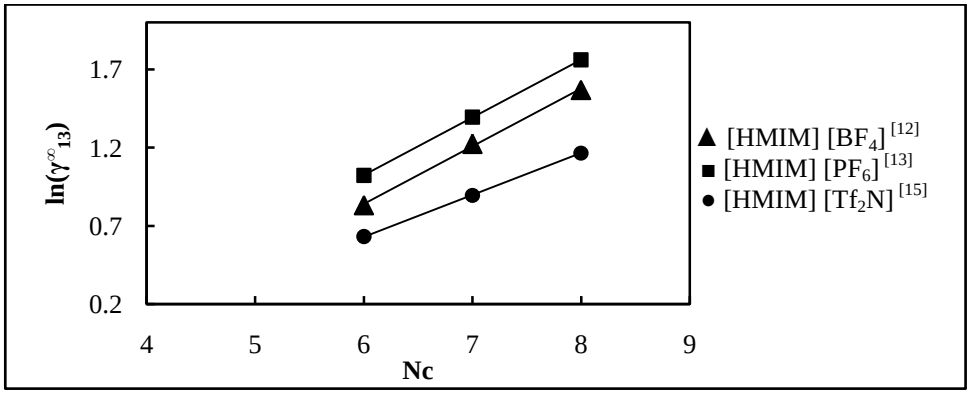

Figure G-35: Plots of $\ln \gamma_{13}^{\infty}$ versus Nc for alk-1-ynes in imidazolium-based FILs comprising $[HMIM]^+$ ion.

3.2. Infinite dilution activity coefficients of alk-1-ynes in phosphonium-based FILs

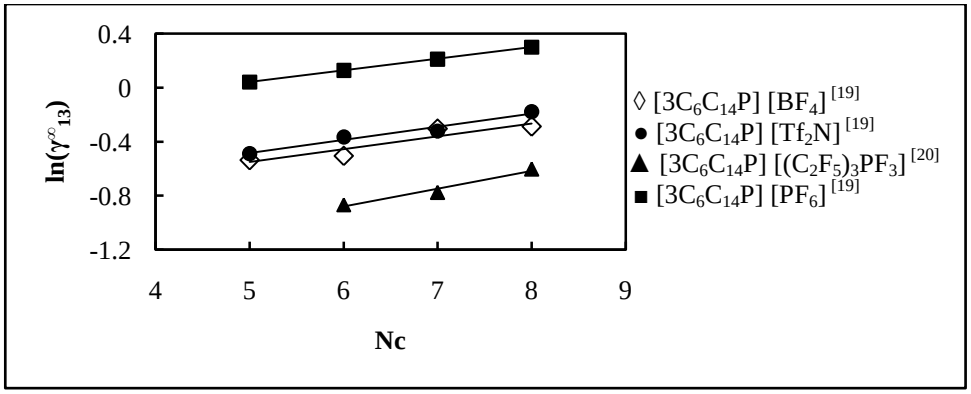

Figure G-36: Plots of $\ln \gamma_{13}^{\infty}$ versus Nc for alk-1-ynes in phosphonium-based FILs comprising $[3C_6C_{14}P]^+$ ion.

3.3. Infinite dilution activity coefficients of alk-1-ynes in ammonium, pyrrolidinium and sulfonium-based FILs

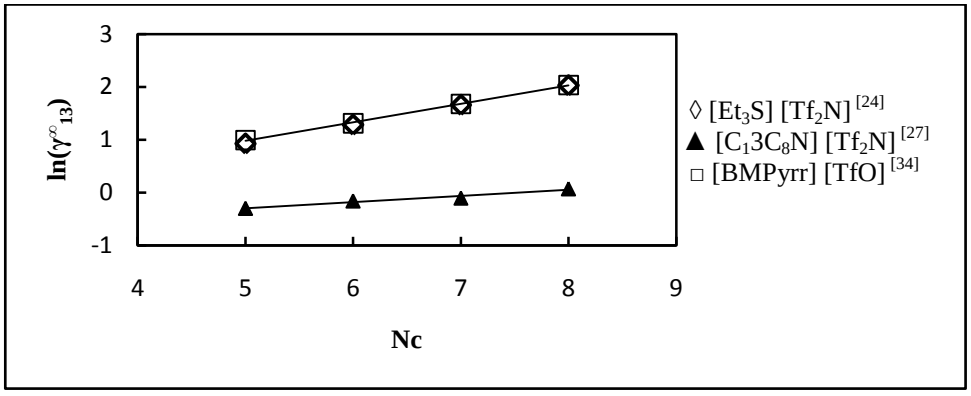

Figure G-37: Plots of $\ln \gamma_{13}^{\infty}$ versus Nc for alk-1-ynes in an ammonium, a pyrrolidinium and a sulfonium-based FILs.

4. Infinite dilution activity coefficients of cycloalkanes in fluorinated ionic liquids.
4.1. Infinite dilution activity coefficients of cycloalkanes in imidazolium-based FILs

4.1.1. Effect of the cation

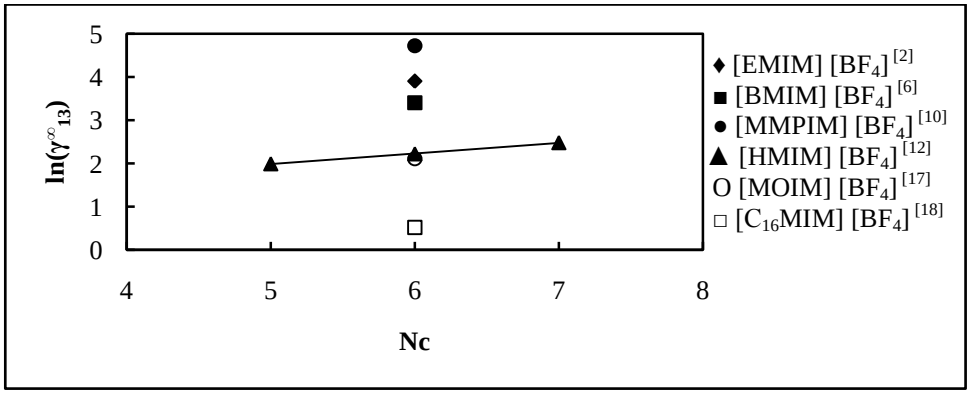

Figure G-38: Plots of $\ln \gamma_{13}^{\infty}$ versus Nc for cycloalkanes in imidazolium-based FILs comprising $[BF_4]^-$ ion.

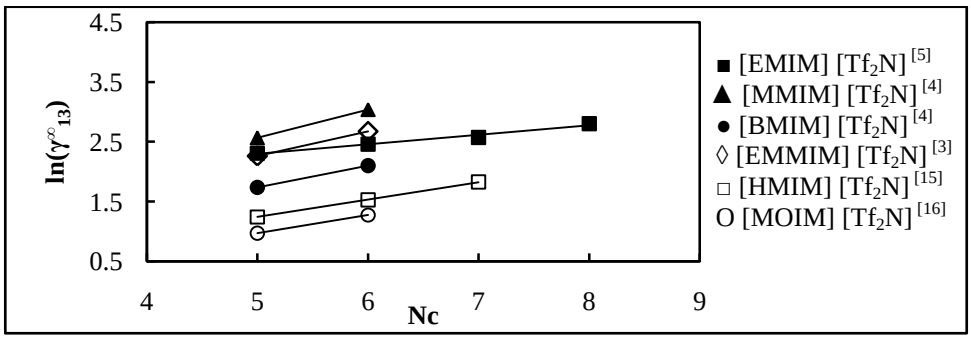

Figure G-39: Plots of $\ln \gamma_{13}^{\infty}$ versus Nc for cycloalkanes in imidazolium-based FILs comprising $[Tf_2N]^-$ ion.

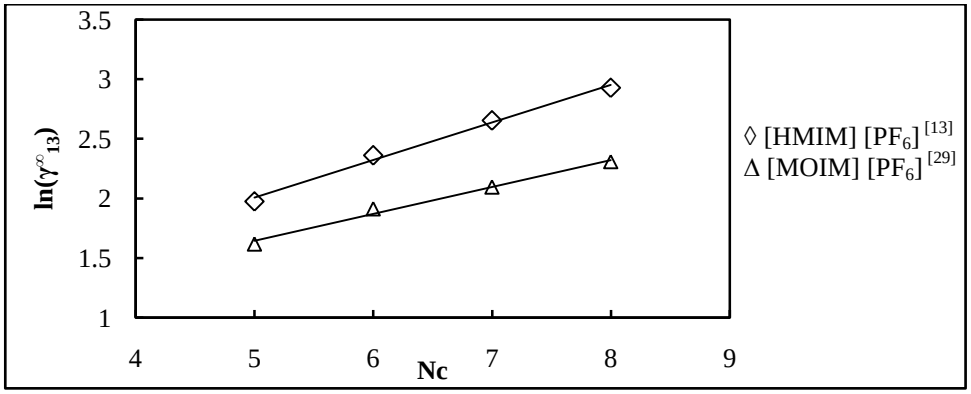

Figure G-40: Plots of $\ln \gamma_{13}^{\infty}$ versus Nc for cycloalkanes in imidazolium-based FILs comprising $[PF_6]^-$ ion.

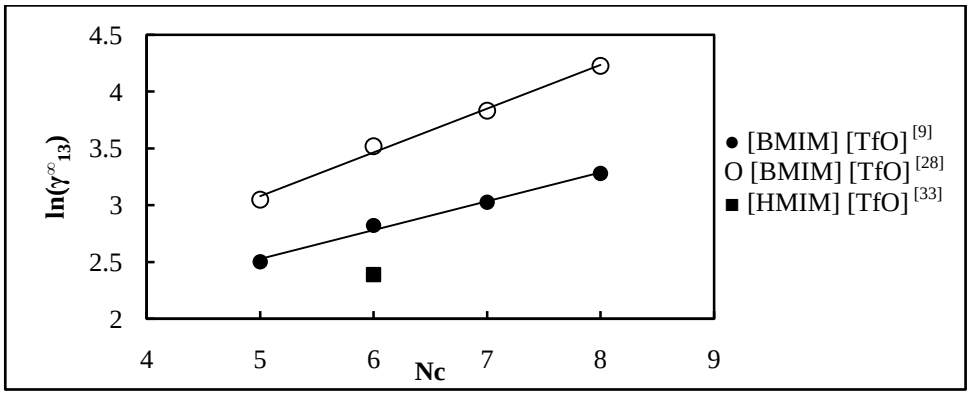

Figure G-41: Plots of $\ln \gamma_{13}^{\infty}$ versus Nc for cycloalkanes in imidazolium-based FILs comprising $[TfO]^-$ ion.

4.1.2. Effect of the anion

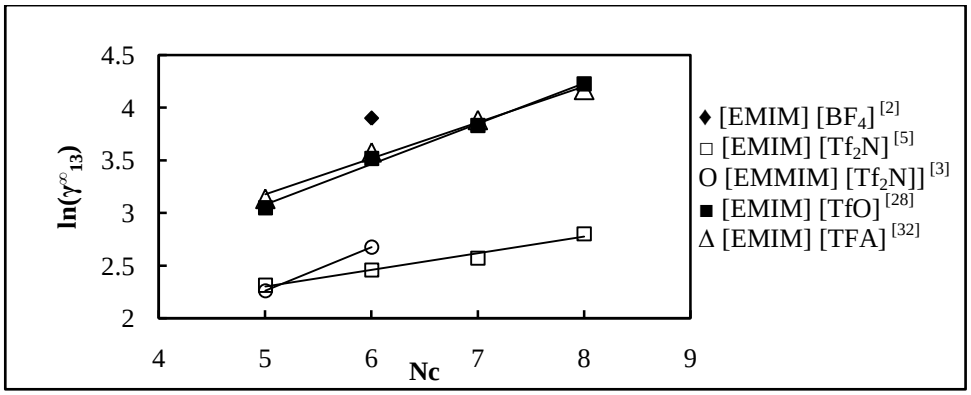

Figure G-42: Plots of $\ln \gamma_{13}^{\infty}$ versus Nc for cycloalkanes in imidazolium-based FILs comprising $[EMIM]^+$ ion.

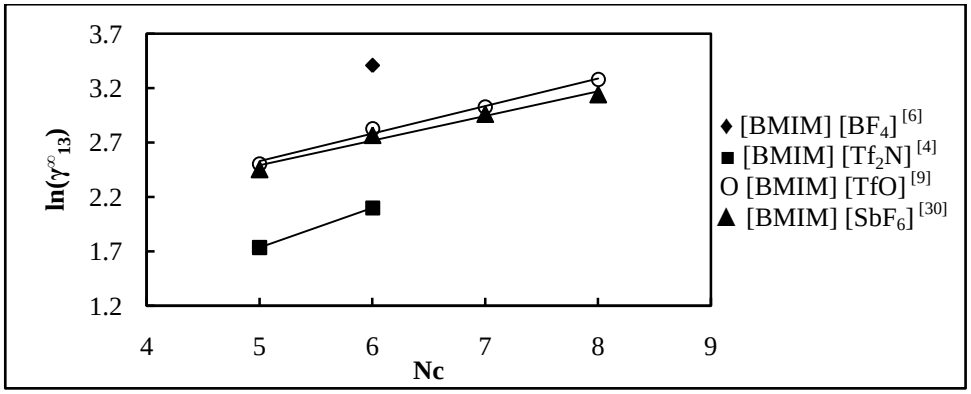

Figure G-43: Plots of $\ln \gamma_{13}^{\infty}$ versus Nc for cycloalkanes in imidazolium-based FILs comprising $[BMIM]^+$ ion.

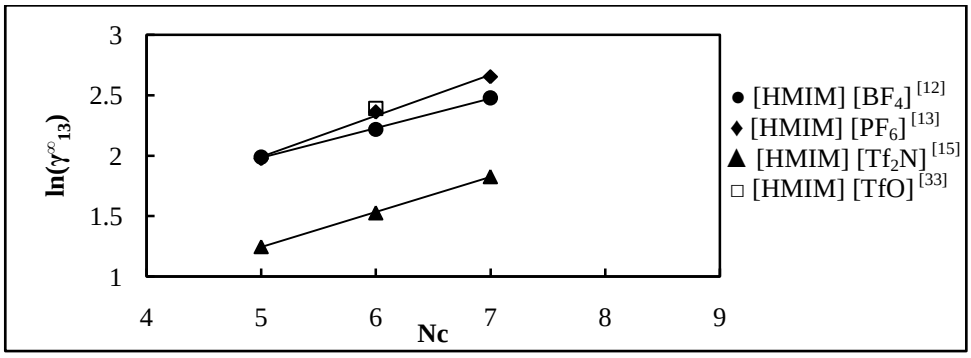

Figure G-44: Plots of $\ln \gamma_{13}^{\infty}$ versus Nc for cycloalkanes in imidazolium-based FILs comprising $[HMIM]^+$ ion.

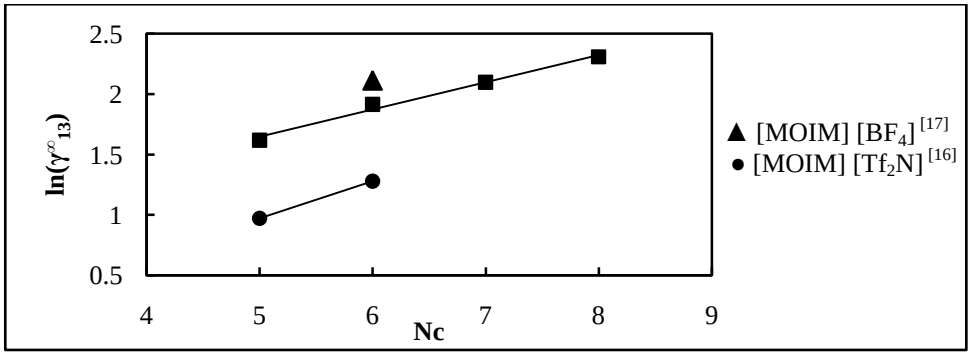

Figure G-45: Plots of $\ln \gamma_{13}^{\infty}$ versus Nc for cycloalkanes in imidazolium-based FILs comprising $[MOIM]^+$ ion.

4.2. Infinite dilution activity coefficients of cycloalkanes in phosphonium-based FILs

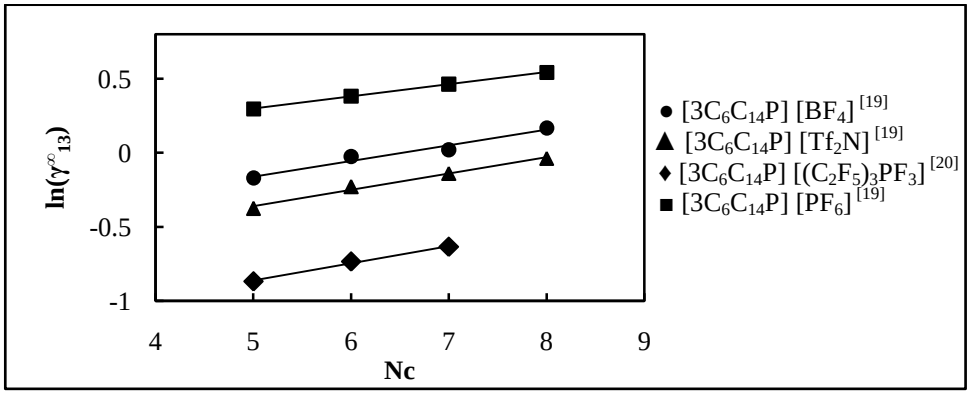

Figure G-46: Plots of $\ln \gamma_{13}^{\infty}$ versus Nc for cycloalkanes in phosphonium-based FILs comprising $[3C_6C_{14}P]^+$ ion.

4.3. Infinite dilution activity coefficients of cycloalkanes in ammonium-based FILs

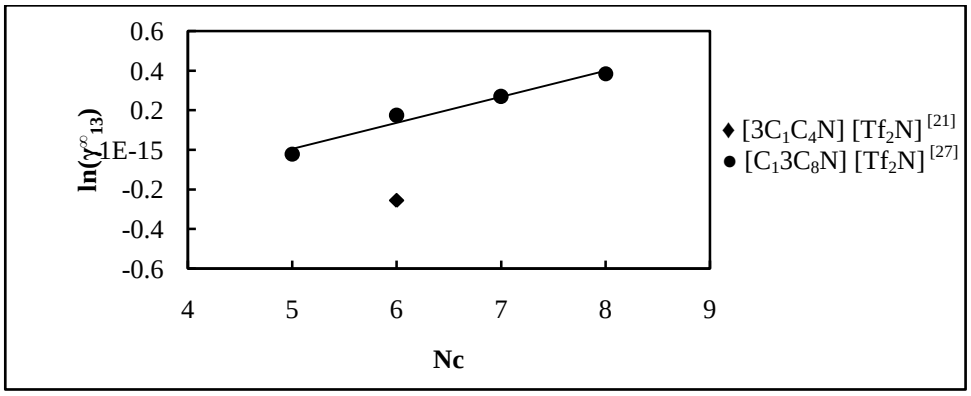

Figure G-47: Plots of $\ln \gamma_{13}^{\infty}$ versus Nc for cycloalkanes in ammonium-based FILs comprising $[Tf_2N]^-$ ion.

4.4. Infinite dilution activity coefficients of cycloalkanes in pyridinium-based FILs

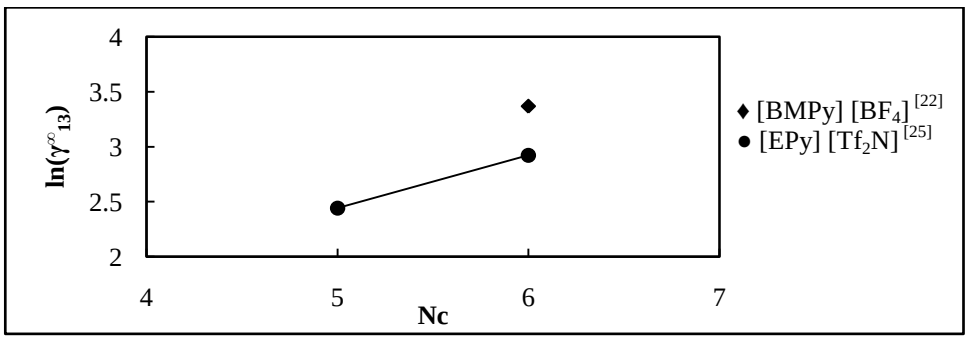

Figure G-48: Plots of $\ln \gamma_{13}^{\infty}$ versus Nc for cycloalkanes in the pyridinium-based FILs [Epy] $[Tf_2N]$ and [BMPy] $[BF_4]$.

4.5. Infinite dilution activity coefficients of cycloalkanes in pyrrolidinium-based FILs

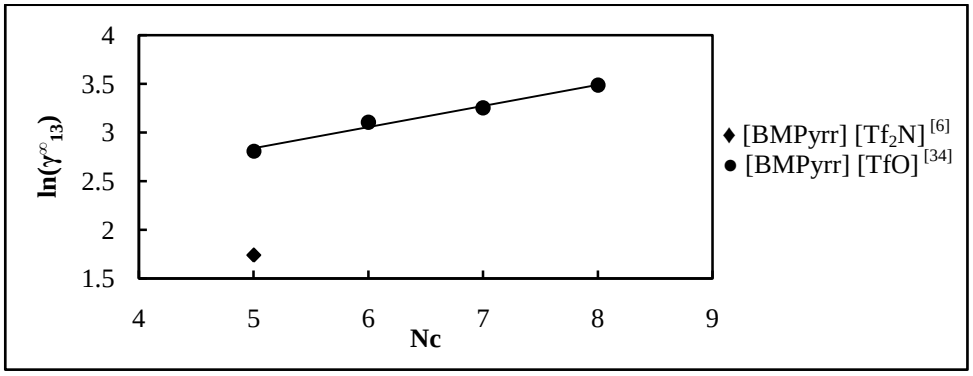

Figure G-49: Plots of $\ln \gamma_{13}^{\infty}$ versus Nc for cycloalkanes in ammonium-based FILs comprising $[BMPyrr]^+$ ion.

4.6. Infinite dilution activity coefficients of cycloalkanes in sulfonium-based FILs

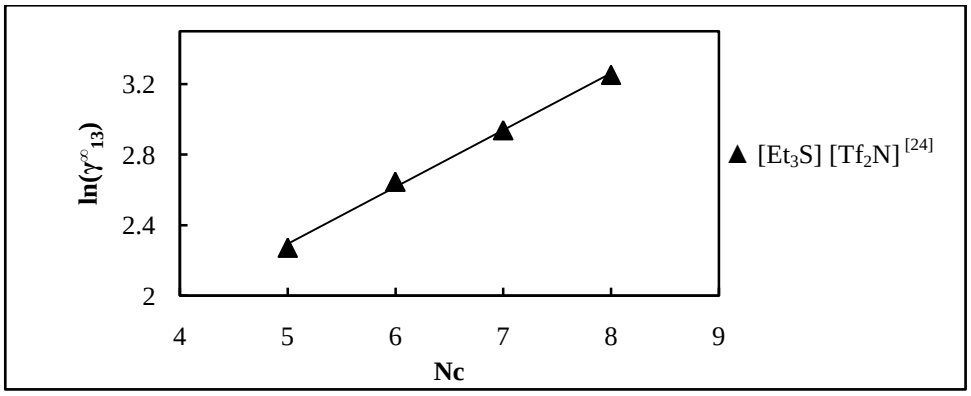

Figure G-50: Plots of $\ln \gamma_{13}^{\infty}$ versus Nc for cycloalkanes in the sulfonium-based FIL $[Et_3S]$ $[Tf_2N]$.

5. Infinite dilution activity coefficients of alkan-1-ols in fluorinated ionic liquids.

5.1. Infinite dilution activity coefficients of alkan-1-ols in imidazolium-based FILs

5.1.1. Effect of the cation

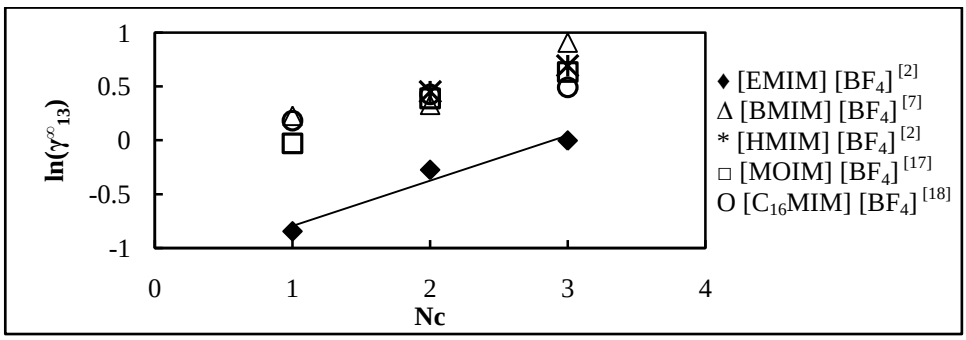

Figure G-51: Plots of $\ln \gamma_{13}^{\infty}$ versus Nc for alkan-1-ols in imidazolium-based FILs comprising $[BF_4]^-$ ion.

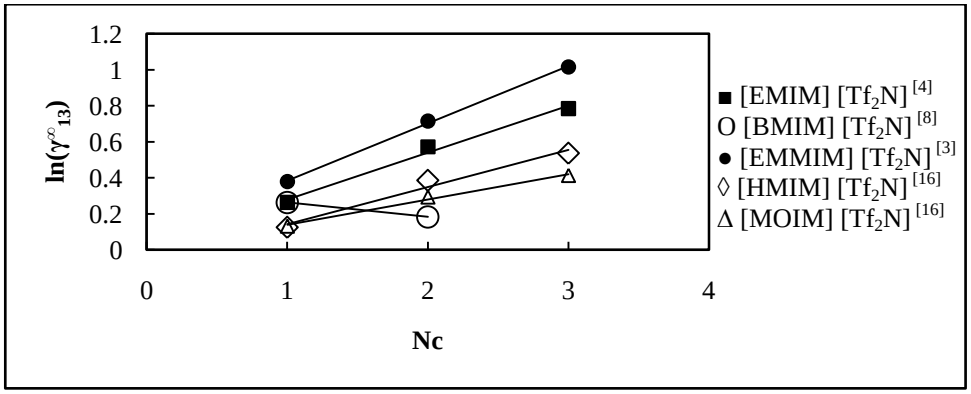

Figure G-52: Plots of $\ln \gamma_{13}^{\infty}$ versus Nc for alkan-1-ols in imidazolium-based FILs comprising $[Tf_2N]^-$ ion.

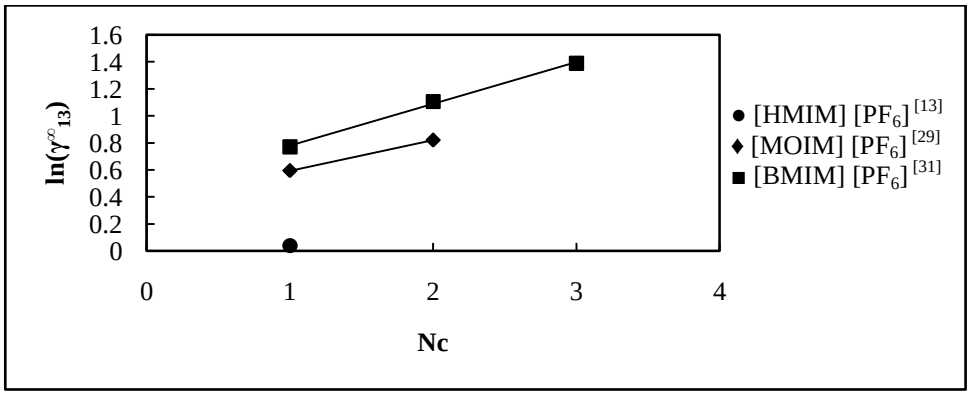

Figure G-53: Plots of $\ln \gamma_{13}^{\infty}$ versus Nc for alkan-1-ols in imidazolium-based FILs comprising $[PF_6]^-$ ion.

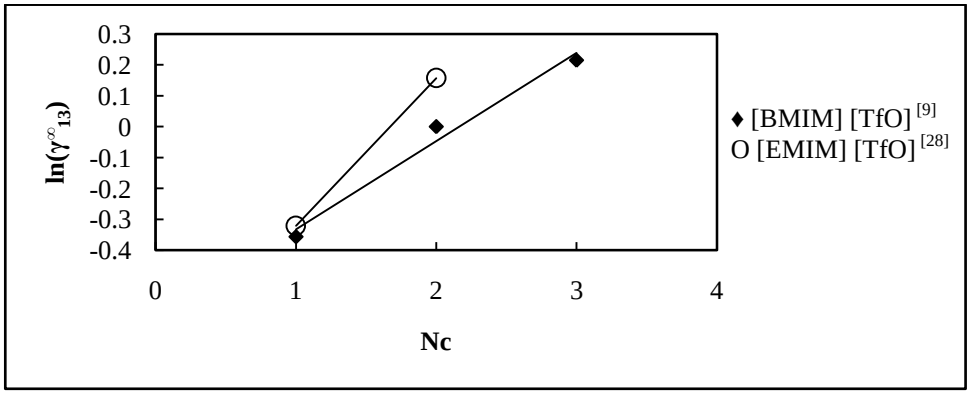

Figure G-54: Plots of $\ln \gamma_{13}^{\infty}$ versus Nc for alkan-1-ols in imidazolium-based FILs comprising $[TfO]^-$ ion.

5.1.2. Effect of the anion

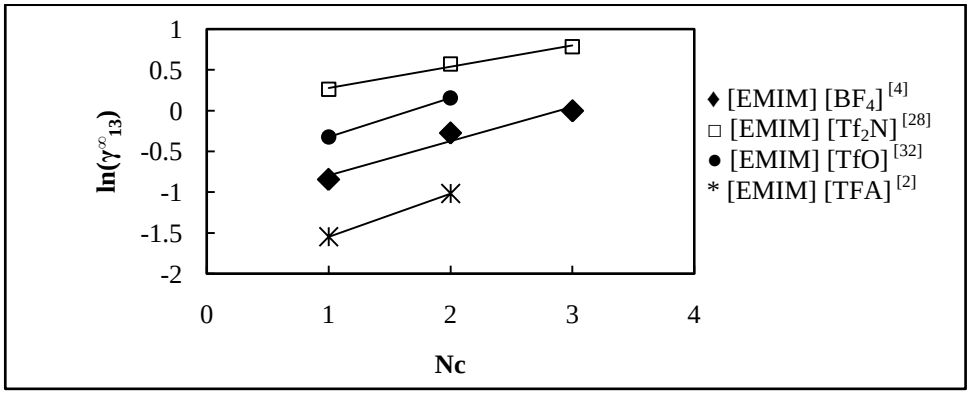

Figure G-55: Plots of $\ln \gamma_{13}^{\infty}$ versus Nc for alkan-1-ols in imidazolium-based FILs comprising $[EMIM]^+$ ion.

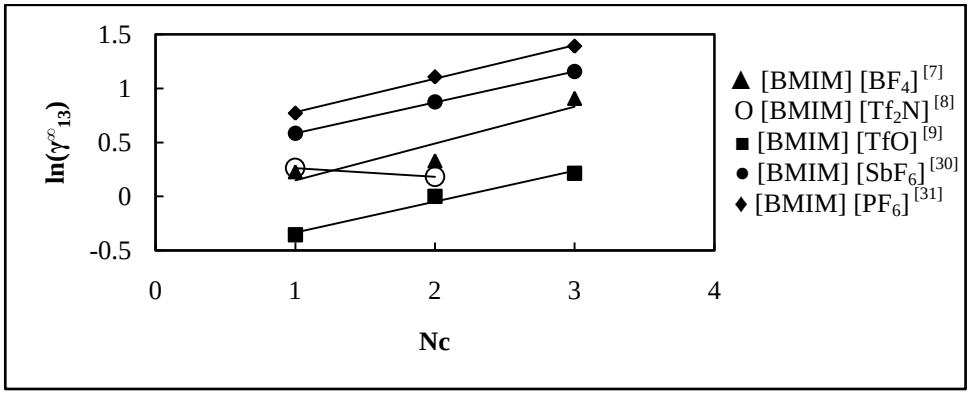

Figure G-56: Plots of $\ln \gamma_{13}^{\infty}$ versus Nc for alkan-1-ols in imidazolium-based FILs comprising $[BMIM]^+$ ion

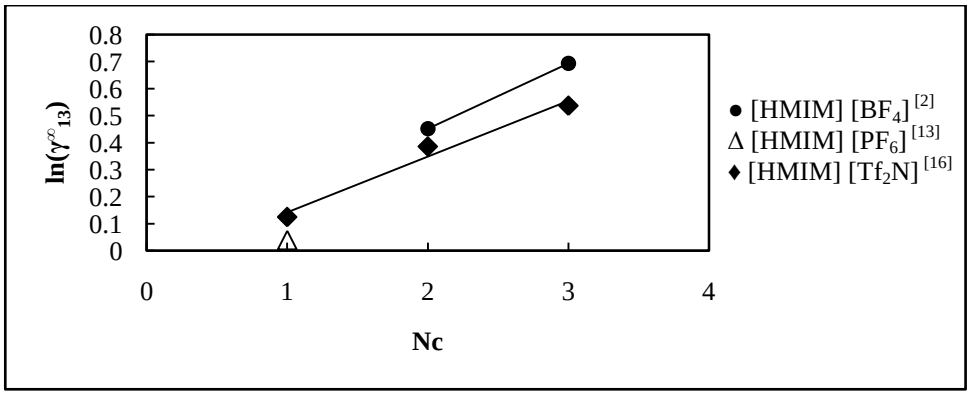

Figure G-57: Plots of $\ln \gamma_{13}^{\infty}$ versus Nc for alkan-1-ols in imidazolium-based FILs comprising $[HMIM]^+$ ion.

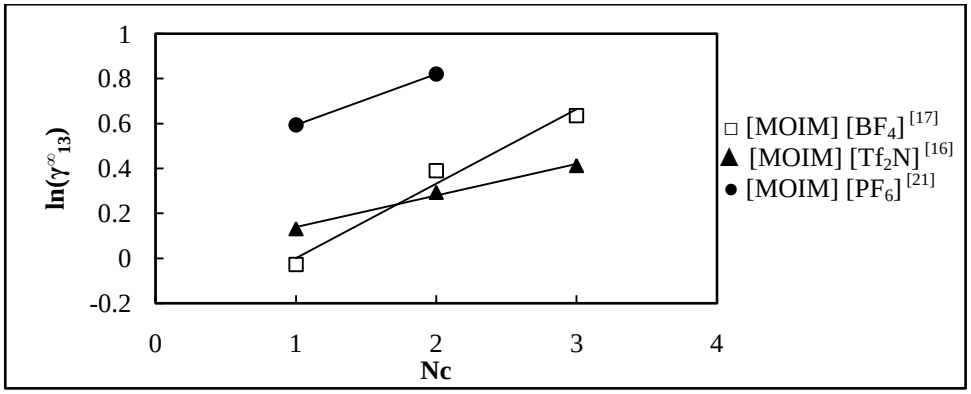

Figure G-58: Plots of $\ln \gamma_{13}^{\infty}$ versus Nc for alkan-1-ols in imidazolium-based FILs comprising $[EMIM]^+$ ion.

5.2. Infinite dilution activity coefficients of alkan-1-ols in phosphonium-based FILs

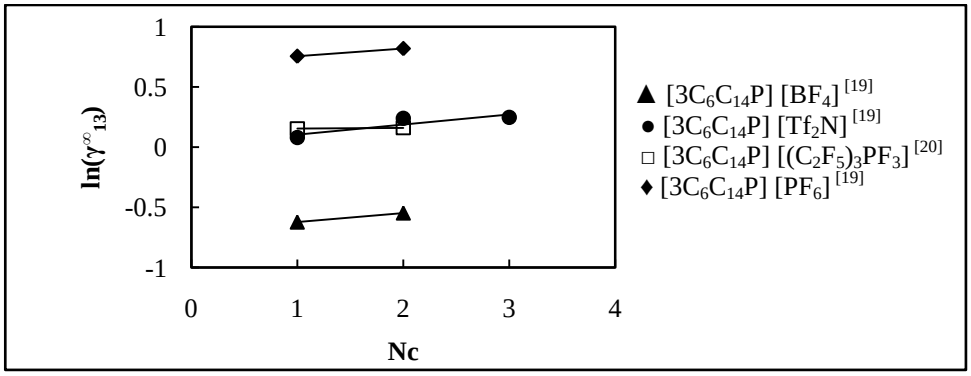

Figure G-59: Plots of $\ln \gamma_{13}^{\infty}$ versus Nc for alkan-1-ols in phosphonium-based FILs comprising $[3C_6C_{14}P]^+$ ion.

5.3. Infinite dilution activity coefficients of alkan-1-ols in ammonium-based FILs

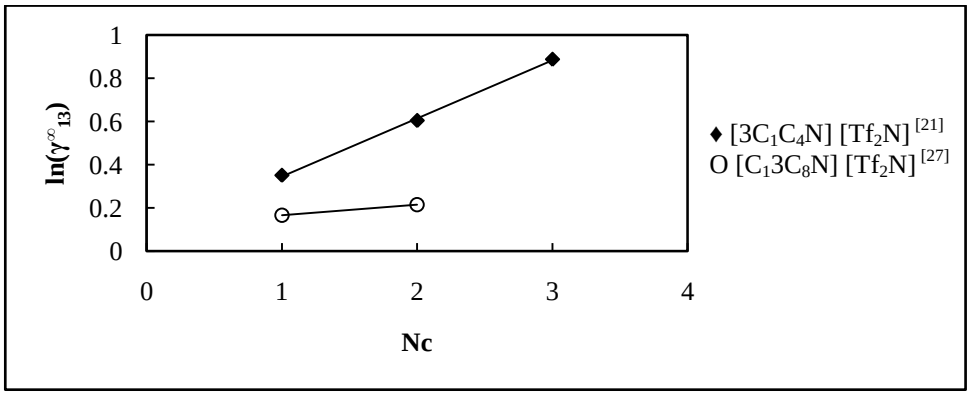

Figure G-60: Plots of $\ln \gamma_{13}^{\infty}$ versus Nc for alkan-1-ols in ammonium-based FILs comprising $[Tf_2N]^-$ ion.

5.4. Infinite dilution activity coefficients of alkan-1-ols in pyridinium-based FILs

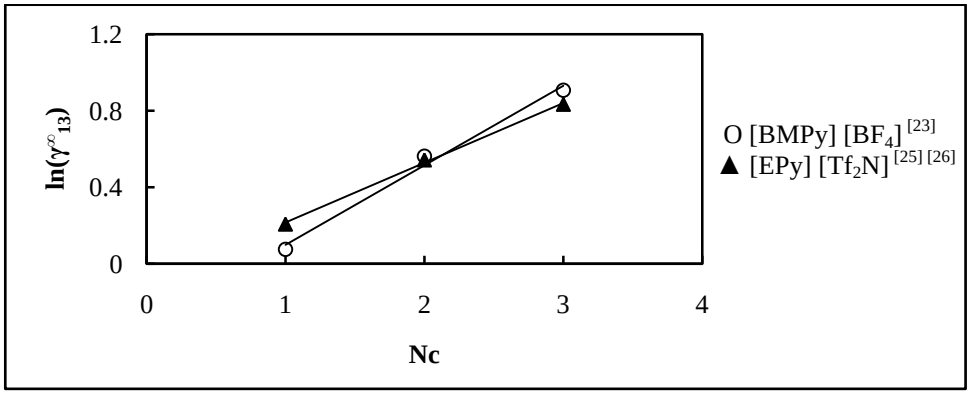

Figure G-61: Plots of $\ln \gamma_{13}^{\infty}$ versus Nc for alkan-1-ols in the pyridinium-based FILs [BMPy] [BF_4] and [Epy] [Tf_2N].

5.5. Infinite dilution activity coefficients of alkan-1-ols in pyrrolidinium-based FILs

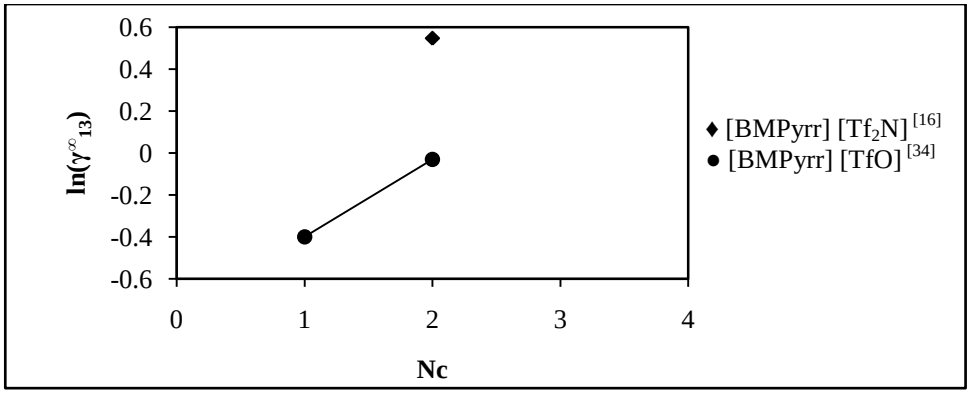

Figure G-62: Plots of $\ln \gamma_{13}^{\infty}$ versus Nc for alkan-1-ols in pyrrolidinium-based FILs comprising $[BMPyrr]^+$ ion.

5.6. Infinite dilution activity coefficients of alkan-1-ols in sulfonium-based FILs

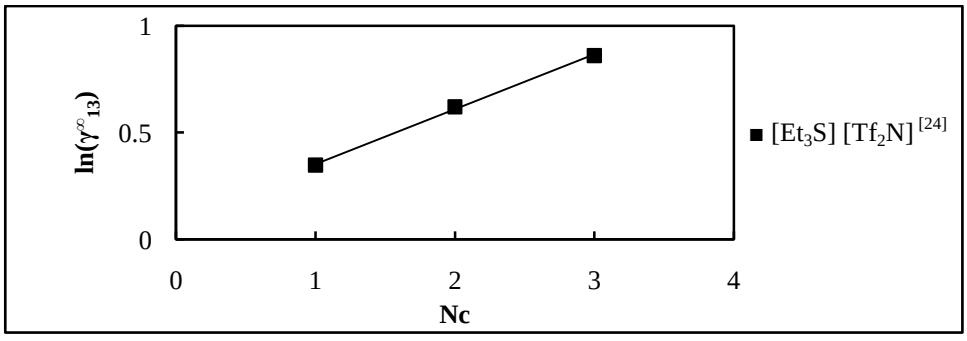

Figure G-63: Plots of $\ln \gamma_{13}^{\infty}$ versus Nc for alkan-1-ols in the sulfonium-based FILs [Et_3S] [Tf_2N].

6. Infinite dilution activity coefficients of alkylbenzenes in fluorinated ionic liquids
6.1. Infinite dilution activity coefficients of alkylbenzenes in imidazolium-based FILs
6.1.1. Effect of the cation

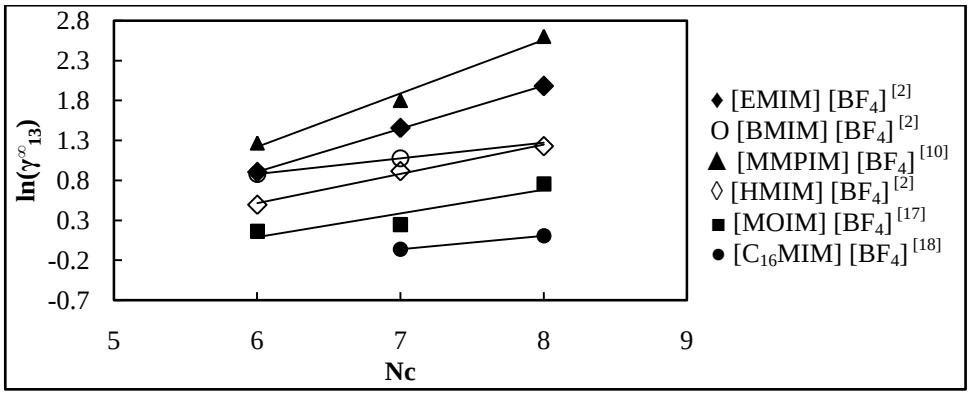

Figure G-64: Plots of $\ln \gamma_{13}^{\infty}$ versus Nc for alkylbenzenes in imidazolium-based FILs comprising $[BF_4]^-$ ion.

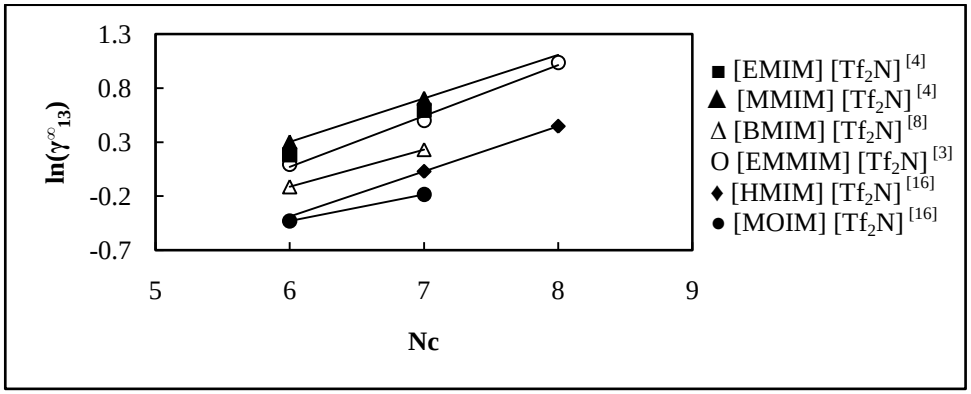

Figure G-65: Plots of $\ln \gamma_{13}^{\infty}$ versus Nc for alkylbenzenes in imidazolium-based FILs comprising $[Tf_2N]^-$ ion.

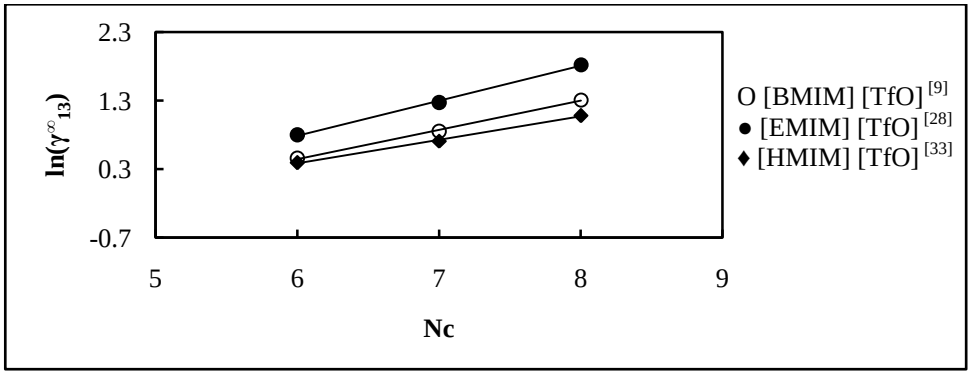

Figure G-66: Plots of $\ln \gamma_{13}^{\infty}$ versus Nc for alkylbenzenes in imidazolium-based FILs comprising $[TfO]^-$ ion.

6.1.2. Effect of the anion

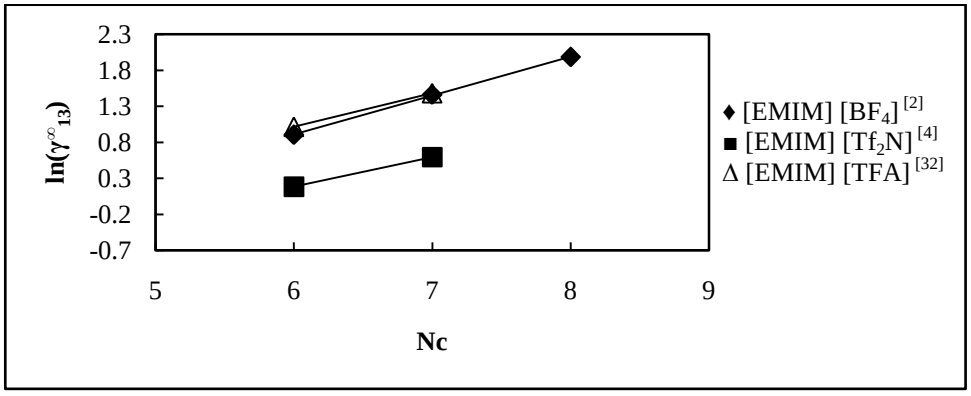

Figure G-67: Plots of $\ln \gamma_{13}^{\infty}$ versus Nc for alkylbenzenes in imidazolium-based FILs comprising $[EMIM]^+$ ion.

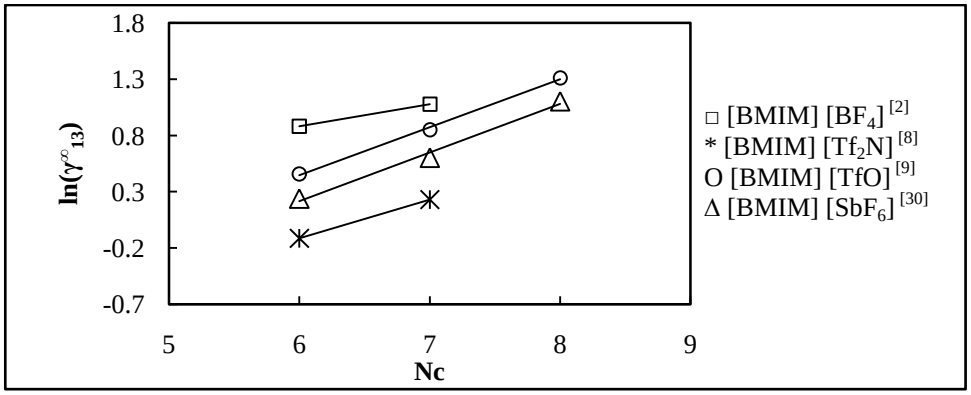

Figure G-68: Plots of $\ln \gamma_{13}^{\infty}$ versus Nc for alkylbenzenes in imidazolium-based FILs comprising $[BMIM]^+$ ion.

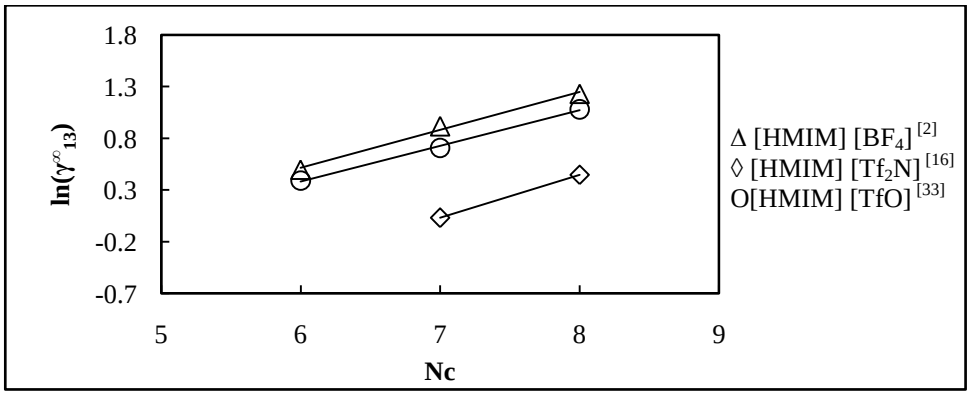

Figure G-69: Plots of $\ln \gamma_{13}^{\infty}$ versus Nc for alkylbenzenes in imidazolium-based FILs comprising $[HMIM]^+$ ion.

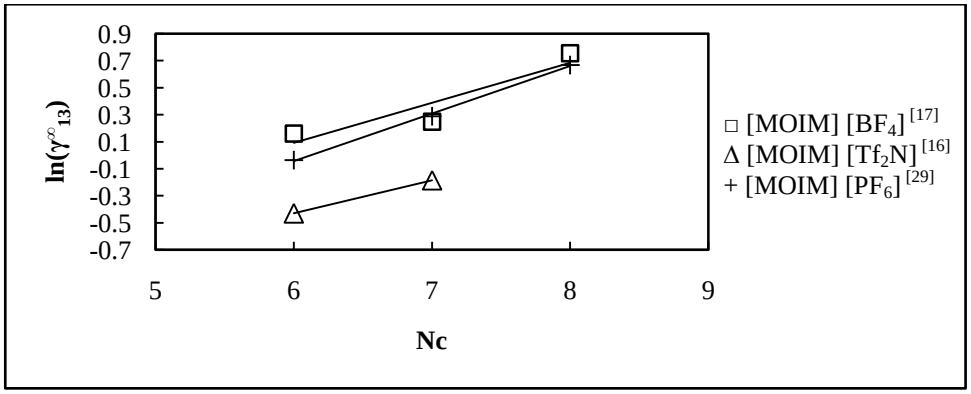

Figure G-70: Plots of $\ln \gamma_{13}^{\infty}$ versus Nc for alkylbenzenes in imidazolium-based FILs comprising $[MOIM]^+$ ion.

6.2. Infinite dilution activity coefficients of alkylbenzenes in phosphonium-based FILs

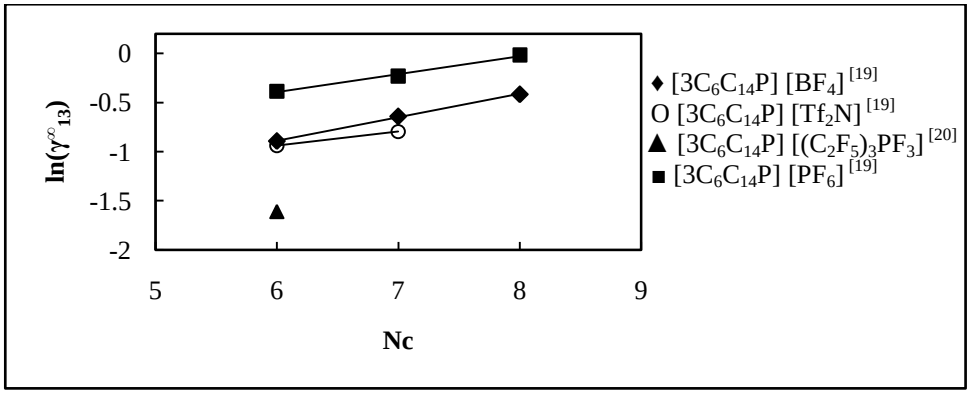

Figure G-71: Plots of $\ln \gamma_{13}^{\infty}$ versus Nc for alkylbenzenes in phosphonium-based FILs comprising $[3C_6C_{14}P]^+$ ion.

6.3. Infinite dilution activity coefficients of alkylbenzenes in ammonium-based FILs

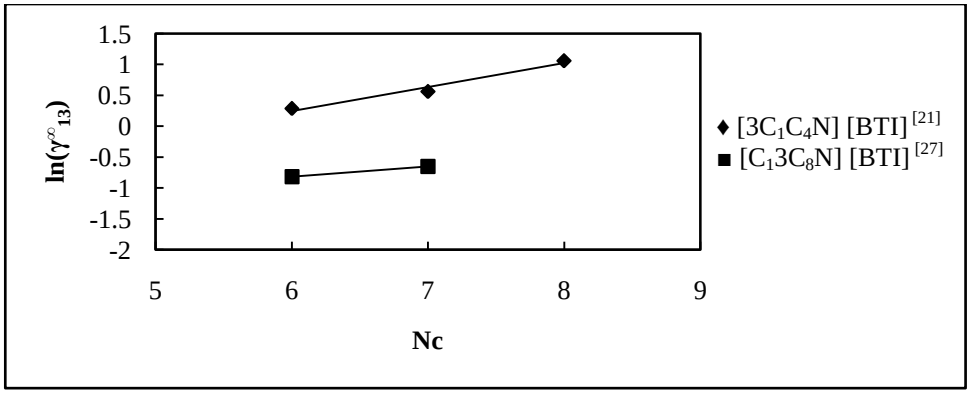

Figure G-72: Plots of $\ln \gamma_{13}^{\infty}$ versus Nc for alkylbenzenes in ammonium-based FILs comprising $[Tf_2N]^-$ ion.

6.4. Infinite dilution activity coefficients of alkylbenzenes in pyridinium-based FILs

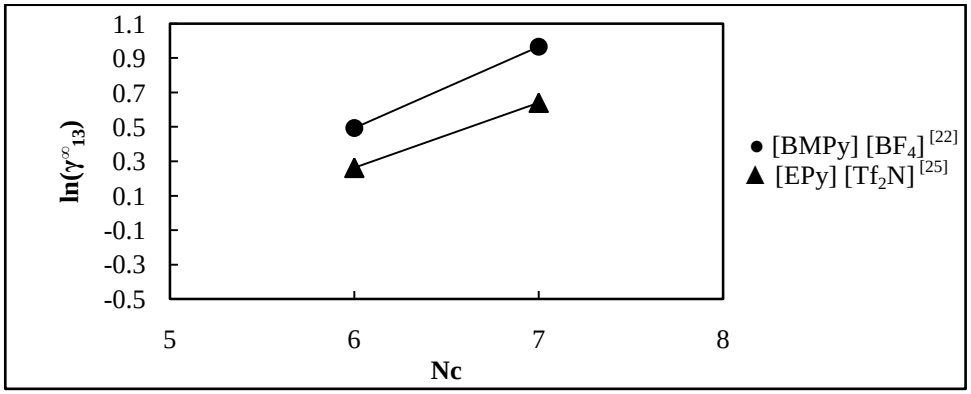

Figure G-73: Plots of $\ln \gamma_{13}^{\infty}$ versus Nc for alkylbenzenes in the pyridinium-based FILs [BMPy] [BF_4] and [Epy] [Tf_2N].

6.5. Infinite dilution activity coefficients of alkylbenzenes in pyrrolidinium and sulfonium-based FILs

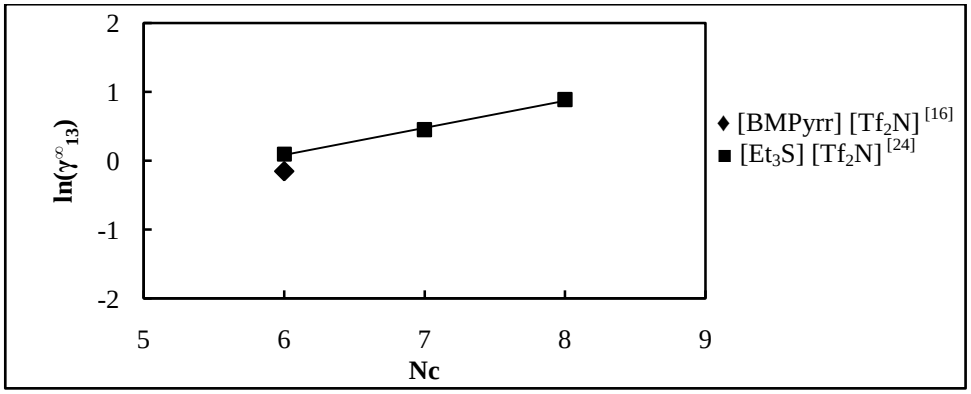

Figure G-74: Plots of $\ln \gamma_{13}^{\infty}$ versus Nc for alkylbenzenes in [BMPyrr] [Tf_2N] and [Et_3S] [Tf_2N].

7. Infinite dilution activity coefficients of ket-2-ones in fluorinated ionic liquids

7.1. Infinite dilution activity coefficients of ket-2-ones in imidazolium-based FILs

7.1.1. Effect of the cation

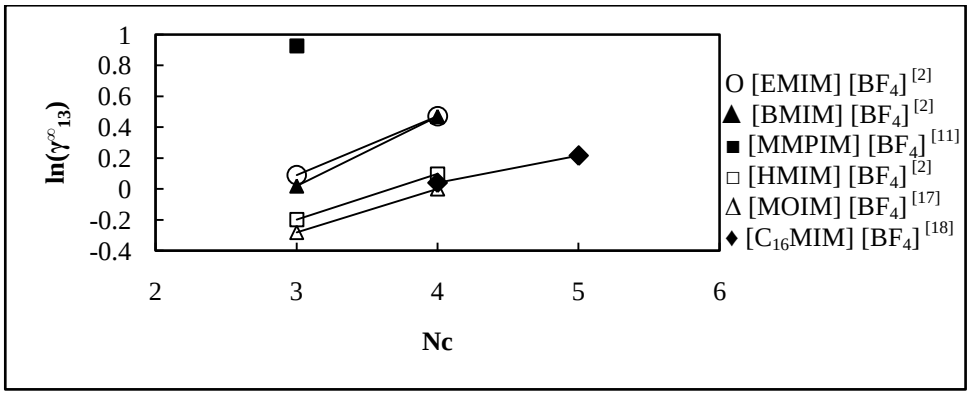

Figure G-75: Plots of $\ln \gamma_{13}^{\infty}$ versus Nc for ket-2-ones in imidazolium-based FILs comprising $[BF_4]^-$ ion.

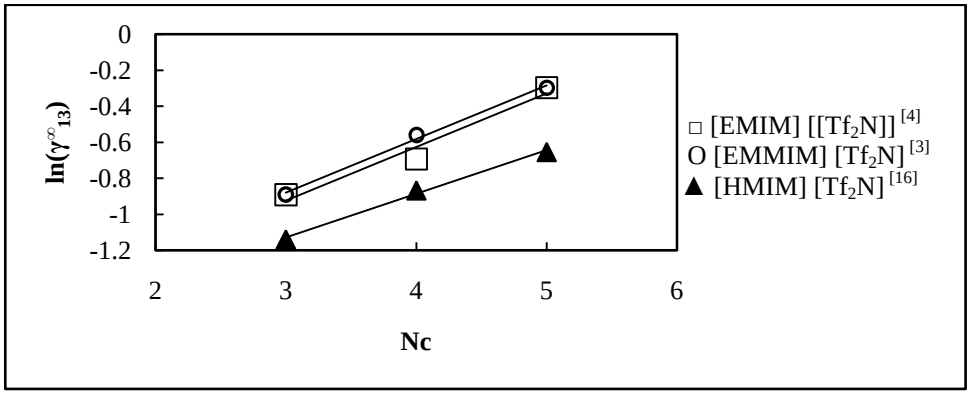

Figure G-76: Plots of $\ln \gamma_{13}^{\infty}$ versus Nc for ket-2-ones in imidazolium-based FILs comprising $[Tf_2N]^-$ ion.

7.1.2. Effect of the anion

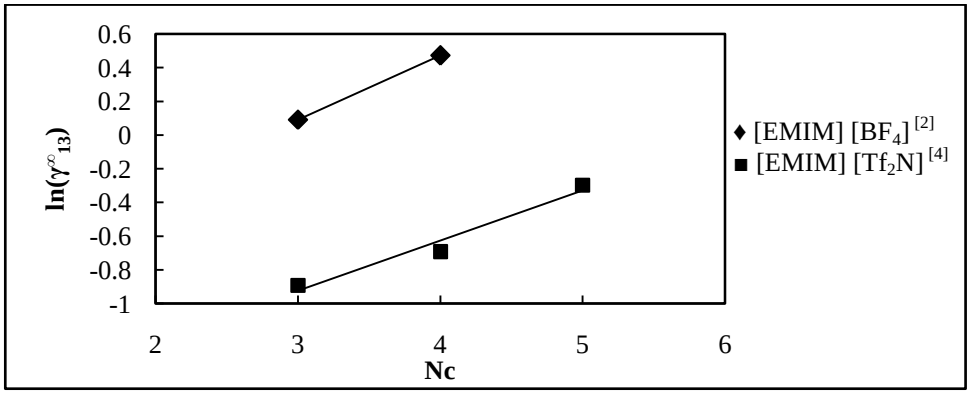

Figure G-77: Plots of $\ln \gamma_{13}^{\infty}$ versus Nc for ket-2-ones in imidazolium-based FILs comprising $[EMIM]^+$ ion.

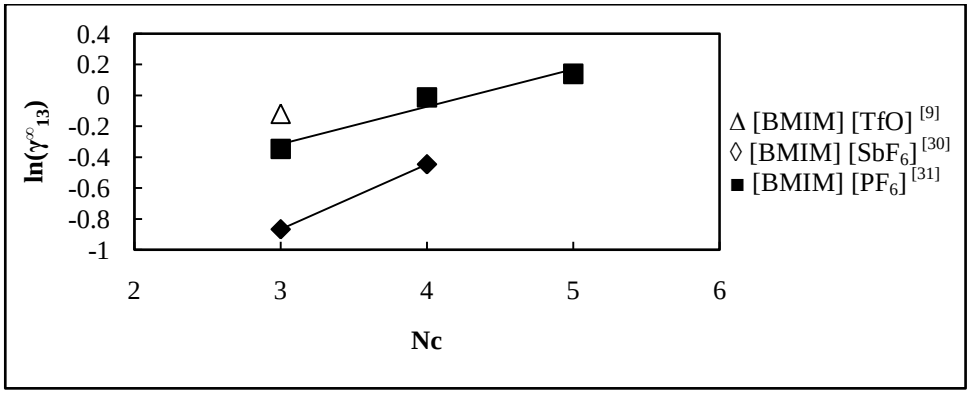

Figure G-78: Plots of $\ln \gamma_{13}^{\infty}$ versus Nc for ket-2-ones in imidazolium-based FILs comprising $[BMIM]^+$ ion.

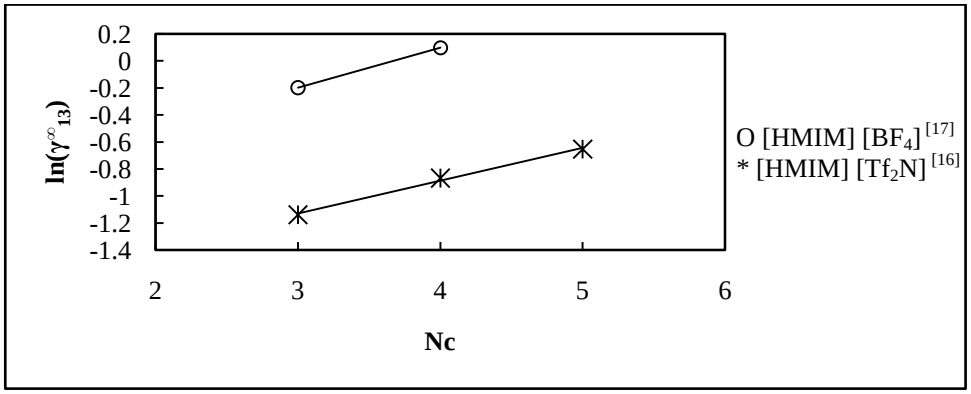

Figure G-79: Plots of $\ln \gamma_{13}^{\infty}$ versus Nc for ket-2-ones in imidazolium-based FILs comprising $[HMIM]^+$ ion.

7.2. Infinite dilution activity coefficients of ket-2-ones in phosphonium-based FILs

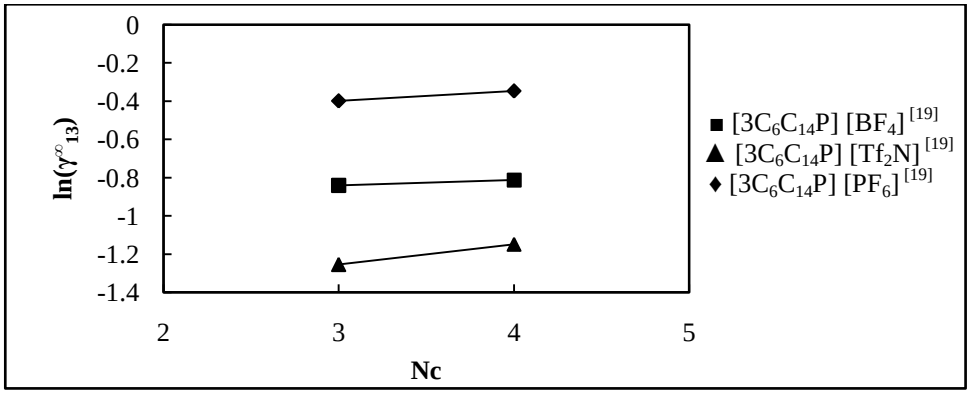

Figure G-80: Plots of $\ln \gamma_{13}^{\infty}$ versus Nc for ket-2-ones in phosphonium-based FILs comprising $[3C_6C_{14}P]^+$ ion.

7.3. Infinite dilution activity coefficients of ket-2-ones in ammonium-based FILs

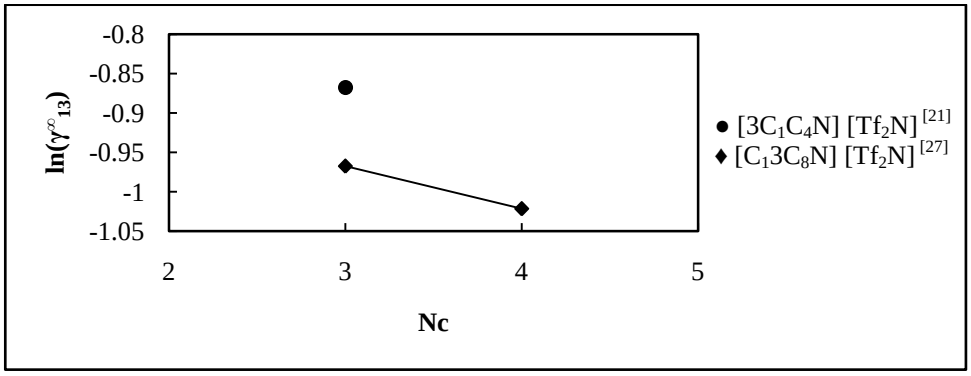

Figure G-81: Plots of $\ln \gamma_{13}^{\infty}$ versus Nc for ket-2-ones in ammonium-based FILs comprising $[Tf_2N]^-$ ion.

7.4. Infinite dilution activity coefficients of ket-2-ones in pyridinium-based FILs

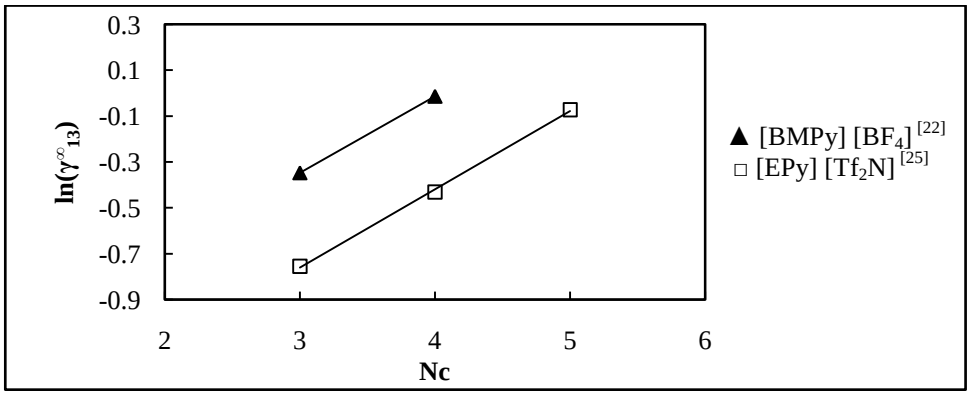

Figure G-82: Plots of $\ln \gamma_{13}^{\infty}$ versus Nc for ket-2-ones in the imidazolium-based FILs [Epy] $[Tf_2N]$ and [BMPy] $[BF_4]$.

7.5. Infinite dilution activity coefficients of ket-2-ones in pyrrolidinium-based FILs

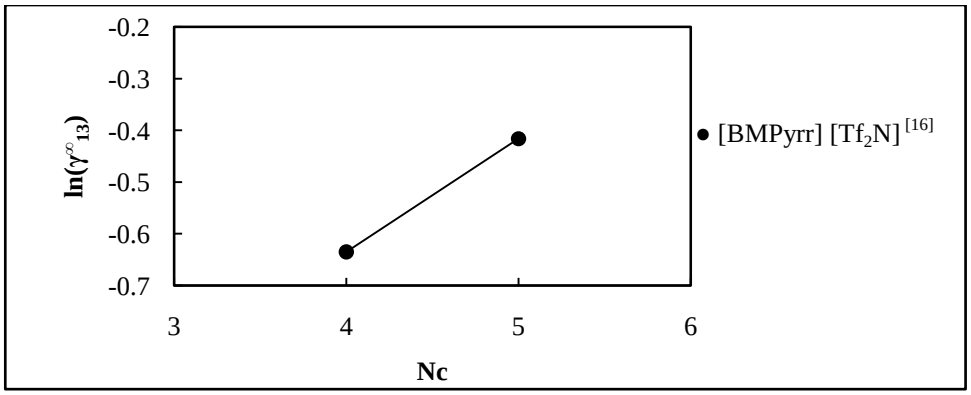

Figure G-83: Plot of $\ln \gamma_{13}^{\infty}$ versus Nc for ket-2-ones in the pyrrolidinium-based FIL [BMPyrr] $[Tf_2N]$.

APPENDIX H: EFFECT OF STRUCTURE ON LIMITING SELECTIVITY AND CAPACITY

1. Benzene/n-hexane separation problem

1.1. Imidazolium-based fluorinated ionic liquids

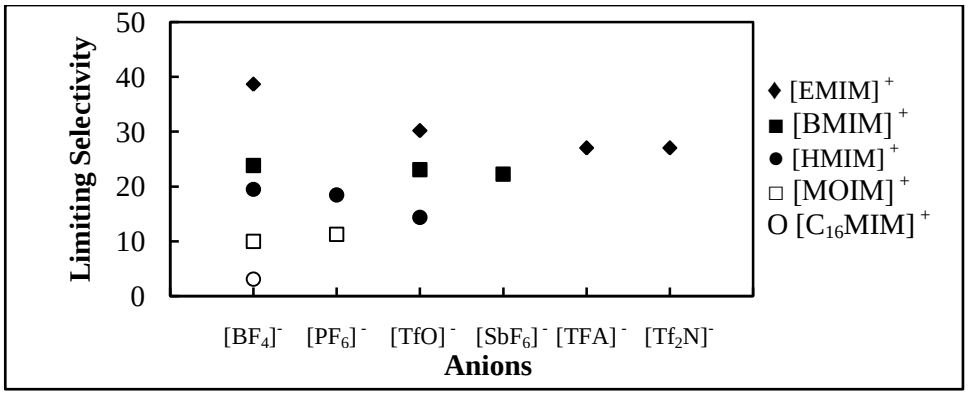

Figure H-1: Limiting selectivity at 313.15 K of imidazolium-based fluorinated ionic liquids for the hexane (1)/benzene (2) system, representing aliphatics/aromatics separation problems. $[EMIM][BF_4]$[1][2];$[EMIM][Tf_2N]$[3][4]; $[BMIM][BF_4]$[2][6] ; $[BMIM][Tf_2N]$[4][8] ; $[BMIM][TfO]$[9] ; $[HMIM][BF_4]$[12][2] ; $[HMIM][PF_6]$[13] ; $[HMIM][Tf_2N]$[14][16] ; $[MOIM][BF_4]$ [17] ; $[MOIM][Tf_2N]$[16] ; $[C_{16}MIM][BF_4]$[18] ; $[EMIM][TfO]$[28]; $[MOIM][PF_6]$[29]; $[BMIM][SbF_6]$[30] ; $[BMIM][PF_6]$[31] ; $[EMIM][TFA]$[32] ; $[HMIM][TfO]$[33].

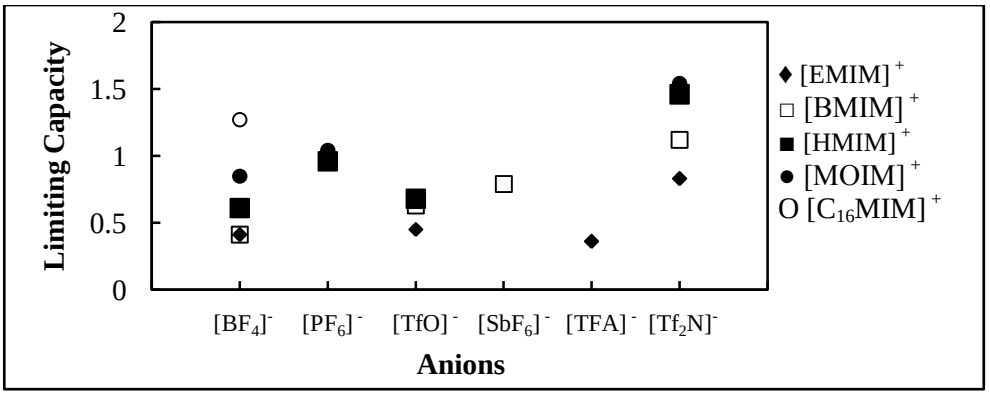

Figure H-2: Limiting capacity at 313.15 K of imidazolium-based fluorinated ionic liquids for the hexane (1)/benzene (2) system, representing aliphatics/aromatics separation problems. $[EMIM][BF_4]$[2];$[EMIM][Tf_2N]$[4]; $[BMIM][BF_4]$[6] ; $[BMIM][Tf_2N]$[8] ; $[BMIM][TfO]$[9] ; $[HMIM][BF_4]$[2] ; $[HMIM][PF_6]$[13] ; $[HMIM][Tf_2N]$[16] ; $[MOIM][BF_4]$ [17] ; $[MOIM][Tf_2N]$[16] ; $[C_{16}MIM][BF_4]$[18] ; $[EMIM][TfO]$[28]; $[MOIM][PF_6]$[29]; $[BMIM][SbF_6]$[30] ; $[BMIM][PF_6]$[31] ; $[EMIM][TFA]$[32] ; $[HMIM][TfO]$[33].

1.2. Phosphonium-based fluorinated ionic liquids

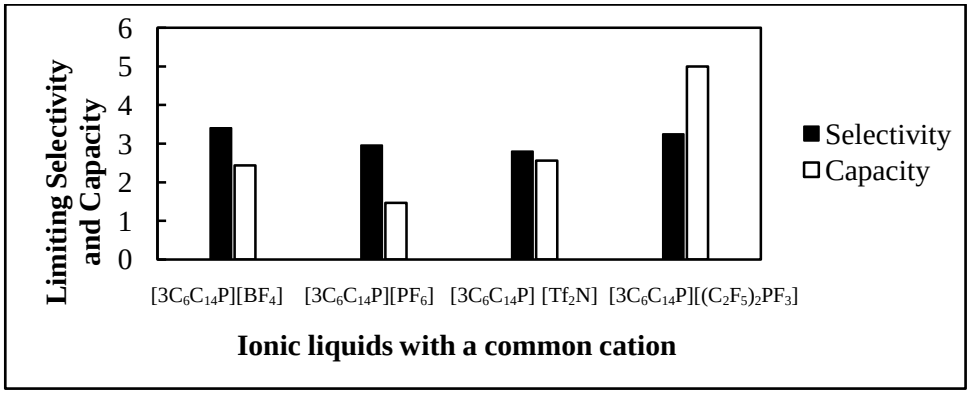

Figure H-3: Limiting selectivity and capacity at 313.15 K of phosphonium-based fluorinated ionic liquids for the hexane (1)/benzene (2) system, representing aliphatics/aromatics separation problems. References: $[3C_6C_{14}P]$ $[BF_4]$ [19]; $[3C_6C_{14}P]$ $[Tf_2N]$ [19]; $[3C_6C_{14}P]$ $[(C_2F_5)_3PF_3]$ [20]; $[3C_6C_{14}P]$ $[PF_6]$ [19].

1.3. Ammonium-based Fluorinated ionic liquids

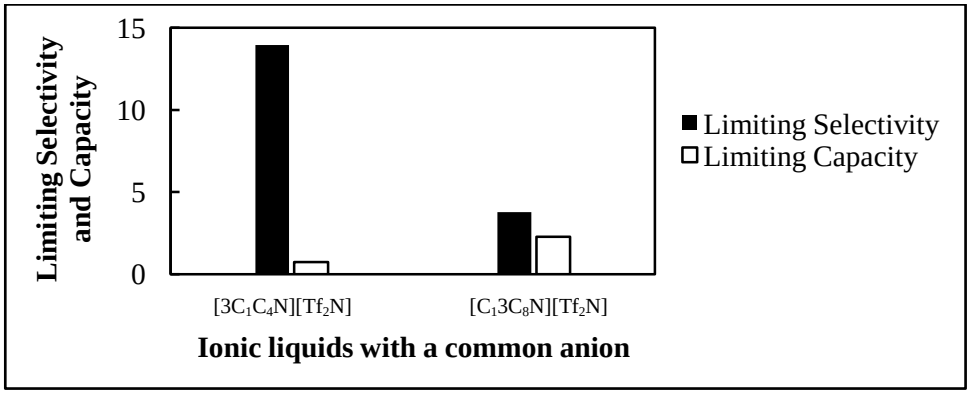

Figure H-4: Limiting selectivity and capacity at 313.15 K of ammonium-based fluorinated ionic liquids for the hexane (1)/benzene (2) system, representing aliphatics/aromatics separation problems. References: $[3C_1C_4N]$ $[Tf_2N]$ [21]; $[C_13C_8N]$ $[Tf_2N]$ [27].

2. Methanol/benzene separation problem

2.1. Imidazolium-based fluorinated ionic liquids

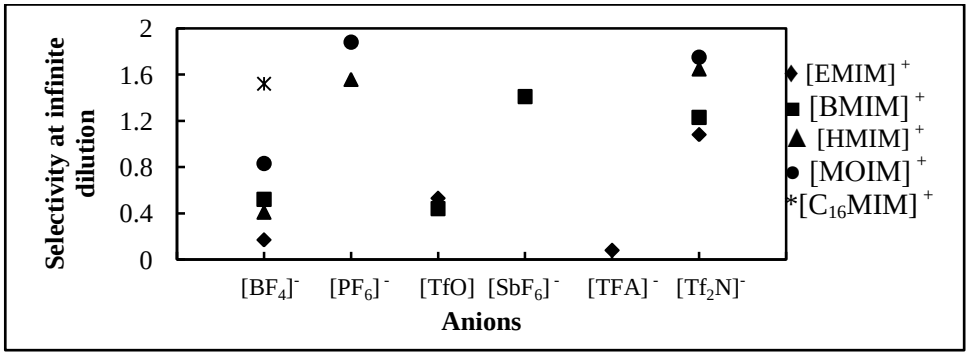

Figure H-5: Limiting selectivity at 313.15 K of imidazolium-based fluorinated ionic liquids for the methanol (1)/benzene (2) system, representing alcohols/aromatics separation problems. References: [EMIM][BF_4][2];[EMIM] [Tf_2N] [4]; [BMIM][BF_4][6][7]; [BMIM] [Tf_2N] [8] ; [BMIM][TfO] [9] ; [HMIM][BF_4] [12] ; [HMIM][PF_6] [13] ; [HMIM] [Tf_2N] [16]; [MOIM][BF_4] [17] ; [MOIM] [Tf_2N] [16] ; [C_{16}MIM][BF_4] [18]; [EMIM][TfO] [28]; [MOIM][PF_6] [29]; [BMIM][SbF_6] [30] ;[EMIM][TFA] [32].

2.2. Phosphonium-based fluorinated ionic liquids

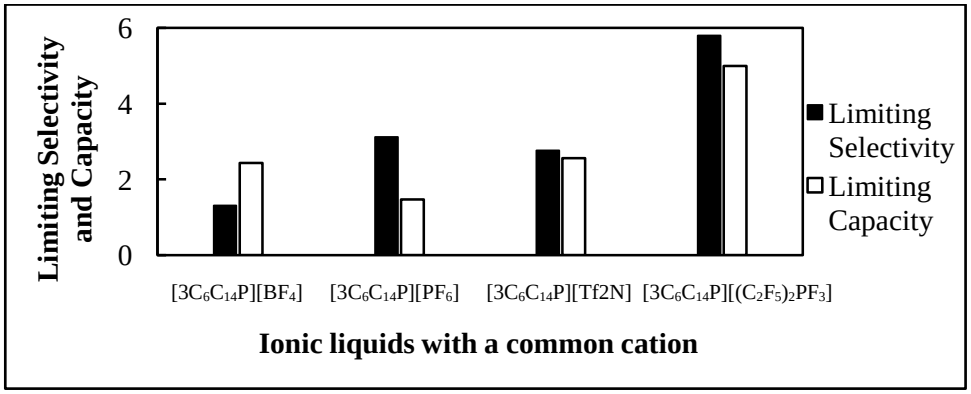

Figure H-6: Limiting selectivity and capacity at 313.15 K of phosphonium-based fluorinated ionic liquids for methanol (1)/benzene (2) system, representing alcohols/aromatics separation problems. References: $3C_6C_{14}P$] [BF_4] [19]; [$3C_6C_{14}P$] [Tf_2N] [19]; [$3C_6C_{14}P$] [$(C_2F_5)_3PF_3$] [20]; [$3C_6C_{14}P$] [PF_6] [19].

2.3. Ammonium-based fluorinated ionic liquids

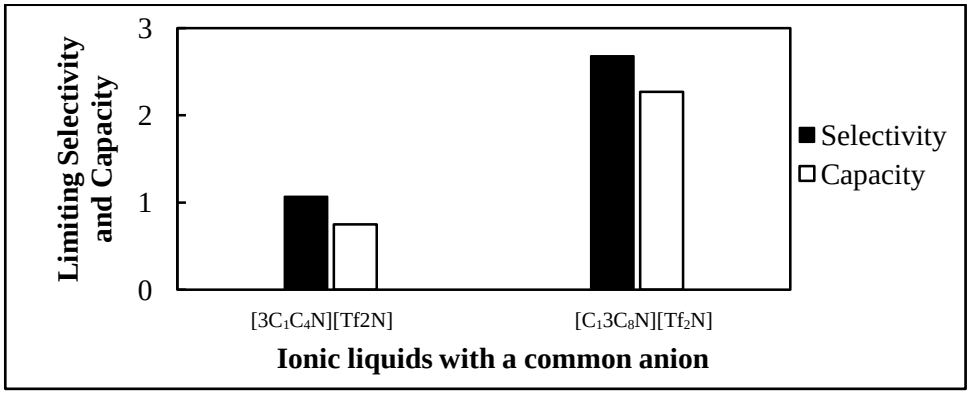

Figure H-7: Limiting selectivity and capacity at 313.15 K of ammonium-based fluorinated ionic liquids for methanol (1)/benzene (2) system, representing alcohols/aromatics separation problems. References: $[3C_1C_4N]$ $[Tf_2N]$ [21]; $[C_13C_8N]$ $[Tf_2N]$ [27].

3. Methanol/acetone separation problem

3.1. Imidazolium-based fluorinated ionic liquids

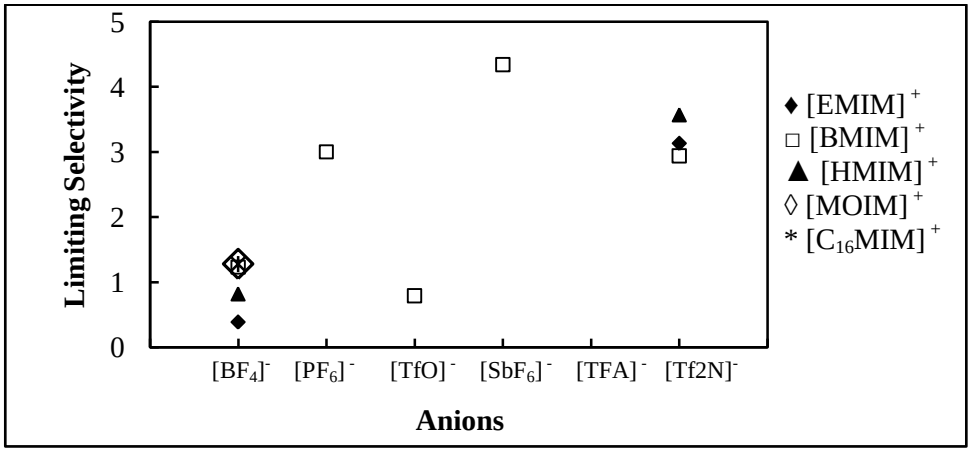

Figure H-8: Limiting selectivity at 313.15 K of imidazolium-based fluorinated ionic liquids for methanol (1)/acetone (2) system, representing alcohols/ketones separation problems. References: $[EMIM][BF_4]$ [2];$[EMIM]$ $[Tf_2N]$ [4]; $[BMIM][BF_4]$ [7] [2] ; [BMIM] $[Tf_2N]$ [8] ; [BMIM][TfO] [9] ; $[HMIM][BF_4]$ [2] ; [HMIM] $[Tf_2N]$ [16]; $[MOIM][BF_4]$ [17] ; $[C_{16}MIM][BF_4]$ [18] ; $[BMIM][SbF_6]$ [30] ; $[BMIM][PF_6]$ [31] .

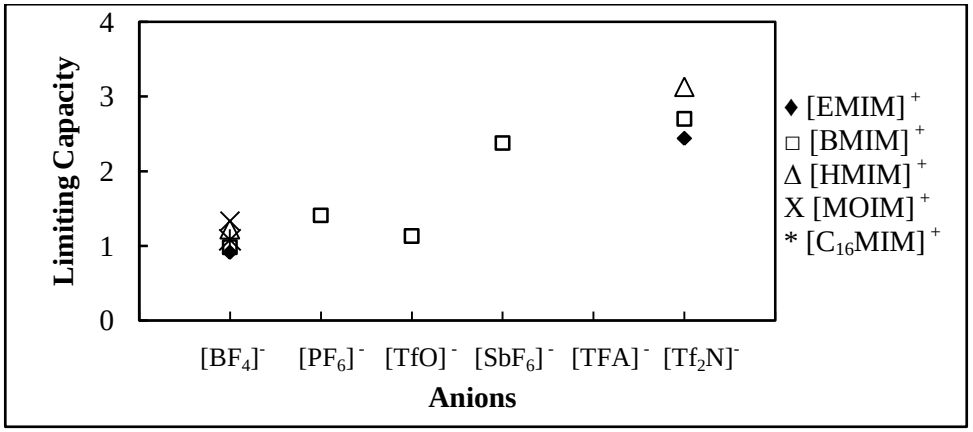

Figure H-9: Limiting capacity at 313.15 K of imidazolium-based fluorinated ionic liquids for methanol (1)/acetone (2) system, representing alcohols/ketones separation problems. References: [EMIM][BF_4][2];[EMIM] [Tf_2N] [4]; [BMIM][BF_4][2] ; [BMIM] [Tf_2N] [8] ; [BMIM][TfO] [9] ; [HMIM][BF_4][2] ; [HMIM] [Tf_2N] [16]; [MOIM][BF_4][17] ; [C_{16}MIM][BF_4] [18] ; [BMIM][SbF_6] [30] ; [BMIM][PF_6] [31].

3.2. Phosphonium-based fluorinated ionic liquids

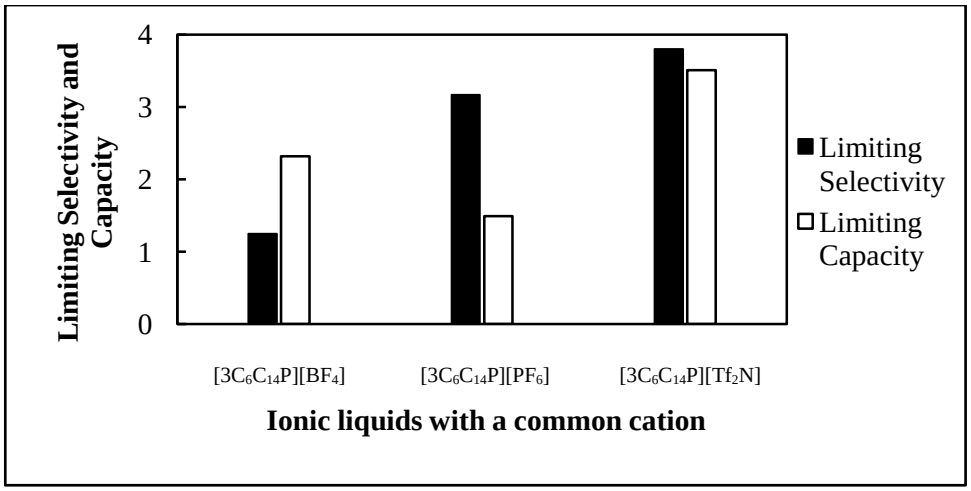

Figure H-10: Limiting selectivity and capacity at 313.15 K of phosphonium-based fluorinated ionic liquids for methanol (1)/acetone (2) system, representing alcohols/ketones separation problems. References: $3C_6C_{14}P$] [BF_4] [19]; [$3C_6C_{14}P$] [Tf_2N] [19]; [$3C_6C_{14}P$] [$(C_2F_5)_3PF_3$] [20]; [$3C_6C_{14}P$] [PF_6] [19].

3.3. Ammonium-based fluorinated ionic liquids

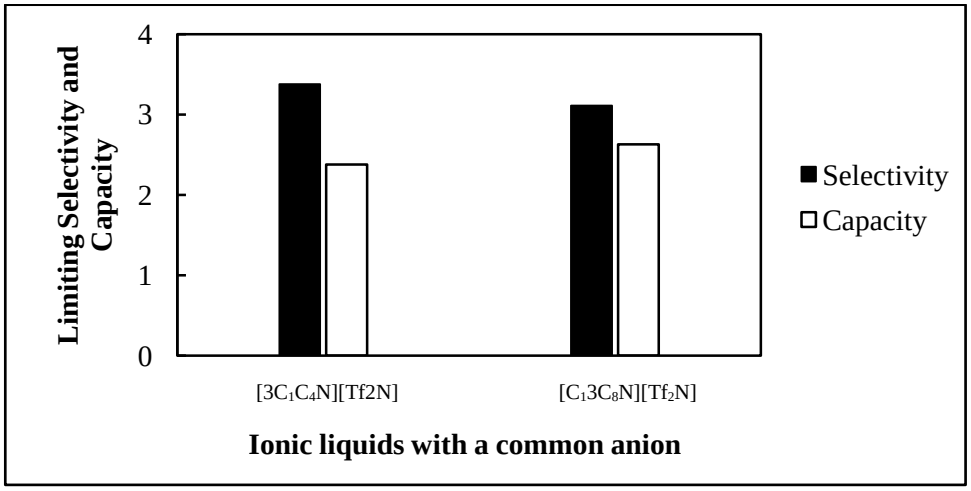

Figure H-11: Limiting selectivity and capacity at 313.15 K of ammonium-based fluorinated ionic liquids for methanol (1)/acetone (2) system, representing alcohols/ketones separation problems. References: [$3C_1C_4N$] [Tf_2N] [21]; [C_13C_8N] [Tf_2N] [27].

4. n-hexane/hex-1-ene separation problem

4.1. Imidazolium-based fluorinated ionic liquids

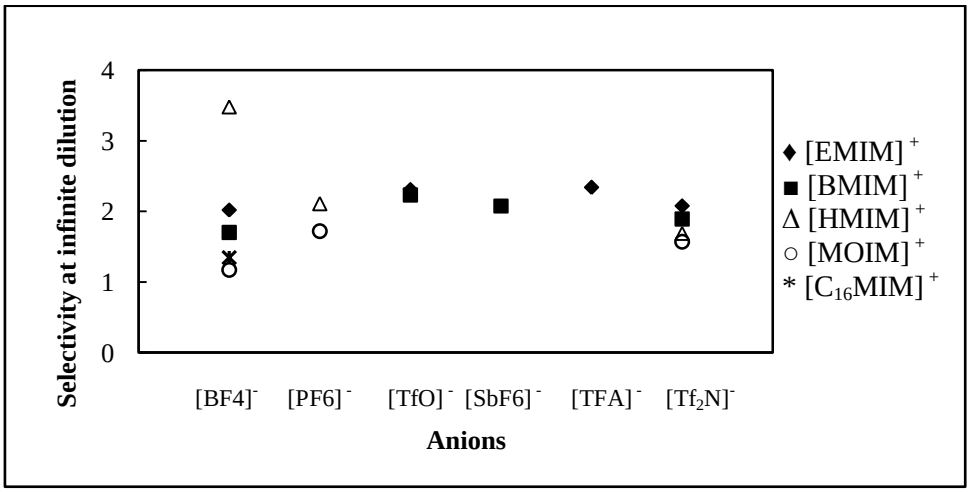

Figure H-12: Limiting selectivity at 313.15 K of imidazolium-based fluorinated ionic liquids for the n-hexane (1)/hex-1-ene (2) system, representing paraffins/olefins separation problems. References: [$EMIM][BF_4$][1][2];[EMIM] [Tf_2N] [3][5]; [$BMIM][BF_4$] [6] [2] ; [BMIM] [Tf_2N] [4]; [BMIM][TfO] [9] ; [$HMIM][BF_4$] [12] ; [$HMIM][PF_6$] [13] ; [HMIM] [Tf_2N] [14] ; [$MOIM][BF_4$] [17] ; [MOIM] [Tf_2N] [16] ; [$C_{16}MIM][BF_4$] [18] ; [EMIM][TfO] [28]; [$MOIM][PF_6$] [29]; [$BMIM][SbF_6$] [30] ; [EMIM][TFA] [32].

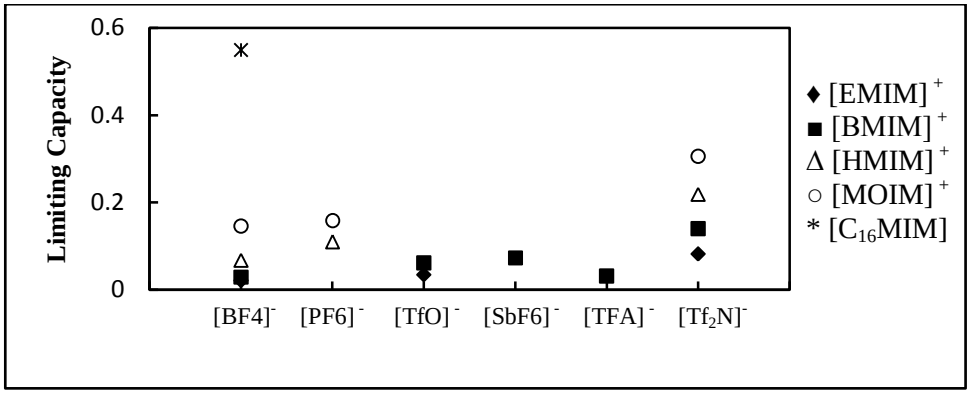

Figure H-13: Limiting capacity at 313.15 K of imidazolium-based fluorinated ionic liquids for the n-hexane (1)/hex-1-ene (2) system, representing paraffins/olefins separation problems. References: $[EMIM][BF_4]$[2];$[EMIM]\ [Tf_2N]$ [5]; $[BMIM][BF_4]$[2] ; $[BMIM]\ [Tf_2N]$ [4] ; $[BMIM][TfO]$ [9] ; $[HMIM][BF_4]$ [12] ; $[HMIM][PF_6]$ [13] ; $[HMIM]\ [Tf_2N]$ [14] ; $[MOIM][BF_4]$ [17] ; $[MOIM]\ [Tf_2N]$ [16] ; $[C_{16}MIM][BF_4]$ [18] ; $[EMIM][TfO]$ [28]; $[MOIM][PF_6]$ [29]; $[BMIM][SbF_6]$ [30] ; $[EMIM][TFA]$ [32].

4.2. Phosphonium-based fluorinated ionic liquids

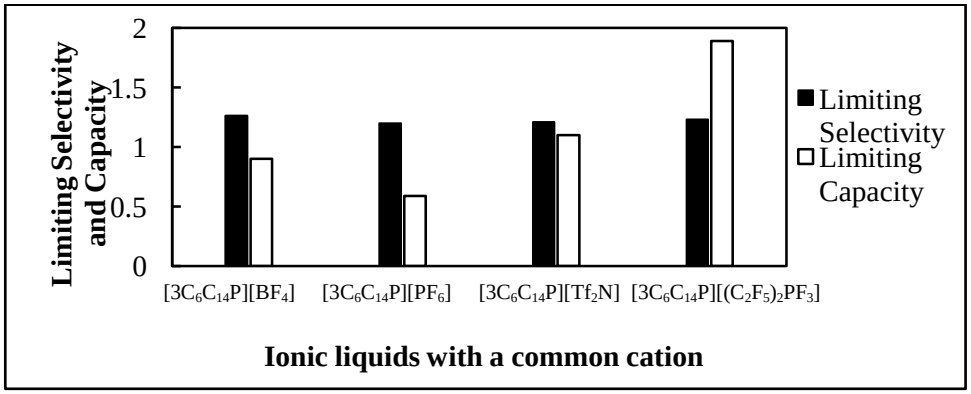

Figure H-14: Limiting selectivity and capacity at 313.15 K of phosphonium-based fluorinated ionic liquids for the n-hexane (1)/hex-1-ene (2) system, representing paraffins/olefins separation problems. References: $3C_6C_{14}P]\ [BF_4]$ [19]; $[3C_6C_{14}P]\ [Tf_2N]$ [19]; $[3C_6C_{14}P]\ [(C_2F_5)_3PF_3]$ [20]; $[3C_6C_{14}P]\ [PF_6]$ [19].

4.3. Ammonium-based fluorinated ionic liquids

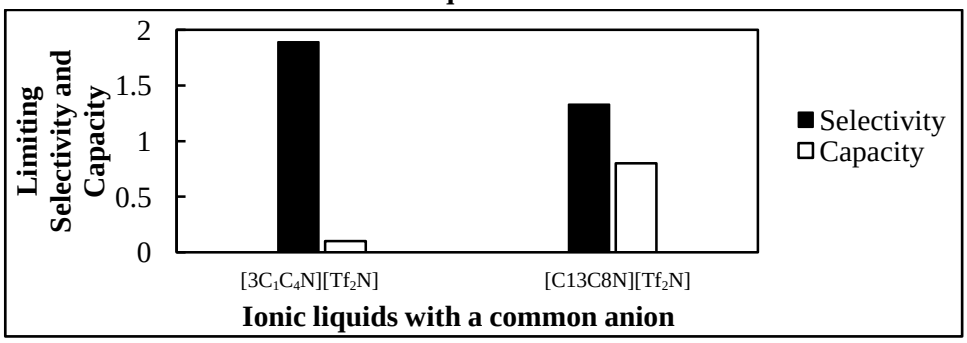

Figure H-15: Limiting selectivity and capacity at 313.15 K of ammonium-based fluorinated ionic liquids for the n-hexane (1)/hex-1-ene (2) system, representing paraffins/olefins separation problems. References: $[3C_1C_4N]\ [Tf_2N]$ [21]; $[C_13C_8N]\ [Tf_2N]$ [27].

4.4. Pyrrolidinium-based fluorinated ionic liquids

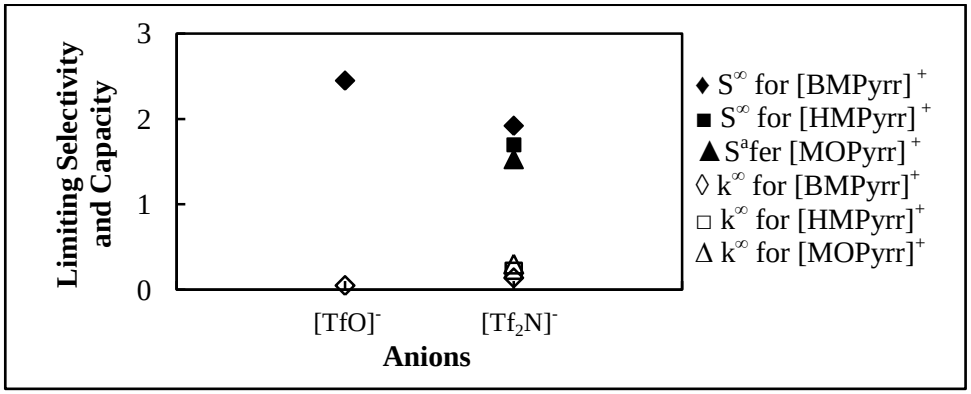

Figure H-16: Limiting selectivity and capacity at 313.15 K of imidazolium-based fluorinated ionic liquids for the n-hexane (1)/hex-1-ene (2) system, representing paraffins/olefins separation problems. References: [BMPyrr] [TfO] [34]; [HMPyrr] [Tf_2N] [35]; [MOPyrr] [Tf_2N] [35].

5. Benzene/butan-2-one separation problem

5.1 Imidazolium-based fluorinated ionic liquids

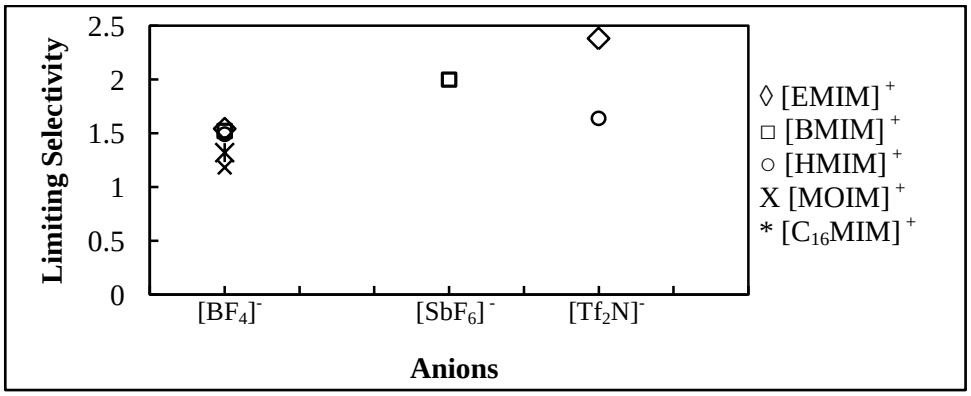

Figure H-17: Limiting selectivity at 313.15 K of imidazolium-based fluorinated ionic liquids for the benzene (1)/butan-2-one (2) system, representing ketones/aromatics separation problems. References: [EMIM][BF_4][2];[EMIM] [Tf_2N] [4]; [BMIM][BF_4] [2]; [HMIM][BF_4][2] ; [HMIM] [Tf_2N] [16] ; [MOIM][BF_4] [17]; [C_{16}MIM][BF_4] [18] ; [BMIM][SbF_6] [30].

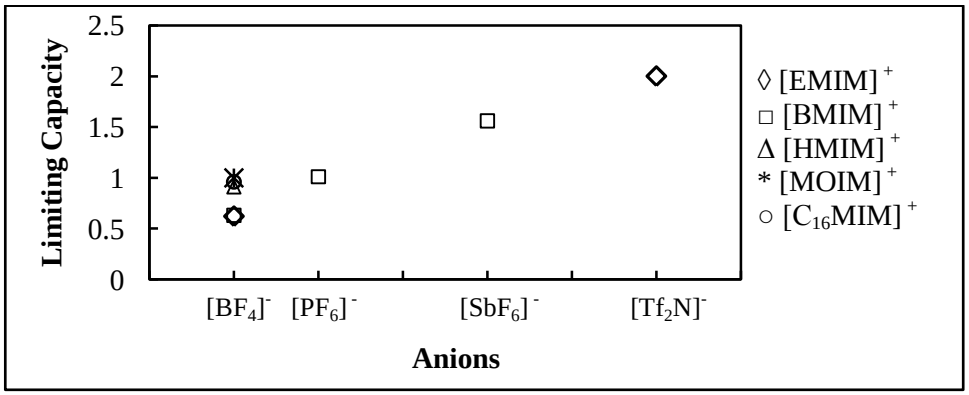

Figure H-18: Limiting capacity at 313.15 K of imidazolium-based fluorinated ionic liquids for the benzene (1)/butan-2-one (2) system, representing ketones/aromatics separation problems. References: [EMIM][BF_4][2];[EMIM] [Tf_2N] [4]; [BMIM][BF_4] [2]; [HMIM][BF_4][2] ; [HMIM] [Tf_2N] [16] ; [MOIM][BF_4] [17]; [C_{16}MIM][BF_4] [18] ; [BMIM][SbF_6] [30].

5.2 Phosphonium-based fluorinated ionic liquids

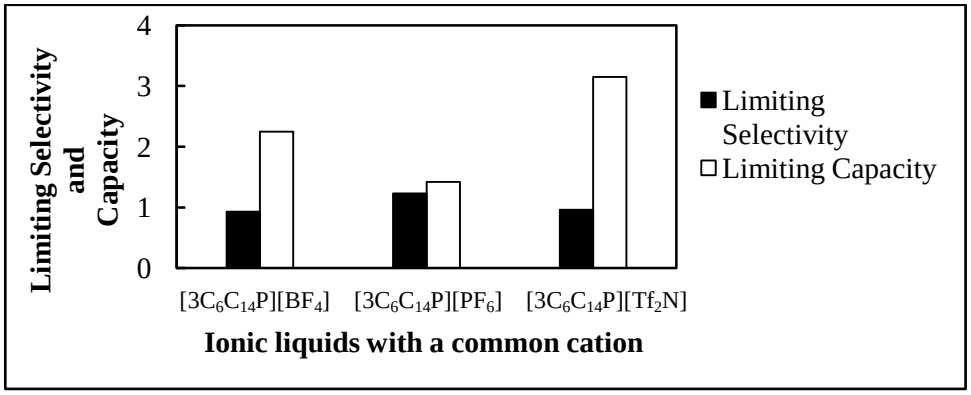

Figure H-19: Limiting selectivity and capacity at 313.15 K of phosphonium-based fluorinated ionic liquids for the benzene (1)/butan-2-one (2) system, representing ketones/aromatics separation problems. References: $3C_6C_{14}P]$ $[BF_4]$ [19]; $[3C_6C_{14}P]$ $[Tf_2N]$ [19]; $[3C_6C_{14}P]$ $[(C_2F_5)_3PF_3]$ [20]; $[3C_6C_{14}P]$ $[PF_6]$ [19].

6. Ethanol/butan-2-one separation problem
6.1 Imidazolium-based fluorinated ionic liquids

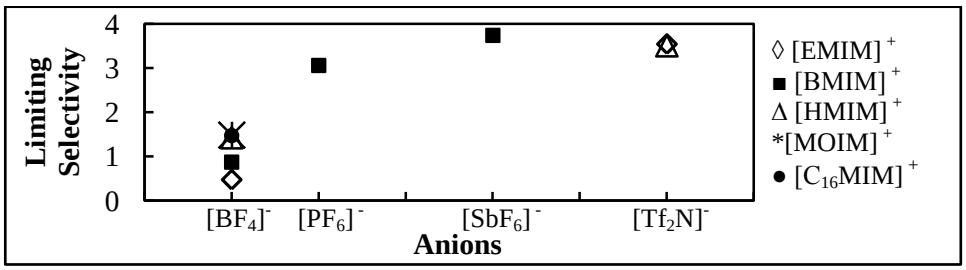

Figure H-20: Limiting selectivity at 313.15 K of imidazolium-based fluorinated ionic liquids for the ethanol (1)/ butan-2-one (2) system, representing alcohols/ketones separation problems. References: $[EMIM][BF_4]$[2];$[EMIM]$ $[Tf_2N]$ [4]; $[BMIM][BF_4]$[7][2]; $[HMIM][BF_4]$[2] ; $[HMIM]$ $[Tf_2N]$ [16] ; $[MOIM][BF_4]$ [17]; $[C_{16}MIM][BF_4]$ [18] ; $[BMIM][SbF_6]$ [30] ; $[BMIM][PF_6]$ [31].

6.2 Phosphonium-based fluorinated ionic liquids

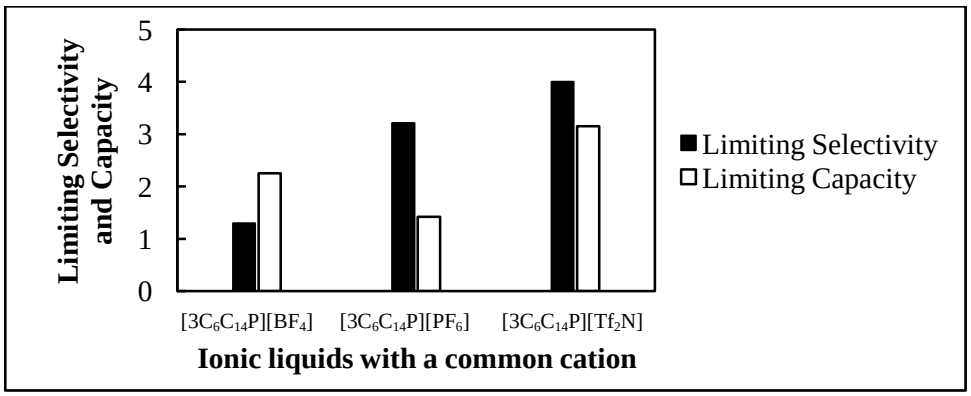

Figure H-21: Limiting selectivity and capacity at 313.15 K of phosphonium-based fluorinated ionic liquids for the ethanol (1)/ butan-2-one (2) system, representing alcohols/ketones separation problems. References: $3C_6C_{14}P]$ $[BF_4]$ [19]; $[3C_6C_{14}P]$ $[Tf_2N]$ [19]; $[3C_6C_{14}P]$ $[(C_2F_5)_3PF_3]$ [20]; $[3C_6C_{14}P]$ $[PF_6]$ [19].

APPENDIX I: CORRELATION OF INFINITE DILUTION ACTIVITY COEFFICIENT, SELECTIVITY AND CAPACITY

1. Infinite dilution activity coefficient correlation with the ionic liquid alkyl chain length

1.1. Imidazolium-based fluorinated ionic liquids

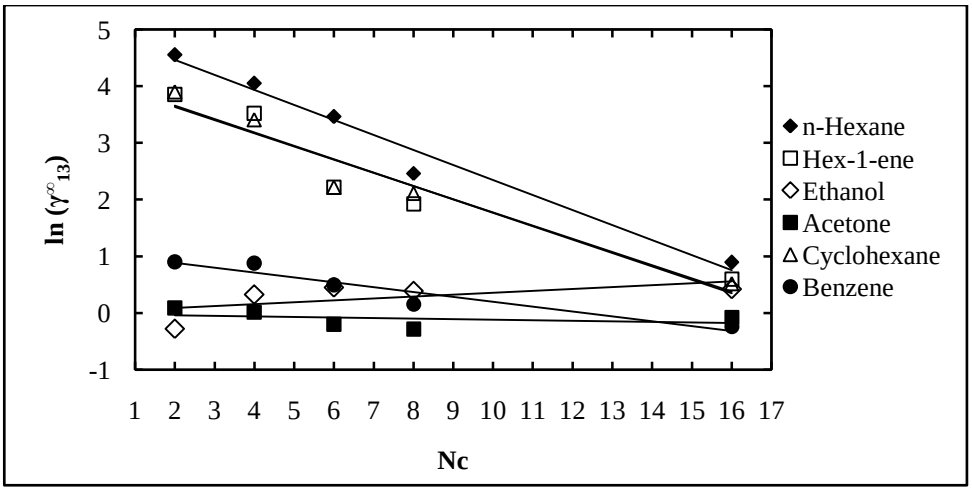

Figure I-1: Variation of limiting activity coefficients of various solutes depending on Nc, the carbon number of the alkyl chain attached to the methylimidazolium group with $[BF_4]^-$ anion. Nc values corresponding to data points are: 2 for [EMIM] $[BF_4]$[1][2], 4 for [BMIM] $[BF_4]$[2][6][7], 6 for [HMIM] $[BF_4]$[2][12], 8 for [MOIM] $[BF_4]$[17] and 16 for $[C_{16}MIM]$ $[BF_4]$[18].

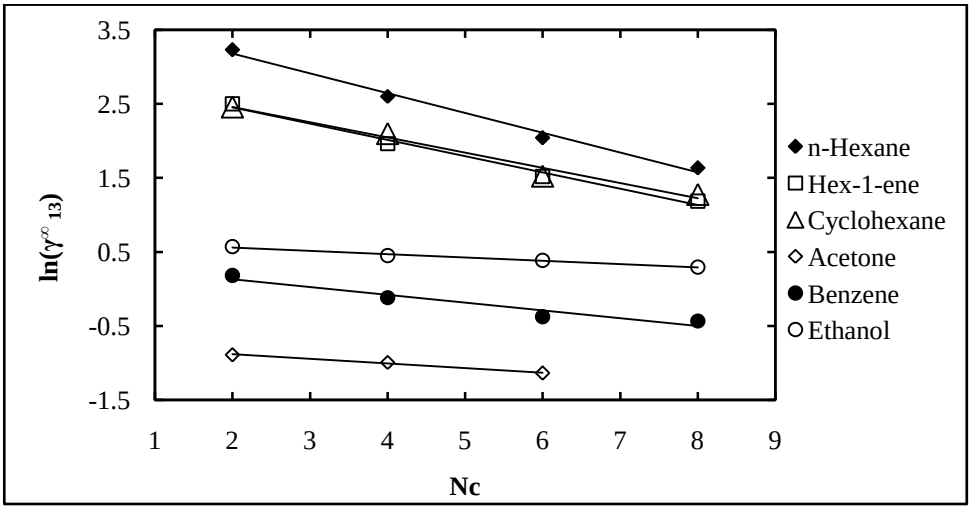

Figure I-2: Variation of limiting activity coefficients of various solutes depending on Nc, the carbon number of the alkyl chain attached to the methylimidazolium group with $[Tf_2N]^-$ anion. Nc values corresponding to data points are: 2 for [EMIM] $[Tf_2N]$ [3][4][5], 4 for [BMIM] $[Tf_2N]$ [4][8], 6 for [HMIM] $[Tf_2N]$ [14][15][16] and 8 for [MOIM] $[Tf_2N]$ [16].

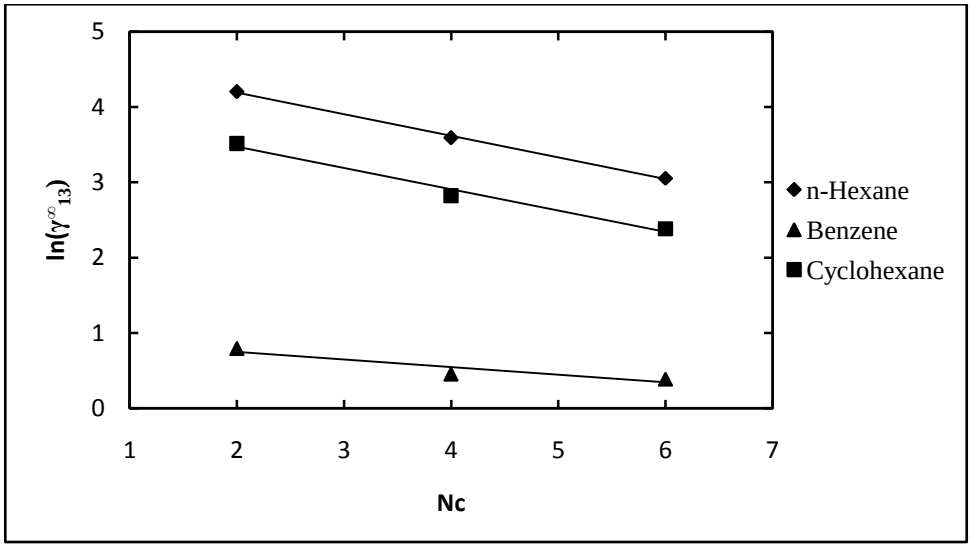

Figure I-3: Variation of limiting activity coefficients of various solutes depending on Nc, the carbon number of the alkyl chain attached to the methylimidazolium group with $[TfO]^-$ anion. Nc values corresponding to data points are: 2 for [EMIM] [TfO] [28], 4 for [BMIM] [TfO] [9] and 6 for [HMIM] [TfO] [33].

1.2. Pyrrolidinium-based fluorinated ionic liquids

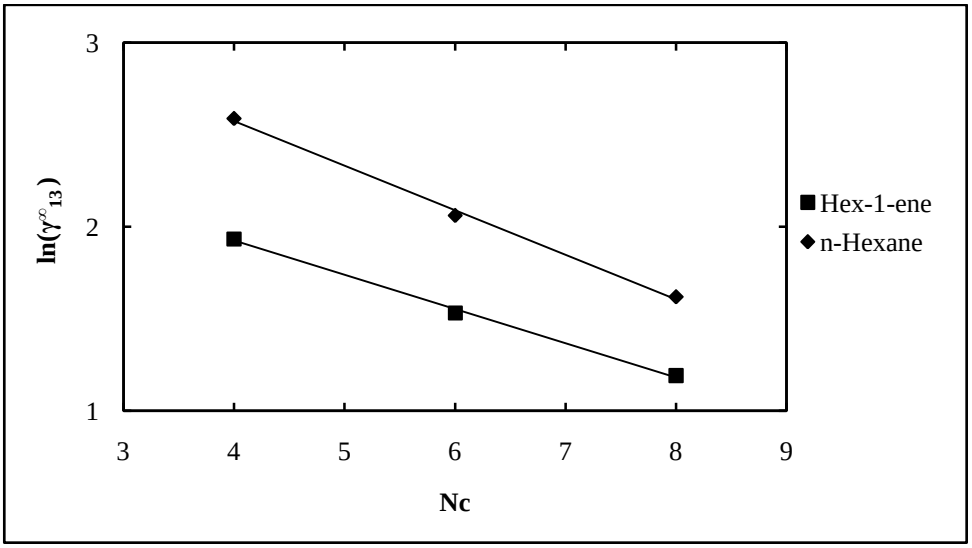

Figure I-4: Variation of limiting activity coefficients of n-hexane and hex-1-ene depending on Nc, the carbon number of the alkyl chain attached to the methylpyrrolidinium group with $[Tf_2N]^-$ anion. Nc values corresponding to data points are: 4 for [BMPyrr] $[Tf_2N]$ [16], 6 for [HMPyrr] [35] and 8 for [OMPyrr] $[Tf_2N]$ [35].

2. Infinite dilution selectivity coefficient correlation with the ionic liquid alkyl chain length

2.1. n-hexane/benzene system

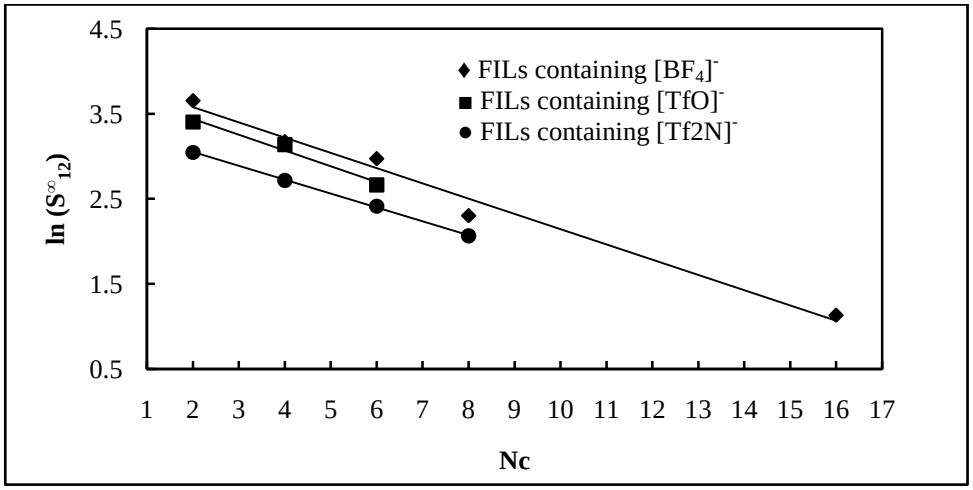

Figure I-5: Variation of limiting selectivities of n-hexane to benzene depending on Nc, the carbon number of the alkyl chain attached to the methylimidazolium group with common $[BF_4]^-$, $[Tf_2N]^-$ and $[TfO]^-$ anions. Nc values corresponding to data points are: 2 for [EMIM] $[BF_4]$[1][2], [EMIM] [TfO][28] and for [EMIM] $[Tf_2N]$ [3][4]; 4 for [BMIM] $[BF_4]$[6][2], [BMIM] [TfO][9] and [BMIM] $[Tf_2N]$ [4][8]; 6 for [HMIM] $[BF_4]$[12][2], [HMIM] [TfO][33] and [HMIM] $[Tf_2N]$ [14][16];8 for [MOIM] $[BF_4]$[17] and [MOIM] $[Tf_2N]$ [16] and 16 for $[C_{16}MIM]$ $[BF_4]$[18].

2-2. n-hexane/hex-1-ene system

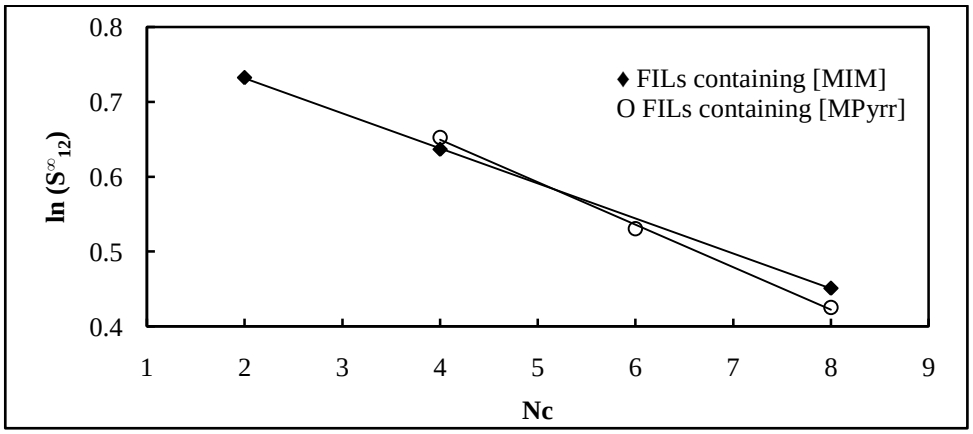

Figure I-6: Variation of limiting selectivity of n-hexane to hex-1-ene depending on Nc, the carbon number of the alkyl chain attached to the methylpyrrolidinium or methylimidazolium group with common $[Tf_2N]^-$ anion. Nc values corresponding to data points are: 2 for [EMIM] $[Tf_2N]$ [3][4]; 4 for [BMIM] $[Tf_2N]$ [4] and [BMPyrr] $[Tf_2N]$ [16] ; 6 for [HMIM] $[Tf_2N]$ [14] and [HMPyrr] $[Tf_2N]$ [35] and 8 for [MOIM] $[Tf_2N]$ [16] and [OMPyrr] $[Tf_2N]$ [35].